

The Silurian Amabel and Guelph
formations of the Bruce Peninsula: insights
into stratigraphy and diagenesis from
petrography and ground-penetrating radar

by

Lona-Kate Dekeyser

A thesis
presented to the University of Waterloo
in fulfillment of the
thesis requirement for the degree of
Master of Science
in
Earth Sciences

Waterloo, Ontario, Canada, 2006

© Lona-Kate Dekeyser 2006

Author's Declaration

I hereby declare that I am the sole author of this thesis. This is a true copy of the thesis, including any required final revisions, as accepted by my examiners.

I understand that my thesis may be made electronically available to the public.

Abstract

Regional study of the Silurian Amabel and Guelph (including the Eramosa Member) formations in the subsurface on the Bruce Peninsula provides petrographic details of these pervasively dolomitized rocks, defines lithofacies changes within each formation, and demonstrates the use of ground-penetrating radar as a tool for shallow subsurface stratigraphic mapping. Detailed stratigraphic logging of core provides insight on the complex depositional history of the pervasively dolomitized Amabel and Guelph formations by highlighting lateral facies changes that are not readily observable in outcrop.

The Lions Head and Colpoy Bay members of the Amabel Formation are continuous in core across the Bruce Peninsula. These members contain characteristic dark grey mottles which are the result of increased porous zones and pyrite, and/or concentrations of undifferentiated organics. Chert nodules and the abundance of silica is most abundant in the upper Lions Head Member where silica-replaced fossils are recognized within the surrounding dolomite. Typical Wiaraton Member crinoidal lithofacies from the upper Amabel Formation are more common in the southern half of the Peninsula. The Eramosa Member is more laterally continuous on the Bruce Peninsula than previously assumed. Although there is a lack of bituminous argillaceous Eramosa lithofacies within core, the laminated Eramosa Member is thick near Wiaraton which suggests that a large restricted less-oxygenated area existed in that vicinity during the Silurian. Thick accumulations of tan-brown fossiliferous undifferentiated Guelph Formation dolostones occur at both the northern and southern ends of the Peninsula.

Petrographic analyses reveal that the Amabel and Guelph formations are dolomitized with no precursor limestone observed. Four types of dolomite were observed within these formations and differentiated based on crystal size. These dolomites are characterized by a uniform dull red luminescence, and range from inclusion-rich anhedral very finely ($< 5 \mu\text{m}$) crystalline dolomite to clearer euhedral coarsely ($> 250 \mu\text{m}$) crystalline dolomite.

Petrographic analyses also revealed secondary minerals such as pyrite, calcite (and dedolomite), silica, sphalerite, fluorite, and glauconite.

Ground-penetrating radar surveys provided high-resolution data, which combined with detailed geologic observations of accessible quarry outcrops and borehole logs, support the conclusion that GPR is a useful tool for locating karstic features, vuggy porosity, and lateral and vertical facies changes in carbonate rocks. Radar profiles may have important implications for the aggregate and building-stone industries as a tool to locate carbonate units of exploration interest or to avoid zones with high impurities.

Acknowledgements

I would like to thank my supervisor, Dr. Mario Coniglio, for teaching me about the world of carbonate petrography and diagenesis. Mario provided answers for my many questions, and taught me how to read more critically during my two years as a graduate student at the University of Waterloo. Mario's patience, efficiency and support were also appreciated. My co-supervisor, Dr. Anthony Endres, taught me how to perform ground-penetrating radar in the field, how to process my data in the lab, and how to appreciate GPR as a tool in stratigraphic mapping. Tony's patience in teaching me about the technology of GPR was also gratefully appreciated. Frank Brunton of the Ontario Geological Survey introduced me to the carbonates of the Niagara Escarpment prior to my study at the University. Frank's enthusiasm for the Silurian and the critters that make up the carbonates was an important motivating factor for this study. Frank's review of the thesis provided additional outcrop and paleontologic feedback, and his support in my efforts was greatly valued. Thanks to Dr. Mike Brookfield from the University of Guelph for his time and review of this thesis as well.

This research was funded by a research grant from Canada's Natural Sciences and Engineering Research Council (NSERC) awarded to Dr. Mario Coniglio. The Ontario Geological Survey provided additional funding for thin section preparation and conference expenses. I would like to thank T. R. Carter at the Oil, Gas, and Salt Resources Centre for his assistance while logging core, and Mike Jackson from the Department of Earth Sciences at Carleton University for thin section preparation.

Finally, I wish to thank my family and friends who have supported me throughout my University career and to Steven Aspden for his love, thoughtfulness, academic and emotional support, and his ability to keep me laughing.

Table of Contents

Chapter 1 : Introduction	1
1.1 Introduction to the Study Area	1
1.2 Objectives of this study	4
1.3 Methodology	5
1.4 Organization of the thesis.....	7
Chapter 2 : Geological Setting.....	8
2.1 Michigan Basin	8
2.2 Geological Setting of the Bruce Peninsula.....	9
2.2.1 Cataract Group.....	9
2.2.2 Clinton Group	10
2.2.3 Albemarle Group	12
2.3 Previous studies on the Amabel and Guelph formations	12
2.3.1 The Amabel Formation.....	13
2.3.2 The Eramosa Member	14
2.3.3 The Undifferentiated Guelph Formation	15
2.4 Paleogeography of the Michigan Basin	17
Chapter 3 : Stratigraphy of the Amabel and Guelph formations	21
3.1 Lithofacies of the Amabel Formation	21
3.1.1 Lions Head Member	22
3.1.2 The Colpoy Bay Member	25
3.1.3 The Wiarnton Member	26
3.2 Lithofacies of the Eramosa Member	29

3.2.1 Eramosa 1 Lithofacies	30
3.2.2 Eramosa 2 Lithofacies	30
3.2.3 Eramosa 3 Lithofacies	34
3.2.4 Eramosa 4 Lithofacies	34
3.3 Lithofacies of the Guelph Formation	35
3.3.1 Guelph 1 Lithofacies	36
3.3.2 Guelph 2 Lithofacies	37
3.3.3 Guelph 3 Lithofacies	37
3.4 The depositional history of the Amabel and Guelph formations	40
3.4.1 The Amabel Formation.....	40
3.4.2 The Eramosa Member	45
3.4.3 The Guelph Formation.....	46
3.5 Conclusions	47
Chapter 4 : Petrography and diagenesis of the Amabel and Guelph formations	50
4.1 Introduction	50
4.2 Diagenesis of the Amabel and Guelph formations.....	51
4.2.1 Pre-dolomitization diagenesis.....	51
4.2.2 Post-dolomitization diagenesis	54
4.2.3 Dolomite distribution and petrography.....	65
4.3 Nature and distribution of silica	72
4.3.1 Distribution of nodules	73
4.4 Distribution of mottles and mottled fabric	77
4.5 Interpretations.....	79

4.5.1 Pre- and post-dolomitization diagenesis.....	79
4.5.2 Dolomitization.....	85
4.5.3 Mottling.....	86
4.6 Dolomitization models of the Bruce Peninsula during the Silurian.....	87
4.7 Conclusions.....	89
Chapter 5 : High Frequency GPR Profiling of Shallow Subsurface Stratigraphy in Silurian Dolostones.....	
5.1 Introduction.....	92
5.2 Geological Setting.....	94
5.3 Methodology.....	96
5.4 Results.....	102
5.4.1 Correlating GPR with geology at OSLW.....	102
5.4.2 Correlating GPR with geology at the Adair Quarry.....	113
5.5 Conclusions.....	116
Chapter 6 : Low Frequency GPR Profiling of Deep Subsurface Stratigraphy in Silurian Dolostones.....	
6.1 Introduction.....	117
6.2 Geological Setting.....	120
6.3 Methodology.....	122
6.4 Results.....	128
6.4.1 Correlating GPR with geology at the Adair Quarry.....	128
6.4.2 Correlating GPR with geology at the OSLW Quarry.....	133
6.4.3 Correlating GPR with geology at Borehole 90-3.....	145

6.5 Conclusions	149
Chapter 7 : Concluding Remarks and Future Recommendations	151
7.1 Overall Conclusions	151
7.2 Recommendations for Future Work	154
7.2.1 Geochemical contributions	155
7.2.2 Georgian Bay Inlet.....	157
7.2.3 Extensive GPR profiles and a three-dimensional GPR-stratigraphy model.....	157
References.....	158
Appendix A Geologic Data.....	165
Appendix B – High Frequency Shallow Subsurface GPR.....	180
Appendix C – Low Frequency Shallow Subsurface GPR	191
Appendix D – Data on CD-ROM	200

List of Figures

Figure 1.1: Geological map of the Paleozoic geology on the Bruce Peninsula.....	2
Figure 1.2: Borehole and GPR survey location map on the Bruce Peninsula	4
Figure 2.1: Nomenclature for Silurian strata on the Bruce Peninsula within the Michigan Basin.....	11
Figure 2.2: Paleogeographic map of the Michigan Basin.....	18
Figure 3.1: Contacts and members of the Amabel Formation.....	24
Figure 3.2: Representative core photographs of the Eramosa lithofacies.....	32
Figure 3.3: Representative core photographs of the Guelph lithofacies.....	40
Figure 3.4: Stratigraphic correlation of eight boreholes on the Bruce Peninsula.....	43
Figure 3.5: Legend to accompany Figure 3.4.....	44
Figure 4.1: Examples of hardground surfaces	53
Figure 4.2: Paragenetic sequence constructed for the Amabel and Guelph formations.....	55
Figure 4.3: Schematic illustration of porosity types within the Amabel and Guelph formations.....	57
Figure 4.4: Photomicrographs of pore-lining and pore-filling calcite and dedolomite.....	58
Figure 4.5: Photomicrographs of replacement silica and pyrite.....	59
Figure 4.6: Core and photomicrographs of sphalerite and fluorite.....	66
Figure 4.7: Photomicrographs of dolomite types in the Amabel and Guelph formations.....	68
Figure 4.8: Core and photomicrographs of nodules and their boundaries.....	74
Figure 4.9: Core and photomicrographs of mottles in the Lions Head and Colpoy Bay members.....	78
Figure 4.10: Photomicrograph of two sutured (peaked) stylolite seams.....	84
Figure 4.11: Paleohydrogeological model.....	89
Figure 5.1: Map of the Bruce Peninsula.....	94
Figure 5.2: Silurian stratigraphic units of the Bruce Peninsula.....	96
Figure 5.3A: 225 MHz Profile of Line 6 at the north end of the OSLW Quarry.....	99
Figure 5.3B: 450 MHz Profile of Line 6 at the north end of the OSLW Quarry.....	100
Figure 5.3C: 900 MHz Profile of Line 6 at the north end of the OSLW Quarry.....	101
Figure 5.4: Map of the west side of the OSLW Quarry.....	103
Figure 5.5: Unannotated 900 MHz profiles of Line 6 and Line 7 from the OSLW Quarry.....	106
Figure 5.6: The annotated 900 MHz profile of Line 6.....	107
Figure 5.7: The annotated 900 MHz profile of Line 7.....	108
Figure 5.8: Dissolution fractures and joints at Line 7 in the OSLW Quarry.....	109
Figure 5.9: The 450 MHz GPR profile along Line 3 overlying the reef mound.....	111
Figure 5.10: Geologic cross section between the three sites near the OSLW Quarry.....	112
Figure 5.11: The 900 MHz profile of Line 2 from the Adair Quarry.....	114
Figure 5.12: Annotated 900 MHz GPR profile at the Adair Quarry.....	115
Figure 6.1: Map of the Bruce Peninsula.....	119
Figure 6.2: Silurian stratigraphic units of the Bruce Peninsula.....	121
Figure 6.3A: 200 MHz profile of Line 2 at the Adair Quarry.....	125
Figure 6.3B: 100 MHz profile of Line 2 at the Adair Quarry.....	126
Figure 6.3C: 50 MHz profile of Line 2 at the Adair Quarry.....	127
Figure 6.4: Location of Line 2 and Line 3 in the Adair quarry with borehole 90-4.....	130
Figure 6.5: 50 and 100 MHz images at Line 2 at the Adair Quarry.....	131
Figure 6.6: The Annotated 50 and 100 MHz profiles at Line 2 in the Adair Quarry.....	132
Figure 6.7: Map of the west side of the OSLW Quarry with the low frequency profiles.....	134
Figure 6.8: 50 MHz GPR profiles of Line 1 and Line 2 at the OSLW Quarry.....	135
Figure 6.9: Annotated 50 MHz profiles of Lines 1 and 2 at the OSLW Quarry.....	136
Figure 6.10: Non-annotated 100 MHz GPR profiles of Lines 1 and 2 at the OSLW Quarry.....	137

Figure 6.11: Annotated 100 MHz GPR profiles of Lines 1 and 2 at the OSLW Quarry..	138
Figure 6.13: 50 MHz and 100 MHz GPR profiles from Line 5 at the OSLW Quarry.	143
Figure 6.14: Annotated 50 MHz and 100 MHz GPR profiles from Line 5 at the OSLW Quarry	144
Figure 6.15: Radar profile from Line 0 at the 90-3 borehole site.....	147
Figure 6.16: Borehole correlation in the vicinity of the OSLW and Adair quarries.	148

List of Tables

Table 1: Summary of observations from the Amabel Formation.....	28
Table 2: Summary of observations from the Eramosa Member.....	33
Table 3: Summary of observations from the Guelph Formation.....	39
Table 4: Crystal size classification.....	65

Chapter 1: Introduction

1.1 Introduction to the Study Area

The Wenlock-Ludlow age Amabel and Guelph formations of southwestern Ontario form the caprock of the Niagara Escarpment and most of the bedrock surface on the Bruce Peninsula (Fig. 1.1). These formations form the Albemarle Group (Bolton, 1957), which overlies the Fossil Hill Formation of the Clinton Group on the Bruce Peninsula.

Silurian strata on the Bruce Peninsula are approximately stratigraphically equivalent to strata exploited for hydrocarbons in southwestern Ontario and to producing strata in southeastern Michigan (see Gill, 1977; Huh et al., 1977; Sears and Lucia, 1980; Cercone and Lohmann, 1987; Armstrong et al., 2002).

The Amabel and Guelph formations have been intensely exploited by the building and chemical stone and aggregate industries, and have been more recently recognized as significant bedrock aquifers in southwestern Ontario. Despite this varied and extensive exploitation over the past century, little detailed work has been carried out on the local and regional stratigraphy, sedimentology, and diagenesis of these strata on the Bruce Peninsula. Therefore, only a rudimentary understanding exists of the relative ages, regional lithofacies, sequence stratigraphy (see Brett et al., 1995), petrography and diagenesis of this carbonate succession.

Moreover, the Amabel and Guelph formations were pervasively dolomitized, as were most Silurian carbonates in the region, and the details of the process are still poorly understood (Sears and Lucia, 1980; Shaver, 1991; Coniglio et al., 2003). These carbonate

rocks are for the most part typical of massive dolostones, with varying preservation of original sedimentary features (e.g., fossils, depositional fabrics, bedding). The Silurian Amabel and Guelph formations contain a variety of diagenetic phases which represent a complex history of multiple stages of diagenesis from limestone lithification to pervasive dolomitization.

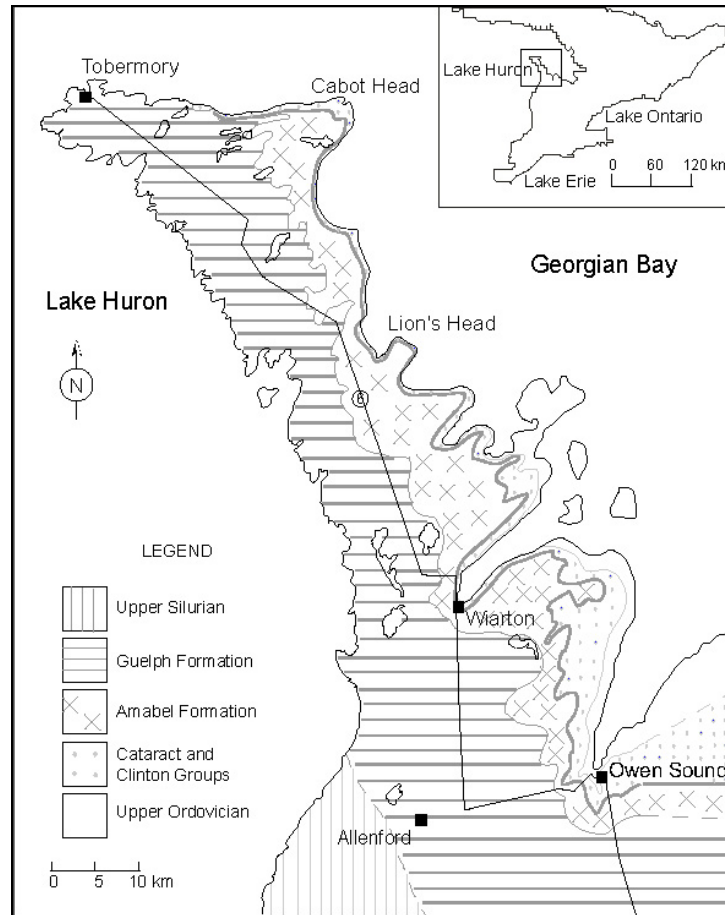


Figure 1.1: Geological map of the Paleozoic geology on the Bruce Peninsula (modified from Armstrong et al., 2002).

This thesis sheds light on aspects of the stratigraphy and diagenesis of these strata by using a two-project approach – the first includes traditional core and petrographic techniques

to study these rocks, and the second explores the vertical and lateral changes in their characteristics using ground-penetrating radar. The stratigraphic study of eight boreholes along the Bruce Peninsula provides a detailed knowledge of the distribution of the lithofacies and members of the Amabel and Guelph formations which aids in the interpretation of their depositional history. Petrographic analyses of the members and lithofacies within the dolostones allows the differentiation of dolomitization fabrics between formations and some lithofacies. As well, petrographic study of mottled fabrics and nodules provides insight into their composition and origin.

Ground-penetrating radar (GPR) has been widely used by stratigraphers in clastics, whereas little GPR work has been done in carbonates. Access to two large bedrock quarries on the Bruce Peninsula provided an opportunity to integrate ground-penetrating radar (GPR) technology into this thesis. GPR surveys were carried out to investigate radar characteristics of facies within the Amabel and Guelph formations and to assess the capability of GPR to image karstic porosity features. GPR is an economical tool that has the potential to optimize costly quarry operations in the search for suitable building and chemical stone, and aggregate.

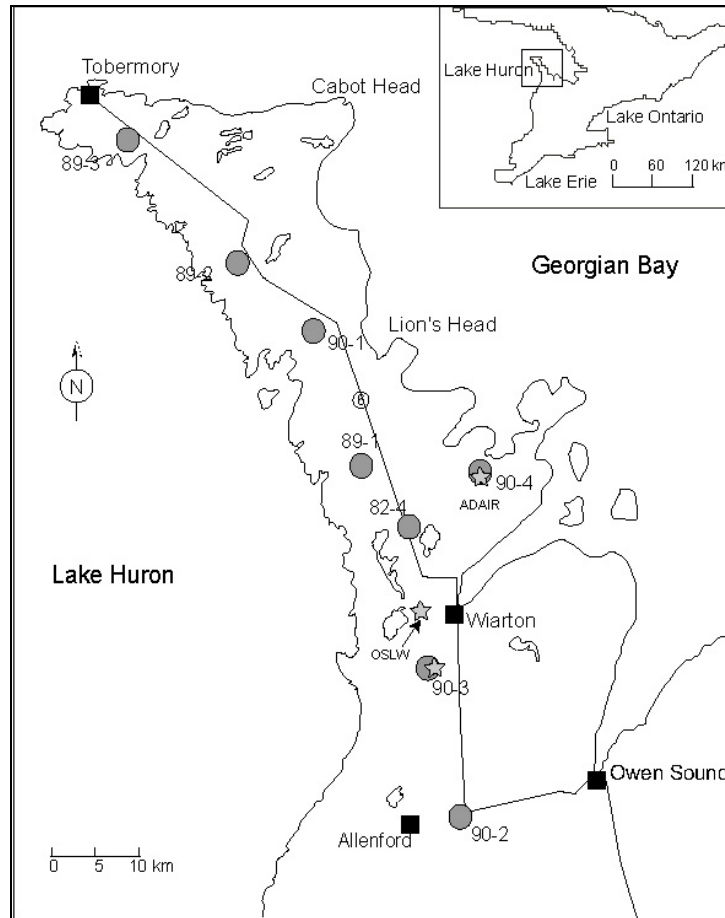


Figure 1.2: Borehole and GPR survey location map on the Bruce Peninsula. Dark grey circles represent borehole locations and light grey stars represent GPR survey locations. The box on inset map of southern Ontario outlines the study area (modified from Armstrong et al., 2002).

1.2 Objectives of this study

The purpose of this study is to examine aspects of the stratigraphy and diagenesis of the Amabel and Guelph formations on the Bruce Peninsula through (1) core and petrographic analyses and (2) GPR. The framework for this study is based on detailed stratigraphic logging of core from eight boreholes along the Peninsula from Tobermory south to Allenford (Fig. 1.2). In addition, quarry outcrop sections were measured and GPR surveys were

conducted at two quarries. Together the two quarries and eight boreholes provide insight into the internal stratigraphy of the Amabel and Guelph formations at a level of detail that is not available based on outcrops alone.

The primary objectives of this thesis are to: (1) correlate in detail lithofacies seen in the eight boreholes on the Bruce Peninsula in order to better understand their distribution and associations of the various depositional facies on the Bruce Peninsula; (2) describe the petrographic characteristics of these carbonates, emphasizing their diagenetic attributes; and (3) illustrate the usefulness of GPR as an exploration tool as applied to aggregate and building stone resources.

1.3 Methodology

The eight boreholes that were examined for this project were drilled from 1982-1990 in support of regional mapping projects by the Ontario Geological Survey (OGS). These boreholes are evenly spaced along the Bruce Peninsula from Tobermory south to Allenford parallel to the Lake Huron shoreline (Fig. 1.2). Stratigraphic logging was carried out in the summer of 2005 at the Oil, Gas and Salt Resource Centre in London, Ontario where the OGS core is currently stored. Each core was subdivided on the basis of observed lithofacies changes. Measurements were recorded in feet to correspond with drilling data, and subsequently converted to metric units. A total of 141 samples were taken based on representative fabrics of each member, and the presence of diagenetic features such as mottles, nodules, stylolites and non-carbonate minerals. The majority of samples were thin sectioned (n = 128) at the Petrographic Services facility of the Department of Earth Sciences

at Carleton University. The stratigraphic locations of the thin sections are illustrated in Appendix A.

All thin sections were examined under cathodoluminescence (CL) prior to covering. The Reliotron CL Instrument provided optimum results using a beam current of ~0.600 mA, a minimum voltage of 10 kV and a beam of ~ 1 cm diameter. After CL examination, thin sections were stained using a combined Alizarin Red S –potassium ferricyanide staining solution to enable differentiation between ferroan and non-ferroan calcite and dolomite. A spray-on lacquer cover slip was applied to all stained thin sections. Observations of crystal size (following Folk, 1959), crystal shape (following Sibley and Gregg, 1987), porosity, mineralogy, stylolite characteristics and abundance, fossil identification and alteration, nodule constituents and boundaries, and mottled fabric properties were made using a binocular petrographic microscope.

Polished thin sections (n = 20) exhibiting various diagenetic features were manufactured for further study by scanning electron microscopy (SEM). A gold coating using a sputter coater was applied to the polished thin sections to make the surface conductive. A LEO FESEM 1530 instrument in the Microscopy and Lithography Lab (Department of Chemistry) was operated at a voltage of 20 kV (greater than 1.5 nm resolution). An integrated energy dispersive x-ray spectrometer provided qualitative elemental compositions.

Geophysical acquisition of data was carried out according to the methods and processing techniques of Annan (2005a, b) and Daniels (2004). Antennae of widely varying frequency (50–900 MHz) were used to conduct ground-penetrating radar (GPR) surveys at

two quarries (Adair Quarry near borehole 90-4 and OSLW Quarry near Wiarnton) and one survey adjacent to borehole OGS-90-3. Chapters 5 and 6 provide further detail on the methods and set-up involved at each site.

1.4 Organization of the thesis

This thesis is presented in six chapters. Chapter 1 introduces the study area, states the objectives of this study, and presents the methodology. The second chapter reviews the geological setting of the Michigan Basin, the regional geological setting, as well as the previous research on the Amabel and Guelph formations. The third chapter is a regional stratigraphic and sedimentological summary based on the core and thin sections from eight boreholes, and includes a discussion of the depositional histories of the Amabel and Guelph formations. Chapter 4 focuses on specific diagenetic attributes of these carbonates, emphasizing dolomitization and silicification, and the origin of mottled fabrics within the Amabel and Guelph formations. Chapter 4 includes a brief discussion of the probable origin of dolomitization of Bruce Peninsula carbonates during the Silurian based on earlier work on correlative carbonates in the subsurface of southwestern Ontario. Chapter 5 reports the results of the high frequency GPR study resolving the small-scale (centimetre-scale) lithologic and diagenetic features of the Amabel and Guelph formations. In Chapter 6, metre-scale lateral and vertical facies changes are examined within the Amabel and Guelph formations using GPR. Chapter 7 is a summary of the overall conclusions of the thesis and makes suggestions for future work.

Chapter 2: Geological Setting

2.1 Michigan Basin

Following the Taconic Orogeny, tectonic activity diminished during the early Silurian. Although the origin of the Michigan Basin is still poorly understood, this nearly circular structure likely attained its present configuration by middle Silurian time (Sanford, 1969). Fauna within the Silurian carbonates suggests that the continental North American plate resided at approximately 10–15 °S latitude (Shaw, 1937; Sanford, 1969). During the early Silurian, the Michigan Basin was a tropical inland seaway that was subjected to repeated transgressions and regressions, subtropical storms, and periodic influxes of terrigenous detritus from the Appalachian Basin and windblown sources (Johnson et al., 1992). During the Late Silurian the relatively rapid subsiding basin centre provided environmental conditions favourable for the prolific growth of carbonate platforms and pinnacle and patch reefs, which formed along the margins of the Michigan Basin (Johnson et al., 1992). Evidence of these reefs was not observed within the core from the Bruce Peninsula.

Terminology

The interpretive phrase “proximal to a bioherm or mound” is used in a broad sense referring to lithofacies within the Amabel and Guelph formations which contain abundant preserved fossils that are typically whole or unfragmented. Fragmented fossils more likely reflect the effects of mechanical (wave- or storm-influenced) breakage, and are interpreted to occur in higher energy settings.

2.2 Geological Setting of the Bruce Peninsula

The Bruce Peninsula is situated between Lake Huron and Georgian Bay in southern Ontario. Ordovician and Silurian rocks make up the bedrock of the Peninsula, which is situated on the northeastern edge of the Michigan Basin. Silurian pinnacle and patch reef belts have been well documented along the southwestern (Ontario) and northern (Michigan) margins of the basin (Textoris and Carozzi, 1964; Mesolella et al., 1974; Fisher, 1977; Shaver et al., 1978; Gill, 1985; Charbonneau, 1990; Smith, 1990; Coniglio et al., 2003). Brett et al. (1995) and Brett et al. (1999) have correlated Silurian strata from western New York and southern Ontario, and attempt to clarify and provide insight between Silurian units in southwestern Ontario and those on the Bruce Peninsula.

Silurian strata on the Bruce Peninsula include the Cataract, Clinton, and Albemarle groups (Johnson et al., 1992). The following is a brief overview of the Silurian stratigraphy on the Bruce Peninsula in the Michigan Basin, and follows the nomenclature of Bolton (1953, 1957; Fig. 2.1). Bolton (1953, 1957) defined the members and formations of the Albemarle Group on the Bruce Peninsula through detailed mapping and his member and formation names continue to be applied today.

2.2.1 Cataract Group

On the Bruce Peninsula, the Lower Silurian Cataract Group includes dolostones of the Manitoulin Formation and shales and sandstones of the Cabot Head Formation. Cataract strata overlie a broad regional platform (Algonquin Arch) composed primarily of Ordovician carbonates with little or no siliciclastics input (Brett et al., 1999). The Cataract strata

represent a transgressive (Manitoulin Formation)-regressive (Cabot Head Formation) cycle of sedimentation (Sanford, 1969).

2.2.2 Clinton Group

The Clinton Group is composed of Dyer Bay Formation dolostones, argillaceous dolostones and shales of the Wingfield Formation, dolostones of the St. Edmund Formation and fossil-rich dolostones of the Fossil Hill Formation (Armstrong et al., 2002). These formations are well exposed in the northern portions of the Bruce Peninsula. Subsidence was more intensive in the northern part of the Michigan Basin as evidenced by thicker accumulations of Cataract strata (Sanford, 1969). Subsidence may have provided the accommodation space that allowed the Wingfield, St. Edmund, and Fossil Hill formations to accumulate (Sanford, 1969). The alternation of shales and carbonates may be indicative of a storm-influenced shelf environment on the margin of the basin (Brett et al., 1999).

Silurian Stratigraphic Units of the Michigan Basin, southern Ontario

Age <small>Harland et al. 1989 Brett et al. 1999</small>	Michigan Basin (Bruce Peninsula) <small>Johnson et al. 1992</small>	
Ludlovian	Albemarle Gp.	Guelph Fm.
~ 424		Eramosa Mb
Wenlockian		Amabel Fm.
		Wiarnton/Colpoy Bay Mb.
		?
		Lion's Head Mb.
~ 430	Clinton Gp.	Fossil Hill Fm.
Llandovery		Wingfield Fm.
		Dyer Bay Fm.

Figure 2.1: Nomenclature for Silurian strata on the Bruce Peninsula within the Michigan Basin (modified from Bolton, 1957; and Johnson et al., 1992).

Following withdrawal of the Cataract sea, the Cabot Head, Dyer Bay, Wingfield, and St. Edmund formations were eroded, and subsequent transgression of Clinton seas established conditions favourable for reef development (Sanford, 1969). The Fossil Hill Formation coral and stromatoporoid biostromes developed in shallow marine waters (Sanford, 1969; Johnson et al., 1992). Middle Clinton strata (Sauquoit shale within eastern New York in the Appalachian Basin) are missing amongst the strata west of the Algonquin

Arch, and an angular unconformity is present in their place (Johnson et al., 1992; Brett et al., 1999). The erosional surface suggests that regional uplift of the Algonquin Arch and possible shifting of the axis of the basin took place (Brett et al., 1999). Tectonic activity likely influenced a regression of the sea following deposition of the Clinton Group (Brett et al., 1999). As the sea re-advanced, the Albemarle Group was deposited.

2.2.3 Albemarle Group

The Albemarle Group, which is the focus of this thesis, is composed of the Amabel and Guelph formations. The contact between the Amabel Formation and underlying Fossil Hill Formation is sharp on the Bruce Peninsula, and correlates with a regional disconformity (Brett et al., 1999). The Amabel Formation includes three members; generally from base to top they are the Lions Head, Colpoy Bay, and Wiarton (Bolton, 1953). Overlying the Amabel Formation is the Eramosa Member assigned as the lowermost member of the Guelph Formation (Sanford, 1969; Armstrong and Meadows, 1988; Johnson et al., 1992) and the overlying undifferentiated Guelph Formation. Based on core observations, the Eramosa Member was subdivided into four lithofacies and the Guelph Formation was subdivided into three lithofacies. Detailed descriptions of the Albemarle Group are discussed in Chapter 3.

2.3 Previous studies on the Amabel and Guelph formations

The majority of early research in southwestern Ontario on the stratigraphic, depositional, and paleoenvironmental interpretations of the Amabel and Guelph formations have been provided by Logan (1863), Williams (1919), Shaw (1937), Bolton (1953, 1957), Sanford (1969),

Liberty and Bolton (1971), and more recently by Armstrong (1988), Johnson et al. (1992), Armstrong et al. (2002), Brunton and Dekeyser (2004), and Brunton et al. (2005). Numerous studies from the United States on the Silurian Amabel Formation (also known as the Lockport Formation or the Grey Niagaran) and the Guelph Formation have added fundamental insight to the stratigraphic and depositional history (Fisher, 1962; Textoris and Carozzi, 1964; Briggs and Briggs, 1974; Mesolella et al., 1974; Briggs et al., 1980; Crowley and Ford, 1980; Sears and Lucia, 1980; Gill, 1985; Droste and Shaver, 1985, 1987; Cercone and Lohmann, 1987; Brett et al., 1990).

2.3.1 The Amabel Formation

According to previous researchers, the Amabel Formation contains both biohermal and interbiohermal strata that are characterized by spatial variations in fossil content and sedimentary fabrics (Liberty, 1966; Liberty and Bolton, 1971; Sanford, 1969; Brunton and Dekeyser, 2004; Brunton et al., 2005). The three members which make up the Amabel Formation (Lions Head, Colpoy Bay, and Wiarton) record the transition from a relatively deeper, low energy environment (Lions Head Member) to a shallow, higher energy shoal environment (Wiarton Member) (Armstrong et al., 2002).

A fourth member, the Eramosa, was considered by earlier workers to be the uppermost member of the Amabel Formation (Bolton, 1957; Liberty and Bolton, 1971); but this assignment was argued by others (Sanford, 1969; Armstrong and Meadows, 1988; Johnson et al., 1992; Armstrong et al., 2002; Brunton and Dekeyser, 2004; Brunton et al., 2005) to be more appropriately included as either a basal member of the Guelph Formation

or a separate rock unit of formational rank (Shaw, 1937; Brett et al., 1995; Brunton et al., 2005). The Eramosa Member is discussed further below.

The three members of the Amabel Formation are distinct in core. In outcrop, however, the Colpoy Bay and Wiarton members are sometimes more difficult to distinguish due to pervasive dolomitization, apparent gradational contacts or lateral facies transitions and similar weathered surfaces. Some researchers have grouped the middle (Colpoy Bay) and upper (Wiarion) members into one unit and refer to it as the Wiarton/Colpoy Bay Member (Sanford, 1969; Johnson et al., 1992; Armstrong et al., 2002; Fig. 2.1).

2.3.2 The Eramosa Member

The Eramosa Member was first introduced in Williams' (1915 a, b) work in southern Ontario as a bituminous dolomite that was continuous and conformable above the underlying Wiarton Member of the Amabel (Lockport) Formation. Shaw (1937) redefined the Eramosa as a separate formation altogether. Based on its inconsistent thickness and presence, Bolton (1957) suggested that this facies was related to the development of bioherms in the Wiarton Member and therefore was associated with the Amabel Formation. However, more recent work has shown this distinctive lithofacies to grade both laterally and vertically into the Guelph Formation (e.g., Armstrong and Meadows, 1988; Johnson et al., 1992; Armstrong et al., 2002).

Eramosa lithofacies have been interpreted to reflect the onset of increasingly restricted conditions and increased salinity, leading to lagoonal deposits situated in and around the apparently reefal sections along the shoreline of the basin (Clarke and

Ruedemann, 1903; Shaw, 1937). Liberty and Bolton (1971) agreed with Shaw (1937) that the Eramosa Member represents a non-reefal facies deposited between Lockport (i.e. Amabel) bioherms. The recent studies of Armstrong and Meadows (1988), Armstrong et al. (2002), Brunton and Dekeyser (2004), and Brunton et al. (2005) show that the Eramosa Member includes fauna that are more closely related to those in the Guelph Formation, and its diagenetic characteristics also supports stratigraphic assignment to the Guelph Formation.

Brett et al. (1995) advanced the Eramosa to its own formational status based on reconnaissance mapping of Silurian stratigraphy in western New York. Although the stratigraphic allocation of the Eramosa Member has not been officially reassigned to the Guelph Formation, the most current stratigraphic work (e.g., Armstrong and Meadows, 1988; Tetreault, 2001; Johnson et al., 1992; Armstrong et al., 2002) considers the Eramosa Member to belong to the Guelph Formation.

2.3.3 The Undifferentiated Guelph Formation

The undifferentiated Guelph Formation constitutes most of the bedrock surface on the western half of the Bruce Peninsula. Previous studies state that the key distinguishing feature between the Amabel and Guelph formations is the faunal turnover from crinoidal, brachiopod, and gastropod fauna of the Amabel to an introduction of bryozoan, microbial and distinctive megalodontid bivalve-gastropod communities which characterize Guelph lithofacies (Bolton, 1957; Liberty and Bolton, 1971; Armstrong et al., 2002; Brunton et al., 2005). Both formations contain several overlapping species (Bolton, 1957). The Amabel and Guelph formations have been mistakenly grouped as one in the past due to the similarities in

their colour, fossil content, and weathered appearance when there was a lack of intervening dark brown Eramosa lithofacies (Bolton, 1957). The Guelph lithofacies generally reflects a more open marine subtidal depositional environment than the less-oxygenated and restricted subtidal lagoons of the Eramosa lithofacies (see Brunton et al., 2005). Fauna within the Guelph Formation suggests that the salinity was higher than within the Amabel Formation (M. Brookfield, personal communication, 2006).

Charbonneau (1990), Smith (1990) and Coniglio et al. (2003) carried out detailed lithologic and petrographic studies of pinnacle and patch reef belts of the Guelph Formation in southwestern Ontario. Charbonneau (1990) and Smith (1990) studied six and three pinnacle and patch reefs, respectively, and interpreted multiple episodes of subaerial exposure that characterized these reefs, based on the presence of laterally extensive enhanced porosity and permeability zones. After the initiation of bioherm growth, tectonic block faulting elevated and intermittently exposed some of the reefs, as suggested by interpreted paleokarstic horizons (Sanford et al., 1985; Smith, 1990; Brett et al., 1999). Charbonneau (1990) proposed that the sea level rose quickly after exposing the Lockport (Amabel) Formation carbonates and these reefs underwent extensive diagenesis from meteoric waters in the phreatic and vadose zones. Evidence of meteoric dolomitization in the vadose zone was shown in both Charbonneau's (1990) and Smith's (1990) petrographic results, based on the presence of pendant and meniscus cements. However, the more than thirty reefs analyzed by Coniglio et al. (2003) petrographically and geochemically have revealed that Silurian seawater was responsible for dolomitization on the platforms. Their petrographic and geochemical evidence does not support any significant role for meteoric water in the

alteration of these carbonates. An overall lack of correlation amongst the geochemistry and petrographic results reflects a diagenetic history composed of a variety of phases of cementation and recrystallization (Coniglio et al., 2003). These case studies show that the Guelph Formation has been influenced by tectonic and climatic controls and has undergone a complex diagenetic history, especially in the southeastern portion of the Michigan Basin.

2.4 Paleogeography of the Michigan Basin

The Michigan Basin comprises a ~ 4800 m-thick succession of largely marine sedimentary rocks ranging in age from late Cambrian through Pennsylvanian (Droste and Shaver, 1985). The Amabel and Guelph formations were deposited along the eastern margin of the Michigan Basin during the late Wenlockian - early Ludlovian (Droste and Shaver, 1985). Marine conditions at this time enabled episodic regional-scale development of stromatoporoid and coral-bearing reefs and reef-associated platformal carbonates such as the more crinoid-rich shoal lithofacies of the Amabel and overlying Guelph formations (Droste and Shaver, 1987; Brunton et al., 1998).

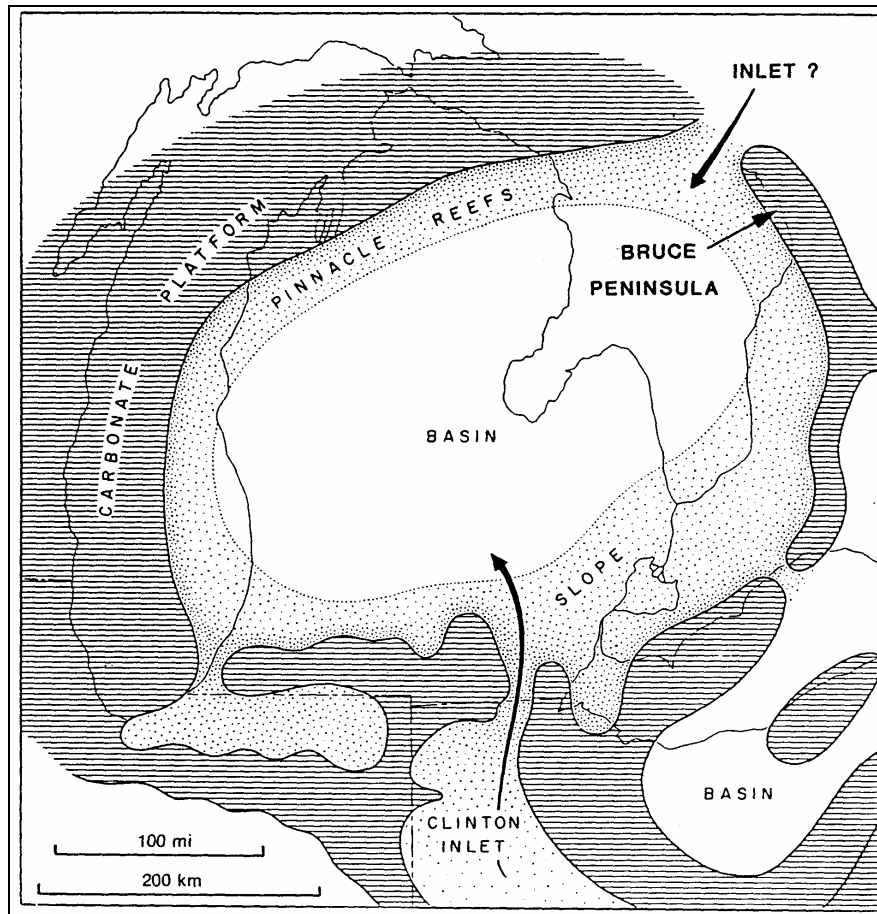


Figure 2.2: Paleogeographic map of the Michigan Basin spanning Early to Late Silurian time (from Briggs et al., 1980; Gill, 1985).

By the Llandovery, basin tectonism induced regional restrictions, preventing open marine waters from entering the basin (Droste and Shaver, 1985). The local climate changed from humid tropical to semi-arid tropical conditions (Droste and Shaver, 1985, 1987). Deeper water Silurian carbonate sediments were deposited in the basin centre and are predominantly limestone. In contrast, platform facies (pinnacle and patch reefs) along the fringes and shelfward are commonly pervasively dolomitized (Sears and Lucia, 1980; Coniglio et al., 2003). A late Wenlockian drop in sea level led to an increase in evaporation

rates, with extreme hypersalinity evidenced by reef demise (Droste and Shaver, 1987). The arid climate and increased evaporation rates led to the deposition of the overlying thick and regionally extensive evaporite deposits of the Salina Formation (Droste and Shaver, 1987).

Silurian paleogeography maps of the Michigan Basin have been drafted by geologists studying the Amabel and Guelph formations (also known as the Lockport, Engadine or Racine formations) from both the Canadian and American sides of the Michigan Basin (e.g., Fig. 2.2). Two inlets into this basin were proposed based on the estimated minor water depth fluctuations, as well as the level of salinity and need for circulation around the basin (Briggs et al., 1980). The inlet which corresponds to the approximate position of the present-day Georgian Bay was hypothesized by Briggs et al. (1980) and Gill (1985) (Fig. 2.2). The Clinton Inlet was discovered by analyzing the distribution of the Silurian strata (Alling and Briggs, 1961). An increase in argillaceous limestones and biota which survive higher salinities overlying Niagaran reefs suggested circulation was later restricted (Briggs et al., 1980). The existence of the Georgian Bay inlet was partially based on the lithofacies of the Lions Head Member of the Amabel Formation. The Lions Head member is composed of finely crystalline, thin-bedded carbonate sediments with low fossil abundances that reflect quieter, low energy conditions (Armstrong et al., 2002). This member has a maximum thickness of 19 m regionally, and averages closer to 5 m on the Bruce Peninsula (Bolton, 1957; Sanford, 1969). The apparent rapid thinning of this member to the south (towards the Algonquin Arch) was interpreted to be caused by a southward shift of the Michigan Basin during the Early Silurian that initiated a transgression within the basin (Sanford, 1969). Armstrong et al. (2002) proposed that there was a lack of shallow shoal lithofacies (Wiarnton

and Colpoy Bay Members) overlying the Lions Head Member at the north end of the Bruce Peninsula. They interpreted local thickening of the Lions Head Member to the north as the only supporting evidence that deeper waters existed north of the Peninsula and that an inlet existed there during the Early Silurian. Although several authors (Sanford, 1969; Gill 1985; Cercone, 1988; Armstrong and Goodman, 1990; Armstrong et al., 2002) have published paleogeographic maps which depict an inlet north of the Bruce Peninsula similar to that shown in Figure 2.2, compelling evidence is lacking to support this hypothesis. The existence of the hypothesized inlet requires more attention. Pervasive dolomitization and bioturbation have obscured the apparent reefal and sedimentary structures, which makes interpreting the depositional environment and recreating the paleogeographic setting of the Bruce Peninsula during the transition between the Early and Late Silurian problematical. Stratigraphic relationships observed in the current study provide additional insight to the Georgian Bay inlet issue (see stratigraphic descriptions in Chapter 3).

Chapter 3: Stratigraphy of the Amabel and Guelph formations

This chapter focuses on the observations made from drilled core from eight boreholes and field observations from the Owen Sound Ledgerrock Wiarion (OSLW) Quarry and the Adair Quarry (Fig. 1.2). The Albemarle Group is divided into the Amabel Formation, the Eramosa Member of the Guelph Formation, and the overlying undifferentiated Guelph Formation.

Further subdivisions are made based on colour, texture, crystallinity size, porosity, fauna, and fabric. Interpretations of each lithofacies are provided in Section 3.4.

3.1 Lithofacies of the Amabel Formation

The Amabel Formation on the Bruce Peninsula is composed of 3 distinct members, which in ascending order are: (1) Lions Head, (2) Colpoy Bay, and (3) Wiarion. These three members are pervasively dolomitized, and contain siliceous nodules and lenses, and abundant pyrite and minor localized MVT-mineralization (e.g., sphalerite and galena). Although fossils are abundant within all members of the Amabel Formation, preservation is variable in core. The recognition of porosity within core was based on visual estimation. There was no limestone found within the eight boreholes studied. An example of each of the members' typical fabric is illustrated in Figure 3.1. The thickness and distribution of these three members is illustrated in Figure 3.4. A summary of the general descriptions of each lithofacies assemblage is provided in Table 1.

3.1.1 Lions Head Member

This member was first named by Nowlan (1935) who included this unit as the uppermost lithofacies of the Clinton Group. Bolton (1953, 1957) named Lions Head after its type section at Lions Head as the lowermost subdivision of the Amabel Formation. The Lions Head Member is characterized by its distinct blocky weathering, massive dense texture and lateral continuity on the Bruce Peninsula (Bolton, 1953). The consistency of the Lions Head Member along the Bruce Peninsula makes it an excellent datum for the construction of cross sections. The Lions Head Member is easily recognizable in core and ranges from 5–15 m in thickness within cores of the study area.

The Lions Head Member is composed of grey to tan, finely crystalline dolostone (Fig. 3.1A, B). In core, this member appears to have a low porosity, typically around ~2 % (biomoldic) and ranges up to ~10 % (biomoldic and vuggy). Porosity is greater in the northernmost and southernmost parts of the study area. Both wispy seam and peaked stylolites occur, and are commonly randomly spaced. Bioturbation within the upper Lions Head Member is profuse, and likely obscures any original sedimentary structures. The Lions Head Member contains small, dark grey to blue-grey millimeter to centimeter-sized, elliptical to elongate irregular mottles (Fig. 3.1B) that are likely a result of bioturbation. These mottled fabrics commonly contain relatively high pyrite content (up to 5 %) made up of 5–25 μm -sized pyrite crystals associated with cloudy finely crystalline dolostone. Very rare calcite cement (crystals up to 40 μm) fills or lines pores. This lithofacies contains chert nodules that are more common in the basal metre, but they are present throughout the Lions Head Member (Fig. 3.1B). Bolton (1953, 1957) similarly noted chert nodules in the basal 4 feet (~

2.5 m). Fossil preservation is commonly poor, and is represented by small patches of coral and shelly fragments (crinoids, gastropods, and/or brachiopods). There are minor fluctuations in the abundance of coral fragments among boreholes within the Lions Head Member.

In the borehole OGS-89-2 on the northern end of the Peninsula, Lions Head type facies are repeated above the Colpoy Bay Member. The recurrence of this facies has also been noted by Sanford (1969, p.10) as “spiraling upward in time to form a basinal facies of the Wiarion in the southern part of the Michigan Basin”.

The contact between the Lions Head Member and the underlying Fossil Hill Formation is sharp and unconformable and is recognized by the abrupt decrease in fossil abundance, and the emergence of new faunas within the Lions Head Member (Armstrong and Goodman, 1990; Stott and von Bitter, 1999; Fig. 3.1A). The upper contact between the Lions Head Member and the Colpoy Bay Member is gradational, and is recognized by an increase in crystal size and fossil content, and a change in the mottled fabric to slightly larger, more irregular shapes (Fig. 3.1C).

The Colpoy Bay Member was observed in the most northerly borehole overlying the Lions Head Member, contrary to Armstrong et al. (2002). Results from this study also indicate that the Lions Head Member is ~ 5 m thick in core at both the north and south ends of the Peninsula (Fig. 3.4). This additional evidence suggests that the proposed Georgian Bay inlet into the Michigan Basin during the Silurian (Gill, 1985; Armstrong et al., 2002) requires more attention. Additional information on this topic is discussed in Section 3.4.

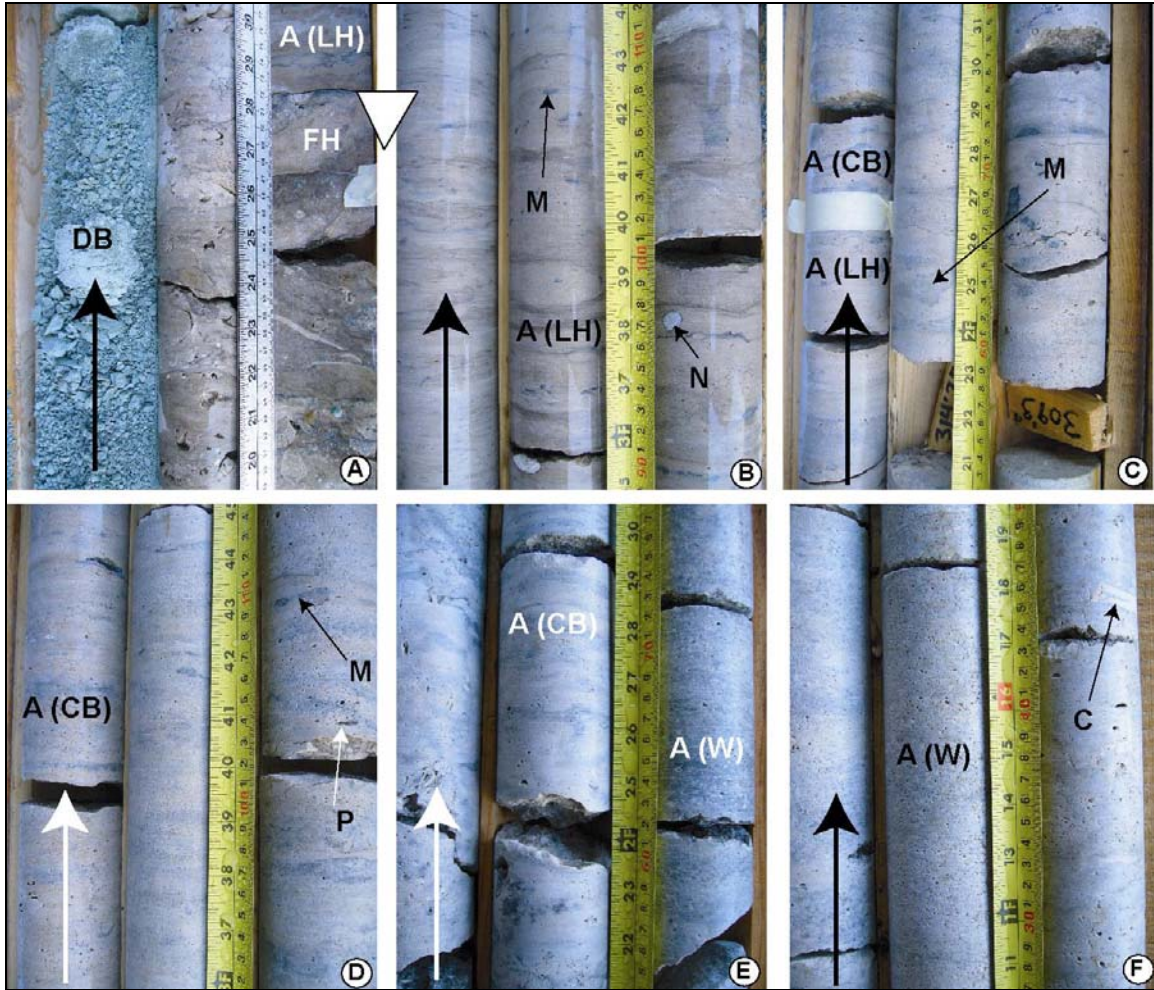


Figure 3.1: Contacts and members of the Amabel Formation. Large arrows in left hand corners of core photographs represent the base of each core, where the top is the upper right-hand corner. All core photographs are from the most southerly borehole, OGS-90-2.

A) The Dyer Bay Formation (DB) underlies the Fossil Hill Formation. The contact between the underlying Fossil Hill Formation (FH) and the Lions Head Member of the Amabel Formation (A(LH)) is sharp and erosional or disconformable (white triangle);

B) Typical Lions Head Member (A(LH)) with small spotty mottles (M) and chert nodules (N);

C) Contact between the underlying Lions Head Member (A(LH)) and the overlying Colpo Bay Member (A(CB)) is gradational (tape in photo). Irregular elongate mottles (M) are common in the Colpo Bay Member;

D) Typical Colpo Bay Member (A(CB)) contains irregular mottles (M) and a slight increase in biomoldic porosity (P);

E) The Colpo Bay Member (A(CB)) and the Warton Member (A(W)) are distinguished by an increase in echinoderm fragments (contact is not shown in photo); and

F) Typical Warton Member (A(W)) is crinoid-rich (C).

3.1.2 The Colpoy Bay Member

This thick package of light to dark grey-tan to blue-grey, fine-medium crystalline dolostones was named after key sections at Colpoy Bay (Bolton, 1953). The Colpoy Bay Member ranges in thickness from 3–20 m within examined core. Porosity, stylolites, bioturbation, and fossil content and abundance vary within this member. The Colpoy Bay Member is noticeably more porous than the Lions Head Member in core, ranging from 5–20% (biomoldic, vuggy, and non-horizontal fractures). Wispy stylolite seams are common within these dolostones, and rare horsetail stylolites are present. Peaked stylolites become more common in the upper portion of this member. Stylolite seams are black and pronounced in the lower portions of this member, becoming lighter in colour and less pronounced in the upper part of the member.

Unlike the Lions Head Member, this mottled fabric is not characterized by the presence of abundant pyrite, although it may be found along the upper or lower edges of the mottle. Mottling within the Colpoy Bay Member is characterized by its shape and evenly-spaced distribution. Typical mottles of the Colpoy Bay Member are elongate parallel to bedding, irregularly shaped, blue-grey, and centimetre-sized in thickness (Fig. 3.1D). Mottles within the Colpoy Bay Member are often 2–3 cm apart. Bioturbation within the base of the Colpoy Bay Member is indicated by irregular banded dark grey mottling parallel to bedding that may only exist in the lower ~1–2 m, followed by a zone of sparse fossils and/or mottling where grey vertical burrow shapes are present. The upper zone of the Colpoy Bay Member may contain ~ 1 m of ‘tiger-striped’ mottling where the tan lithofacies appears intertwined

with dark grey irregular mottles. This uppermost mottling pattern may also be present within the Wiarion Member.

Calcite commonly lines or fills vugs and fractures with crystals ranging from 10–475 μm . Chert nodules are less common than in the Lions Head Member. The abundance of tabulate corals decreases upwards whereas stromatoporoids and shell fragments (crinoids, brachiopods, bivalves, and gastropods) become more abundant. Fragments of fossils are rarely observed in concentrated zones parallel to bedding within the core. The Colpoy Bay Member is laterally continuous on the Bruce Peninsula, and has a gradational contact with the underlying Lions Head Member in all eight boreholes. The lower contact of this member is recognized by the increase in biomoldic, vuggy and fracture porosity, fossil content, and extensive irregular diffuse mottles that resulted from bioturbation (Fig. 3.1D). The contact between the Colpoy Bay Member and the overlying Wiarion Member is gradational, with a change in fauna to more crinoid-rich lithofacies, and a decrease in the mottled fabric (Fig. 3.1E).

3.1.3 The Wiarion Member

The light to dark grey-brown, medium-coarse crystalline crinoidal dolostones of the Wiarion Member were named after their type section at Wiarion by Nowlan (1935). The Wiarion Member is generally quite porous in core, ranging from 10–25 % (biomoldic and vuggy) porosity. Both wispy and peaked stylolite seams rarely occur. Calcite both lines and fills vugs and sub-millimetre-wide fractures with crystals up to 350 μm in size. Minor 5–25 μm -sized crystals of pyrite are associated with fossils and biomoldic porosity. The characteristic

feature of the Wiaraton Member is the abundance of crinoid fragments (Fig. 3.1F), which can range from 20–80 % of this facies, with fragmented stems reaching up to 4 cm in length. Corals become more abundant within the southernmost borehole. The Wiaraton Member does not show the same lateral continuity as the Lions Head and Colpoy Bay members, which are present in each of the boreholes logged. The Wiaraton Member ranges from absent at Tobermory to 15 m thick within the southernmost borehole. This facies is encountered in four of the eight boreholes examined.

Difficulty arises in distinguishing the Wiaraton Member where the size and abundance of crinoids is not great. Where the Guelph Formation directly overlies the Wiaraton Member, the contact is commonly represented by a faunal change, with the introduction of megalodontid bivalves and/or an increase in gastropods and bryozoans. The crystal size and tan-grey colour that sometimes characterizes the Wiaraton Member and the overlying Guelph Formation may be similar and the contact is commonly difficult to determine. In contrast, where the Eramosa Member of the Guelph Formation overlies the Wiaraton Member, the contact is abrupt with a change in colour to darker brown and a reduction in crystal size from medium-coarsely crystalline dolomite to finely crystalline dolomite in the Eramosa Member.

Table 1: Summary of observations in the Amabel Formation

Member	Lions Head Member	Colpo Bay Member	Wiarion Member
Core Observations	Grey-tan, massive, bioturbated fcd, blue-grey spotted (mm-cm) mottling, p= ~2%, wispy ss and peaked ss, minor coral and sf; calcite and chert occur in bp, pyrite occurs in mottles	Light grey-tan, massive, heavily bioturbated, mcd with dark blue-grey irregular mottling, bp and vp= 5–20%, wispy and horsetail ss to peaked ss; abundant sf, coral, stromatoporoid; calcite, chert and minor pyrite are found in bp and nodules	Light tan-grey, massive, heavily bioturbated, mcd with blue-grey irregular mottling, bp and vp= 10–25%, wispy ss and peaked ss, minor sf, abundant crinoids and corals, calcite with minor chert and pyrite in vugs, nodules and bp
Petrographic Observations	Anhedral to subhedral fcd, ~1% ixst, ~2% bp; minor wispy or peaked ss; fp: replaced with fcd or mcd or mixture of microquartz and dolomite, or mimically-replaced with dolomite; pyrite along ss; megaquartz, chalcedony and calcite fill pores	Anhedral to subhedral fcd–ehedral ccd; ~1% ixst, ~10% bp; fp: replaced with fcd, drusy quartz, or mixture of microquartz and mcd; minor pyrite with calcite lining vugs	Subhedral–ehedral fcd–mcd; ~1% ixst; 3–15% bp; fp: mimically-replaced with dolomite; calcite, pyrite, minor diagenetic quartz
Distribution and thickness * from outcrop (Armstrong and Dubord, 1992)	Ranges from 4–12 m in thickness. Lower contact with the Fossil Hill Fm is sharp. Occurs in all 8 boreholes. *Thin- to thick-bedded, platy to blocky parted	Ranges from 5–19 m in thickness. The lower contact with Lions Head Mb is typically gradational. Occurs in all 8 boreholes. *Thick- to massively bedded	Ranges from 3–15 m in thickness. The lowermost contact with the Colpo Bay Mb is typically gradational. Occurs in 4 of the 8 boreholes. *Thick-bedded
Depositional Environment	Low energy, relatively deeper water environment.	Shallow high-energy shoaling non-biohermal environment.	Proximal to bioherms or shoals with crinoids, corals and stromatoporoids.

vfd = very finely crystalline dolostone, fcd = finely crystalline dolostone; mcd = medium crystalline dolostone; ccd = coarsely crystalline dolostone; ixst = intercrystalline porosity; bp= biomoldic porosity; vp=vuggy porosity, ss= styloseams; p = porosity; sf = shelly fragments; fp= fossil preservation

3.2 Lithofacies of the Eramosa Member

The Eramosa Member was first named by Williams (1915) to refer to the bituminous dolostones outcropping along the Eramosa River in southern Ontario. This study has included the Eramosa Member as a basal part of the Guelph Formation. The Eramosa Member contains four lithofacies on the Bruce Peninsula, which have been subdivided by the author into the: (1) Eramosa 1 (E1), (2) Eramosa 2 (E2), (3) Eramosa 3 (E3), and (4) Eramosa 4 (E4). Examples of each of the lithofacies are illustrated in Figure 3.2. The four lithofacies of the Eramosa Member show vertical and/or lateral facies changes across the Bruce Peninsula. Armstrong and Meadows (1988) also observed four similar subdivisions of the Eramosa Member based on quarry outcrop data. Their study of the Eramosa involved thorough research within seven quarries concentrated in the Wiarton area as well as detailed mapping of nearby outcrop locations.

The lower contact of this member with the Amabel Formation is commonly sharp and is recognized by a change in colour from grey-tan to brown, a change from medium-coarse to fine crystallinity, a decrease or lack of mottles, and a decrease in both fossil abundance and faunal type to one with few to no crinoids (Fig. 3.2A). The Eramosa Member varies in thickness from 0–35 m and displays both gradational and sharp litho- and biofacies changes within it. Contacts among lithofacies E1–E3 are generally gradational, whereas the E4 lithofacies is composed of dark bituminous or argillaceous dolostone which makes it prominent within the stratigraphy. These observations suggest changing environmental conditions both temporally and spatially throughout the depositional history of this

significant rock unit. The thickness and distribution of these facies is illustrated in Figure 3.4. A summary of each facies is provided in Table 2.

3.2.1 Eramosa 1 Lithofacies

This lithofacies is composed of grey-brown, massive, finely crystalline dolostone. Porosity estimates from core range from 2–15 % (biomoldic and vuggy). The E1 lithofacies contains an abundance of wispy stylolite seams that are commonly spaced ~ 10 cm apart (Fig. 3.2A). Groups of stylolites ~ 1 cm apart may separate fossil-rich intervals within the E1 lithofacies. Calcite commonly lines vugs and biomoldic pores with crystals up to 2.4 mm in diameter. Pyrite crystals are rarely found associated with stylolite seams. One occurrence of glauconite was observed along a stylolite seam. A variety of shell fragments occur within this facies, including crinoids, brachiopods, bivalves, and possible gastropods.

Although the E1 lithofacies is found within five of the eight boreholes logged on the Bruce Peninsula, this lithofacies does not have a consistent stratigraphic position between the underlying Amabel Formation and the overlying Guelph Formation. The E1 lithofacies may overlie the bituminous laminated dolostones of the E4 lithofacies or the Amabel Formation at the northern end of the Peninsula, and it is also found overlying E2 and E3 lithofacies at the southern end of the Peninsula.

3.2.2 Eramosa 2 Lithofacies

The difference between the E1 and the E2 lithofacies is a colour change from grey-brown (E1) to dark brown (E2) and the introduction of larger-sized coral and brachiopod fragments

(Fig. 3.2B). The E2 lithofacies is composed of dark brown, massive, fine to medium crystalline dolostone. Porosity within this lithofacies ranges from ~5–15 % (biomoldic and vuggy) in core. Wispy stylolite seams occur in groups ~10 cm apart. Minor pyrite crystals are found within stylolite seams, and calcite crystals up to 500 µm line vugs and fractures. Although the majority of nodules found within the E2 lithofacies are mixed dolomite and chert (see Section 4.3.1.2), chert nodules are more abundant in this lithofacies than the E1, E3, or E4 lithofacies. Bioturbation within this lithofacies is not abundant (<10 %), and burrows are not obvious. Similar to the E1 lithofacies, the E2 lithofacies contains a variety of fossils, including shelly fragments (crinoid, brachiopods, gastropods), as well as scattered coral fragments and stromatoporoids. The E2 lithofacies has the greatest abundance of fossils of the four lithofacies. Although preservation of fossils within the E1 and E2 lithofacies was variable within core, Tetreault (2001) recovered a diverse selection of biota from the Eramosa Member at the OSLW Quarry north of Wiarton. Trace fossils, a few rare marine plant fossils, high density shell beds, sponges, trilobites, and stromatolites were found within the various lithofacies of the Eramosa Member, with greater fossil content found in the “interbedded unit”, which most likely corresponds with the E1 or E2 lithofacies (Tetreault, 2001).

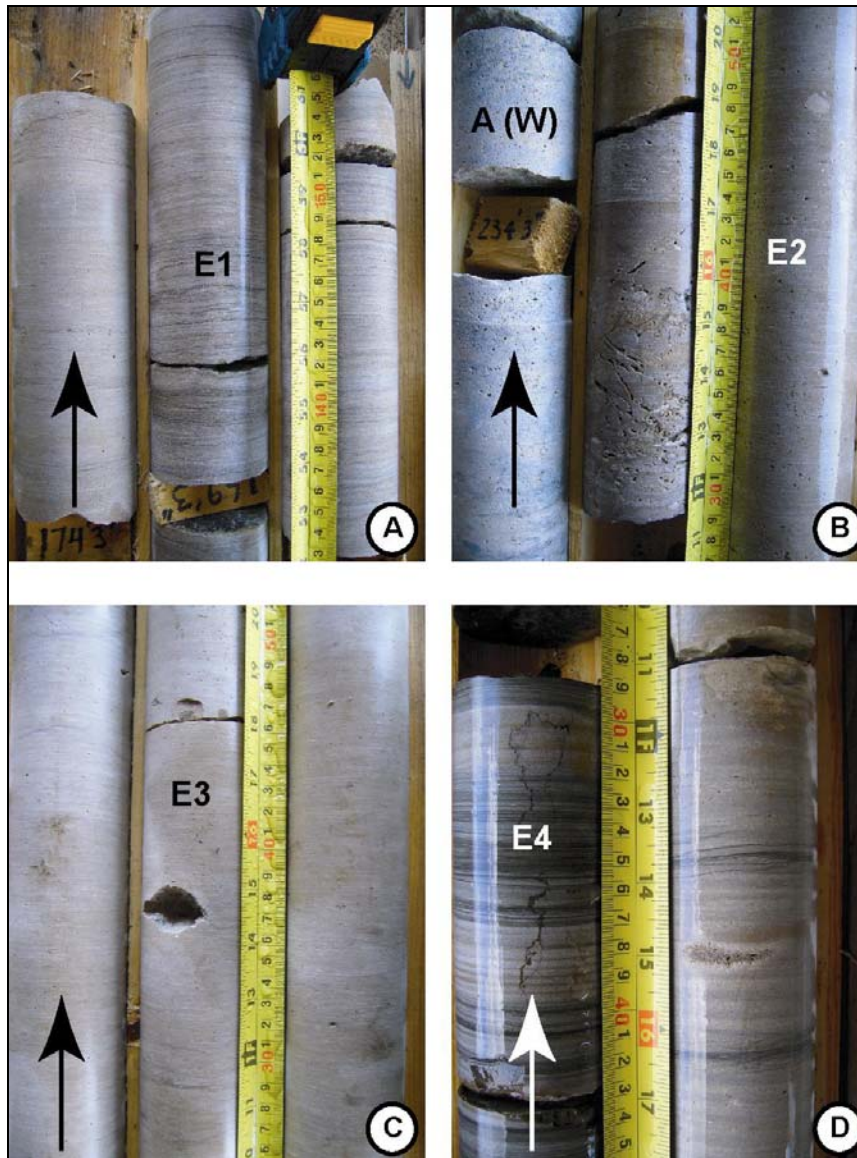


Figure 3.2: Representative core photographs of the Eramosa lithofacies. Large arrows in lower left-hand corners of photographs represent the base of each core, where the top is the upper right-hand corner. Photographs A - C are from borehole OGS-90-2, and photograph D is from borehole OGS-89-2.

- A)** Eramosa 1 lithofacies (E1) is finely crystalline and contains abundant stylolite seams;
- B)** Eramosa 2 lithofacies (E2) is shown here sharply overlying the Warton Member (A (W)) and is dark brown and fossiliferous. The contact is not shown within this photograph;
- C)** Eramosa 3 lithofacies (E3) is light grey-tan, finely crystalline, and contains vuggy porosity;
- D)** Eramosa 4 lithofacies (E4) is dark brown and grey, laminated, very finely crystalline, and bituminous.

Table 2: Summary of observations in the Eramosa Member

Lithofacies	Eramosa 1: Grey-brown abundant ss, dolostone	Eramosa 2: Dark brown fossiliferous, nodular dolostone	Eramosa 3: Light brown vuggy dolostone	Eramosa 4: Bituminous dark brown and grey laminated dolostone
Core Observations	Grey-brown, massive, abundant ss; rare vp; chert and mixed chert and dolomite nodules, upper boundary may contain fossils	Light to dark brown, massive, fcd-mcd, locally fossiliferous: sf, coral, stromatoporoids; mixed chert and dolomite nodules also locally abundant	Light tan to grey- tan, massive, fcd- mcd, thin zones of wispy ss (anastomosing or rare horsetail), locally vug-rich, thick-bedded, rare corals	Very thinly laminated, dark brown/black and grey/blue-grey fcd, no visible fossils or vugs.
Petrographic Observations	Subhedral fcd- mcd, with rare euhedral, ixst ~1-2 %, 3% bp; fp: replaced with mcd, rarely with quartz; pyrite, microquartz fills some vp	Subhedral fcd- mcd, with rare euhedral crystals, ixst ~1-5%, up to 5% bp and vp, fp: few - replaced with microquartz, mcd; minor quartz and calcite (in vp)	Subhedral, vfcd- mcd, ~1% ixst, ~2% bp, fp: few- bp, lath-shaped pores; <1% diagenetic quartz, pyrite, calcite	No thin sections from core, thin section from OSLW: vfcd-mcd, <1% ixst, 1% vp, fp: replaced with mcd; pyrite, calcite, minor quartz
Distribution and thickness	Ranges from 4-17 m in thickness. Occurs in 5 of the 8 boreholes.	Ranges from 4-15 m in thickness. Occurs in 6 of the 8 boreholes.	Ranges from 5-15 m in thickness. Occurs in 3 of 8 boreholes, and repeats itself in 90- 2.	Ranges from 30 cm-2 m in thickness; spatially associated with Eramosa 2 facies. Occurs in 2 of 8 boreholes.
Depositional Environment	Inter-reef	Proximal to a bioherm or mound	Inter-biohermal, low energy	Low energy, lagoon, anoxic?

vfcd = very finely crystalline dolostone, fcd = finely crystalline dolostone; mcd = medium crystalline dolostone; ccd = coarsely crystalline dolostone; ixst = intercrystalline porosity; bp= biomoldic porosity; vp=vuggy porosity, ss= styloseams; p = porosity; sf = shelly fragments; fp= fossil preservation

The E2 lithofacies is found in six of the eight boreholes on the Bruce Peninsula, making it the most common Eramosa lithofacies. The E2 lithofacies occurs at the top of the Eramosa Member directly underlying the Guelph Formation within the stratigraphic

sequence at the north end of the Peninsula and it directly overlies the Wiarion Member of the Amabel Formation at the south end of the Peninsula (Fig. 3.4).

3.2.3 Eramosa 3 Lithofacies

This lithofacies is composed of light tan to grey-tan, massive, finely crystalline dolostone, with intervals of medium crystalline dolostone. Biomoldic and vuggy porosity is commonly <2 % in core; however, vuggy porosity locally reaches up to 25 %. Calcite crystals up to 300 μm are found lining some vuggy pores, and calcite cement may partially or completely fill lath-shaped “swallow-tail” (Lowenstein, 1983) (precursor gypsum?) pores. Minor corals and shelly fragments (crinoids, brachiopods) are rare within this facies (Fig. 3.2C). Wispy stylolite seams occur randomly throughout this lithofacies and may form anastomosing or more rarely horsetail arrangements. The E3 lithofacies is less common than the E1 and E2 lithofacies and has only been observed within the boreholes on the southern half of the Peninsula, where it is repeated within the most southerly borehole (Fig. 3.4).

3.2.4 Eramosa 4 Lithofacies

The bituminous, thinly-laminated (~ 1 mm to 1 cm thick), dark brown to black very fine to finely crystalline dolostones of the E4 lithofacies are readily recognized in core from the Bruce Peninsula (Fig. 3.2D). This lithofacies is only present in two of the boreholes on the Bruce Peninsula, where it ranges from 1–3 m in thickness. The E4 is thickest in the Wiarion area (up to 3.5 m) and has been recognized as far south as the Niagara Peninsula (Bolton, 1957).

The E4 is known as the ‘Marble Beds’ in quarries around the Warton area where this lithofacies can be up to 3.85 m thick (Armstrong and Meadows, 1988). Minor mollusc fossil fragments were observed in carbonate laminae within the E4 lithofacies in core. The E4 lithofacies has a low (1 %) porosity (minor vuggy or biomoldic) observed in core. Wispy and low-amplitude peaked stylolite seams are common and contribute significantly to the laminated character of this lithofacies.

3.3 Lithofacies of the Guelph Formation

The youngest Silurian carbonates logged on the Bruce Peninsula are dolostones of the Guelph Formation. Williams (1919) mapped the Guelph Formation from Niagara Falls as far north as Fitzwilliam Island, just north of the Bruce Peninsula. The Guelph Formation comprises thick buff brown-tan dolostone beds proximal to biostromes and bioherms, and extensive lagoonal mudflats, which appear to conformably overlie bituminous, argillaceous, less fossiliferous dolostones of the Eramosa Member. The formation possesses a distinctive coarse sucrosic dolomite texture that is visible in weathered outcrop sections. The Guelph Formation is exposed along the western and northern portions of the Bruce Peninsula, and is up to 75 m thick at Tobermory. Key distinguishing faunal elements include the abundance of high- and low-spiral gastropods and spatially associated megalodontid bivalves, and trimerellid brachiopods.

In the eight boreholes logged for this thesis, three distinct lithofacies were observed in core and are informally referred to as: (1) Guelph 1 (G1), (2) Guelph 2 (G2), and (3) Guelph 3 (G3) lithofacies. The characteristic features of each lithofacies are illustrated in Figure 3.3.

Biohermal and non-biohermal facies divisions were recognized by Armstrong (1988) in the Guelph Formation. Within this study no bioherms were confirmed, though two lithofacies contain abundant fossils and are differentiated by a change in colour. These lithofacies have been interpreted to be located proximal to a bioherm. Although colour is the main differentiating characteristic between these two lithofacies, the author believes it is important to recognize and distinguish the units. Due to pervasive dolomitization and the effects of weathering on the outcrop, the subtle differences among the G1, G2, and G3 lithofacies are likely difficult to observe in outcrop. The thickness and distribution of these lithofacies is illustrated in Figure 3.4 where it is evident that the Guelph Formation is thickest in the most northerly borehole and there is no consistent stratigraphic order of the individual lithofacies. A summary of the general descriptions of each lithofacies is provided in Table 3.

3.3.1 Guelph 1 Lithofacies

The G1 lithofacies occurs within four of the eight boreholes and is generally found directly overlying the Eramosa Member (Fig. 3.4). This lithofacies ranges in thickness from ~ 1–24 m in core, and is composed of light tan, massive, fine to medium crystalline dolostone (Fig. 3.3A). The G1 lithofacies is locally vuggy in core, where biomoldic and vuggy porosity averages ~5–10 %, with rare zones up to 30 %. The G1 lithofacies contains wispy stylolite seams that occur in small groups spaced ~10–20 cm apart. In some of the boreholes there are no stylolite seam patterns, and stylolites occur with random spacing. Pyrite is of minor importance, with crystals ranging from 5–25 μm in size, typically occurring along stylolite seams. Calcite crystals up to 140 μm line vuggy pores and fractures. Minor bioturbation was

observed within this lithofacies. A wide variety of shelly fragments (gastropods, brachiopods, crinoids) are found within this lithofacies, as well as corals and stromatoporoids.

3.3.2 Guelph 2 Lithofacies

The G2 lithofacies is the most common lithofacies encountered, and ranges in thickness in core from ~ 6–19 m. This lithofacies is the most representative of the Guelph Formation. The G2 lithofacies is characterized by its abundant fossil content and size. The G2 lithofacies is distinguished by its tan-brown colour and presence of megalodontid bivalves up to 5 cm in diameter, corals ~1.5 cm in size, stromatoporoids up to 4 cm in length, and shelly fragments (crinoid ossicles ~1cm, brachiopods up to 5 cm, and gastropods ~1.5 cm). It is composed of tan to light brown, massive, medium crystalline dolostone (Fig. 3.3B). Within the northernmost boreholes, there are also rare occurrences of thinly-laminated argillaceous dolostone beds (< 0.5 m thick) which range in colour from blue-grey to dark brown and black. Biomoldic and vuggy porosity ranges from 10–30 % in core. Wispy stylolite seams are relatively common in the northern boreholes, whereas peaked stylolite seams dominate in the southern boreholes. Calcite crystals up to 4 mm line and/or fill vuggy and biomoldic pores.

3.3.3 Guelph 3 Lithofacies

The G3 lithofacies is a medium crystalline fossiliferous dolostone and is similar in most respects to the G2 lithofacies except for the darker brown colour of the G3 lithofacies (Fig. 3.3C). The G3 lithofacies ranges in thickness within core from ~ 7–10 m. The vuggy and biomoldic porosity in this lithofacies is generally ~15–20 % in core. Similar to the G2

lithofacies, this lithofacies contains thinly-laminated beds that are only 3–20 cm thick. The G3 lithofacies rarely contains randomly spaced, peaked stylolite seams. Calcite crystals up to 4 mm fill and line vugs as well as biomoldic pores. Bioturbation is evident in the form of minor marble-coloured mottling. Brachiopods and corals range from 5 mm–3 cm within the G3 lithofacies, with fragments of bivalves and crinoids that are generally <1 cm. The abundance of these fauna suggests that this lithofacies was deposited proximal to a bioherm, and minor laminated beds possibly represent flanking sediments or perhaps a slight deepening of the waters.

The G3 lithofacies only occurs in the most northerly boreholes, and is found at different stratigraphic levels.

Table 3: Summary of observations in the Guelph Formation

Lithofacies	Guelph 1: Light tan fossiliferous (non-biohermal) dolostone	Guelph 2: Tan biohermal dolostone	Guelph 3: Dark brown biohermal dolostone
Core Observations	Light tan, fcd–mcd, massive, minor peaked and wispy ss; locally vuggy, local sf of coral, brachiopod, gastropod, and crinoids	Tan, mcd, massive, rare ss; <i>abundant</i> coral, brachiopod, bivalve, gastropod, sf; thinly laminated beds < 0.40 m thick	Dark brown, mcd, massive, rare ss; coral, brachiopod, bivalve, gastropod, sf; thinly laminated beds ~ 0.30m thick
Petrographic Observations	Subhedral mcd with fcd and rare euhedral ccd; ~1–2% ixst, ~5–25% bp and vp fracture porosity; ss; fp: poor- replaced with mcd–ccd; crinoids, sf; former evaporites, pyrite, quartz fills vp and bp, minor calcite	Subhedral mcd–Euhedral ccd with rare subhedral fcd; ~1% ixst, ~2–10% bp and vp; few peaked and wispy ss; fp: replaced with ccd, mimically-replaced with dolomite; minor pyrite, microquartz fills bp	Subhedral mcd–euhedral ccd; ~1% ixst, ~5% bp vp; few peaked ss, fp: poor, few mimically replaced with dolomite, ccd; 1–15% pyrite, calcite
Distribution and thickness	Ranges from 2–25 m in thickness. Occurs in 4 of the 8 boreholes.	Ranges from 7–20 m in thickness. Occurs in all boreholes containing the Guelph (5 of 8).	Ranges from 9–12 m in thickness. Occurs in 2 northerly boreholes.
Depositional Environment	Inter-biohermal?	Shallow marine water, proximal to a bioherm	Shallow marine water, proximal to a bioherm

vfd = very finely crystalline dolostone, fcd = finely crystalline dolostone; mcd = medium crystalline dolostone; ccd = coarsely crystalline dolostone; ixst = intercrystalline porosity; bp= biomoldic porosity; vp=vuggy porosity, ss= styloseams; p = porosity; sf = shelly fragments; fp= fossil preservation

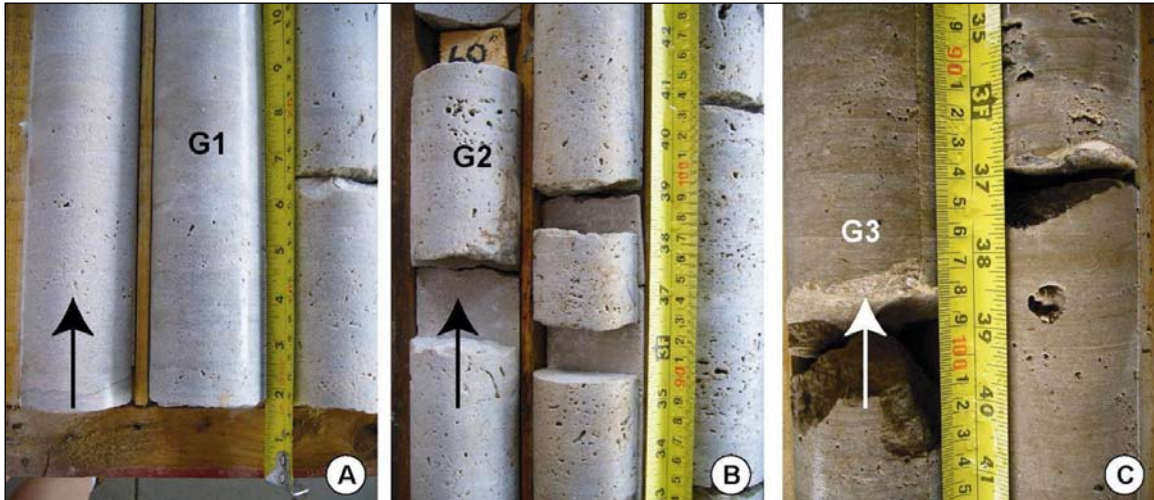


Figure 3.3: Representative core photographs of the Guelph lithofacies. Large arrows in lower left-hand corners represent the bottom of the core with the top in the upper right-hand corner. Photographs A and B are from borehole OGS-90-2, and photograph C is from borehole OGS-89-3.

- A) Guelph 1 lithofacies is light tan-grey fine-medium crystalline with minor fossils;
- B) Guelph 2 lithofacies is light tan medium crystalline fossiliferous dolostone; and
- C) Guelph 3 lithofacies is dark brown, medium-coarse crystalline, sucrosic, and fossiliferous.

3.4 The depositional history of the Amabel and Guelph formations

3.4.1 The Amabel Formation

The lowermost lithofacies of the Amabel Formation is the Lions Head Member, which is composed of thin- to thick-bedded dolostone with few identifiable fossils. The apparently low abundance of recognizable fossils within this facies may be due to pervasive dolomitization. Fossils that are recognizable include crinoid and coral fragments. The low abundance of fossils and their random scattering in the upper portions of the Lions Head Member reflects a depositional environment removed from the ideal carbonate factory environment, which could be below wave base (e.g., Gill, 1985) in a slightly down-slope setting. The fine crystal size of the Lions Head Member may also reflect a tidal flat-lagoon or

quieter water conditions. It is likely that the material which makes up the Lions Head Member was deposited within relatively deeper waters than those in the overlying Colpo Bay Member (Johnston et al., 1992; Armstrong et al., 2002). Observations of a potential hardground surface at the base of the Lions Head Member suggests that there was a hiatus in deposition that resulted from a lack of sedimentation where the surface may have been exposed on the seafloor, thus encouraging lithification (e.g., Brett and Brookfield, 1984).

Johnson et al. (1992) described the Lions Head Member as thickening towards the north, and that a lateral facies change of the Lions Head occurred with the Colpo Bay facies to the south. Although there is a repetition of the Lions Head Member in borehole OGS-89-2 on the north end of the Peninsula, the Colpo Bay Member is still present in between the repeated facies (Fig. 3.1). There were no lateral facies changes evident between these two members within the eight boreholes logged.

The overlying Colpo Bay Member contains abundant shell fragments (crinoids, brachiopods), and coral fragments that may occur in concentrated zones. The concentrated zones of fauna suggest possible storm influxes of fossil debris from a shallow high energy shoal environment (Armstrong et al., 2002). In addition, the Amabel sea may have undergone a relatively rapid shallowing (Sanford, 1969) during the deposition of the Colpo Bay Member that initiated conditions ideal for carbonate production. This lowered sea level would increase the penetration depth of the sunlight within the water column, warming the temperature of the water in a subtidal environment suitable for bioherm development in close proximity. The Colpo Bay Member has been interpreted as a transitional facies between the Lions Head and Wiarion members (Sanford, 1969).

The present study shows that the Colpoy Bay Member was deposited between the lower Lions Head Member and either the overlying biohermal Wiarthon Member, the fossiliferous E2 lithofacies, or the E1 lithofacies along the Bruce Peninsula. A gradual shift from quiet water deposits to slightly more fossiliferous facies suggests that the marine environment gradually changed to more ideal carbonate producing conditions.

Figure 3.4 (next page): Stratigraphic correlation of eight boreholes on the Bruce Peninsula. Boreholes are oriented from north (left) to south (right). Elevation axes are on either end of the diagram and units are shown in metres above sea level (m.a.s.l). Thick solid lines represent correlation between formations or members; thin solid lines correlate members; dashed lines represent hypothesized correlations; and jagged zigzag lines suggest a facies change occurred between boreholes. Legend is shown in Figure 3.5 on page 44.

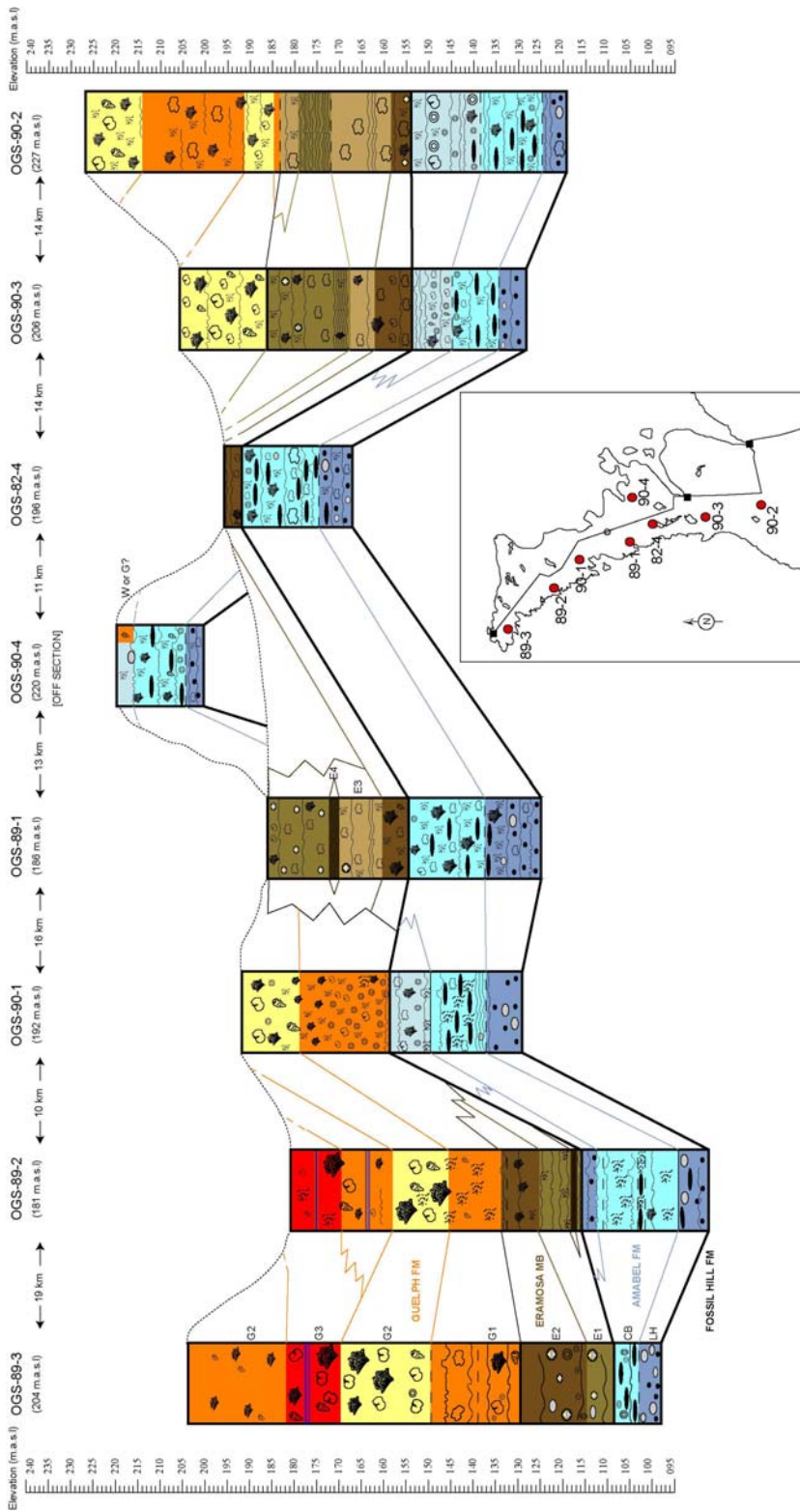


Figure 3.4: Figure caption is on previous page. Legend is on next page.

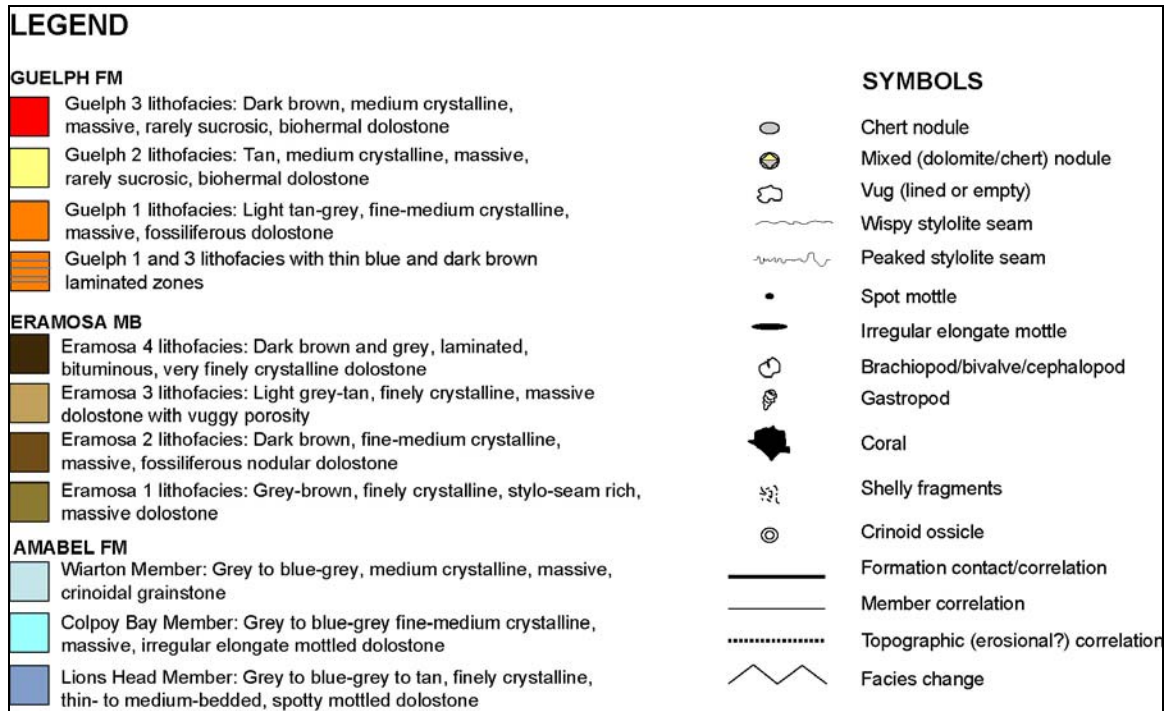


Figure 3.5: Legend to accompany Figure 3.4, the stratigraphic correlation between boreholes. Each lithofacies is represented by a colour scheme. The lowermost Amabel Formation is coded in shades of blue, the Eramosa Member is in shades of brown, and the Guelph Formation is shown in red, orange, and yellow. Symbols and definition of various correlation lines used in the stratigraphic logs are shown on the right.

The uppermost Wiarion Member likely represents local shoal growth along shallower portions of the basin margin, which is indicated by the increase in crinoids. An increase in corals in the boreholes south of Wiarion may indicate their proximity to a bioherm. There was no fault or displacement evidence within these boreholes. The lateral extent of each lithofacies and the possible proximal distance to a bioherm is unavailable from information provided by each of the boreholes which are separated by ~ 13 km.

3.4.2 The Eramosa Member

Gradational contacts among the E1–E3 lithofacies on the Bruce Peninsula indicate that the depositional environment at this time was undergoing minor fluctuations. The E1 and E2 lithofacies contain fragments of crinoids and brachiopods that rarely occur in isolated intervals, suggestive of a slope or flanking environment which may receive detrital fragments possibly from a nearby shoal or bioherm. Tetreault (2001) proposed that storms periodically destroyed bottom communities, which would produce similar intervals of fossil fragments. The E3 lithofacies commonly occurs between the E1 and E2 lithofacies in the southernmost boreholes. The E3 lithofacies is massive, and contains only minor fossil content. Groups of stylolites ~ 1 cm apart may also separate fossil-rich intervals within the E1 and E3 lithofacies. The E3 lithofacies contains little to no fossils and appears as a transitional facies between the E1 and E2 lithofacies in the southerly boreholes. The E3 lithofacies may represent an inter-biohermal unit or an increased salinity or anoxic zone.

Within the core on the Bruce Peninsula the laminated E4 lithofacies is localized and may indicate a rare restricted back-barrier-reef lagoon environment that existed in and around bioherms on the Bruce Peninsula along the borehole cross-section in this study area (e.g., Shaw, 1937; Bolton, 1957; Sanford, 1969). The lack of fossils within the E4 lithofacies suggests water salinity was high (Tetreault, 2001), making the lagoons a hostile environment for all metazoan life. Alternatively, the E4 lithofacies may represent relatively deeper anoxic waters.

The local absence of the entire Eramosa Member at borehole OGS-90-1 may be due to deposition on an irregular paleotopography. Bolton (1957) suggested that the Eramosa

Member is a transitional facies between the Warton Member and the Guelph Formation, and that it has been found overlying and laterally grading into Warton bioherms. This study has shown that the Eramosa Member contains a variety of facies changes that indicate that there was more than one depositional environment transition between the underlying Warton Member and overlying Guelph Formation. The Eramosa lithofacies indicate a variety of salinities, oxygenation levels, and water depths during the time of deposition. This study assigns the Eramosa Member as a basal lithofacies of the Guelph Formation, and there are no lateral facies changes between the Warton Member and the overlying Eramosa Member (Fig. 3.4). This study has shown that the Eramosa Member contains similar fauna as the undifferentiated Guelph Formation, and likely represents the base of a regressive sequence to the overlying Guelph Formation.

3.4.3 The Guelph Formation

The three lithofacies of the Guelph Formation were interpreted to result from an overall increase in water depth that provided increased water circulation and changed ecologic patterns (Tetreault, 2001). However, coarser crystal sizes and bryozoan, brachiopod, and bivalve faunas more likely indicate an overall shallowing upwards sequence. The fossiliferous deposits of the G2 and G3 lithofacies are commonly separated by the non-biohermal dolostones of the G1 lithofacies. The pause in fossil abundance, as indicated by the presence of the G1 lithofacies, supports a change in sea level or salinity that initiated an unfavourable environment for the organisms of the surrounding Guelph Formation sediments. There were no observations made of reefs or bioherms in the core and lath-shaped

(“sparrow-tail”) pores were observed within the G1 lithofacies indicating the presence of precursor evaporites. Gypsum or anhydrite may have been present based on southwestern Ontario studies by Zheng (1999) and Coniglio et al. (2003).

The G2 lithofacies contains large brachiopods up to 5 cm in diameter, gastropods and corals. The fauna within the G2 and G3 lithofacies showed good zonation (Armstrong et al., 2002), and were abundant and whole, which may be indicative of their close proximity to a biohermal complex. Where intervals of shelly fragments occur, storms may have contributed pulses of debris to the bioherm facies.

The G3 lithofacies was deposited within a similar environment as the G2 lithofacies that may have contained larger quantities of organics as indicated by the darker brown colour, and may be proximal to a bioherm (Armstrong et al., 2002). Based on the pattern of eroded Paleozoic strata (Fig. 1.1), the thickness of the Guelph Formation and the observed presence of the G3 lithofacies at the northern tip of the Peninsula (Fig. 3.4) may be related to the reduced amount of erosion that occurred at these locations compared to the locations of the southern boreholes.

3.5 Conclusions

From stratigraphic logging of eight boreholes and two quarries on the Bruce Peninsula a lithostratigraphic framework was constructed for the Amabel and Guelph (including the Eramosa Member) formations. The Amabel Formation is composed of three lithofacies (also recognized as formal members), the Eramosa Member of the Guelph Formation has been

subdivided into four lithofacies, and the upper Guelph Formation is made up of three lithofacies.

The lowermost member of the Amabel Formation, the Lions Head, is easily recognizable in core as the blue-grey to tan grainstone that contains dark grey spotty mottles and chert nodules, and in outcrop as the thin- to thick-bedded blocky weathering blue-grey grainstone. The overlying grey to blue-grey Colpoy Bay Member of the Amabel Formation is consistent across the Bruce Peninsula and contains irregular elongate blue-grey mottles and an increase in shelly fragments and corals compared with the underlying Lions Head Member. The Lions Head and Colpoy Bay members of the Amabel Formation are consistently present across the Bruce Peninsula, although their thickness varies. The uppermost Wiarthon Member of the Amabel Formation is not laterally continuous across the Peninsula, and is only present within four of the eight boreholes logged in this study. This member is a crinoidal grainstone that also contains minor corals and brachiopods.

The Eramosa Member is prominent in both core and outcrop as a light- to dark brown vuggy, fossiliferous, argillaceous laminated dolostone. In this study, the Eramosa Member has been subdivided into four lithofacies that each contains distinct lithologic and diagenetic features. The E2 lithofacies is present in six of the eight boreholes and is dark brown and fossiliferous. The brown sparsely fossiliferous E1 lithofacies, the massive light tan vuggy E3 lithofacies, and the rare argillaceous dark brown and black laminated E4 lithofacies are much less consistent in their presence in core on the Bruce Peninsula.

The Guelph Formation makes up the uppermost Silurian strata on the Bruce Peninsula within the core from this study. In outcrop, the Guelph Formation may be hard to distinguish

from the Amabel Formation based on their similar weathering characteristics. Within core, the characteristic fauna of the Guelph Formation allow differentiation from the underlying Amabel Formation. The light grey-tan fossiliferous G1 lithofacies, the tan medium crystalline to sucrosic fossiliferous G2 lithofacies, and the dark brown medium crystalline fossiliferous lithofacies are laterally inconsistently deposited across the Bruce Peninsula. The G2 lithofacies is the most commonly occurring lithofacies of the Guelph Formation.

Overall the Amabel Formation represents a transition from quieter waters, as represented by the Lions Head Member to shallower water in the Colpoy Bay Member which led to the crinoidal shoal lithofacies of the Wiarton Member where bioherms may have developed in close proximity as suggested by the increasing occurrence of corals and stromatoporoids. The Eramosa Member does not represent a transitional facies between the underlying Wiarton Member of the Amabel Formation and the overlying Guelph Formation as previously claimed by Bolton (1957). This member is composed of sparsely fossiliferous and laminated lithofacies, as well as fossiliferous lithofacies. The fine crystal size of the Eramosa Member suggests possible deposition in quiet slightly deeper waters. The dolostones of the Guelph Formation likely represent an overall decrease in water depth from the environment in which the Eramosa Member was deposited, which was only habitable by few select fauna.

Chapter 4: Petrography and diagenesis of the Amabel and Guelph formations

4.1 Introduction

Interest in the Silurian Amabel and Guelph formation carbonates began in southwestern Ontario over a century ago due to their production of hydrocarbons (Sanford, 1969; Armstrong et al., 2002). Silurian reefs have produced nearly 900 oil and/or gas pools in southwestern Ontario, southeastern Michigan, and northern Michigan (Armstrong et al., 2002). The Guelph Formation has been stratigraphically and petrographically analyzed in the subsurface of southwestern Ontario (Charbonneau, 1990; Smith, 1990; Coniglio et al., 2003), but there have not been comparable subsurface and field-based studies on the Bruce Peninsula. There are only a few published petrographic studies on the Amabel (Lockport) Formation that focus on pinnacle and patch reefs in southwestern Ontario (Charbonneau, 1990; Smith, 1990), and there are no documented petrographic studies on the Bruce Peninsula. The Amabel Formation has not been as thoroughly studied in Ontario as the overlying Eramosa Member and the undifferentiated Guelph Formation. Due to its resource potential (Armstrong and Meadows, 1988; Armstrong et al., 2002) and stratigraphic variability, the Eramosa Member and its relationship with the overlying Guelph Formation has been the primary focus of more recent research (Brunton and Dekeyser, 2004; Brunton et al., 2005). This study focuses on the northeastern margin of the Michigan Basin along the Bruce Peninsula, where the Amabel and Guelph formations have been pervasively dolomitized.

This is the first diagenetic study of Silurian carbonates on the Bruce Peninsula that combines data from borehole observations, transmitted light, cathodoluminescence, and scanning-electron microscopy. The dolomite distribution and diagenetic history, including nodules and mottled fabrics, of both the Amabel and Guelph formation dolostones are interpreted from eight boreholes.

4.2 Diagenesis of the Amabel and Guelph formations

Grainstones and wackestones associated with a variety of fauna which have undergone intense bioturbation make up the Amabel Formation, and possible boundstones and brachiopod-, gastropod- and bivalve-rich units make up the Guelph Formation. These formations were altered to a texturally heterogeneous limestone during early burial diagenesis (Charbonneau, 1990; Zheng, 1999; Coniglio et al., 2003).

4.2.1 Pre-dolomitization diagenesis

The Amabel and Guelph formations record a complex diagenetic history (Fig. 4.2) where pre-dolomitization events have been largely obscured by pervasive dolomitization. Evidence of pre-dolomitization alteration within the lowermost Amabel Formation includes a possible hardground surface at its basal contact with the Fossil Hill Formation. There is no evidence of pre-dolomitization alteration within the Guelph Formation (including the Eramosa Member).

Coniglio et al. (2003) studied dolomitized reefs and platformal carbonates of the Guelph Formation in southwestern Ontario where evidence of pre-dolomitization calcite

cements were found. In southwestern Ontario, both the underlying Lockport (i.e., Amabel) and Guelph formations are composed of a mixture of dolostone and limestone. These formations were also studied by Charbonneau (1990) and Smith (1990) who observed blocky and fibrous calcite cements within six and three Lockport (i.e., Amabel) Formation dolostone and limestone pinnacles respectively. Dolostones of the Bruce Peninsula in the current study area show rare preservation of fibrous cement that has been dolomitized, and no evidence of pendant or meniscus cements. Overall, Silurian carbonates on the Bruce Peninsula are pervasively dolomitized; therefore, a lack of evidence of pre-dolomitization fabrics exists.

4.2.1.1 Hardground

Within the majority of the eight boreholes logged, a dark, pyrite-rich planar to hummocky surface occurs in the lowermost ~1 m of the Lions Head Member of the Amabel Formation, just above the contact with the underlying Fossil Hill Formation. This surface likely represents a pause in sedimentation where the marine seafloor was exposed and hardened. The nature of the contact between the underlying Fossil Hill Formation and the Lions Head Member is represented by a sharp break in sedimentation at several locations (Bolton, 1953, 1957) suggesting that the contact represents a disconformity (Liberty and Bolton, 1971). The hardground surface is composed of cloudy, finely crystalline dolomite and commonly contains 5-25 μm sized pyrite crystals along the surface (Fig. 4.1D).

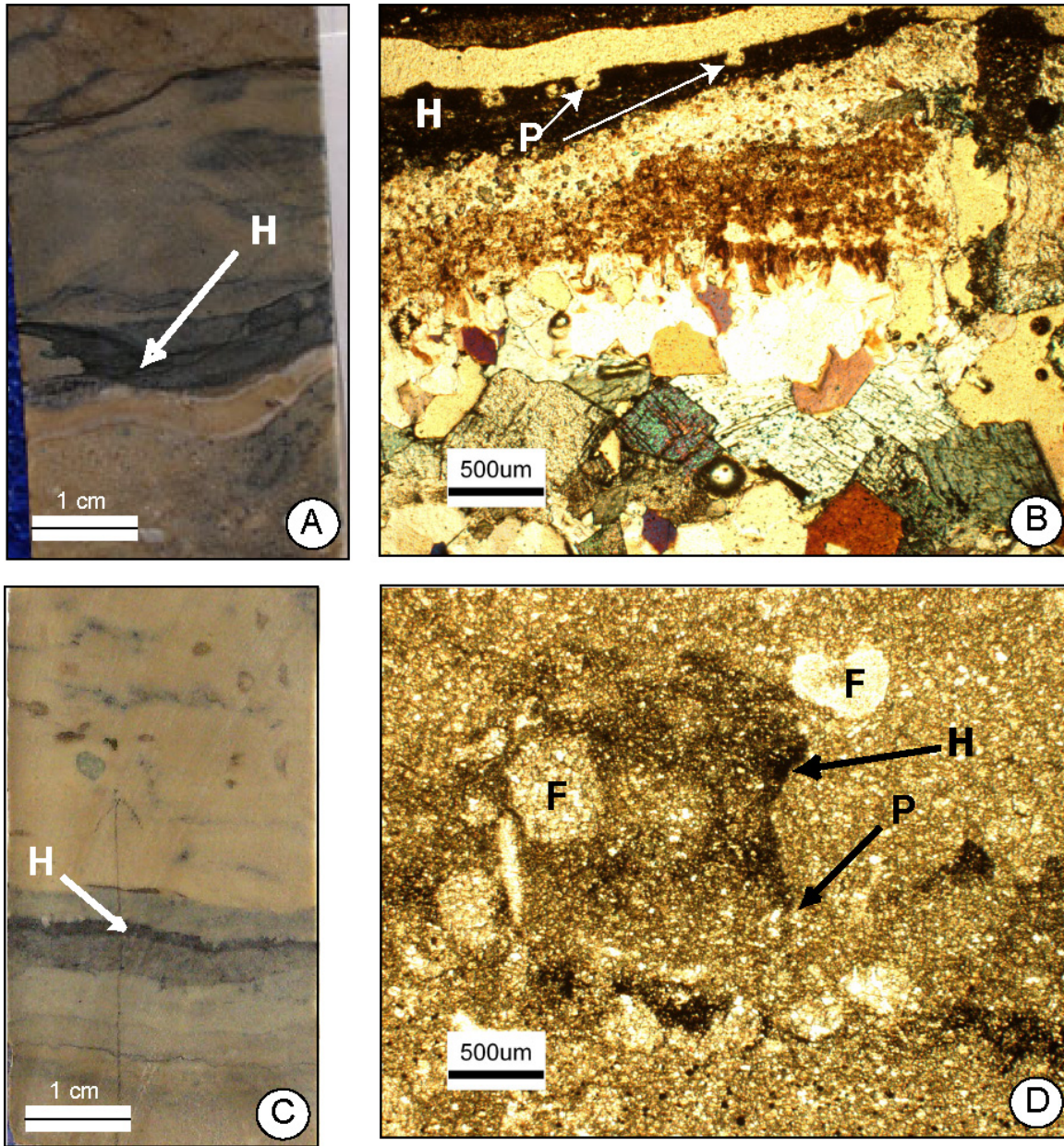


Figure 4.1: A, C) Two core samples of hardground (H) examples (A is from borehole 89-2, and C is taken from borehole 89-3) developed in the lower Lions Head Member;

B and D) Cross-polarized photomicrographs of cores in A and C illustrate a hardground (H) depicted by dark, pyrite-rich surfaces that are pitted (P) or bored by organisms.

D) Preservation of fossils (F) with cloudy finely crystalline dolomite and mimically-replacing dolomite (upper right fossil - F) along the hardground surface (H) is similar to the surrounding dolomite.

The hardground surface may appear pitted, possibly the result of boring by organisms (Fig. 4.1B, D). Poorly preserved fossils replaced with clearer medium crystalline dolomite or possible echinoderms replaced with mimically-replacing dolomite crystals appear concentrated along the hardground surface (Fig. 4.1D).

Although there are chert nodules and silicified fossils within the uppermost Fossil Hill Formation near the contact with the Amabel Formation, chert nodules and lenses within the Lions Head Member only begin to appear within the metre above this potential hardground surface.

4.2.2 Post-dolomitization diagenesis

The post-dolomitization diagenetic events which occurred within the Amabel and Guelph formations include dolostone dissolution, evaporite cementation and dissolution, secondary mineralization (silica, calcite, pyrite, fluorite, sphalerite, and glauconite), fracturing, chemical compaction and the formation of stylolite seams, dedolomitization, and accumulation of hydrocarbons. The relative timing of the diagenetic events is illustrated in Figure 4.2.

4.2.2.1 Porosity

Porosity was estimated from petrographic thin sections based on Flugel's (1982) porosity comparison charts. The major porosity types that occur within the Amabel and Guelph formations in order of abundance are biomoldic and vuggy, intercrystalline, fracture, and intraskeletal porosity (Fig. 4.3).

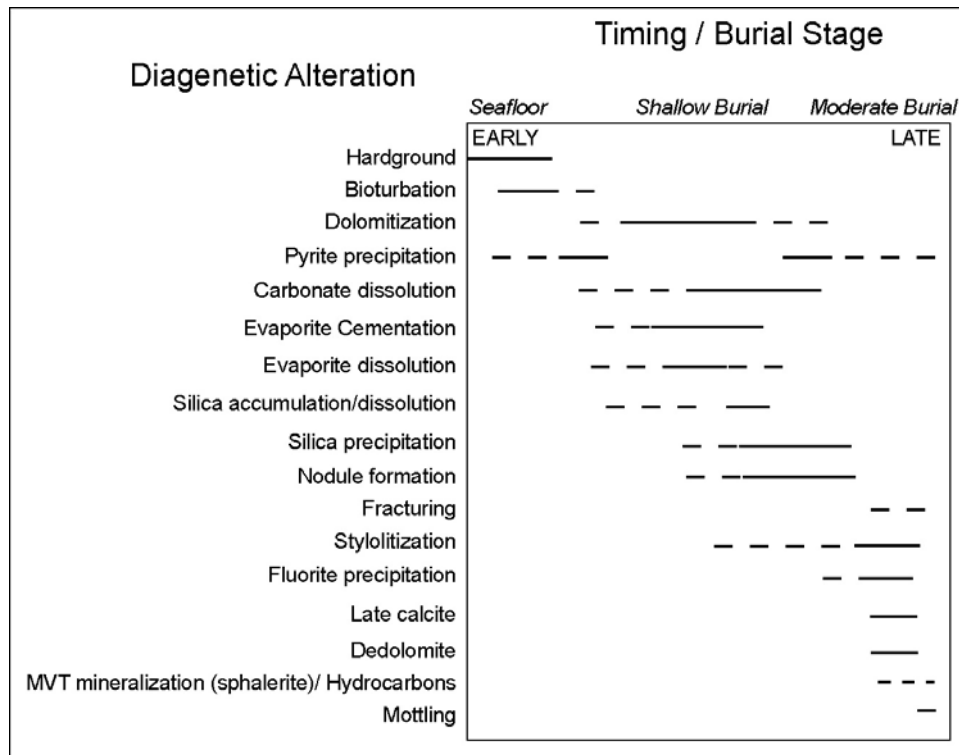


Figure 4.2: Paragenetic sequence constructed for the Amabel and Guelph formations in the study area. Dashed lines are inferred.

Biomoldic and vuggy porosity percentages are grouped together where there is uncertainty as to whether the porosity is biomoldic or vuggy. The term vuggy porosity is used where there is nothing to suggest a biologic origin, even though it is recognized that many such vugs may have originated as solution-enhanced biomolds. Biomoldic porosity is only defined where it is clear that the pores were derived from the dissolution of fossils.

In general, irregularly-shaped vuggy pores that are the same size as associated fossils when they occur (millimetre to centimetre-sized) are likely the result of solution-enhanced biomolds. Vugs that have irregular to rounded shapes and that are in excess of 2 cm in size are likely a result of enhanced dissolution of smaller vuggy or biomoldic pores.

Alternatively, these larger vugs may have formed along fracture planes where larger

volumes of fluids would have been available to dissolve the surrounding rock. Biomoldic and vuggy porosity are commonly higher in the Guelph Formation than in the Amabel Formation. Within the Amabel Formation, biomoldic and vuggy porosity makes up ~ 5-10% of the rock. Vugs occur within the Eramosa Member (2-5%) and are most common within the Guelph Formation (2-25%). Blade or lath-shaped pores, which are evidence of former evaporites, are common within both the Eramosa Member and the Guelph Formation.

Intercrystalline porosities range from ~ 1–2 % within the Amabel Formation, and ~ 1–5 % in both the Eramosa Member and the Guelph Formation. Intercrystalline porosity resulted from the recrystallization of the precursor limestone.

Fracture porosity is difficult to quantify within the Amabel and Guelph formations. Although the carbonates are fractured in various orientations across the core, fractures are generally lined or completely filled with calcite cement which decreases the porosity. Remaining porosity after calcite cementation within fractures is less common in the Amabel Formation (~1 %) than the Eramosa Member (2–3 %) and Guelph Formation (~ 3 %) on the Bruce Peninsula.

Bioclasts are poorly preserved and their internal structure is commonly obscured by dolomitization or replaced by microquartz rather than left as biomoldic pores. Corals and stromatoporoids in correlative units in southwestern Ontario contain up to 5 % intraskeletal porosity (Zheng, 1999). Intraskeletal porosity within dolostones on the Bruce Peninsula makes up less than 1 % of the total porosity.

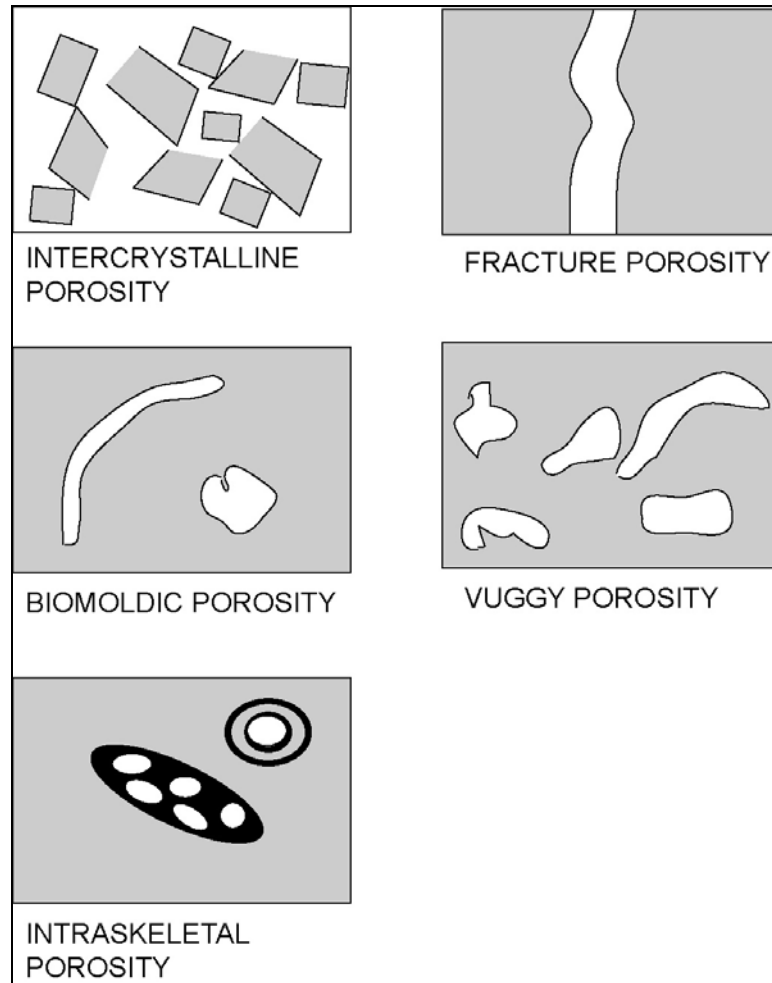


Figure 4.3: Schematic illustration depicting the major porosity types within the Amabel and Guelph formations. Dolostone is grey, dolomitized or silicified bioclasts are shown in black with pore space represented by the white areas (modified after Zheng, 1999).

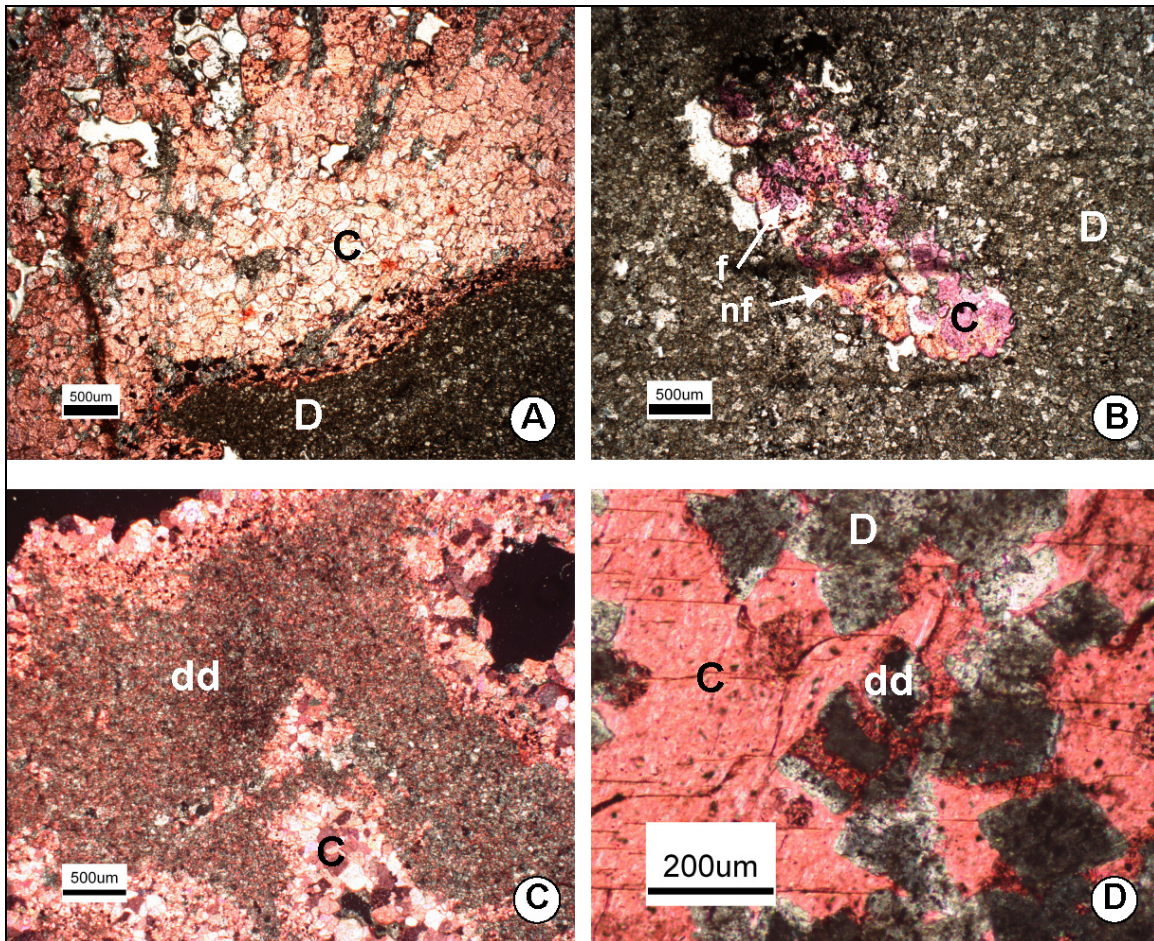


Figure 4.4: Photomicrographs of pore-lining and pore-filling calcite (A, B), and dedolomite (C, D).

A) Plane polarized light photomicrograph of blocky subhedral calcite crystals (C) that partially fill a vug within finely crystalline dolomite (D) from the Eramosa Member in borehole 90-2;

B) Plane polarized light photomicrograph of pore-filling calcite (C) exhibits minor ferroan (f) and nonferroan (nf) zoning from the Colpoy Bay Member in borehole 90-2;

C) Cross-polarized light photomicrograph of dedolomite (dd) surrounded by blocky equant calcite cement (C) from the Guelph Formation in borehole 89-3;

D) Plane-polarized light photomicrograph of a replaced dolomite rhomb (dd) shows optical discontinuity with the surrounding calcite (C) from the Guelph Formation in borehole 89-3.

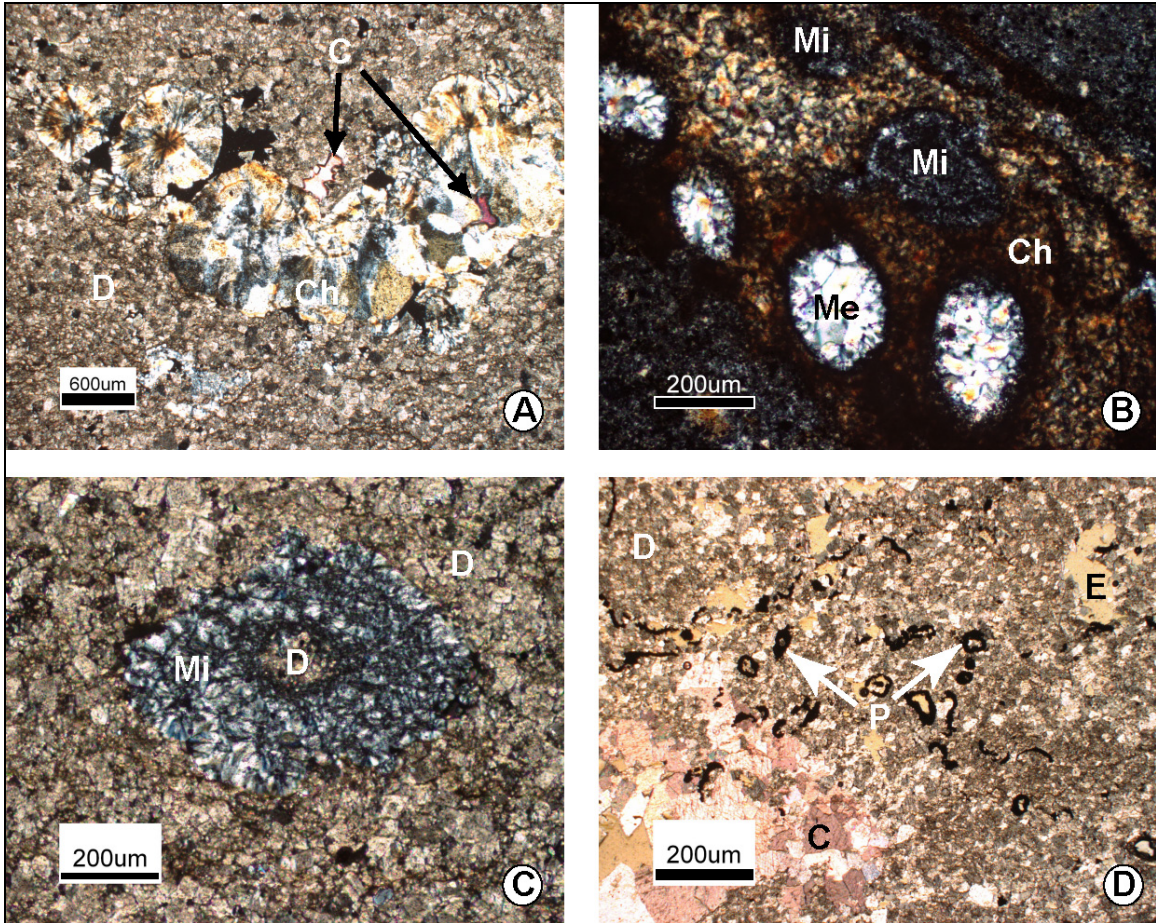


Figure 4.5: Cross-polarized light photomicrographs of replacement silica (A-C) and pyrite (D).

A) Pore-filling chalcidonic spherules (Ch) and calcite (C) cement within surrounding dolomite (D) from the Lions Head Member in thin section FRB-9-045 from borehole 89-1;

B) Replacement of a bioclast (likely a bryozoan fragment) with microquartz (Mi), megaquartz (Me), and chalcidonic fibres (Ch) within the surrounding dolomite (D) of the Eramosa Member in thin section 128 from borehole 82-4;

C) Replacement of a crinoid ossicle with microquartz (Mi). Dolomite (D) fills the intraskeletal pore in the centre and is surrounding the fragment from the Lions Head Member in thin section 016 from borehole 90-2;

D) Plane polarized light photomicrograph illustrates pyrite (P) crystals that form rings that likely replaced portions of unidentified bioclasts. The center of these features may be filled with slightly clearer dolomite or they contain orange-coloured epoxy (E). These pyrite rings were only observed in the Eramosa Member in thin section FRB-93-564A from borehole 90-3 amongst pore-filling blocky calcite cement (C) and dolomite (D). Orange-coloured epoxy (E) also fills intercrystalline pores.

4.2.2.2 Pore-filling minerals

Most biomoldic and vuggy pores within the Amabel Formation are filled with several types of silica (microquartz and megaquartz), blocky calcite cement and dolomite (replacement euhedral to subhedral crystals). Pores within the Eramosa Member and the undifferentiated Guelph Formation commonly contain dolomite (replacement euhedral to subhedral crystals and rarely radiaxial cement), minor silica or calcite, or they are empty. Slightly ferroan euhedral dolomite rarely lines pores (Fig. 4.7F).

Very rare occurrences of sphalerite (Fig. 4.6A-C), fluorite (Fig. 4.6D-F) and glauconite have also been observed within intercrystalline and vuggy pores. Where intercrystalline porosity is greater (i.e., sucrosic G2 and G3 lithofacies), calcite cement may be present. The dolomite distribution and petrography is described in section 4.2.3. The nature and distribution of silica within the Amabel and Guelph formations are discussed in section 4.3.

Calcite Cement

Within both the Amabel and Guelph formations on the Bruce Peninsula, equant non-ferroan and rare slightly ferroan calcite cement occurs as euhedral to subhedral calcite spar ranging from 25–750 μm in size. This blocky, bright orange zoned luminescent calcite cement lines or completely fills the vuggy, biomoldic, and fracture pores in which it is found (Fig. 4.4). On one occasion, bladed prismatic calcite cement was observed lining a vug in the Eramosa Member. Calcite cement is estimated to comprise ~ 2–3 % of the Amabel Formation,

whereas the Guelph Formation (including the Eramosa Member) contains closer to 1 % calcite.

Dolomite Cement

Sparry dolomite cement rarely occurs within the Amabel Formation and the Eramosa Member as euhedral medium to coarse crystals lining vuggy pores or fractures. Medium crystalline euhedral crystals may exhibit slight ferroan (blue) staining (Fig. 4.7F). Crystals are generally less cloudy (i.e., less inclusion-rich) than surrounding dolomite, and may exhibit minor zoning of cloudy cores and clear rims (Fig. 4.7C). Dolomite cement lining pores and fractures in replacement dolomite are confirmed by cathodoluminescence as overgrowths of the adjacent matrix dolomite. In CL, the dolomite cement has identical dull red luminescence as the surrounding replacement dolomite.

Pyrite and other minor mineral phases

Pyrite is the most common non-carbonate mineral within the Amabel and Guelph formations. Pyrite is generally associated with stylolite seams, centimeter-sized vugs and nodules, and finely crystalline cloudy dolomite. Pyrite also partially replaces fossil fragments (Fig. 4.5D). Pyrite is more common in the Amabel Formation, ranging from 2–10 % in abundance. The Eramosa Member contains ~ 1–5 % pyrite, and the Guelph Formation commonly contains 1–3 % pyrite, with the rare occurrence of large clusters of crystals (crystals range in size from <5–250 μm) near vugs. Crystal shapes range from equant octagons to elongate needle-shaped crystals. Crystals are often combined into irregularly-shaped clusters.

Fluorite was observed with calcite crystals, where calcite crystals were ~ 250 µm in size, lining or partially filling vugs (Fig. 4.6D-F). The fluorite was not obvious using transmitted light microscopy and required SEM to be revealed. This rare mineral was only observed within the Eramosa Member.

One observation of sphalerite, also within the Eramosa Member, replaced finely crystalline dolomite and filled intercrystalline pore space (Fig. 4.6A-C). Crystal size of sphalerite was difficult to discern as the mineral is opaque in transmitted light (Fig. 4.6B). Clusters of sphalerite were >2 mm in diameter. Sphalerite appeared very dark to non-luminescent in CL. There was no evidence of an association with biomoldic or vuggy porosity.

Rare occurrences of glauconite were observed within the Lions Head facies along thick stylolite seams. The glauconite was a deep green colour, pleochroic, and did not show any grain or crystal shape.

4.2.2.3 Evidence of evaporites and evaporite dissolution

Within the E2, E3, G1, and G2 lithofacies, the former presence and complete dissolution of evaporites is confirmed by the presence of lath-shaped pores subsequently filled with calcite cement or left empty (e.g., Fig. 4.6E, F). The shape of the pores suggests that the original evaporite was anhydrite or gypsum. Anhydrite was observed within patch and pinnacle reefs in southwestern Ontario within the Guelph Formation (Zheng, 1999; Coniglio et al., 2003).

4.2.2.4 Stylolites

Stylolites are common within the Amabel and Guelph formations. Stylolites may form low or high-amplitude peaked solution seams, or they may have wispy, horsetail, or anastomosing characteristics. Based on the amplitude of peaked stylolite seams, up to 3 cm of material may be dissolved. Stylolites generally occur parallel to bedding, and are less commonly found at angles between 15–90 degrees to bedding. Stylolites are mostly continuous across the core width, but some wispy horsetail or anastomosing seams are laterally discontinuous.

The distribution of stylolites is variable. The Amabel Formation includes wispy stylolite seams at the base of the Lions Head Member which grade upward into low-amplitude peaked stylolites in the overlying Colpoy Bay Member. The Wiarnton Member grainstone is dominated by high-amplitude peaked stylolites. Wispy stylolite seams are more common than peaked seams within the Eramosa Member, and are more abundant within the E1 lithofacies than in the E2-E4 lithofacies. Low-amplitude peaked stylolites are the most common stylolite type that occurs within each of the Guelph lithofacies.

Clusters or individual pyrite crystals and detrital feldspar (very fine blue grains in CL) are often associated with stylolite seams.

Amber coloured elliptical features are rarely found in the Eramosa Member amongst wispy stylolite seams and may represent collapsed algal cysts. They range from ~ 100–200 μm in width.

4.2.2.5 Dedolomite

Rare dedolomite is observed within the Colpoy Bay Member of the Amabel Formation and within the G1 lithofacies of the Guelph Formation within two boreholes on the Bruce Peninsula. Replacement of dolomite by calcite is indicated by corroded dolomite rhombs which are partially made up of calcite and show optical discontinuity with the surrounding calcite (Fig. 4.4D). Calcite which replaces dolomite generally has a poikilotopic texture, and is made up of fine to coarse (<5-300 μm) euhedral to subhedral crystals. Euhedral medium crystalline dolomite rhombs commonly have corroded edges and appear in two dimensions to float within the calcite. In CL, dolomite rhombs are a dull red colour and are distinct from the associated dull orange luminescent calcite crystals. Late stage calcite and calcite identified as dedolomite are likely cogenetic based on their similar CL and petrographic properties. Although observed dedolomite is rare, this phase of calcite is likely more common based on the abundance of late stage calcite cements.

4.2.2.6 Hydrocarbons

Very dark brown to opaque substances, probably hydrocarbons, also occur with no discernable shape within intercrystalline pore spaces and appear concentrated along stylolite seams. Undifferentiated organics are also associated with mottled fabrics, which are described below in section 4.4 and illustrated in Figure 4.9.

4.2.3 Dolomite distribution and petrography

The Amabel and Guelph (including the Eramosa Member) formations are pervasively dolomitized with none of the original limestone preserved in core or outcrop within the study area. Limestone or partially dolomitized Eramosa Member lithofacies have been observed in Hepworth near Wiarton within the study area (F. Brunton, personal communication, 2006). Dolomite on the Bruce Peninsula can be divided into 4 categories, on the basis of crystal size, based on the crystal size definitions from Folk (1959, Table 4): (1) anhedral cloudy very finely crystalline dolomite (crystals < 15 µm in size), (2) subhedral cloudy finely crystalline dolomite (crystals 15-60 µm in size), (3) subhedral to euhedral clearer medium crystalline dolomite (crystals 60-250 µm in size), and (4) coarse euhedral crystalline to mimically replacing dolomite and replacement cement (variety of crystal sizes > 250 µm). The presence of micrometre to sub-micrometre-sized organics and unidentified solid and liquid inclusions results in the cloudy appearance of individual dolomite crystals. Cloudiness is associated with finely crystalline dolomite, which is the common crystal size within the Amabel Formation and the Eramosa Member, whereas slightly clearer medium to coarse crystalline dolomite makes up the Guelph Formation. Each of the four types of dolomite may appear within the various lithofacies of both the Amabel and Guelph formations.

Table 4: Crystal Size Classification (from Folk, 1959)

Extremely coarsely crystalline	≥ 4 mm
Very coarsely crystalline	1–4 mm
Coarsely crystalline	0.25–1 mm
Medium crystalline	0.062–0.25 mm
Finely crystalline	0.016–0.062 mm
Aphanocrystalline (very finely crystalline)	0.004–0.016 mm

Figure 4.6 (next page): Core photographs (**A** and **D**), transmitted light photomicrographs (**B** and **E**) and SEM photomicrographs (**C** and **F**) of sphalerite and fluorite.

A) Sphalerite (S) appears as light grey patches in core within surrounding tan-grey dolostone (D) from the Eramosa/Guelph transition zone in borehole 82-4. The large arrow on the right is a marker on the core that indicates stratigraphic right way up;

B) Plane polarized light photomicrograph of sphalerite (S), which is dark brown to opaque. Dolomite crystals (D) are present amongst and surrounding the sphalerite;

C) SEM photomicrograph illustrates sphalerite (S) as very light grey in colour and dolomite (D) as grey;

D) Fluorite (F) forms a brown rim with calcite (dedolomite?) and dolomite (C & D) lining a vug in core from the Eramosa Member in borehole 89-3;

E) Plane polarized light photomicrograph of brown and cloudy fluorite in a polished thin section from the same sample as **D**. Lath-shaped pores from former evaporites (E) are partially filled with calcite (C) and extend from the fluorite rims; and

F) Same field of view as E. In SEM fluorite (F) is dark grey and calcite and dolomite (C & D) are light and medium grey in colour.

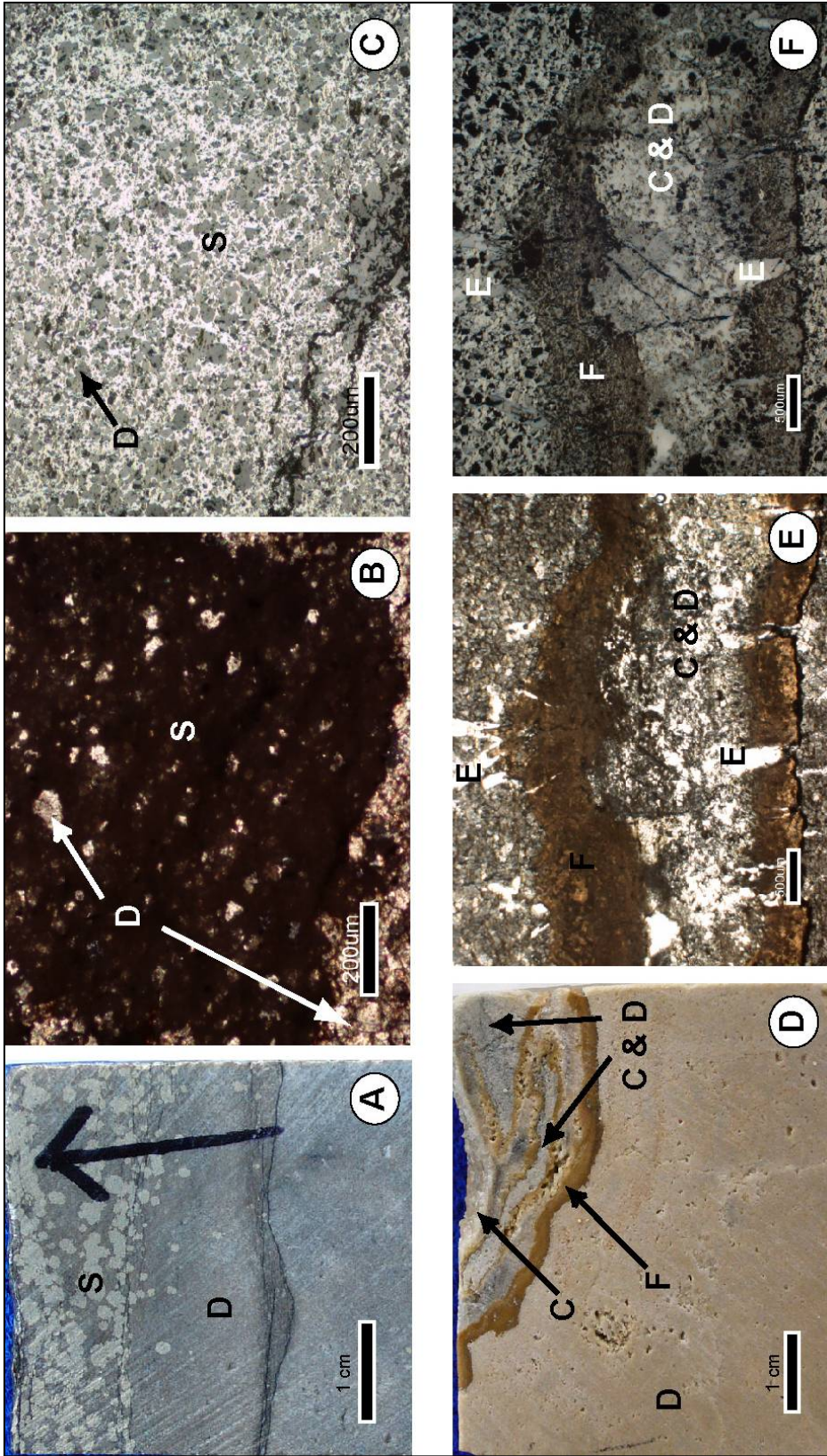


Figure 4.7 (next page): Photomicrographs of dolomite types in the Amabel and Guelph formations.

A) Cross-polarized light photomicrograph of mimically-replaced echinoderm fragment (M) surrounded by finely crystalline dolomite (fcd) from the Guelph Formation in borehole 89-2;

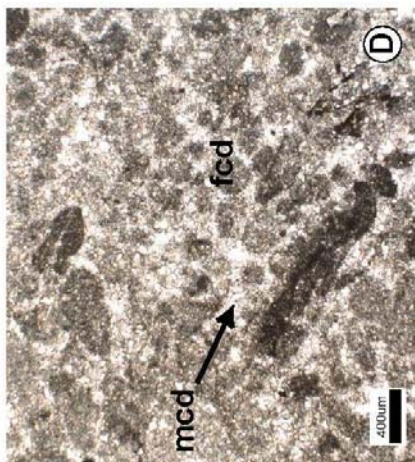
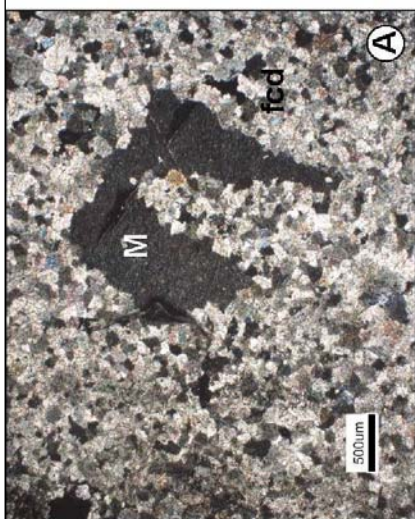
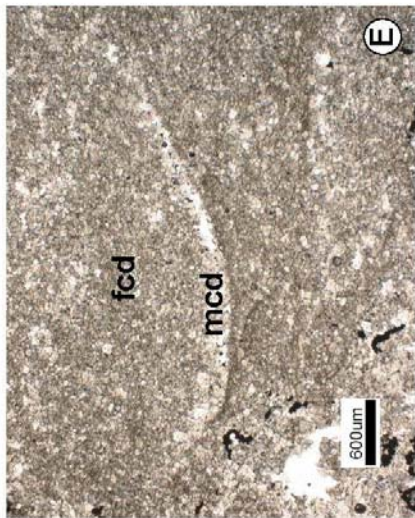
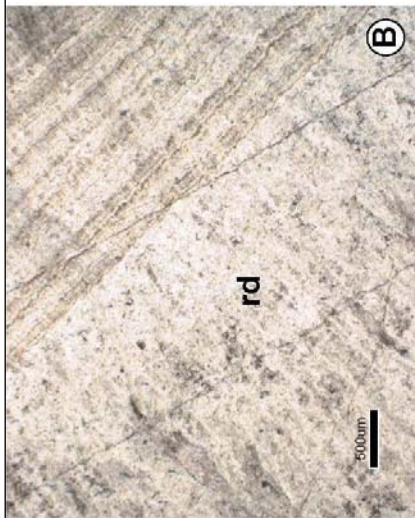
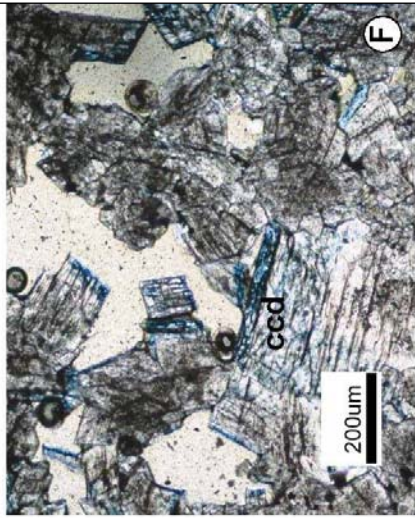
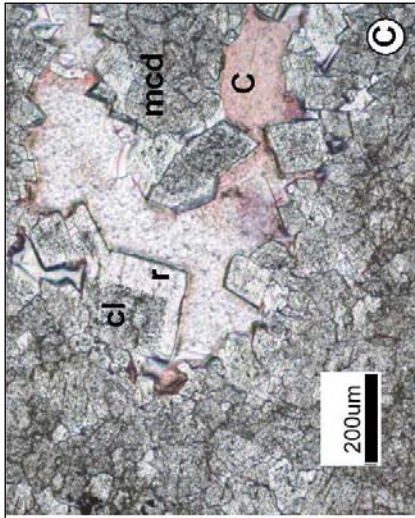
B) Plane-polarized light photomicrograph of radiaxial dolomite (rd) replaces a portion of a stromatoporoid in the Guelph Formation from borehole 89-3;

C) Plane-polarized light photomicrograph of euhedral medium crystalline dolomite (mcd) rhombs with cloudy (cl) cores and clear rims (r). Calcite cement (C) partially lines vuggy pore. This example is from the Lions Head Member of borehole 89-1;

D) Plane-polarized light photomicrograph of cloudy finely crystalline dolomite (fcd) replacing peloids within medium crystalline dolomite (mcd);

E) Plane-polarized light photomicrograph of medium crystalline dolomite (mcd) replacing a shell fragment within surrounding finely crystalline dolomite (fcd). Lower edge of replaced fossil is lined with a stylolite; and

F) Plane-polarized light photomicrograph of a rare example of slightly ferroan euhedral coarsely crystalline dolomite (ccd) from the Lions Head Member in borehole 90-2.



4.2.3.1 The Amabel Formation

Replacement dolomite within the Amabel Formation is commonly fine to medium crystalline in size, exhibits a variety of crystal shapes, and extinguishes sharply. The Lions Head Member of the Amabel Formation is composed of cloudy, anhedral to subhedral fine to medium (10–100 μm in size) crystalline dolomite, whereas slightly clearer, subhedral to euhedral medium (150–200 μm) crystalline dolomite constitutes the overlying Colpoy Bay and Wiarton members. The similarity in dolomite replacement fabrics between the Colpoy Bay and Wiarton members makes them more difficult to distinguish petrographically.

Fossil preservation in the Amabel Formation is generally poor, with fossil identification based largely on fragment morphologies. Fossils within the lower Lions Head and Colpoy Bay members of the Amabel Formation are generally replaced by silica, cloudy finely crystalline dolomite or slightly clearer medium crystalline dolomite. Fossils within the upper Wiarton Member of the Amabel Formation are commonly replaced with clearer medium to coarsely crystalline dolomite. Each member of the Amabel Formation contains echinoderm fragments mimically replaced with dolomite where internal microstructure is generally poorly preserved (Fig. 4.7A).

4.2.3.2 The Eramosa Member

The E1, E2, and E3 lithofacies are identical petrographically, whereas the E4 lithofacies is more distinct. Dolomite within all of the Eramosa Member lithofacies is generally cloudy and subhedral in shape, and ranges in size from fine to medium (15–125 μm) crystalline. More rarely the E1, E2, and E3 lithofacies contain zones of anhedral finely crystalline or euhedral

slightly coarser crystalline mosaics. The E4 lithofacies is easily distinguished by its abundance (> 75 %) of wispy and low amplitude peaked stylolite seams, which are found within the laminations of this lithofacies.

Within each of the lithofacies of the Eramosa Member fossil preservation is generally poor in thin section. The E2 lithofacies contains more fossil fragments than the other 3 lithofacies. Replacement of fossils with slightly clearer medium crystalline dolomite is common, and more rarely echinoderm fragments are mimically replaced by dolomite. Although diverse plant and animal fauna were well preserved within the outcrop at the OSLW Quarry (Tetreault, 2001), this degree of preservation is not apparent in thin section.

4.2.3.3 The Guelph Formation

The 3 lithofacies that comprise the Guelph Formation are petrographically similar. The Guelph Formation is mostly composed of subhedral to euhedral, fine to medium crystalline (10–175 μm) dolomite with rare patches of more coarsely crystalline dolomite. Rarely, euhedral dolomite rhombs contain distinct cloudy cores with clear rims (Fig. 4.7C).

The three lithofacies of the Guelph Formation have similar fossil preservation. Mimically-replacing dolomite commonly replaces echinoderm or other shelly fossil fragments throughout the Guelph Formation. Clearer medium to coarsely crystalline replacement dolomite stands out amongst cloudy finely crystalline matrix dolomite where stylolite seams separate the crystal sizes (Fig. 4.7E). In contrast, cloudy finely crystalline replacement dolomite stands out when surrounded by clearer medium crystalline replacement dolomite (Fig. 4.7D). Replacement radial dolomite was observed within the Guelph

Formation in the two most northerly boreholes, where it replaces echinoderms, shelly fragments, or portions of a stromatoporoid (Fig. 4.7A, B).

4.3 Nature and distribution of silica

Silica is most commonly found in the form of chert nodules within the Amabel and Guelph formations. Diagenetic silica includes both microquartz (including chalcedonic fibres) and megaquartz. Microquartz is defined as equant crystals less than 20 μm in size or chalcedonic fibres of unspecified length (Folk and Pittman, 1971). Megaquartz is defined as coarser than 20 μm in size. Silica partially or fully replaces bioclasts within nodules and occurs as cement filling biomoldic and vuggy pores.

Microquartz (chert) is indistinguishable between the Amabel and Guelph formations. Within the Lions Head Member of the Amabel Formation, megaquartz commonly fills vuggy and biomoldic pores. In contrast, biomoldic and vuggy pores within the Colpoy Bay Member are commonly lined with microquartz and megaquartz crystals up to 150 μm in size, which either produces a drusy quartz mosaic or the centre remains empty. Rarely, fibrous chalcedony precipitated on pore-lining equant microquartz with megaquartz filling the centre of the pore. Where pore space is sufficiently large, chalcedonic fibres may fill the entire pore resulting in chalcedonic spherulites (Fig. 4.5A) that range from 25–400 μm in size. The Wiarton Member of the Amabel Formation and the Guelph Formation (including the Eramosa Member) typically contain lower abundances of silica than elsewhere in these units.

4.3.1 Distribution of nodules

Chert nodules are irregular in shape and commonly resemble burrows. Chert nodules range from 1–6 cm (the maximum core width) in diameter and are generally composed of microquartz (Fig. 4.8D). Chert nodules are porous and non-luminescent in CL. Contacts between nodules and surrounding dolomite may be sharp and accompanied by a stylolite seam, or gradational with surrounding dolomite (Fig. 4.8A-F). Fossils within nodules, and within the surrounding dolomite, may be preserved by microquartz (equant crystals and fibrous chalcedony spherules), megaquartz, medium (75–175 μm) crystalline dolomite, or a combination of these phases. Within chert nodules poorly preserved echinoderm, brachiopod, bivalve, gastropod, possibly bryozoan or chain coral and possible radiolarian and sponge spicules were observed.

4.3.1.1 The Amabel Formation

Chert nodules are typically most abundant in the Lions Head Member of the Amabel Formation. Chert nodules also occur in the overlying Colpoy Bay Member and are less common within the upper Wiarton Member. Within the Lions Head Member, chert may also form in discontinuous lenses parallel to bedding. In general, nodules have sharp pyrite-rich stylolitic boundaries with the surrounding rock. Detrital silt-sized feldspar and quartz may also be associated with the stylolitic nodule boundary.

Figure 4.8 (next page): Core and cross-polarized light photomicrographs of nodules and their boundaries.

A) An example of a chert nodule (N) with a sharp stylolitic contact with the surrounding dolomite of the Lions Head Member of the Amabel Formation in borehole 90-2;

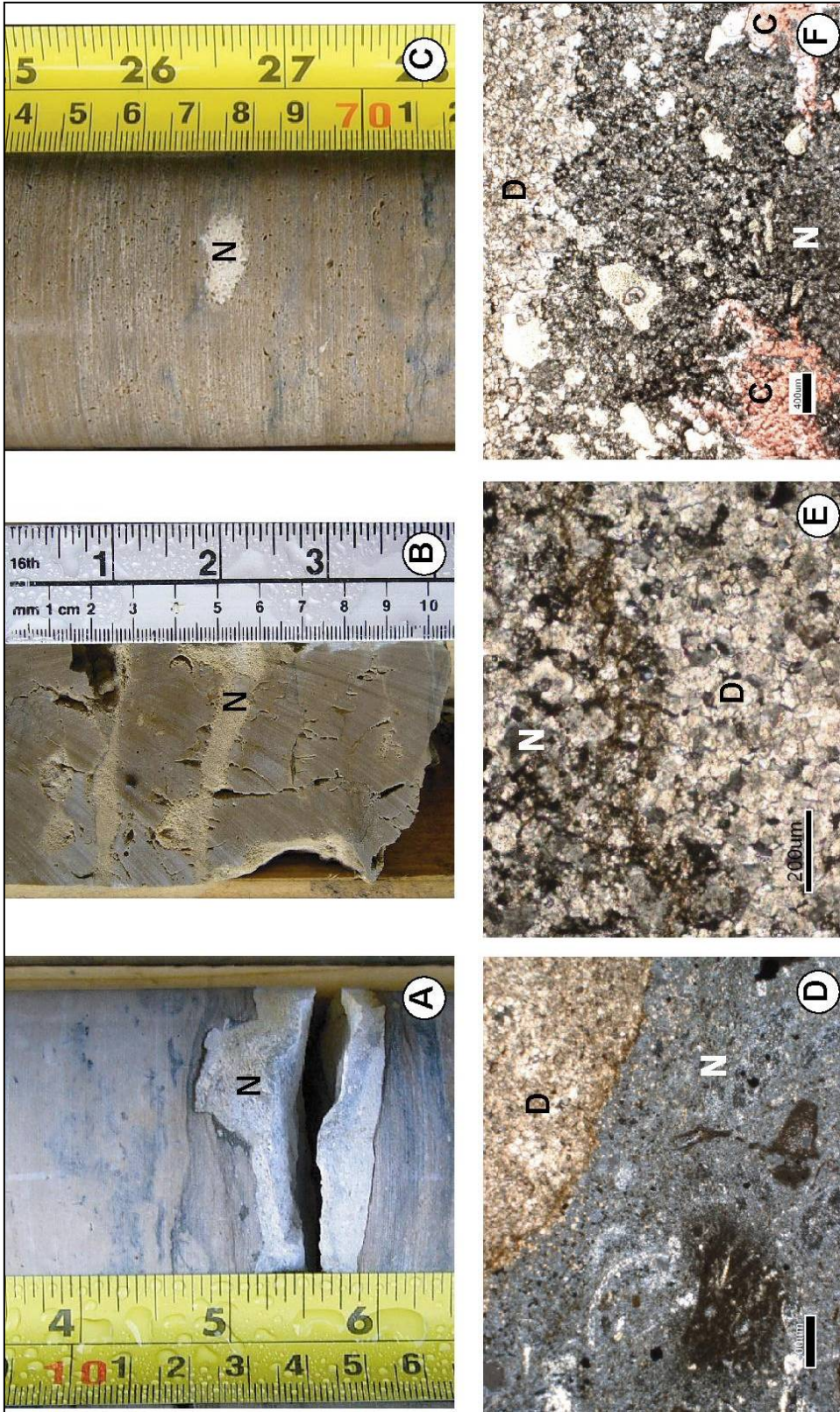
B) A dolomitic nodule (N) in core which has a gradational boundary with the surrounding dolomite. This example is from the Guelph Formation in borehole 89-1;

C) A mixed chert and dolomite nodule (N) within surrounding dolomite with a gradational, non-stylolitic boundary from the Amabel Formation in borehole 90-3;

D) Cross-polarized light photomicrograph of a chert nodule (N) with a sharp stylolitic boundary with the surrounding dolomite (D) from the Eramosa Member in borehole 82-4;

E) Cross-polarized light photomicrograph of a dolomite nodule (N) that is more porous than the surrounding dolomite (D) from the Guelph Formation in borehole 89-1;

F) Cross-polarized light photomicrograph of a mixed chert and dolomite nodule (N) that has a gradational boundary with the surrounding dolomite (D). Calcite cement (C) fills pores within the nodule. This example is from the Eramosa Member of borehole 90-3.



4.3.1.2 The Eramosa Member

Subhedral to euhedral medium dolomite crystals are observed individually and in small groups mixed with chert both within nodules (Fig. 4.8F) and silica-filled biomoldic pores in the Eramosa Member. In nodules where dolomite is 10 % or more of the nodule's volume, the term 'mixed chert and dolomite nodule' is used. Mixed chert and dolomite nodules are more common within the Eramosa Member and the undifferentiated Guelph Formation than in the Amabel Formation. Chert nodules commonly have gradational or partially stylolite-defined boundaries. Porosity is slightly greater within the mixed chert and dolomite nodules than within more chert-rich nodules, where chert is ≥ 90 % of the nodule. The E2 lithofacies is more fossiliferous than the other three Eramosa lithofacies, and commonly contains more nodules as well. Although preservation of fossils is generally poor, possible sponge spicules and radiolarians were observed within one of the nodules sampled from both the Amabel Formation and the Eramosa Member. The presence of silica-producing fauna suggests that the origin of silica could be biogenic.

4.3.1.3 The Guelph Formation

Nodules within the Guelph Formation are commonly partially surrounded by a stylolitic boundary and are composed of porous medium to coarsely crystalline dolomite (Fig. 4.8B). There are few occurrences of dolomitic nodules with microquartz partially filling the intercrystalline pore spaces. Rarely, microquartz is found within the Guelph Formation replacing fossil fragments in dolomitic nodules. In general, very little chert occurs within the Guelph Formation compared to the underlying Amabel Formation.

4.4 Distribution of mottles and mottled fabric

Two types of mottled fabrics are recognized in the Albemarle Group. Finely (<5–100 µm) crystalline cloudy dolomite with authigenic pyrite makes up mm- and cm-sized dark elliptical grey mottles within the Lions Head Member of the Amabel Formation (Fig. 4.9A, B). The second mottled fabric is dominated by dark grey, cm-sized irregular and diffuse shapes parallel to bedding (Fig.4.9C, D). This mottling most commonly occurs in the Colpoy Bay Member of the Amabel Formation, and may occur within the uppermost Wiaraton Member. The amount of mottling observed in all members of the Amabel Formation likely depends on the abundance of burrowing organisms which inhabited these environments. The abundance of crinoid-rich facies within the Wiaraton Member suggests that the depositional environment was of higher energy and did not offer suitable conditions for burrowing organisms, which likely contributed to the general lack of mottling observed.

The dark grey irregular and elongate appearance of the mottles within the Colpoy Bay Member results from the presence of undifferentiated organic material within intercrystalline and mm- to cm-sized vuggy pore spaces. CL did not reveal any textural differences between mottled fabrics and surrounding dolomite. SEM analysis revealed slight increases in porosity associated with mottled fabrics.

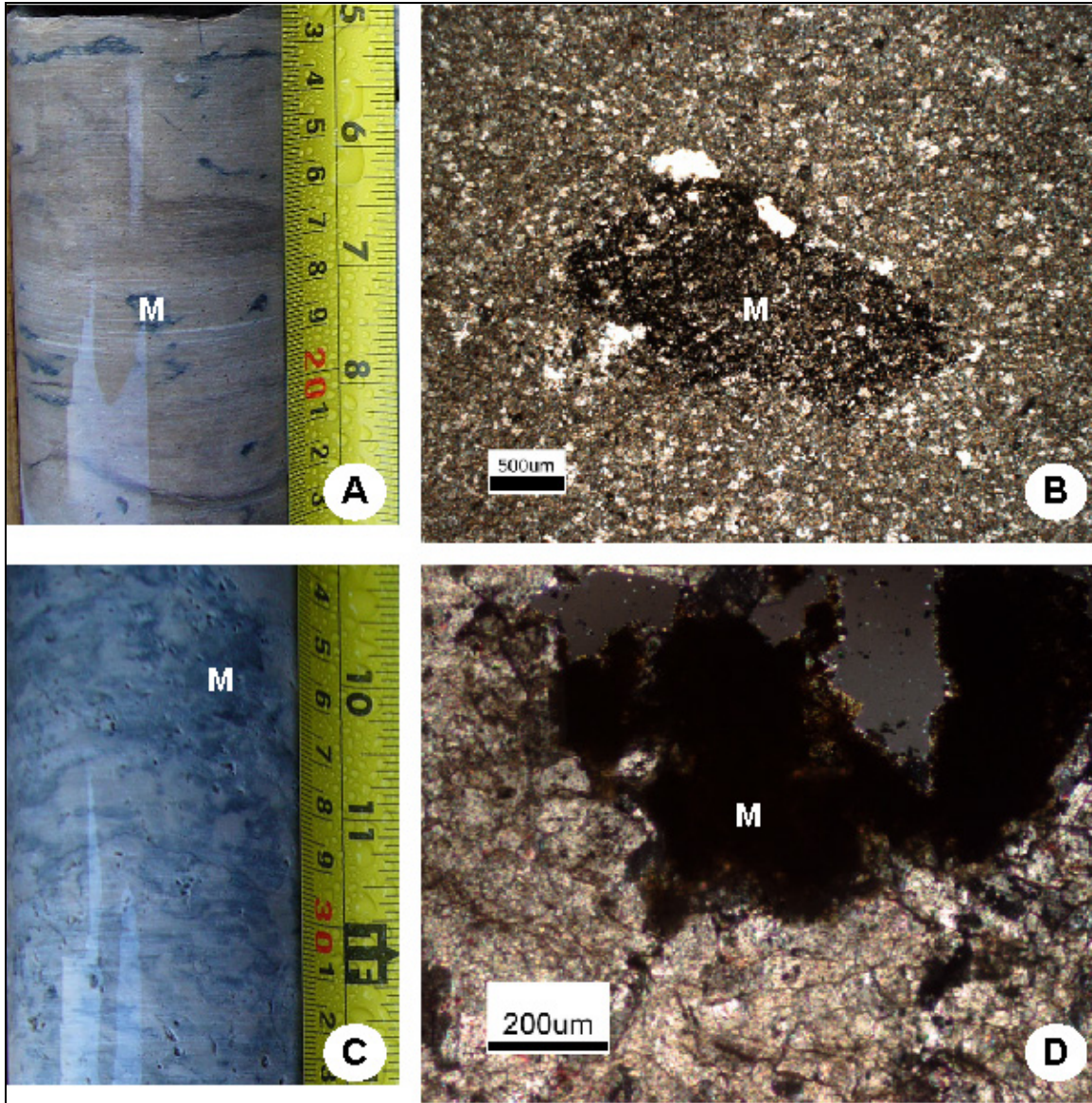


Figure 4.9: Core and photomicrographs of mottles in the Lions Head (**A and B**) and Colpoy Bay (**C and D**) members. All photos are from borehole 90-2.

A) Core view and **B)** corresponding cross-polarized light photomicrograph illustrates elliptical pyrite-rich mottles (M) characteristic of the Lions Head Member of the lower Amabel Formation. These mottles rarely occur within the overlying Colpoy Bay Member. The pyrite-rich spotty mottles provide a good visual marker to identify this stratigraphic horizon;

C) Core photograph illustrating irregular, diffuse mottles (M) in the Colpoy Bay Member of the Amabel Formation; and

D) Cross-polarized light photomicrograph shows that mottles (M) within the Colpoy Bay Member contain undifferentiated organics and are porous.

4.5 Interpretations

4.5.1 Pre- and post-dolomitization diagenesis

4.5.1.1 Hardground

Evidence of pre-dolomitization diagenesis was observed in the form of a potential hardground surface. The presence of a pronounced sharp surface in the lower Lions Head Member of the Amabel Formation suggests that a widespread area was lithified following deposition of the Fossil Hill Formation, when a regional regression of the sea commenced (Sanford, 1969). Bioerosion evidence in the form of possible pitting or boring was observed in thin section (Fig. 4.1). Evidence of subaerial exposure from previous studies in southwestern Ontario Silurian reefs (Charbonneau, 1990; Smith, 1990) is found within the same stratigraphic level as the hardground observed in this study on the Bruce Peninsula. The planar eroded appearance of the hardground surfaces, in addition to subaerial exposure events interpreted from southwestern Ontario (Charbonneau, 1990; Smith, 1990), suggests that there was an extensive area of the northeastern margin of the Michigan Basin that was exposed and possibly eroded during the regression of the sea prior to the deposition of the Amabel Formation during the Early Silurian (Sanford, 1969). According to Brett and Brookfield's (1984) hardground morphology classification, the pyrite-rich hardgrounds with planar and possibly hummocky morphologies observed at the base of the Lions Head Member are characteristic of well-sorted grainstones that may have formed in an intershoal environment. The morphology of the hardground surface is difficult to classify from the lack of lateral information adjacent to the borehole, as well as the pervasive dolomitization of the rock.

4.5.1.2 Porosity

Pre-dolomitization porosity within originally porous fossiliferous lithofacies was likely enhanced by diagenetic pore-waters that recrystallized the limestone and precipitated dolomite. Post-dolomitization porosity such as the intraskeletal, biomoldic and vuggy porosity observed within the dolostones likely reflects the primary porosity within precursor limestones. Fracture porosity was likely associated with tectonic movement or late isostatic rebound within the basin, though no fault or displacement evidence was observed within the core in this study.

4.5.1.3 Source of silica

The presence of silica-producing fauna (siliceous sponges or radiolarians) suggests that the origin of silica is biogenic. In addition, the abundance of silica within nodules in the Lions Head Member at the base of the Amabel Formation suggests that the source of silica may have been derived from the underlying Fossil Hill Formation, which is characterized by an abundance of silicified fossils, including sponge spicules (Eley and Jull, 1982; Eley and von Bitter, 1989). Dense shell beds in the underlying Fossil Hill Formation would have been associated with large amounts of organic matter that may have affected pore water chemistry by reducing the pH in pore water, encouraging the dissolution of siliceous skeletal fragments, and the precipitation of silica within the sedimentary succession (Siever, 1962; Eley and Jull, 1982).

Alternatively, the Precambrian quartzite now exposed in the La Cloche Mountains to the northeast were islands within the Silurian Sea that would have provided a large source of

detrital silica (Eley and Jull, 1982) but the evidence for dissolution of detrital silicates originating from this source is lacking. Fluctuations in the abundance of silica were similar between boreholes.

The porous nature of the chert nodules likely reflects the inherited pre-lithification sediment porosity (Eley and von Bitter, 1989). Multiple combinations of varying silica phases and dolomite fill vuggy pores and preserve fossils. The combination of microquartz and megaquartz replacement of fossils is likely a result of the availability of silica, and the initial replacement silica which is commonly microquartz (Eley and von Bitter, 1989). Cross-formational fluid flow, perhaps related to vertical fractures, could have assisted in the precipitation order of each silica phase by introducing fluids of varying concentrations, but this speculation remains to be tested. Although the types of fossils that are preserved within these formations are generally robust (i.e., crinoid ossicles, brachiopod and gastropod fragments), there were no signs of compaction of fossils preserved within nodules or within the surrounding dolomite.

Higher abundances of silica within the lower Amabel Formation compared with the overlying Guelph Formation is likely due to preferential precipitation within the heavily bioturbated sediments which likely made the rock more permeable. Mixed chert-dolomite nodules characterized by more gradational boundaries with surrounding dolomite likely resulted from lower concentrations of dissolved silica in pore fluids. Dissolved silica concentrations continued to decrease further up-section, explaining the absence of chert in the porous dolomitic nodules within the Guelph Formation.

4.5.1.4 Timing of silicification

Evidence of silicified fossils within chert nodules in the Amabel Formation indicates that silicification preceded the widespread dolomitization of the Amabel Formation on the Bruce Peninsula. The lack of compaction of microquartz nodules and fossil fragments within them suggests that silicification was an early diagenetic process. Laboratory analyses from Folk and Weaver (1952) indicate that the chemistry and growth of microquartz rapidly replaces limestone, and chalcedonic and megaquartz form at a slightly slower rate within the carbonate rocks which likely correlates with the drusy mosaics commonly observed.

Although silica-bearing solutions preferentially alter fossil fragments first (Eley and von Bitter, 1989), complete silicification likely post-dated widespread dolomitization. The presence of fine to medium-sized dolomite crystals within ~ 60 % of pore-filling bioclast replacement silica, within ~ 80 % of chert nodules, and euhedral rhombs completely entombed by silica supports the hypothesis that widespread dolomitization preceded complete silicification. Dolomite within the nodules has the same dull red luminescence as the surrounding dolomite suggesting a cogenetic relationship between the two phases. Within the Eramosa Member and the Guelph Formation, the abundance of dolomite is much greater than the volume of silica within vuggy and biomoldic pores and nodules. The decrease in silica within the Guelph Formation dolostones suggests that the silica concentration within diagenetic pore waters declined in the upper strata.

4.5.1.5 Evaporite cements

The presence of evaporite lath-shaped pores is interpreted to indicate the former presence of anhydrite or gypsum. Lithofacies that contain these pores provide evidence of hypersaline seawater resulting from restriction of seawater and slightly arid conditions. Although their occurrence is relatively minor, the presence of moldic pores after evaporites is observed within the Wiarton, E2 and E3 lithofacies and the G1 and G2 lithofacies. Evaporite cementation may have corresponded with dolomitization (Fig. 4.2), but occurs prior to widespread calcite cementation, which partially or fully fills the former evaporite pores.

4.5.1.6 Stylolites and chemical compaction

The presence of low and high-amplitude peaked stylolites with amplitudes up to 3 cm indicates pressure dissolution of the dolomite crystals likely dissolved small (< 2–3 cm) portions of the dolostones (Fig. 4.10). Peaked stylolite seams appear to preferentially occur within dolostones of higher purity (i.e., the Colpo Bay and Wiarton members of the Amabel Formation). Authigenic pyrite is abundant along stylolite seams in both the Amabel and Guelph formations suggesting that undifferentiated organics may have been gathered by sulfide-rich pore waters along the stylolite seams. Glauconite was rarely found along the stylolite seams in the Lions Head Member of the Amabel Formation, which may be related to the amount of siliciclastic clay within this depositional environment. The presence of the sutured seams, which dissolved dolomite crystals and contain late-stage secondary minerals as well as detrital feldspar, postdated dolomitization. The distinct shape of the peaked

stylolite, with a sharp black continuous seam, suggests that the stylolite post-dated dolomitization rather than forming during limestone lithification (Coniglio et al., 2003).

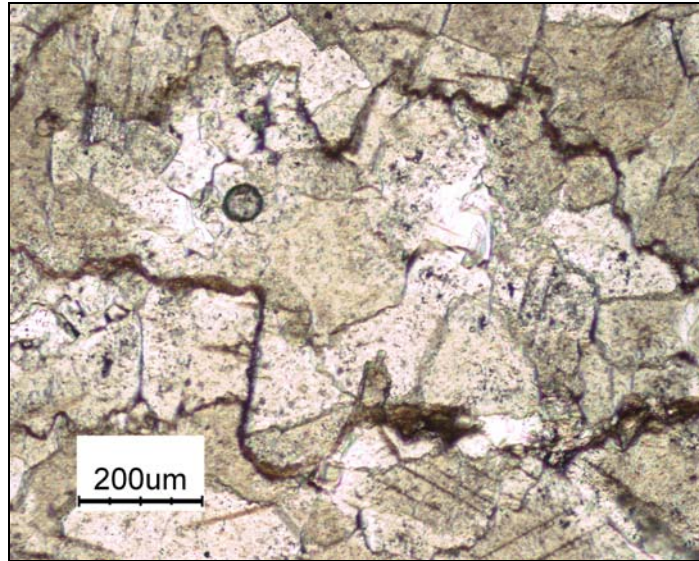


Figure 4.10: Example of two sutured (peaked) stylolite seams within partially dissolved dolomite. This photomicrograph is from sample 90-2-030, which is from the G1 lithofacies.

4.5.1.7 Calcite precipitation

Calcite cement within the Amabel Formation is typically blocky and pore-filling. The Eramosa Member and the Guelph Formation contain greater abundances of vuggy porosity, which is commonly lined or filled with large crystals of equant drusy calcite. The presence of abundant late-stage pore-filling calcite cement, which rarely shows distinct zoning in CL, is indicative of seawater-derived pore fluids that occur in moderate burial settings (Choquette and James, 1990). The lack of meniscus or pendant calcite cement suggests that late stage calcite cementation did not occur within the meteoric environment.

4.5.1.8 Dedolomite

Dedolomitization rarely occurs within the dolostones of the Amabel and Guelph formations and is a late diagenetic process, likely corresponding with calcite cementation (Coniglio, 2003). The minor occurrences of dedolomite suggest slight chemistry alterations within burial pore fluids due to rock-water interaction that dissolved and replaced former dolomite.

4.5.1.9 Pyrite and hydrocarbons

The widespread occurrence of pyrite within the dolostones of the Amabel and Guelph formations suggest that organics were profuse and available for reduction by non-oxygenated waters. Pyrite appears to have precipitated both during early dolomitization and late post-dolomitization, as it is associated with both stylolite seams and late-stage calcite cement. The long duration of pyrite precipitation suggests that sulphate must have been readily available within both early and late dolomitizing fluids and post-dolomitizing pore fluids.

The presence of hydrocarbons as a non-mineral phase within intercrystalline pores indicates that the dolostones were permeable and contained sufficient organic content within pore fluids to leave hydrocarbon residue. Similarly, an opaque residue is commonly found along stylolite seams.

4.5.2 Dolomitization

Dolomitization significantly altered the carbonates, preserving little of the original sedimentary fabric. These dolostones emit a uniform dull red cathodoluminescence, which suggests that the dolomitizing fluids rarely fluctuated geochemically (Coniglio et al., 2003).

This study does not have any supporting geochemical data that may provide an alternative explanation for the lack of cathodoluminescence zoning.

The density of nucleation sites and the mechanism of crystal growth controlled the dolomite replacement texture (Sibley and Gregg, 1987). The similarities between replacement dolomite types 1–4 mentioned in section 4.2.3 reflect the precursor texturally homogeneous limestone. The variety of crystal sizes and shapes provides an assortment of nucleation sites which enabled the precipitation of anhedral to subhedral finely crystalline dolomite. Where subhedral to euhedral dolomite occurs, the precursor fabric may have had a more homogeneous distribution of nucleation sites or contained larger pore spaces that allowed for optimum crystal growth. Dolomite mimically replaces echinoderm fragments with a single crystal. The pervasive dolomitization of the Amabel and Guelph formations suggests a high permeability existed within the precursor limestones that enabled flow of dolomitizing pore fluids.

4.5.3 Mottling

Overall, mm- to cm-sized pyrite-rich mottles within the lower Amabel Formation are associated with small localized increases in porosity. Both the small elliptical shape of the mottles in the Lions Head Member of the Amabel Formation and the irregular diffuse mottles of the Colpo Bay Member appear closely related to burrows. In general, mottles extend parallel to bedding. The occurrence of pyrite within or surrounding small mottles in the Lions Head Member (Fig. 4.9B) suggests new organic material may have been introduced into the burrows by the burrowing organism (Kendall, 1977).

Irregular diffuse dark grey mottles of the Colpoy Bay Member contain less pyrite than those in the Lions Head Member. SEM analysis revealed organics concentrated within porous zones. Bioturbation likely created the increased porosity in the sediment that may have later been filled with sediment and organic material from organisms, or organics may have resulted from dissolved fossils within limestone.

4.6 Dolomitization models of the Bruce Peninsula during the Silurian

Numerous dolomitization models have been proposed for regional reefal and basinal dolomitization, such as: the burial dolomitization model (Jodry, 1969), the reflux-hypersaline model (Sears and Lucia, 1980), and the evaporative drawdown model (Cercone, 1988). Coniglio et al. (2003) summarized the various types of evidence used to support the dolomitization models that have been applied to Silurian reefs in the Michigan Basin. The model that best explains the dolomitization within the Michigan Basin, and supports the observations presented in this thesis from the Bruce Peninsula, is the evaporative drawdown model (Cercone, 1988).

Eight boreholes studied for this thesis from the Bruce Peninsula contain pervasively dolomitized Silurian carbonates with no precursor limestone preserved. These boreholes are located on the northeastern side of the Michigan Basin. Similar observations of dolostone along the margins of the basin and limestone deposited towards the basin centre (Coniglio et al., 2003) indicate that the concentration of Mg within the dolomitizing fluids was greater along the basin rim.

The evaporative drawdown model (see Fig. 4.11 based on the model proposed by Cercone, 1988) infers that dolomitizing fluids originated from beyond the basin margins where dolostone prevails. According to Cercone (1988) and Coniglio et al. (2003), Mg-rich dolomitizing fluids that were derived from beyond the basin margin migrated by gravity-driven reflux through porous and permeable carbonates (such as reefs, bioherms, and storm deposits), gradually losing the ability to dolomitize as the source and availability of Mg declined towards the basinal strata. The localized dolomitization of pinnacle and patch reefs in southwestern Ontario is explained by upwelling of dolomitizing fluids through these more permeable features (Zheng, 1999; Coniglio et al. 2003).

Shaver (1991) disagreed with the drawdown model because it does not take into account the interconnectedness of the carbonates among the Michigan Basin, the Illinois Basin and the Wabash Platform. The distribution of dolostone and limestone between the Illinois Basin and the Wabash Platform that border the Michigan Basin does not support the evaporative drawdown hypotheses of a Mg source originating beyond the Michigan Basin (Shaver, 1991). Although Shaver (1991) disagreed with the drawdown model of the Michigan Basin during the Late Silurian, this model remains to be the best explanation for the rim of preferential dolomitization around the basin, as well as localized dolomitization of patch and pinnacle reefs in southwestern Ontario (Zheng, 1999; Coniglio et al., 2003).

Within the study area no bioherms, pinnacle or patch reefs were observed. There was no evidence of limestone within the boreholes closer to the basin centre which made it difficult to assess the extent of dolomitization from the margin towards the centre of the basin. The Amabel and Guelph formations were completely dolomitized in the study area.

Further geochemical and petrographic study of carbonates laterally adjacent to the borehole cross-section would be required to gauge the extent at which pervasive dolomitization occurs from the margin towards the centre of the basin.

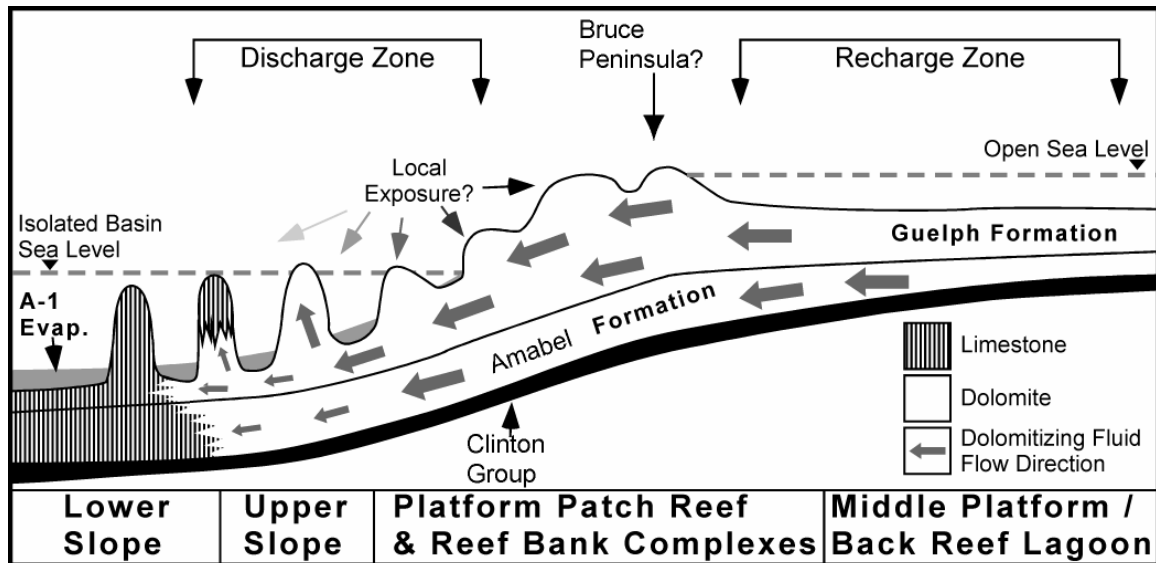


Figure 4.11: Paleohydrogeological flow system driven by evaporative drawdown (gravity-driven reflux) (modified from Coniglio et al., 2003).

4.7 Conclusions

Petrographic study of the diagenetic features of each lithofacies in the Amabel and Guelph (including the Eramosa Member) formations has provided a better understanding of the diagenetic history of these carbonates on the Bruce Peninsula.

Silurian carbonates on the Bruce Peninsula are pervasively dolomitized and contain little evidence of pre-dolomitization diagenetic alteration. A single possible hardground

surface at the base of the Albemarle Group, within the lower Lions Head Member of the Amabel Formation was observed. Bioturbation in the form of mottled fabrics throughout the Amabel Formation and in parts of the Guelph Formation was also observed. Post-dolomitization alteration includes the presence of secondary porosity, silica precipitation, evidence of precursor evaporites, stylolitization, calcite cementation and dedolomitization, dolomite cementation, and secondary mineralization (pyrite, sphalerite, fluorite, and glauconite), and the formation of hydrocarbons.

Silica was likely biogenetically-derived from the underlying Fossil Hill Formation as well as from possible minor sponge spicules and radiolarians within the lower Eramosa Member. Silica precipitation generally occurred prior to widespread dolomitization, although dolomite rhombs completely entombed in silica suggest some silicification followed dolomitization.

Dolomitization of the Amabel and Guelph (including the Eramosa Member) formations is characterized by 4 different types of replacement dolomite: (1) anhedral cloudy very finely crystalline dolomite, (2) subhedral cloudy finely crystalline dolomite, (3) subhedral to euhedral clearer medium crystalline dolomite, and (4) coarse euhedral crystalline to mimically replacing dolomite. Although overall fossil preservation is poor, fossil preservation with silica is generally better in the Amabel Formation than in the Guelph Formation. Fossils, which include: crinoids, brachiopods, bivalves, cephalopods, gastropods, stromatoporoids and corals, are most often preserved by microquartz, macroquartz, and/or dolomite or a combination of these phases.

The paleohydrological model that best explains the widespread dolomitization of the Silurian carbonates in southwestern Ontario is the evaporative drawdown model proposed by Cercone (1988) and applied by Coniglio et al. (2003) in southwestern Ontario to explain the regional distribution of dolomitization along the margins of the Michigan Basin, where a progressive decrease in dolomitization towards the centre of the basin occurs.

:

Chapter 5: High Frequency GPR Profiling of Shallow Subsurface Stratigraphy in Silurian Dolostones

5.1 Introduction

Silurian age carbonates in the Bruce Peninsula region are among the best exposed and intensely exploited bedrock units in southern Ontario, particularly as sources of building stone and industrial minerals. Despite their regional scale exposure and economic importance, these rock units have not been extensively studied using ground-penetrating radar (GPR). GPR is an effective tool for defining shallow stratigraphy within carbonate buildups (Asprion and Aigner, 2000) as well as the internal architecture of bioherms (Pratt and Miall, 1993; Asprion et al., 2004). Whereas a significant body of work has focused on unconsolidated clastic deposits (e.g. Roberts et al., 2003), comparatively little work has been done on consolidated carbonates.

Building-stone quarries on the Bruce Peninsula provide an excellent opportunity to study the application of GPR profiling of carbonate strata. Both the OSLW Quarry and the Adair Quarry (Fig. 5.1) offer three-dimensional exposures of outcrop with little or no overburden and a lowered water table, providing conditions that are ideal for GPR surveys. A previous GPR study conducted on the Amabel Formation along the Niagara Escarpment in southern Ontario (Pratt and Miall, 1993) was able to delineate lithologic variability between carbonate beds and argillaceous lenses. More recently, a GPR study on the stratigraphy in the OSLW Quarry was carried out using more modern equipment and signal processing techniques (Tetreault, 2001). These earlier studies were unable to refine fine-scale

stratigraphic details (10's of centimetres) due to the low frequency antennae (50 and 100 MHz, respectively) used. To achieve this level of resolution, high frequency antennae (i.e., 225 MHz or greater) are required. However, there have been very few documented investigations within carbonate rocks using these high frequencies (e.g., Kruger et al., 1997).

The purpose of this field study was to investigate the high frequency (225–900 MHz) GPR profiling for imaging shallow stratigraphic and karstic features in carbonate rocks. Furthermore, we assessed the predictive capabilities of this method for delineating building stone resources (i.e., lateral continuity and thicknesses of key building stone units).

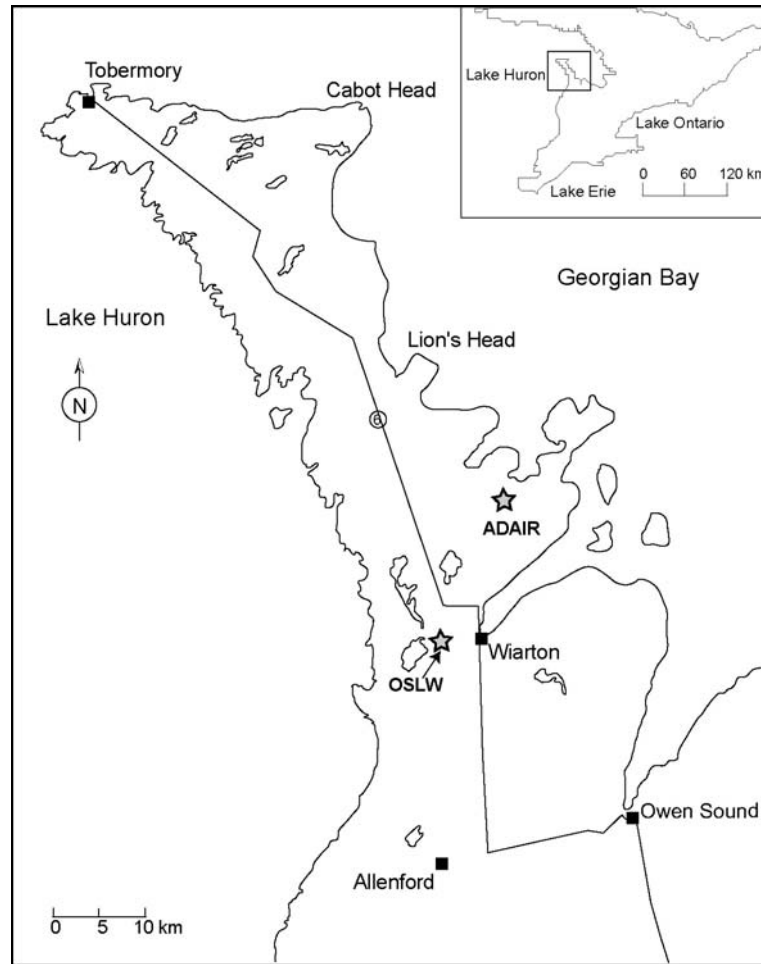


Figure 5.1: Map of the Bruce Peninsula. Stars represent the OSLW and Adair quarries where GPR surveys were conducted. Squares are located at main cities on the Peninsula. Inset map of southern Ontario highlights the study area with a box (adapted from Armstrong et al., 2002).

5.2 Geological Setting

Dimension stone and aggregate quarry operations are a significant local industry on the Bruce Peninsula, with much of the activity concentrated in the Eramosa Member of the Guelph Formation and the underlying Warton/ Colpoy Bay members of the Amabel Formation (Fig. 5.2). The Wenlock-Ludlow (Silurian) Amabel and Guelph formations of southwestern Ontario form the caprock of the Niagara Escarpment and most of the bedrock

surface on the Bruce Peninsula. Lithofacies within these formations record depositional environments proximal to bioherms and shoals that reflect partially restricted marine to more open marine conditions along the eastern margin of the Michigan Basin. The OSLW Quarry exposes ~ 8 m of thin- to thick-bedded deep lagoonal dolostones of the Eramosa Member. This distinctive unit is characterized by cm- to m-scale laminated dark brown argillaceous dolostone that is finely crystalline and bituminous, and contains chert nodules associated with calcite, pyrite and more rarely fluorite. The Adair Quarry, which is located ~ 30 km to the northeast of the OSLW Quarry, reveals ~ 10 m of the underlying Amabel Formation. At the Adair Quarry, the Amabel Formation consists of cream-tan and blue-grey mottled dolomitized grainstones that form medium to coarsely crystalline beds, containing wide (1–30 cm) solution joints and fractures. Although both the Eramosa Member and the Amabel Formation are pervasively dolomitized, the exposed Amabel Formation is more homogeneous.

Silurian Stratigraphic Units of the Michigan Basin, southern Ontario

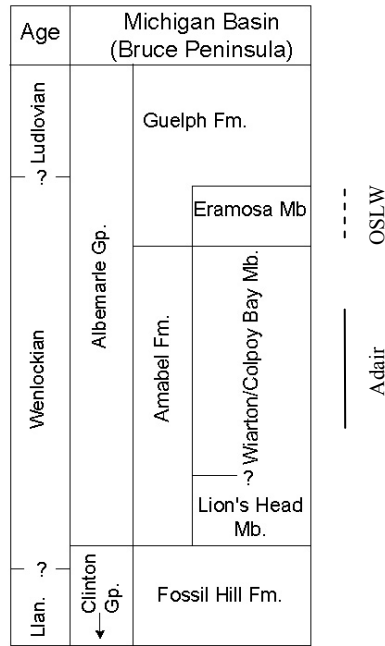


Figure 5.2: Silurian stratigraphic units of the Bruce Peninsula (adapted from Bolton, 1957; Johnson et al., 1992). The solid line indicates the stratigraphic section imaged at the Adair Quarry and the dashed line indicates the stratigraphic section imaged at the OSLW Quarry.

5.3 Methodology

GPR surveys were conducted at the OSLW Quarry in July 2004 and August 2005. Survey lines were located on top of and oriented parallel to existing quarry faces. Each survey was performed with a PulseEKKO 1000 system using a range of high frequencies (225-900 MHz). 900 MHz antennae provide better resolution of a GPR profile, which results in the ability to correlate specific diffraction events and reflectors with diagenetic features (such as vugs and nodules) and lithologic boundaries, respectively (Fig. 5.3).

In this chapter, we present the correlation between radar images and carbonate geology using the 450 MHz profiling for one profile line, and the 900 MHz data for three

other profile lines. The 450 MHz profiling was acquired using a station spacing of 0.05 m; the 900 MHz data was obtained with 0.025 m station spacing. For both frequencies, the time sampling was 100 ps, and the stacking number was 64. Processing of each profile included the use of the following procedures:

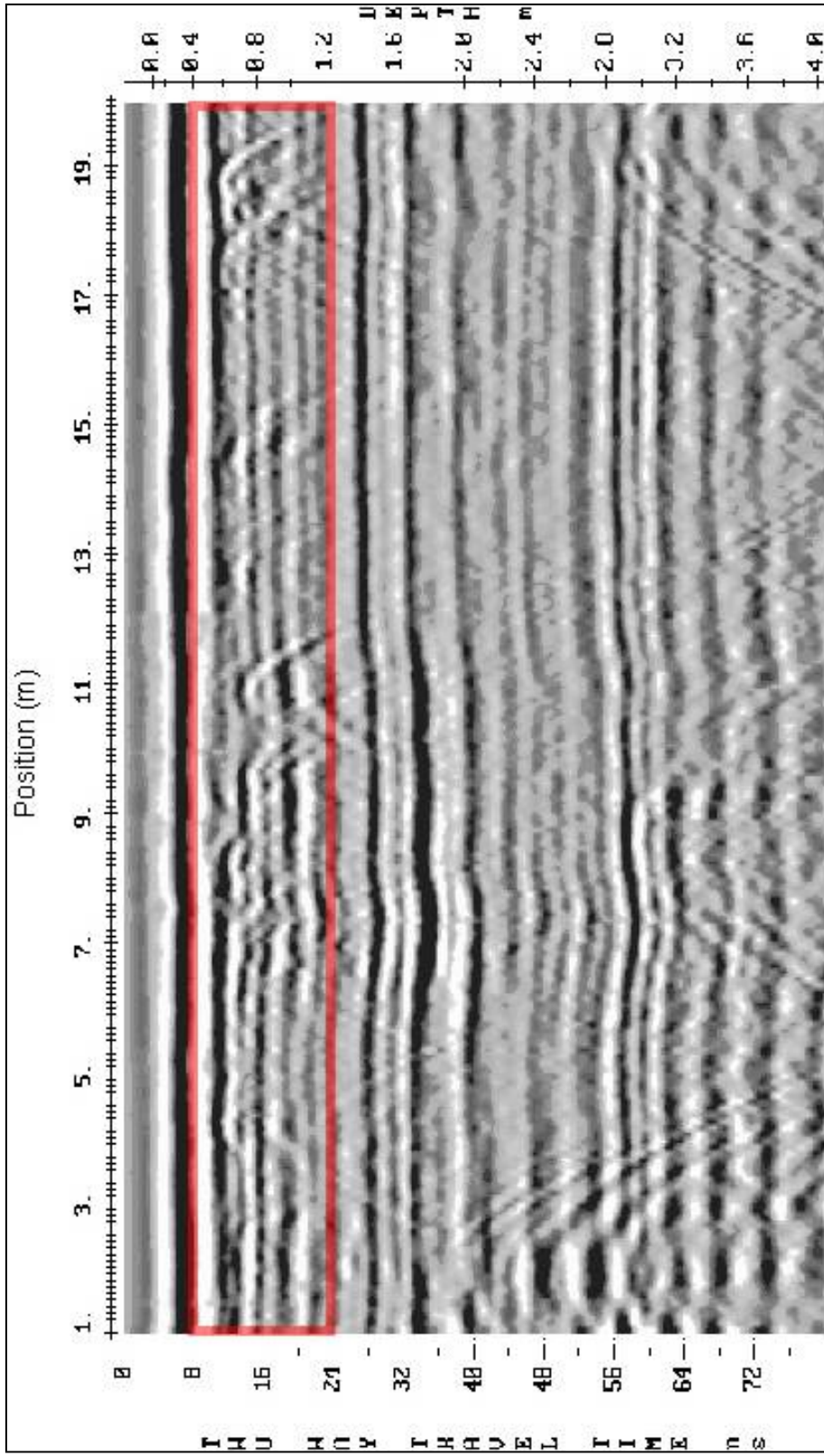
- Dewow
- Spreading and exponential compensation (SEC) gain
- Down the trace averaging (3 and 5 samples for 900 and 450 MHz, respectively)
- Topographic correction

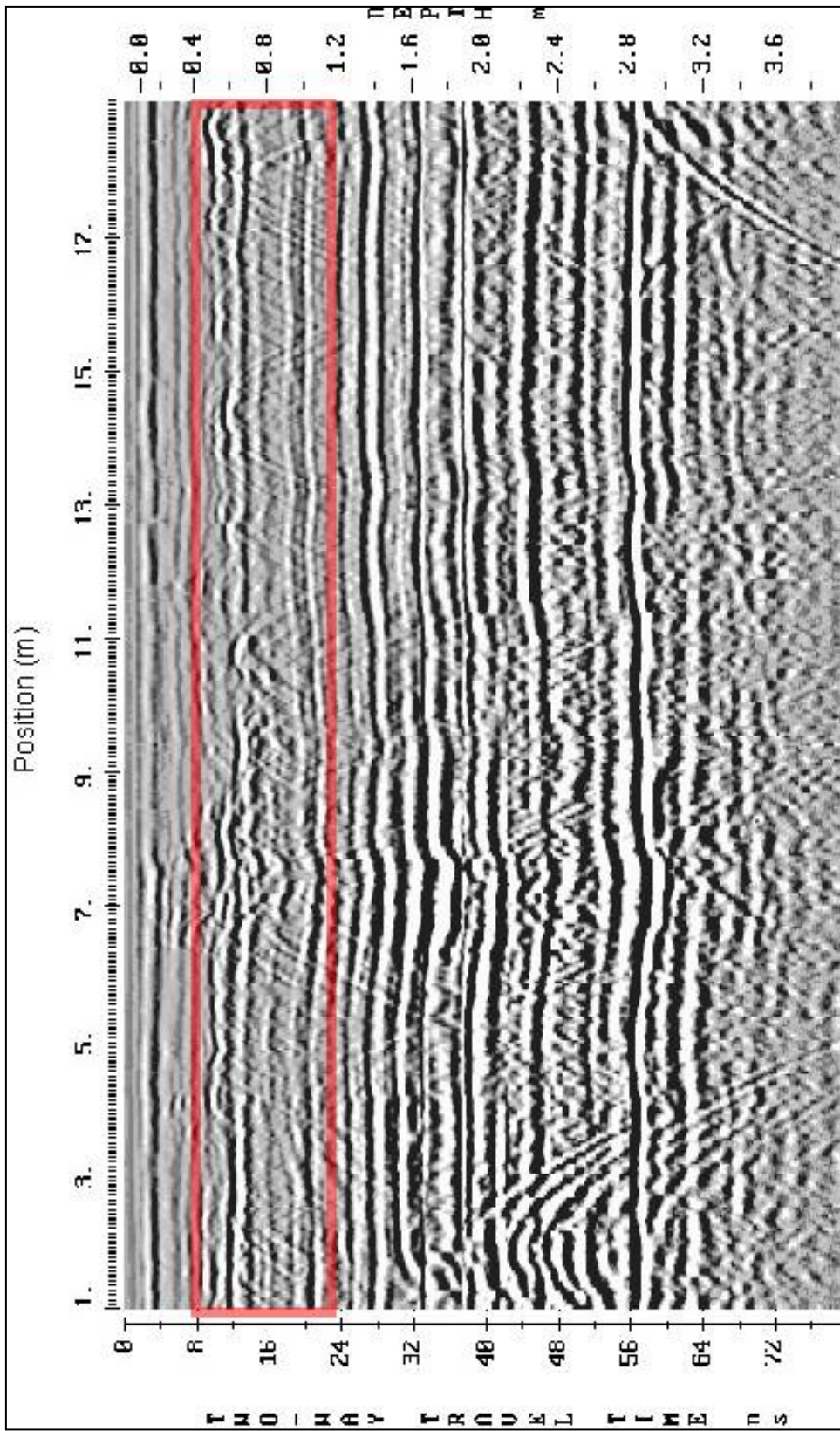
Velocity analyses were performed using common midpoint (CMP) and wide-angle reflection-refraction (WARR) surveys. Velocities were obtained using the CMP/WARR analysis module in the Deluxe EKKO View software packages. Velocities obtained (0.098-0.101 m/ns) were used for depth estimates and topographic correction. Tables B1–B3 in Appendix B shows the results of velocity analyses for each line. Stratigraphic units were measured and described in detail in both the OSLW and Adair quarries and compared to the high resolution GPR profiles. The reconstruction of facies types from radar patterns (e.g., Asprion et al., 2000) was used in conjunction with outcrop information to identify major radar facies packages and radar relationships to the stratigraphy at each site.

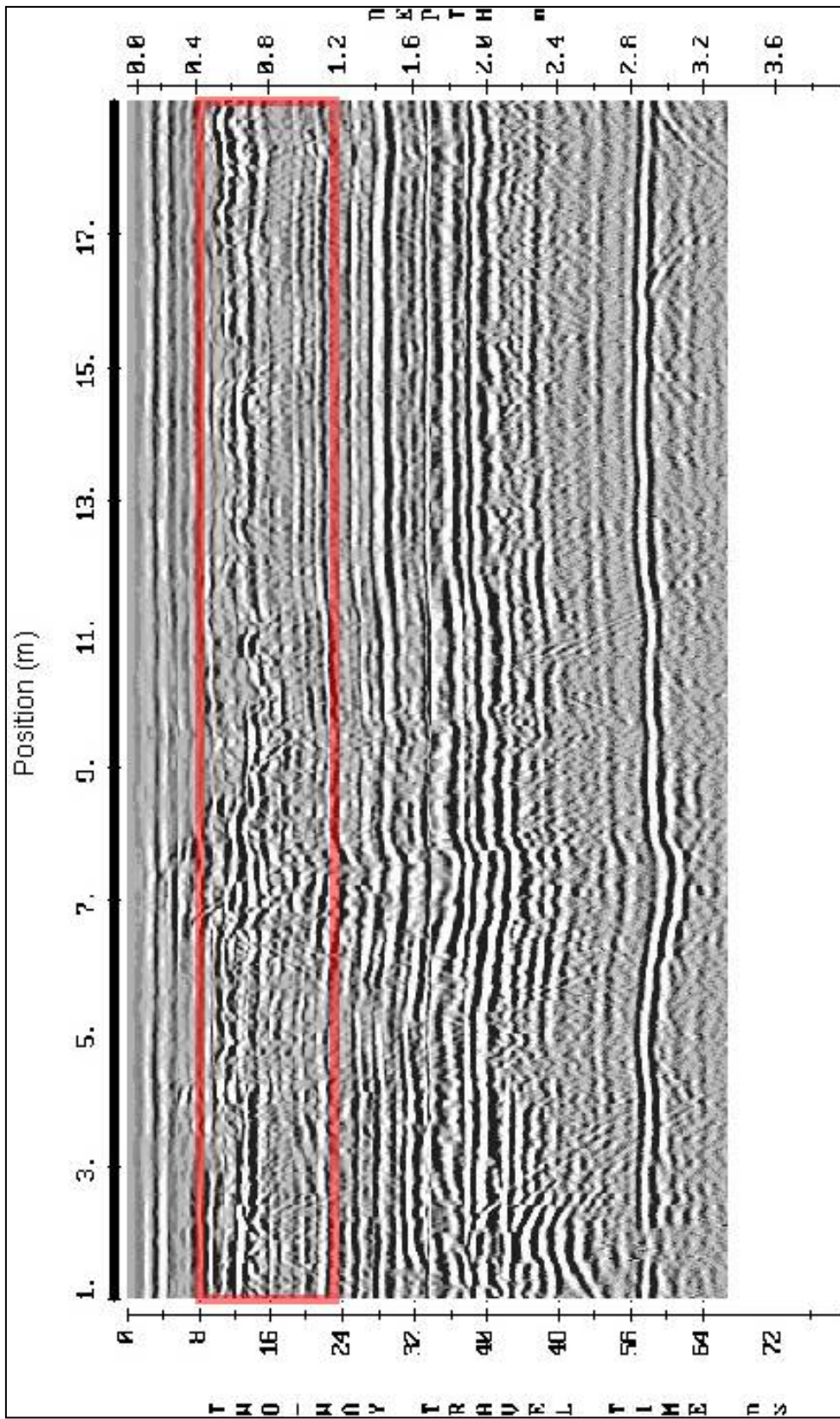
Figure 5.3A (see page 99): 225 MHz Profile of Line 6 at the north end of the OSLW Quarry. The velocity obtained for this line was 0.10 m/ns. The profile was acquired using a station spacing of 0.05 m; the time sampling was 100 ps, and the stacking number was 64. Processing of this profile included the application of a SEC gain of 1000; attenuation = 1; down the trace averaging of 5 samples, and traces per inch = 20. The red box indicates a zone corresponding to abundant small-scale heterogeneities (vugs and nodules) in the uppermost meter of the exposed section.

Figure 5.3B (see page 100): 450 MHz Profile of Line 6 at the north end of the OSLW Quarry. The velocity obtained for this line was 0.099 m/ns. The profile was acquired using a station spacing of 0.05 m; the time sampling was 100 ps, and the stacking number was 64. Processing of this profile included the application of a SEC gain of 1000; attenuation = 0.8; down the trace averaging of 3 samples, and traces per inch = 40. The red box indicates a zone corresponding to abundant small-scale heterogeneities (vugs and nodules) in the uppermost meter of the outcrop with greater resolution than illustrated in Fig. 5.3A.

Figure 5.3C (see page 101): 900 MHz Profile of Line 6 at the north end of the OSLW Quarry. The velocity obtained for this line was 0.099 m/ns. The profile was acquired using a station spacing of 0.025 m; the time sampling was 100 ps, and the stacking number was 64. Processing of this profile included the application of a SEC gain of 1000; attenuation = 0.8; down the trace averaging of 3 samples, and traces per inch = 60. The red box indicates a zone corresponding to abundant small-scale heterogeneities (vugs and nodules) in the uppermost meter of the outcrop with greater resolution than illustrated in Fig. 5.3A and B.







5.4 Results

5.4.1 Correlating GPR with geology at OSLW

The change in resolution between the 225 MHz, 450 MHz, and 900 MHz profiles is apparent in Figure 5.3. The higher frequency antennae (900 MHz) reveal finer details (10's of centimetres) that correspond to those mapped on a geological scale (centimetres to 10's of centimetres). For example, a red box has been drawn on the radar images to emphasize a zone corresponding to vuggy pores and nodules in the uppermost metre. The comparison among Figures 5.3A, 5.3 B and 5.3C shows the progressive resolution improvement in the heterogeneous imaging with increasing frequency. The overlapping diffractions on the lower frequency profiles obscure the depth and position of the small-scale heterogeneities. The profile obtained using 900 MHz antennae provided the best definition of the depth and location of the apex of individual diffractions, allowing improved imaging of these heterogeneities. Radar surveys performed in this study yielded high resolution images at shallow depths down to ~ 4 m. Although resolution is greatly improved with higher frequency antennae, the depth of penetration of the radar unit decreases as the frequency is increased. The GPR transmission characteristics of the carbonates allow high resolution imaging to depths comparable to the outcrop scale. Lower frequency antennae (50–200 MHz) units are utilized in Chapter 6 to delineate lateral and vertical facies changes to depths ~ 27 m.

The locations of the high frequency profiles are illustrated in Figure 5.4. The consistency and accessibility to the geology in the controlled area of the quarries allowed for accurate geologic correlation with GPR reflection events. For the correlation with the

carbonate facies, we present the 900 MHz profiling which provided the highest resolution data at both the north and south end of the OSLW Quarry. 225 MHz and 450 MHz profiles from each location within the quarry are provided in Appendix B. 450 MHz antennae were the only antennae used to profile and examine the potential reef mound near the center of the quarry.

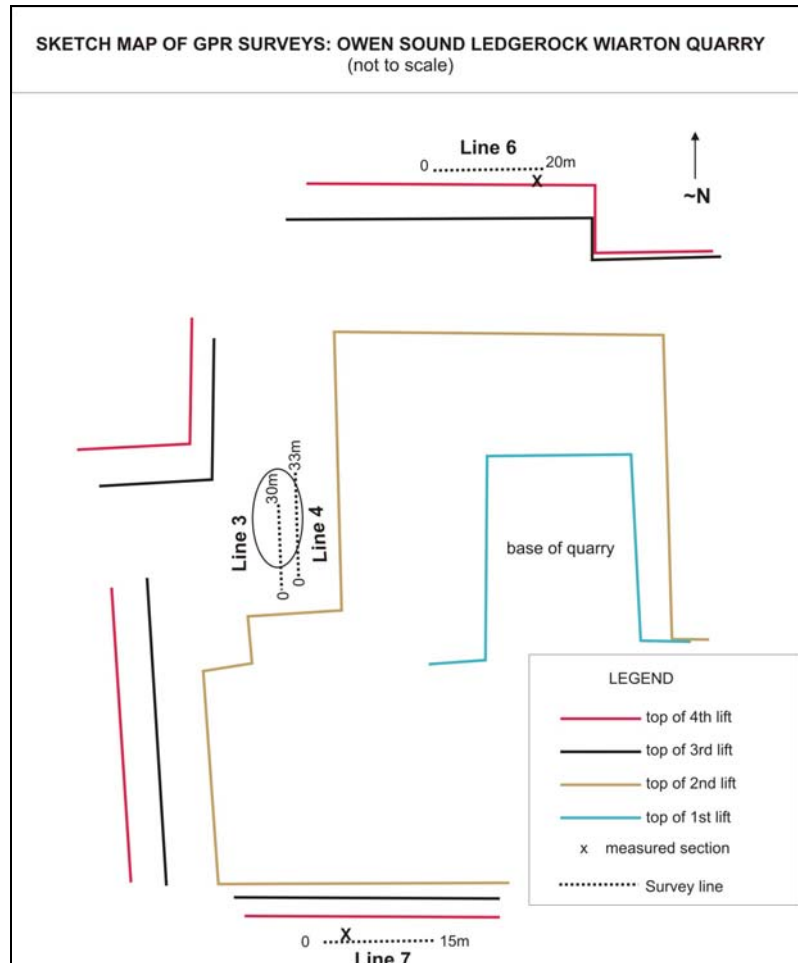


Figure 5.4: Map of the west side of the OSLW Quarry. Line 6 is situated at the north end of the quarry on top of the 4th lift. Line 3 (reef mound) is located in the center on top of the 2nd lift, with Line 4 located on the mound's flank. Line 7 is at the south end of the quarry located on top of the 4th lift.

5.4.1.1 Line 6 and Line 7

The 900 MHz profiles along Lines 6 and 7 (Figs. 5.5–5.7) resolve fine detail in the upper 3 m of the OSLW Quarry. Non-annotated 900 MHz GPR profiles of Line 6 and 7 are illustrated in Figure 5.5. Detailed correlation between the radar images of Lines 6 (Fig. 5.6) and 7 (Fig. 5.7) with the quarry geology illustrates that strata in both the north and south end of the quarry are very similar. The notable exception is the uppermost ~ 80 cm at Line 6 which is absent at the Line 7 site. This uppermost section (Reflector E in Fig. 5.6) contains additional material that is heterogeneous, deformed, and vug- and nodule-rich. In the south end of the quarry at Line 7, this material is absent likely due to pinch-out or erosion.

The lowermost reflection (A) is very strong and found at a relatively consistent depth (2.75 m at Line 6; 2.6 m at Line 7) throughout the quarry. It corresponds with the contact between a lower tan-grey massive ‘2-foot’ bed that is vuggy (vugs range from 1 mm–5 cm and are calcite, and/or pyrite-, and/or more rarely fluorite-lined) and a tan-brown strongly bioturbated stylolitic unit that is traceable across the quarry. An apparent increase in the visibly vuggy porosity and crystallinity in the lower vuggy ‘2-foot’ bed is a likely explanation for this strong reflector. Reflector A (dashed in the photo in Fig. 5.5) occurs less than 5 cm below the quarry floor at Line 6 and 7 locations (Fig. 5.6 and 5.7 respectively).

Reflector B is also prominent from the north end at Line 6 to the south end at Line 7 of the quarry. It correlates with the top of the informally named ‘I-beam’ bed, which is a porous tan-brown unit bounded by thick stylolite seams that tend to form localized fracture planes and includes a minor number of vugs up to 2 by 4 cm in size.

Reflector C is found at approximately 1.1 m depth at Line 7 and at 1.58 m depth at Line 6. It correlates with the contact between an underlying strongly bioturbated stylonitic unit and a massive, porous bed similar to the 2-foot bed but is somewhat less vuggy. In addition, a continuous 1 cm-thick horizontal seam containing dry to moist fine soil and plant debris, which is visible on the quarry face, occupies the solution-enhanced joint at this contact. The presence of this organic material probably contributes to the contact reflectivity.

Reflector D is related to an extensive horizontal break between an upper massive porous unit and an underlying thick (0.5 m) dark black and gray-brown prominently laminated argillaceous bed with relatively minor porosity.

Package E (Line 6 only) is a series of small diffractions generated by small-scale heterogeneities within a bed that contains vugs and nodules, has deformed laminae, and undulating contacts.

Vertical joints and fractures exposed on the surface at positions 4, 9, and 11 m appear to cause diminished signal penetration along the radar profile at Line 7. Fractures, their widths, and relative orientations along Line 7 are illustrated in Figure 5.8. Fractures are up to 0.18 m wide and are filled at the surface with dry to moist soil and plant debris. The depth at which the fractures extend is variable from centimetres to metres.

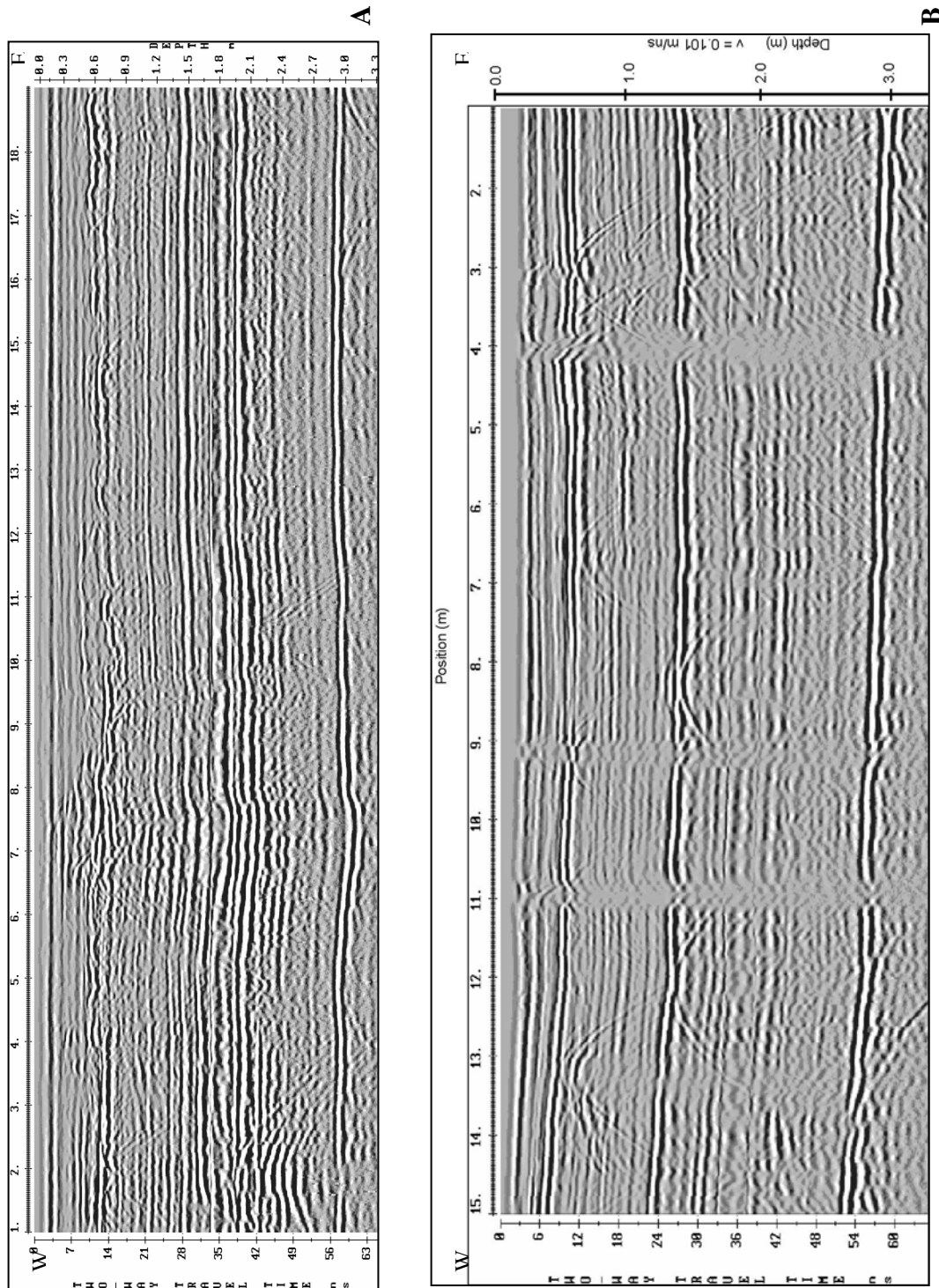


Figure 5.5: The 900 MHz profile of Line 6 (A) and Line 7 (B) from the north and south ends of the OSLW Quarry, respectively. The velocities obtained for these lines were 0.099 m/ns and 0.101 m/ns. The profiles were acquired using a station spacing of 0.025 m; the time sampling was 100 ps, and the stacking number was 64. Processing of this profile included the application of a SEC gain of 1000; attenuation = 0.8 and 0.6; down the trace averaging of 3 samples, and traces per inch = 40.

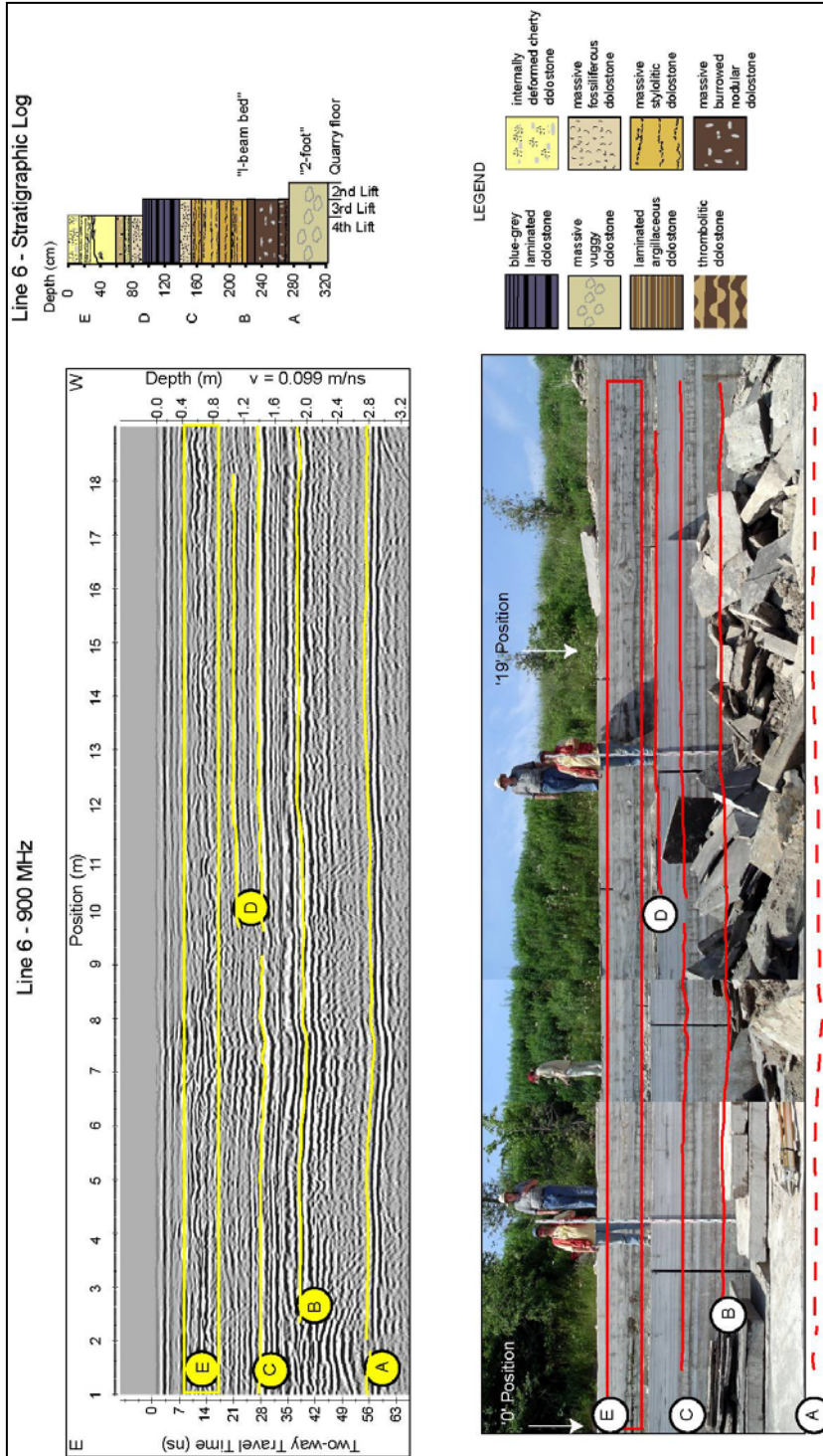


Figure 5.6: The 900 MHz profile of Line 6 has strong reflectors (A-D) as well as a shallow vuggy zone represented by multiple diffractions (E). The stratigraphic log shown to the right was measured at position '0' on the survey line.

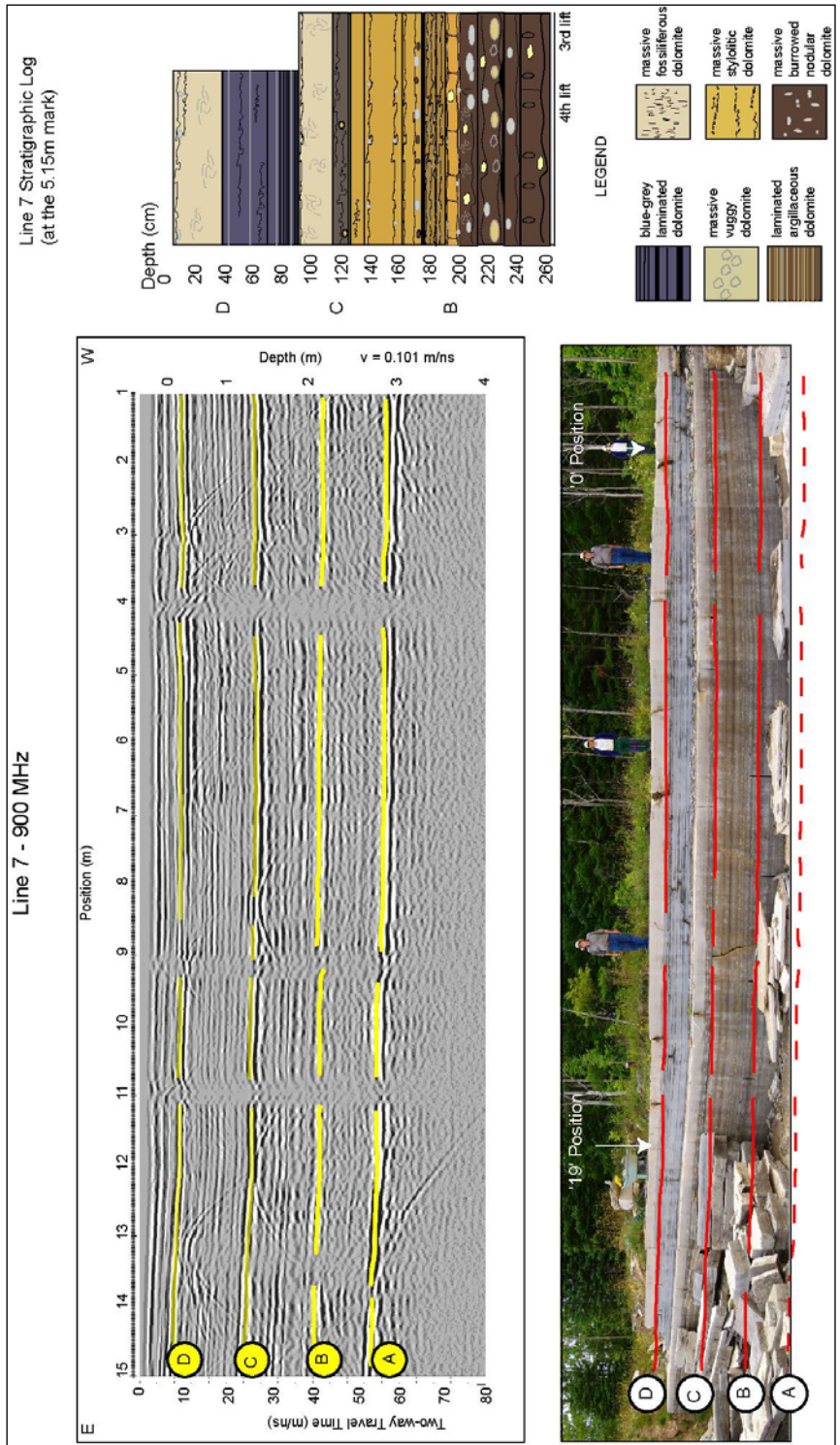


Figure 5.7: The 900 MHz profile of Line 7 has strong reflectors (A-D), and is missing the upper ~1 m of rock compared with Line 6 (package E). The stratigraphic log shown to the right was measured at 5.15 m on the profile.

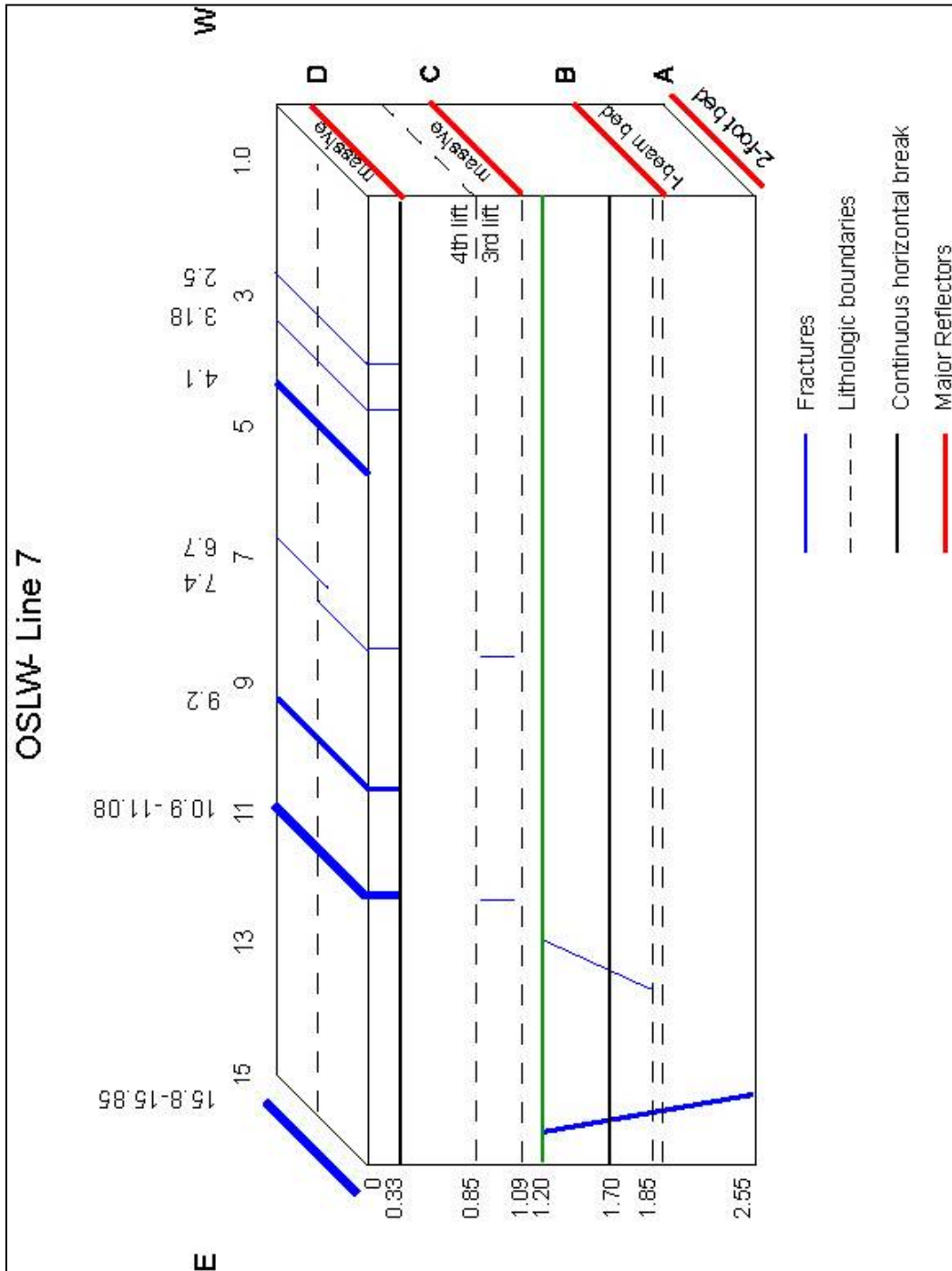


Figure 5.8: Vertical breaks in the continuity of reflections due to the dissolution-enhanced joints and fractures (thick blue lines) at Line 7. Major horizontal breaks (black and green) occur at or near lithologic boundaries.

5.4.1.2 Line 3: Potential reef mound

Two surveys were performed parallel to the length of the reef mound. Line 3 was carried out along the top of the reef mound and Line 4 was run along the flank of the mound. Line 3 is illustrated in Figure 5.9, i.e. the GPR profile of Line 4 does not provide additional information about the internal structure of the reef mound and is provided in Appendix B.

Strong planar reflectors were imaged to the south of the reef mound. Although it was not possible to conduct a visual transect directly into the mound, the closest quarry face indicates that the reef mound sits directly on top of the 2-foot bed. Thus, Reflector A is correlated with the top of the 2-foot bed. Reflector X is likely the base of the 2-foot bed where visibly vuggy porosity dramatically decreases as the lithology changes downward to more finely crystalline, argillaceous dolostone referred to locally as the ‘Marble Beds’. Below Reflector X, the discontinuous planar reflectors collectively named Reflector Y represent these Marble Beds (Fig. 5.9). The lowermost Reflector Z was inferred from core located ~ 800 m to the southwest of the mound that revealed a vuggy, more porous unit found below the Marble Beds.

The GPR signature of the mound at the north end of the profile (see box in Fig. 5.9) is predominantly composed of diffractions. This scattering is due to the small-scale heterogeneities associated with the mound’s expected heterogeneous interior. This dispersion impedes the propagation of electromagnetic waves to the underlying strata causing a shadow effect below the mound.

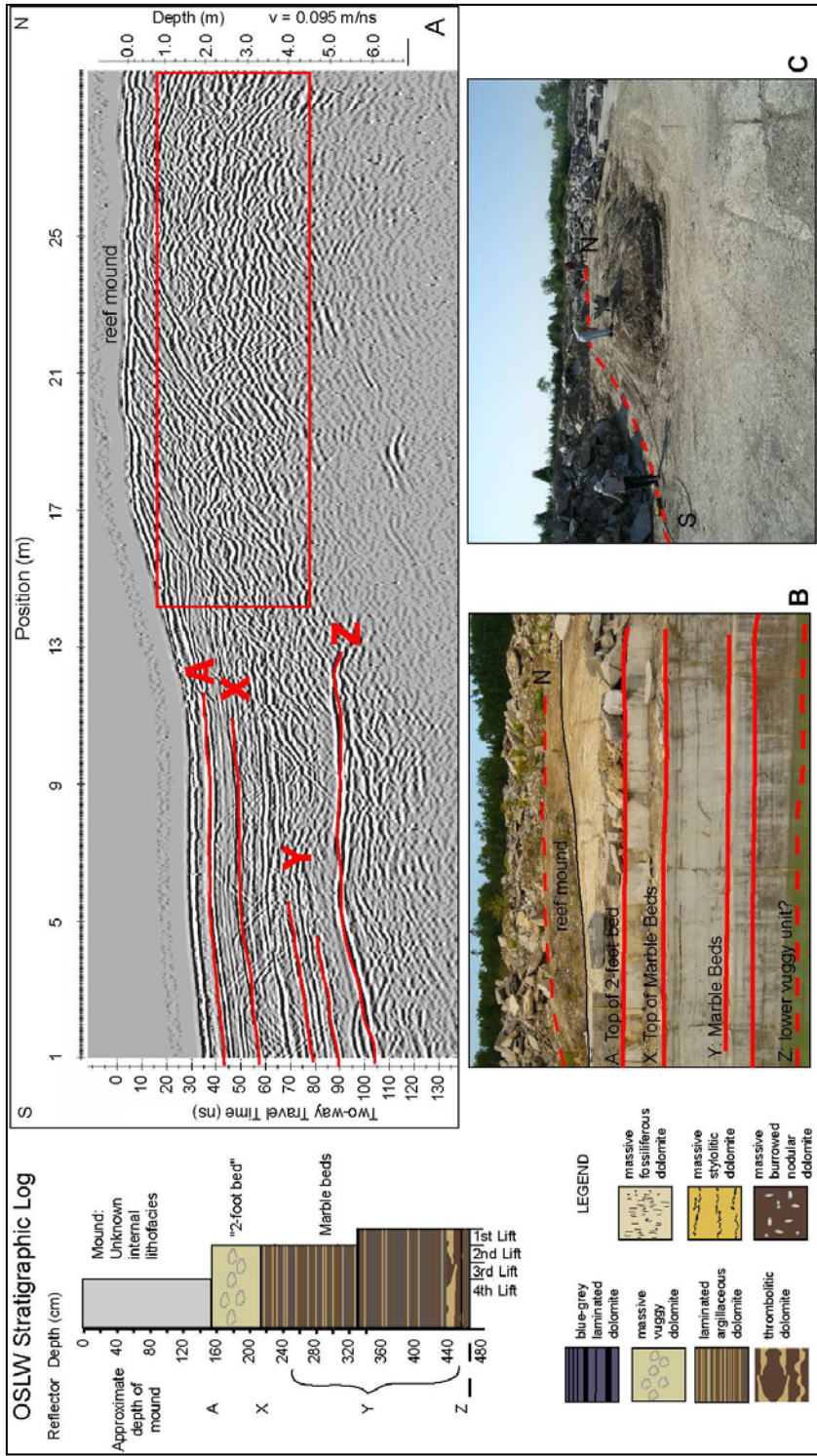


Figure 5.9: A) The 450 MHz GPR profile along Line 3 overlying the reef mound; B) Photograph showing units underlying the reef mound; and C) Photograph showing the reef mound with the position of Line 3 indicated. Stratigraphic log shown at left illustrates the stratigraphy at the Line 3 site.

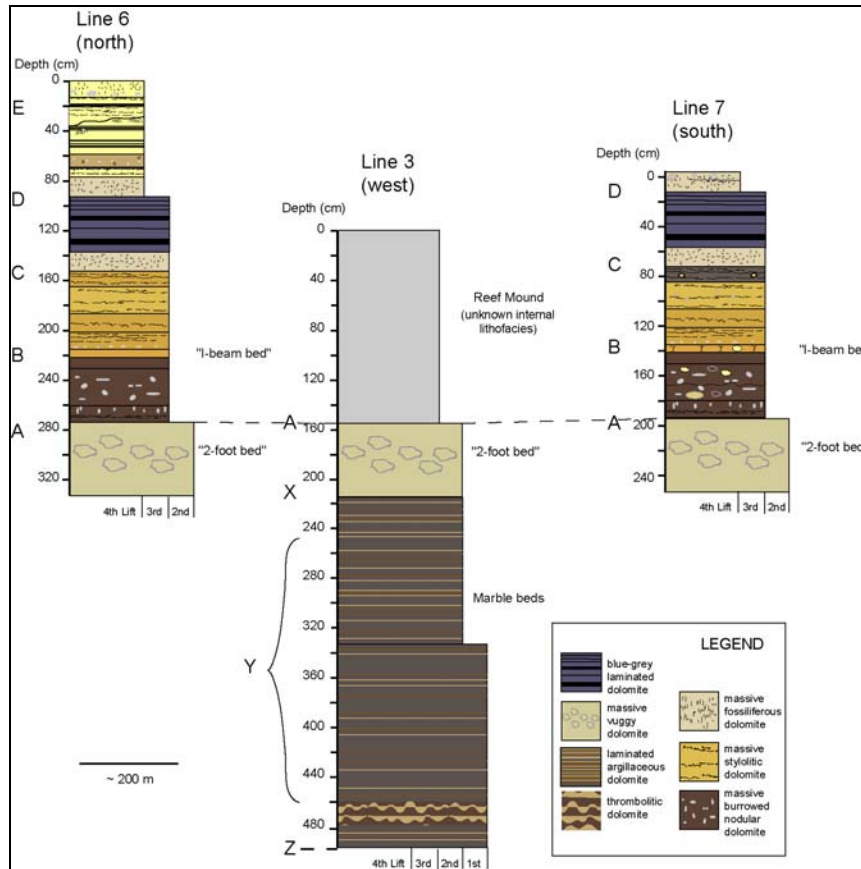


Figure 5.10: Geologic cross section between the three sites in the vicinity of the OSLW Quarry. At each site the ‘2-foot’ bed provides a strong marker horizon (Reflector A). The legend in the lower right corner illustrates the various lithofacies of the Eramosa Member in the OSLW Quarry.

A composite stratigraphic section at each site within the OSLW Quarry is illustrated in Figure 5.10. Geologic properties such as porosity and density show similar radar responses across the OSLW Quarry. Reflector A is consistently imaged throughout the quarry and correlates to the ‘2-foot’ bed, which is also a valuable marker horizon for interpreting the local geology.

5.4.2 Correlating GPR with geology at the Adair Quarry

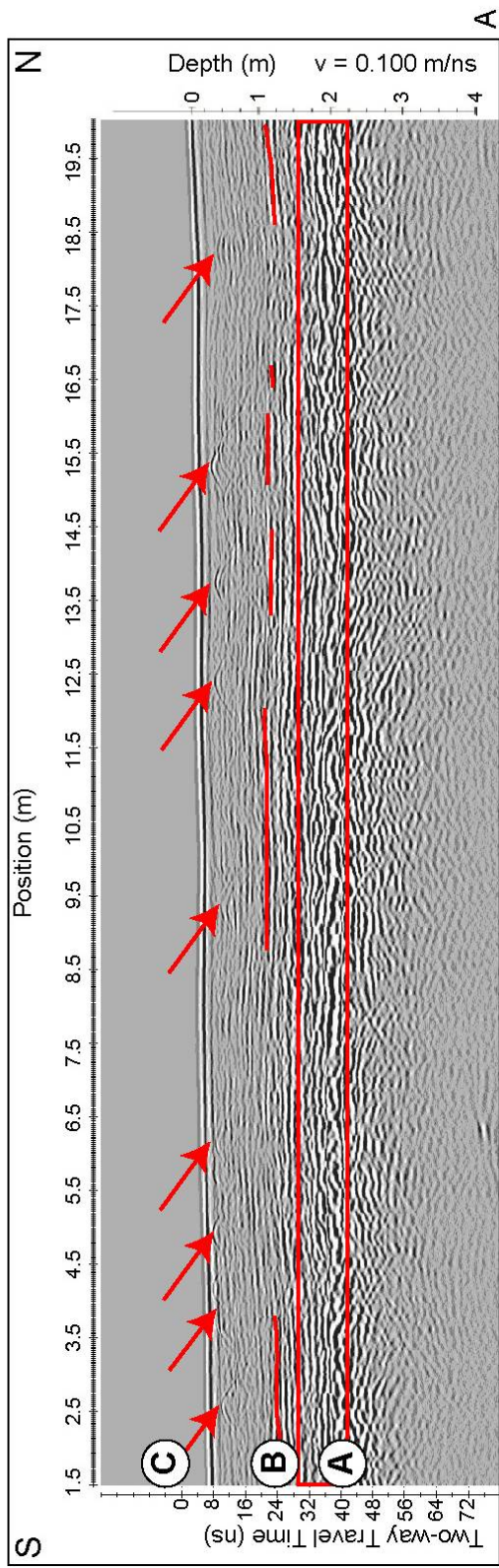
The Amabel Formation is found at surface on the eastern side of the Bruce Peninsula, where the Adair Quarry is situated. Karstic features within the Amabel Formation are mainly large cavities and solution-enhanced fractures and joints. In the vicinity of the GPR profile at the Adair Quarry, a prominent solution-enhanced horizontal fracture was observed in the quarry wall.

Figures 5.11 and 5.12 give the unannotated and interpreted 900 MHz profiles, respectively; the corresponding 225 and 450 MHz profiles are given in Appendix B. On the radar profile in Figure 5.12 the fracture zone, highlighted with a red box (Reflector A in Fig. 5.12), is characterized by discontinuities in the reflections and strong diffractions. Above the fracture zone, outcrop study reveals that bioturbated beds and minor stylolite seams within the Amabel Formation probably produced discontinuous planar features seen in the radar image highlighted in red (Reflector B in Fig. 5.12). Diffractions in the upper 50 cm likely represent vugs and/or nodules (Reflector C in Fig. 5.12).

Figure 5.11 (see page 114): The 900 MHz profile of Line 2 from the Adair Quarry. The velocity obtained for this line was 0.10 m/ns. The profile was acquired using a station spacing of 0.025 m; the time sampling was 100 ps, and the stacking number was 64. Processing of this profile included the application of a SEC gain of 600; attenuation = 1.4; down the trace averaging of 3 samples, and traces per inch = 60.

Figure 5.12 (see page 115): **A)** 900 MHz GPR profile at the Adair Quarry. Radar image reveals a small-scale heterogeneous reflectivity within the Amabel Formation. The red box (**A**) highlights a solution-enhanced horizontal fracture with varying opening widths along the quarry face (photo in **B**), indicating the presence of one or more karstic horizons. Reflector B is indicated by the discontinuous red line. Red arrows (**C**) point to the apex of small diffractions in the upper 50 cm, which correlate to vuggy pores and/or nodules.

Adair Quarry
Line 2 - 900 MHz



5.5 Conclusions

High frequency GPR profiling was successfully used to image stratigraphic, karstic, and diagenetic features identified at both the OSLW and Adair quarries on the Bruce Peninsula. We observed that vertical facies changes within the stratigraphy at the OSLW quarry (Line 6 and 7) were evident as continuous planar reflections with the high frequency (900 MHz) unit. Our study also found that lateral facies changes were clearly imaged in the radar profile at the potential reef mound (Line 3). Furthermore, we correlated diagenetic features such as vugs and nodules, as well as dissolution horizons, with radar events (e.g., diffractions) at both the OSLW and Adair quarries.

Solution-enhanced joints and fractures, vugs and mounds are a negative attribute of these carbonates that, if imaged with high frequency GPR, can be avoided by quarry operators in their search for suitable building-stone or aggregate. For example, impurities within the Amabel Formation that are found within vugs, nodules and karstic horizons are a detriment to building stone and aggregate quality. GPR is an economical tool that provides quarry operators with the locations of such features that is otherwise costly to acquire. This field-based study clearly demonstrates that high-resolution GPR techniques in combination with detailed geologic mapping can be employed as a cost effective exploration method for resource estimates in building-stone quarries, especially where the lack of subsurface data limits other means of assessing the resource potential.

Chapter 6: Low Frequency GPR Profiling of Deep Subsurface Stratigraphy in Silurian Dolostones

6.1 Introduction

Ground-penetrating radar (GPR) is an effective tool for defining deep (~30 m) stratigraphic changes within carbonates (Asprion et al., 2000) as well as their internal architecture (Pratt and Miall, 1993). Whereas a significant body of work has focused on unconsolidated clastic deposits (e.g., Roberts et al., 2003), comparatively little work has been done on consolidated carbonates. Within carbonates, GPR has been utilized as a tool for identifying large-scale sedimentary structures such as cross-bedding, defining variations in lithologies (Dagallier et al., 2000), and for imaging the lateral extent of karstic caves and fractures (Chamberlain et al., 2000).

One would reasonably expect GPR to be a valuable geophysical method for subsurface imaging of Silurian dolostones; however, very little work has been done in carbonates. A previous GPR study conducted on the Amabel Formation along the Niagara Escarpment in southern Ontario (Pratt and Miall, 1993) was able to delineate lithologic variability between carbonate beds and argillaceous lenses. More recently, a GPR study on the stratigraphy in the OSLW Quarry was carried out using more modern equipment and signal processing techniques (Tetreault, 2001).

The purpose of this field study was to investigate the low frequency (50-200 MHz) GPR profiling for imaging deep (20-30 m) stratigraphic and karstic features in carbonate rocks. Furthermore, we assessed the predictive capabilities of this method for delineating

building stone resources (i.e., lateral continuity and thicknesses of key building stone units). Building-stone quarries on the Bruce Peninsula provide an excellent opportunity to study the application of GPR profiling of deep carbonate strata. Both the OSLW and Adair quarries (Fig. 6.1) offer three-dimensional exposures of outcrop with little or no overburden and a lowered water table, providing conditions that are ideal for GPR surveys. The Ontario Geological Survey (OGS) drilled several boreholes from 1982-1990 in support of a regional mapping project. Three of the boreholes were stratigraphically logged during the summer of 2005 as a part of this thesis, and are relatively close to the GPR sites.

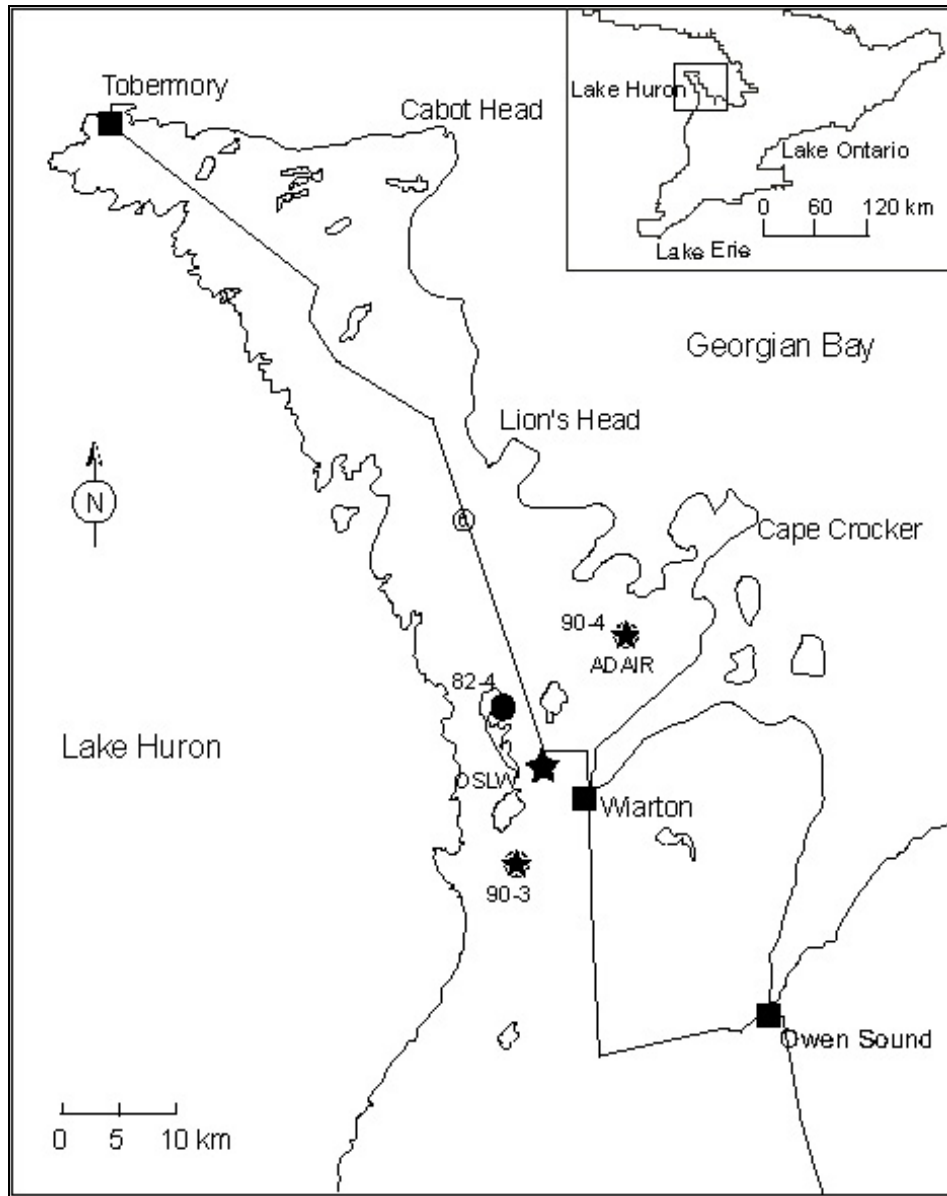


Figure 6.1: Map of the Bruce Peninsula. Stars represent the locations of GPR surveys, and circles represent the location of boreholes. Squares are located at main cities on the Peninsula. Inset map of southern Ontario highlights the study area with a box (adapted from Armstrong et al., 2002).

6.2 Geological Setting

Figure 6.2 illustrates the Silurian stratigraphic nomenclature for our study area on the Bruce Peninsula. Although the lowermost Dyer Bay Formation dolostones of the Clinton Group were not imaged with the GPR in this study, the boundary between the top of the argillaceous dolostones and shales of the Wingfield Formation and the overlying fossil-rich dolostones of the Fossil Hill Formation were observed. Alternating shale and dolostone units of the lower Clinton Group represent oscillating sea levels during this time (Sanford, 1969). The Fossil Hill Formation, deposited at the end of the Clinton time, records an abundance of shelly fossils representative of a shallow marine depositional environment. The overlying Amabel and Guelph formations record depositional environments that reflect partially restricted marine to more open marine conditions along the eastern margin of the Michigan Basin. Dimension stone and aggregate quarry operations are a significant local industry on the Bruce Peninsula, with much of the activity concentrated in the Eramosa Member of the Guelph Formation and the underlying Wiarton and Colpoy Bay members of the Amabel Formation (Fig. 6.2).

The three GPR survey sites were selected where different lithofacies of the Silurian stratigraphy on the Bruce Peninsula could be imaged (Fig. 6.2). The Adair Quarry, which is located ~ 13 km to the northeast of the OSLW Quarry, reveals ~ 10 m of the Amabel Formation. At the Adair Quarry, the Amabel Formation consists of cream-tan and blue-gray mottled dolomitized grainstones that form medium to coarsely crystalline beds, containing wide (1–30 cm) solution joints and fractures visible in the upper 3–4 m. Borehole OGS-90-4,

located within ~ 15 m of the survey line, reveals the carbonate stratigraphy from the Amabel Formation down to the Dyer Bay Formation.

The OSLW Quarry exposes ~ 8 m of thin-to thick-bedded relatively deeper lagoonal dolostones of the Eramosa Member. This distinctive unit is characterized by cm- to m-scale laminated dark brown argillaceous dolostone that is finely crystalline and bituminous, and contains chert nodules associated with calcite, pyrite and more rarely fluorite.

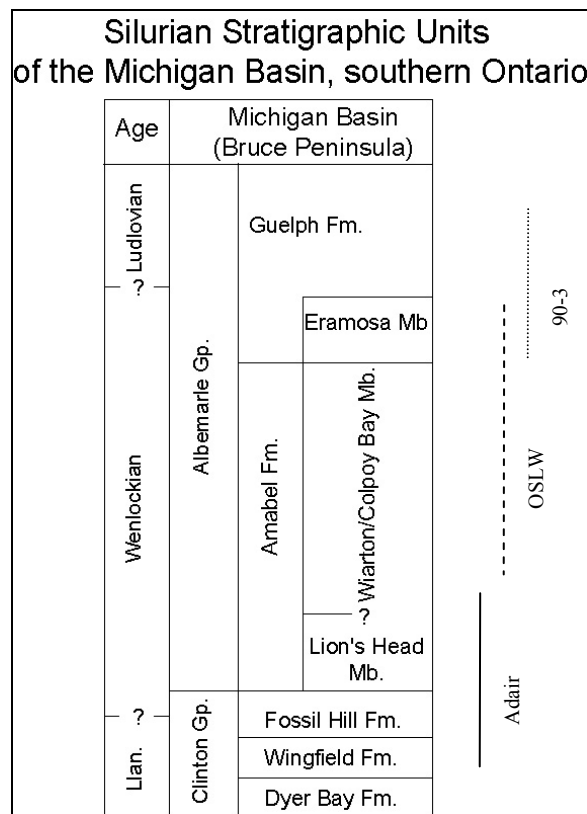


Figure 6.2: Silurian stratigraphic units of the Bruce Peninsula (adapted from Bolton, 1957; Johnson et al., 1992). The solid, dashed and dotted lines represent the stratigraphy imaged using GPR at the Adair Quarry, the OSLW Quarry, and the 90-3 borehole site, respectively.

The third site was at the location of borehole OGS-90-3, which was drilled ~ 7 km southwest of OSLW, where less than 1 m of overburden covers the Guelph Formation at surface. This borehole reveals medium crystalline, massive tan dolomitic grainstone of the Guelph Formation overlying the bituminous argillaceous Eramosa Member. Although the Guelph Formation, Eramosa Member, and the Amabel Formation are pervasively dolomitized, the Guelph and Amabel formations are more homogeneous than the Eramosa Member.

6.3 Methodology

GPR surveys were conducted at the OSLW Quarry in July 2004 and 2005, and at the Adair Quarry in August 2005. Survey lines were located on top of and oriented parallel to existing quarry faces. In August 2005, a GPR survey was also conducted along a gravel road adjacent to the 90-3 borehole. Each survey was performed with a PulseEKKO 100 system using three antenna frequencies (50, 100, and 200 MHz).

The 50 MHz antennae provide the greatest depth penetration (Fig. 6.3C) and, therefore, have the ability to correlate deeper lithologic boundaries with radar reflectors. In comparison, the 100 MHz antennae achieve a reasonable compromise between resolution and penetration depth. In this chapter, we present the correlation between radar images and carbonate geology using the 50 MHz profiling for four sites. In addition, we also present the 100 MHz profiling at three sites to provide higher resolution images of the shallow stratigraphy.

The 50 and 100 MHz profiling were acquired using a station spacing ranging from 0.10–0.25 m. The time sampling was 800 ps, and the stacking number was 64. Processing of each profile included the use of:

- Dewow
- Spreading and exponential compensation (SEC) gain
- Down the trace averaging (5 - 9 samples)
- Topographic correction

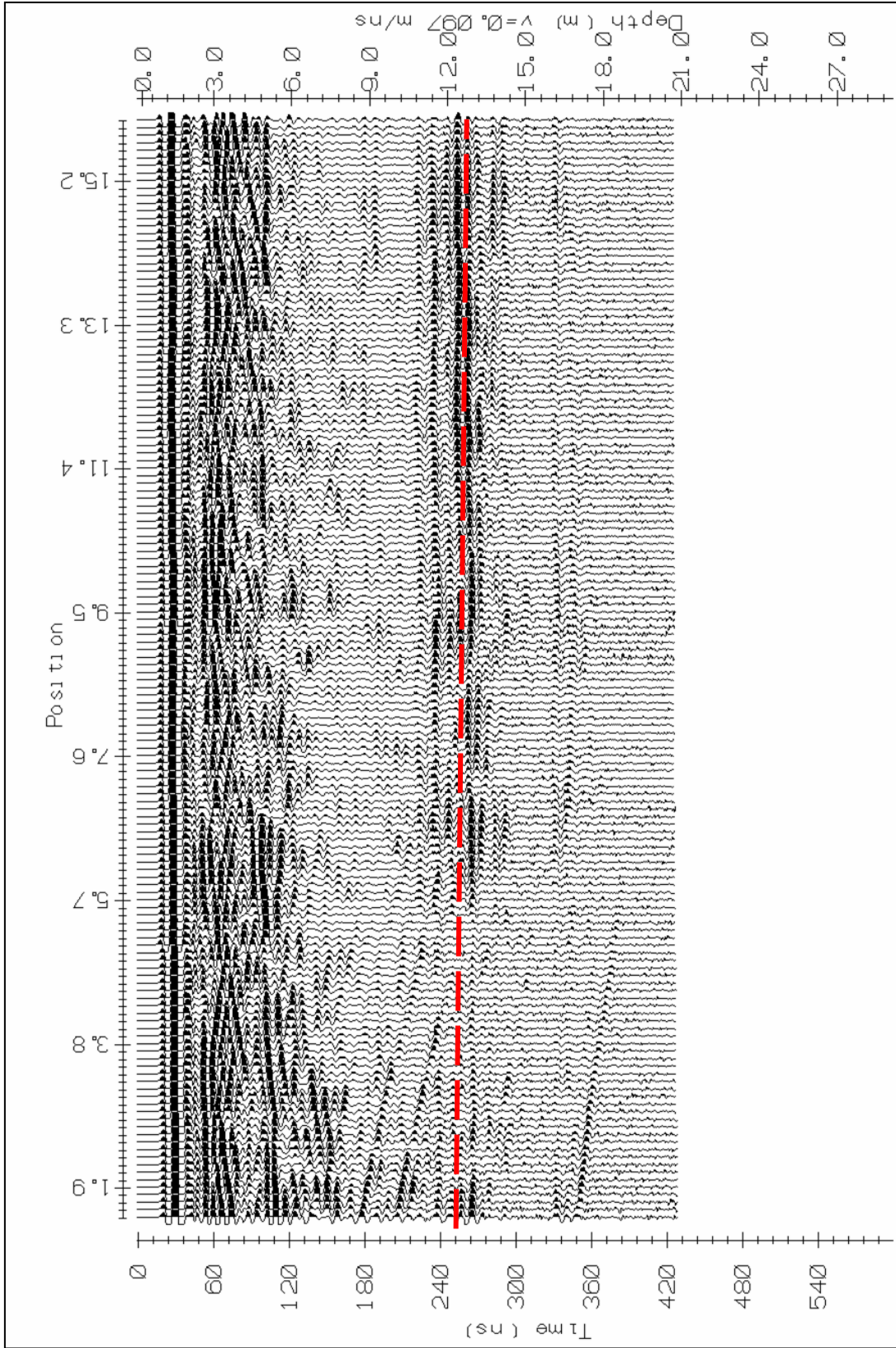
Velocity analyses were performed using common midpoint (CMP) surveys.

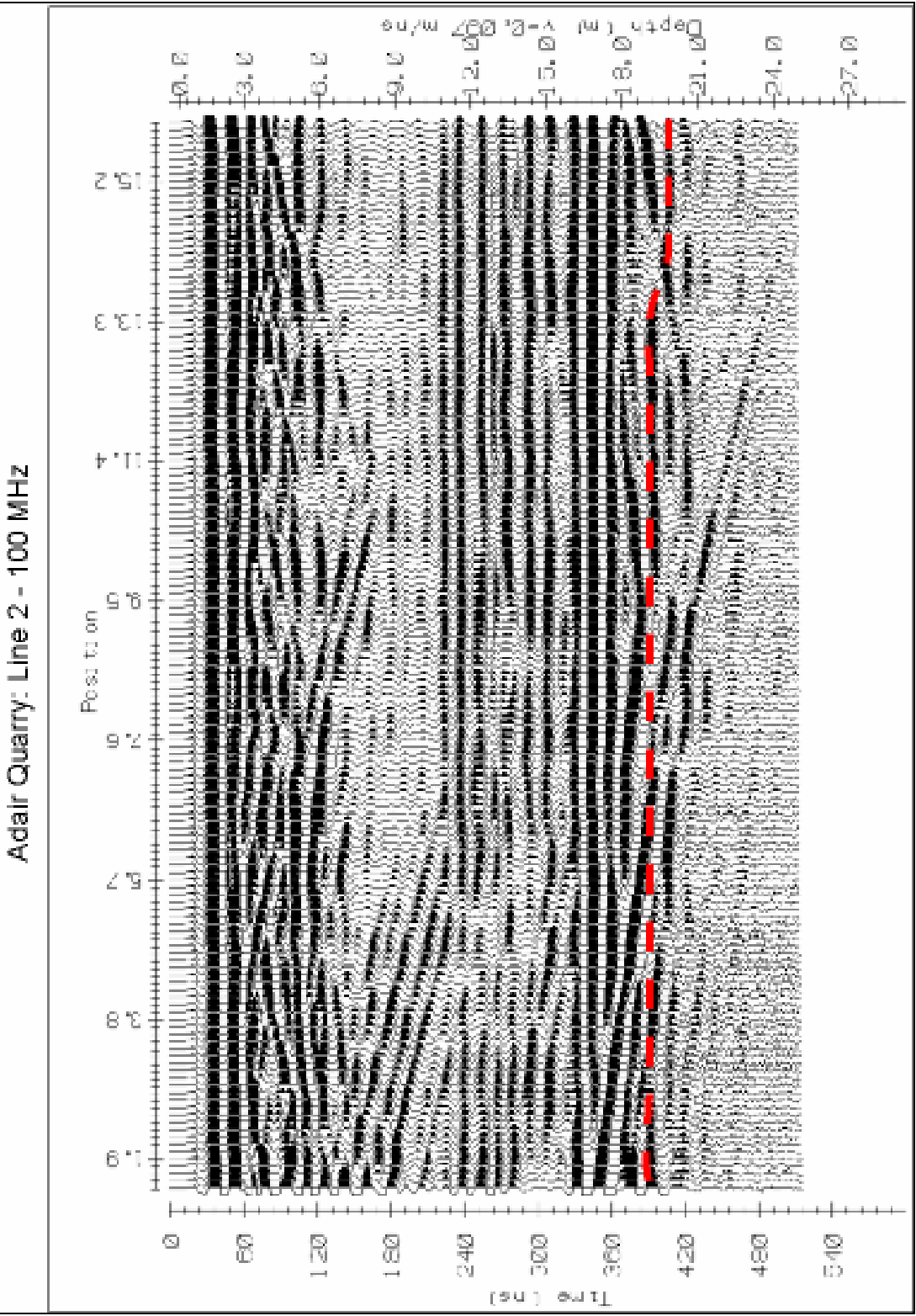
Velocities obtained (0.096-0.101 m/ns) were used for depth estimates and topographic correction. Boreholes 90-3 and 90-4 were logged in detail and major facies boundaries were correlated with the low frequency GPR profiles. Formation thicknesses observed within borehole 82-4 were used to guide the interpretation of GPR profiles from the OSLW Quarry, allowing for the ~ 10 km separation between these two locations. The reconstruction of facies types from radar patterns (e.g., Asprion et al., 2000) was used in conjunction with outcrop and borehole information to identify major radar facies packages at each site.

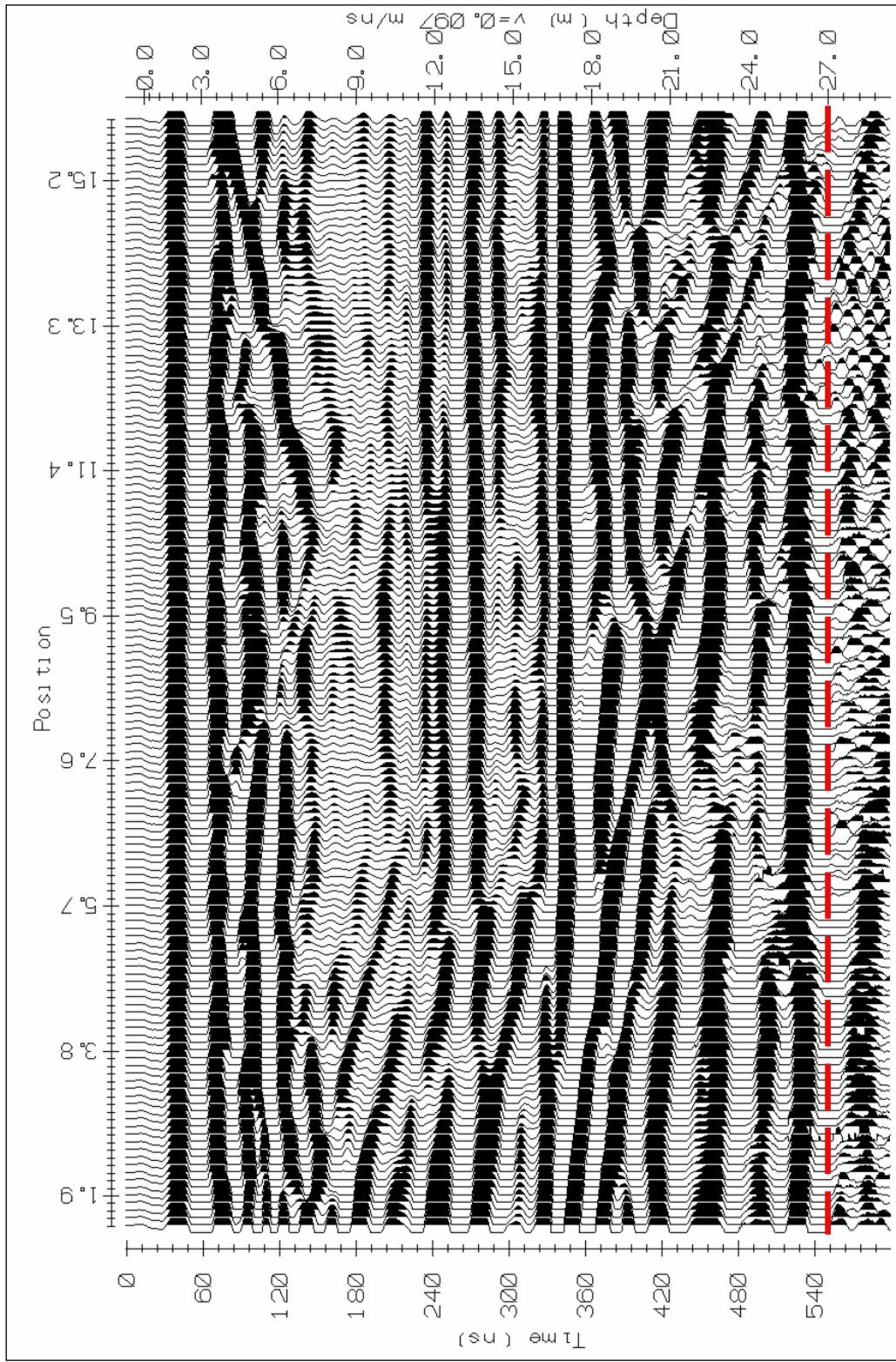
Figure 6.3A (see page 125): 200 MHz profile of Line 2 at the Adair Quarry. The velocity obtained for this line was 0.097 m/ns. The profile was acquired using a station spacing of 0.10 m; the time sampling was 800 ps, and the stacking number was 64. Processing of this profile included the application of a SEC gain of 1000; attenuation = 1.2; down the trace averaging of 1 sample, and traces per inch = 20. The red dashed line indicates the effective depth of penetration at ~ 14 m.

Figure 6.3B (see page 126): 100 MHz profile of Line 2 at the Adair Quarry. The velocity obtained for this line was 0.097 m/ns. The profile was acquired using a station spacing of 0.10 m; the time sampling was 800 ps, and the stacking number was 64. Processing of this profile included the application of a SEC gain of 1000; attenuation = 0.6; down the trace averaging of 3 samples, and traces per inch = 20. The red dashed line indicates an effective depth of penetration at ~ 20 m.

Figure 6.3C (see page 127): 50 MHz profile of Line 2 at the Adair Quarry. The velocity obtained for this line was 0.097 m/ns. The profile was acquired using a station spacing of 0.10 m; the time sampling was 800 ps, and the stacking number was 64. Processing of this profile included the application of a SEC gain of 1000; attenuation = 0.6; down the trace averaging of 9 samples, and traces per inch = 20. The red dashed line indicates an effective depth of penetration at ~ 27 m.







6.4 Results

6.4.1 Correlating GPR with geology at the Adair Quarry

Although the resolution decreases with the use of lower frequency antennae, greater depths of penetration for the GPR signal are achieved. This trade-off is illustrated by comparing the GPR profiles from the Adair Quarry (Fig. 6.3). In this series of figures, one can clearly see the depth of investigation progressively increase from 14 m with the 200 MHz antennae (Fig. 6.3A) to 27 m with the 50 MHz antennae (Fig. 6.3C).

We present the geologic correlation with the 50 and 100 MHz radar surveys performed at Line 2 within this quarry. 50–200 MHz profiling was also performed along Line 3 which is oriented perpendicular to Line 2 (Fig. 6.4B). Data from Line 3 did not further contribute to our comparison between GPR imaging and stratigraphy; these images are provided in Appendix C. The locations of these two profile lines within the Adair Quarry are illustrated in Figure 6.4B.

6.4.1.1 Line 2 at the Adair Quarry

The 50 and 100 MHz antennae provided the ability to compare the radar response with measured facies changes and formation contacts that could be confirmed in borehole stratigraphic logs (Figs. 6.5 and 6.6). From a detailed stratigraphic log of borehole 90-4 located within 15 m of the radar survey, the GPR profile revealed continuous strong reflectors where abrupt changes in porosity were observed within the core. In general, porosity changes correspond to stratigraphic boundaries. Dipping linear events from the

south side of the survey are probably direct radar waves scattered off the quarry step face at the south end of the line.

The lowermost reflector, referred to as 'W', is found at ~ 24 m depth at the Adair Quarry. The strong planar reflector correlates with the transition from lower argillaceous dolostones of the Wingfield Formation (W) to overlying porous fossil-rich dolostones of the Fossil Hill Formation (FH) (Fig. 6.6). The abrupt change in porosity as well as the high electrical conductivity of the underlying argillaceous Wingfield Formation is likely the cause for this strong reflection. Above the 'W' Reflector, the Fossil Hill (FH) Formation is composed of both horizontal planar and low angle onlapping prograding internal reflectors.

A strong continuous planar reflector found at ~16 m depth and referred to as 'FH' correlates with the contact between the lower porous, fossil-rich dolostones of the Fossil Hill Formation, and the overlying massive, dense dolostones of the Lions Head Member of the Amabel Formation. In borehole OGS-90-4, this contact has an apparent sharp decrease in porosity and fossil content. The internal reflectors corresponding to the Lions Head Member are composed of fairly continuous planar bedding which may correspond with progradation of beds at a larger scale within these dolostones.

The uppermost strong reflector, referred to as A (LH), is found at ~ 11 m depth and correlates with the contact between the Lions Head Member and the overlying Colpoy Bay Member of the Amabel Formation (Fig. 6.6). The presence of this sharp planar reflector may be related to the observed increase in porosity in the overlying dolostones. Shallow diffractions apparent in the Colpoy Bay Member are scattering due to the shallow karstic features. Observed within the quarry face, solution-enhanced fractures and joints, and vugs

and nodules are present to ~ 4 m depth. However, the Colpoy Bay Member generally appears to have a much lower internal reflectivity than either the Lions Head Member or the Fossil Hill Formation. The 100 MHz profile gives a higher resolution image of the shallower section at the Adair Quarry (Figs. 6.5 and 6.6). The horizontal internal reflections within the Lions Head Member interval are more clearly defined. The low reflectivity of the Colpoy Bay Member is also better defined in the 100 MHz profile which again suggests that there is a lower dielectric contrast between the stratigraphic horizons. In addition, the combination of the improved resolution and shorter duration direct wave arrival allows us to clearly image a significant horizontal GPR reflection at ~ 4 m depth (A and yellow line in Fig. 6.6) on the 100 MHz section which is not well defined on the 50 MHz profile (Figs. 6.4 and 6.6). While the cause for this marker has not been determined, it corresponds with the lower limit of the enhanced vuggy porosity.

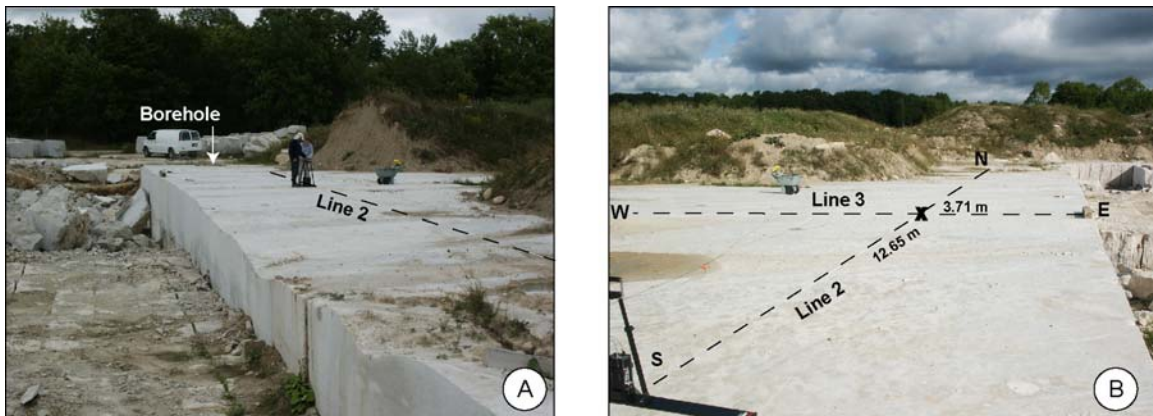


Figure 6.4: **A)** The orientation of Line 2 in the quarry with the relative position of borehole 90-4, which is superimposed on the left of the radar survey; **B)** The intersection point between Line 3 and Line 2 and its relative position in the quarry.

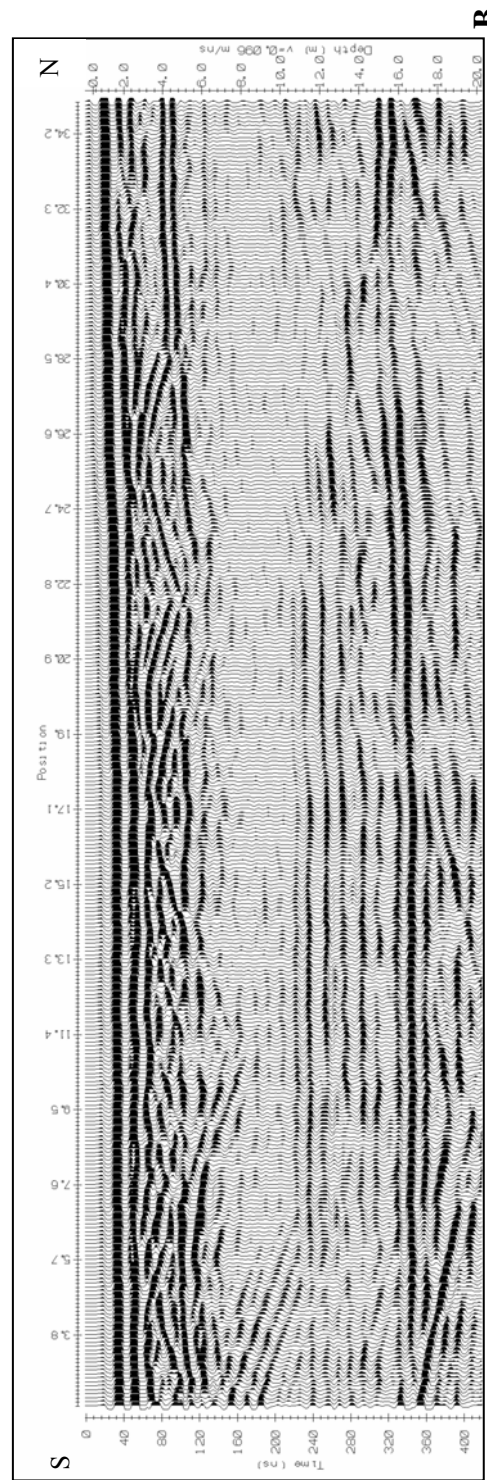
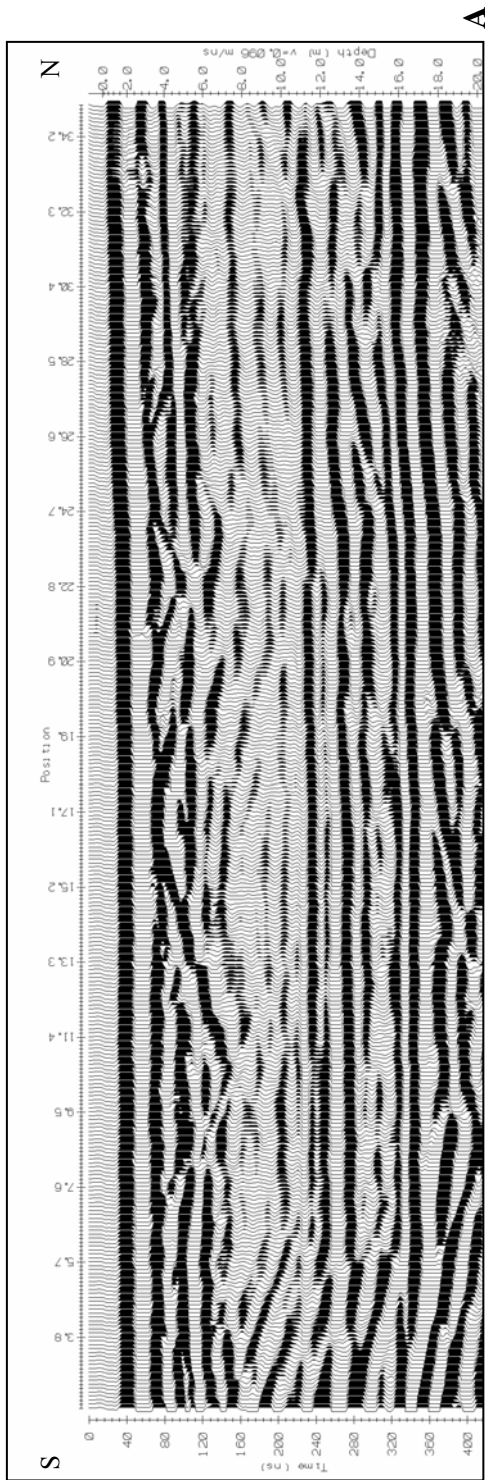


Figure 6.5: Line 2 at the Adair Quarry. **A)** The 50 MHz image amalgamates traces to form reflectors that have less definition than the reflectors in the 100 MHz image. **B)** The 100 MHz profile better resolves the planar reflectors as well as the location of the diffraction apices.

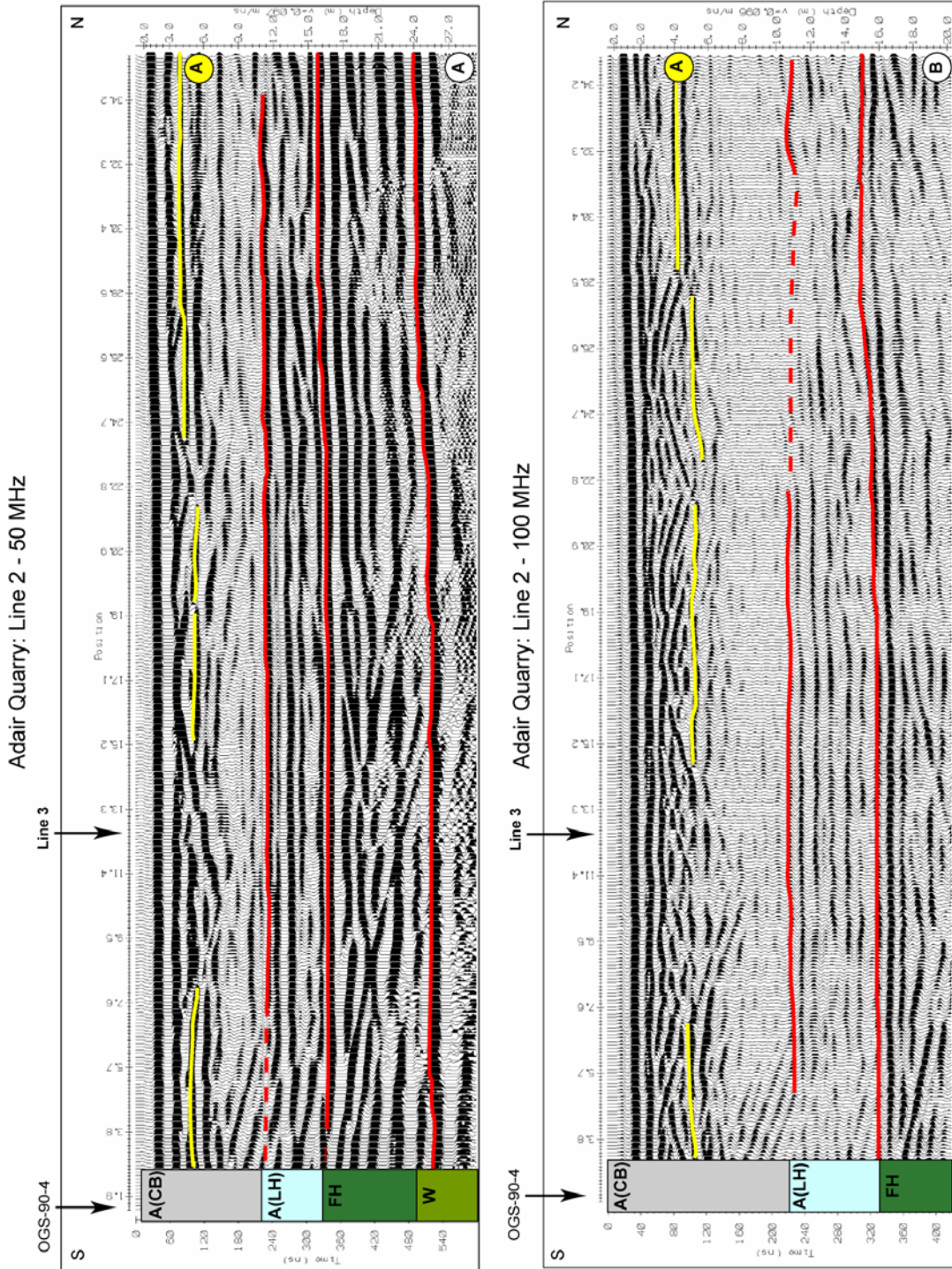


Figure 6.6: The 50 and 100 MHz profiles at Line 2 in the Adair Quarry have strong reflectors (W, FH, A (LH)). A discontinuous internal reflector (A) is shown in yellow near the top of the Colpo Bay Member. The intersection point of Line 3 on Line 2 is labeled with an arrow. Although depth penetration is greater in the 50 MHz profile (A), contacts are better resolved in the 100 MHz (B) profile.

6.4.2 Correlating GPR with geology at the OSLW Quarry

GPR profiling using 50, 100, and 200 MHz antennae was done to image the carbonate rocks at the OSLW Quarry (Fig. 6.7). Three profile lines were performed. Two radar surveys were carried out in the northwest quadrant of the quarry and intersect at right angles to each other (Lines 1 and 2 in Figs. 6.8–6.11). The third survey was performed in the southwest quadrant of the quarry (Line 5 in Figs. 6.13 and 6.14) where the quarry has not yet been developed.

For the correlation with the carbonate facies, we present the 50 MHz profiling, which provided the greatest depth penetration data, and the 100 MHz profile which resolves finer details of the individual reflectors. The 200 MHz profiles of each survey performed are in Appendix C. At least 8 m of the Eramosa Member has been observed within the quarry, and is imaged within the radar profile. The closest deep (> 30 m) borehole (OGS-82-4) to the OSLW Quarry is located ~ 10 km to the northwest (Fig. 6.1). The correlation between the GPR reflecting boundaries and deeper lithologic contacts (Colpoy Bay and Lions Head members) can only be approximated from the thicknesses observed from borehole OGS-82-4 (Figs. 6.8–6.14).

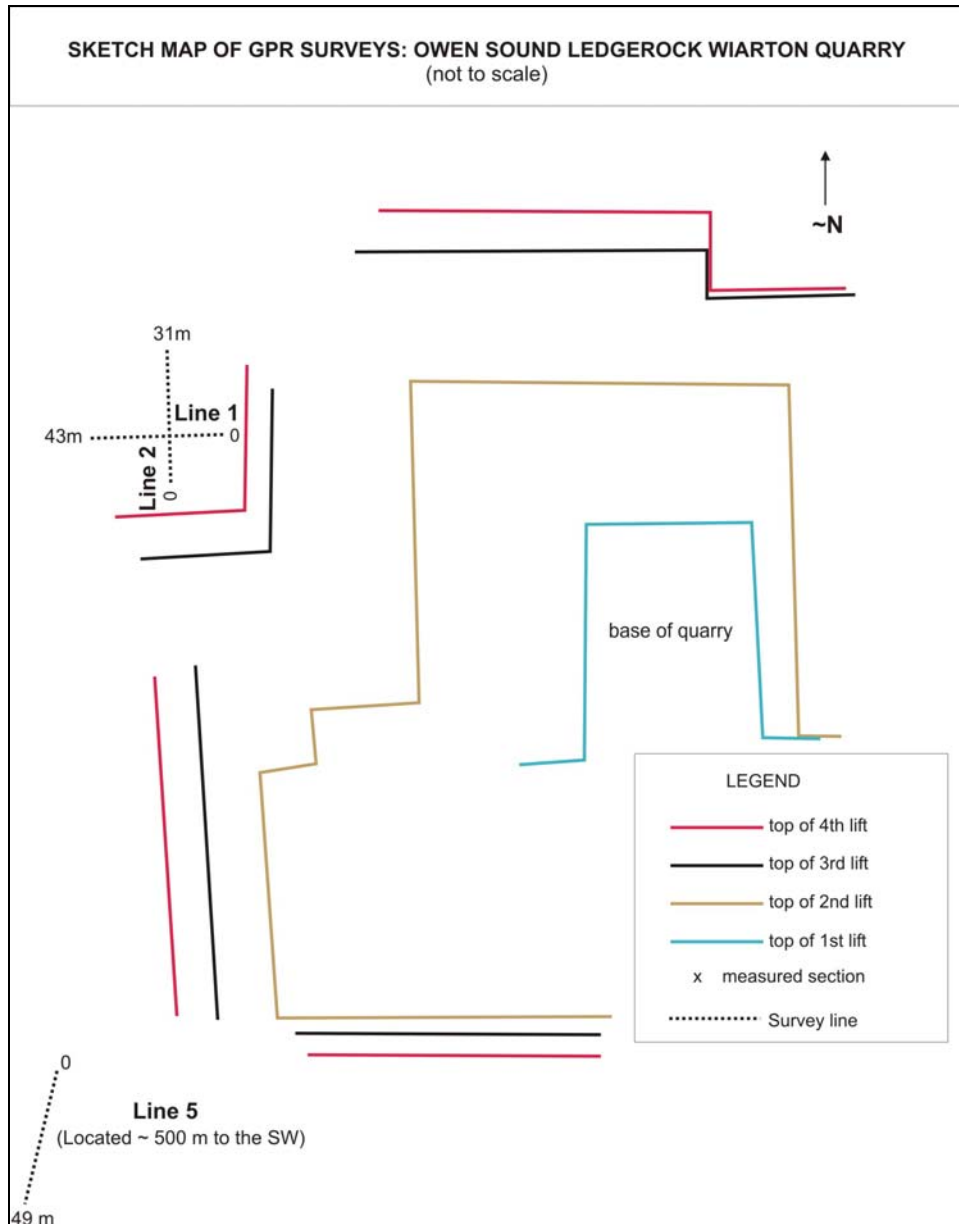


Figure 6.7: Map of the west side of the OSLW Quarry. Lines 1 and 2 are situated in the northwest end of the quarry on top of the 4th lift. Line 5 is located ~ 500 m to the southwest of the quarry, presumably on top of the 4th lift.

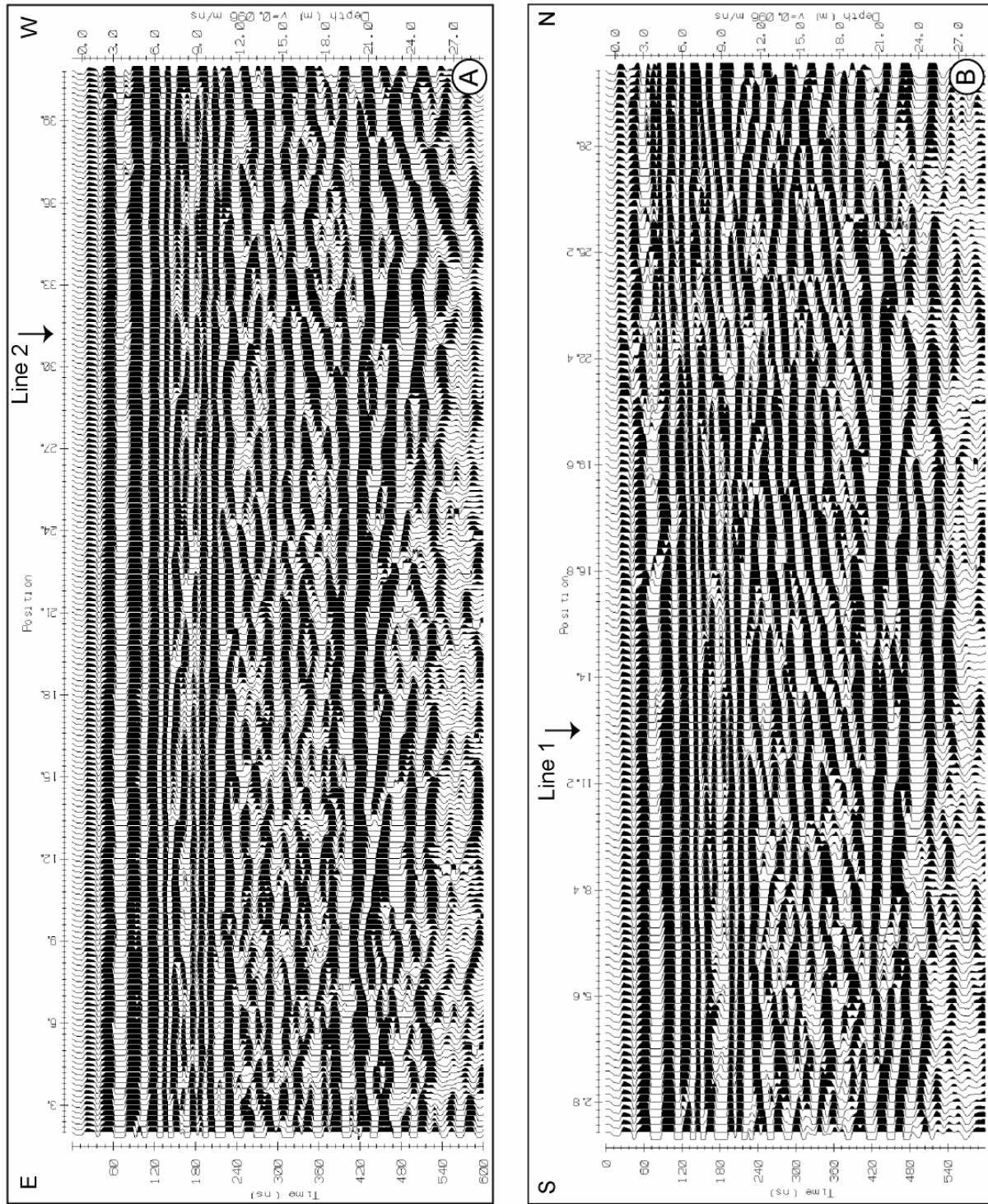


Figure 6.8: 50 MHz GPR profiles of Line 1 (left) and Line 2 (right). These two lines are perpendicular to each other. The intersection point of the two lines is labeled on both sections. Line 2 (right) illustrates overlapping radar facies from the south, onto a prograding feature in the north.

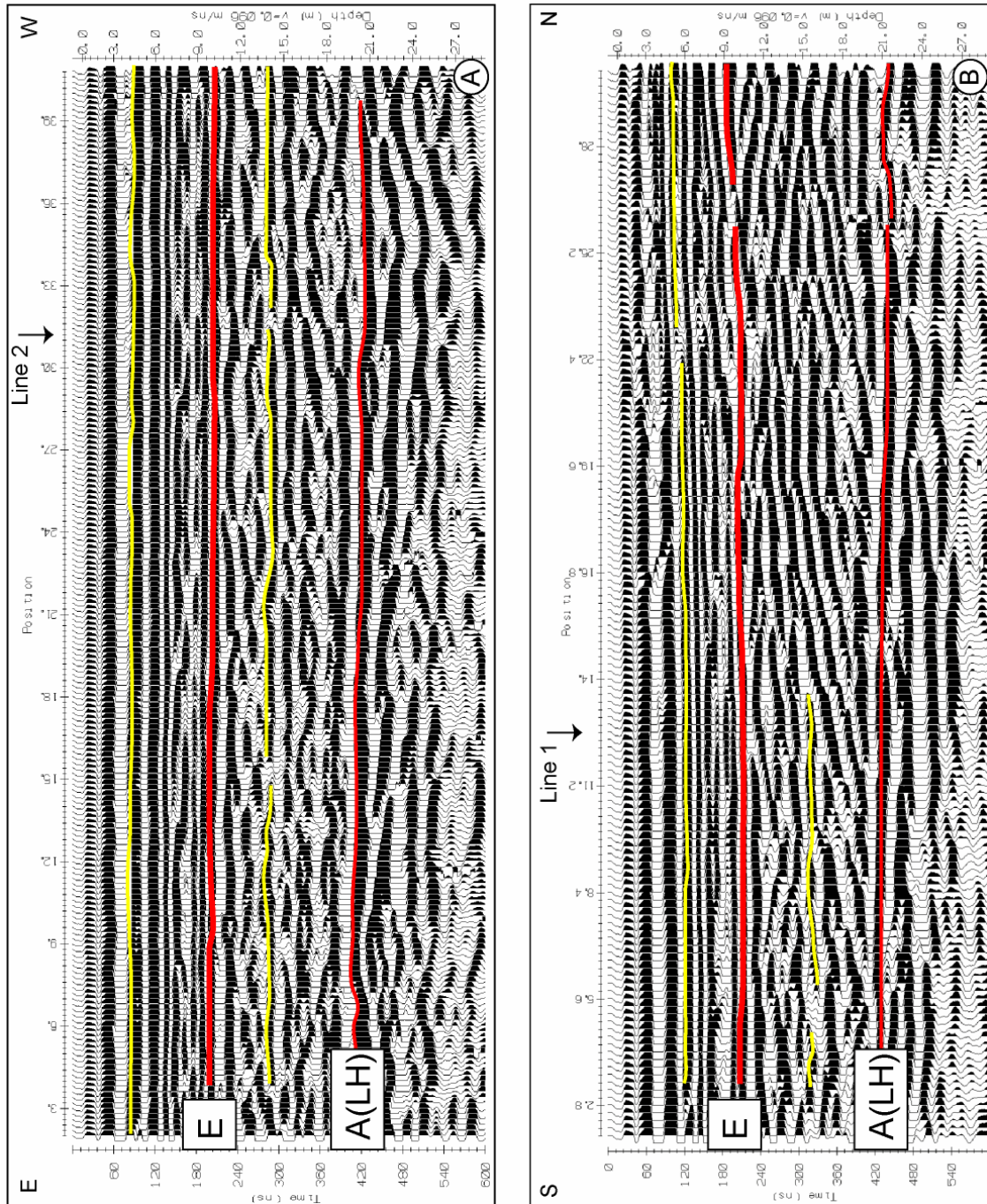


Figure 6.9: 50 MHz profiles from Lines 1 (left) and 2 (right). **A)** Line 1 from the OSLW Quarry has strong reflectors shown in red (A (LH) and E) which divide the Eramosa, Colpo Bay, and Lions Head members. Yellow lines represent strong internal reflectors; **B)** Line 2 from the OSLW Quarry reveals similar strong reflectors A (LH) and E (red). The orientation of the line provides a different view of the stratigraphy. Both survey lines indicate the intersection point of the two lines with an arrow. The thickness of the Colpo Bay and Lions Head members is inferred from borehole 82-4. The yellow lines represent strong internal planar reflectors within the Eramosa and Colpo Bay members.

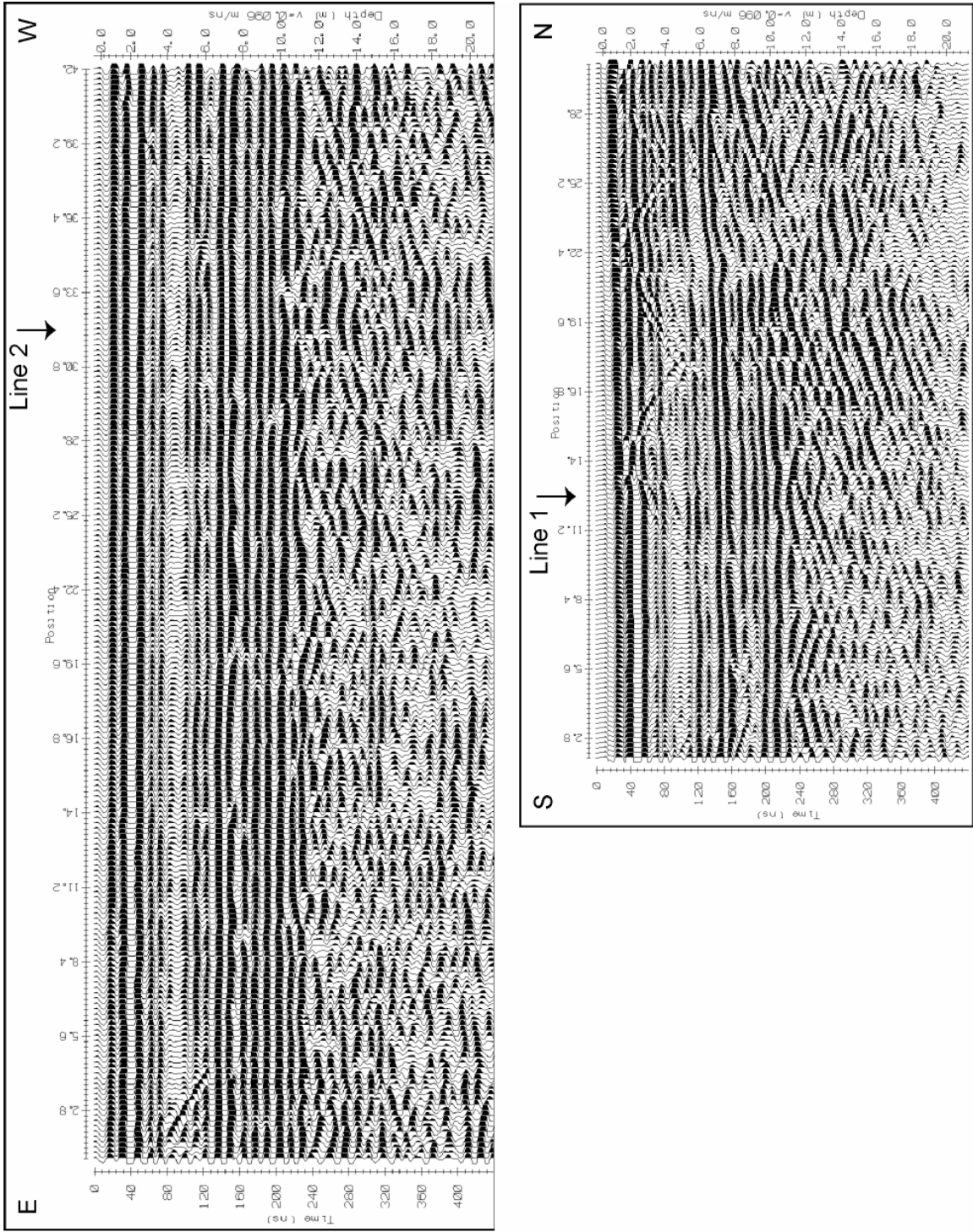


Figure 6.10: 100 MHz GPR profiles of Lines 1 (left) and 2 (right) at the OSLW Quarry. 100 MHz radar images better resolve the subsurface stratigraphy and provide good depth penetration down to ~ 20 m. Contacts between members are better defined with the higher frequency antennae.

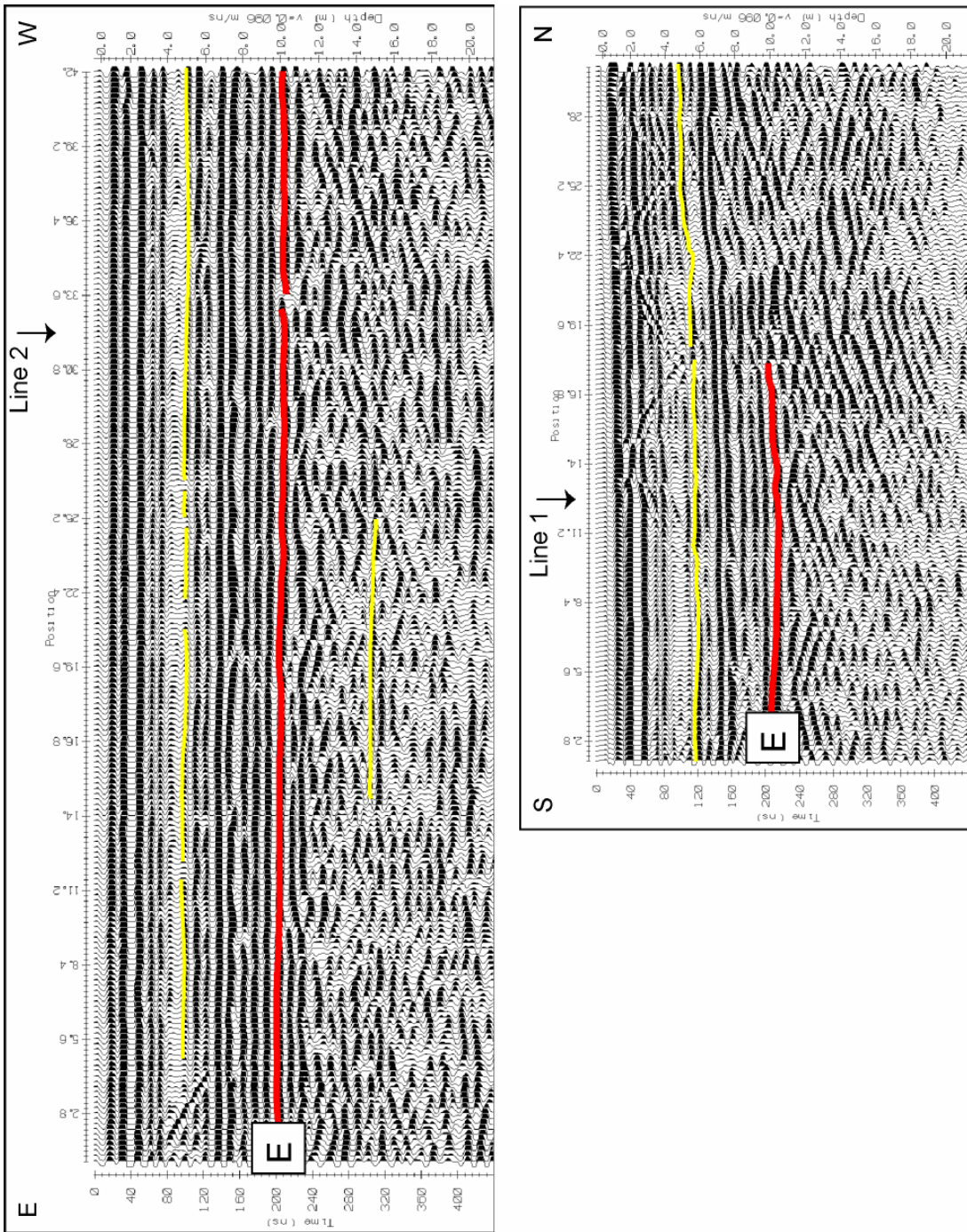


Figure 6.11: 100 MHz GPR profiles of Lines 1 (left) and 2 (right) at the OSLW Quarry. 100 MHz radar images provide good depth penetration down to ~ 20 m. The red lines correlate with the contact between the underlying Colpo Bay Member of the Amabel Formation and the overlying Eramosa Member (E). The yellow lines correlate with strong planar internal reflections within the Eramosa and Colpo Bay members.

6.4.2.1 Lines 1 and 2 at the OSLW Quarry

Figures 6.8–6.11 illustrate the GPR profiles along Lines 1 and 2. While facies packages are slightly different between Lines 1 and 2, major GPR events can be related to stratigraphic horizons. While exposures within the quarry can be used to correlate shallow stratigraphy with GPR response, member thicknesses observed in the stratigraphic log for borehole 82-4 can be used to infer deeper lithologic boundaries in the OSLW Quarry. The lowermost reflector is referred to as A (LH) for the contact between the Lions Head Member and the Colpoy Bay Member of the Amabel Formation, and is only observed within the 50 MHz profiles. This reflector marks the change in GPR response from more continuous undulating facies of the Lions Head Member to more chaotic, discontinuous and heterogeneous GPR facies of the Colpoy Bay Member. An apparent porosity difference of > 10 % exists between the lower Lions Head Member (Fig. 6.12A) and the overlying Colpoy Bay Member (Fig. 6.12B). At the Adair Quarry, the Colpoy Bay Member exhibits a similar discontinuous heterogeneous GPR reflection response. At both the OSLW and Adair quarries, a planar discontinuous to continuous reflector exists within the Colpoy Bay Member. At both the Adair and OSLW quarries, this reflector (A - yellow) is present ~ 6 m above the A (LH) contact (Figs. 6.6 and 6.9). Although the heterogeneous, mottled texture within the Colpoy Bay Member (Fig. 6.12E) observed in the Adair Quarry is similar to that in the borehole OGS-82-4 (correlated with OSLW), the Colpoy Bay Member appears more porous in borehole OGS-82-4 (Fig. 6.12B) than at the Adair Quarry.

At the OSLW Quarry in the Line 1 profile, the upper 10 m is represented by planar, continuous reflectors interpreted to represent the planar bedded argillaceous Eramosa

Member dolostones. In the Line 2 profile, similar strong reflectors occur at the same depths (Figs. 6.9 and 6.11). The N-S orientation of Line 2 provides insight to the lateral variations of the internal structure of these facies. Rather than observing chaotic discontinuous reflectors in the base of the Colpoy Bay Member at Line 1, Line 2 reveals prograding reflections from the north with onlapping reflectors from the south. The uppermost ~ 10 m of the profile along Line 2 contains planar continuous reflectors and exhibits progradation in its lower portion (i.e., between 6–10 m depth). In addition, the shallowing of the major reflection events in the northward direction could indicate a bioherm or mound to the north of this site.



Figure 6.12A: Example of the Lions Head Member from borehole OGS-82-4. Note the low porosity. Arrow is located at the base of the core.



Figure 6.12D: Example of the Lions Head Member from borehole OGS-90-4. Note the low porosity. Arrow is located at the base of the core.



Figure 6.12B: Example of the Colpo Bay Member from borehole OGS-82-4. Note the increased vuggy porosity. Arrow is located at the base of the core.

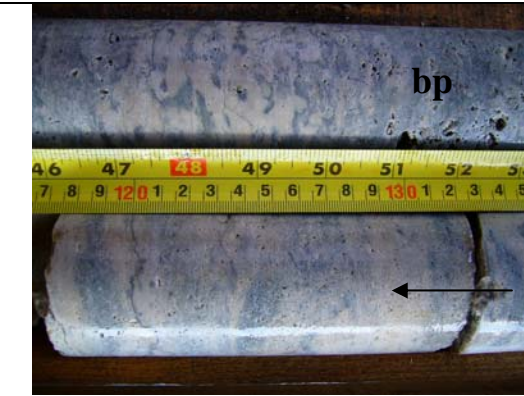


Figure 6.12E: Example of the Colpo Bay Member from borehole OGS-90-4. Note the increased biomoldic porosity (bp). Arrow is located at the base of the core.



Figure 6.12C: Example of the Eramosa Member from borehole OGS-82-4. Note the decreased porosity and horizontal stylolites (S). White arrow is located at the base of the core.



Figure 6.12F: Example of the Eramosa Member 'Marble Beds' from the OSLW Quarry. Note the decreased porosity and planar laminations (L).

6.4.2.2 Line 5 at the OSLW Quarry

The 50 MHz profile performed at Line 5 in the OSLW Quarry is located ~ 500 m south of Lines 1 and 2. Line 5 was performed in the same orientation as Line 2 from north to south. Similar facies packages were observed within the Line 5 profile as at Lines 1 and 2, where ~ 12 m of strong planar reflectors of the Eramosa Member are imaged. Along the Line 5 profile (Figs. 6.13 and 6.14) the lowermost reflector (yellow) at ~ 20 m depth is likely a strong planar internal reflector within the lower Colpoy Bay Member, based on a thickness of ~ 15 m inferred from borehole OGS-82-4. The Lions Head Member was not imaged at this site. The reflectors in the Colpoy Bay Member (yellow) are similar to the onlapping units observed on the south side of the Line 2 profile and likely represent continuous deposition of the carbonates.

GPR profiles for Lines 1, 2, and 5 at the OSLW Quarry and Line 2 at the Adair Quarry exhibit similar internal radar reflections for the Colpoy Bay Member. At both sites, this member possesses discontinuous, chaotic reflections having relatively lower reflectivity than its neighbouring units. While there are similarities between the Adair and OSLW quarries for the Colpoy Bay Member, it is not apparent for the Lions Head Member. This may be due to reduced resolution and/or reduced depth of penetration at the OSLW Quarry. Within the Colpoy Bay Member, planar internal reflectors (yellow) are apparent, and may indicate that facies changes from the Colpoy Bay Member to the heterogeneous, porous Warton facies. Although the Warton Member was not observed within borehole OGS-82-4, both OGS-90-3 and OGS-90-4 contain the crinoidal lithofacies. A similar strong internal reflector was observed at the Adair Quarry (Reflector A in Fig. 6.6).

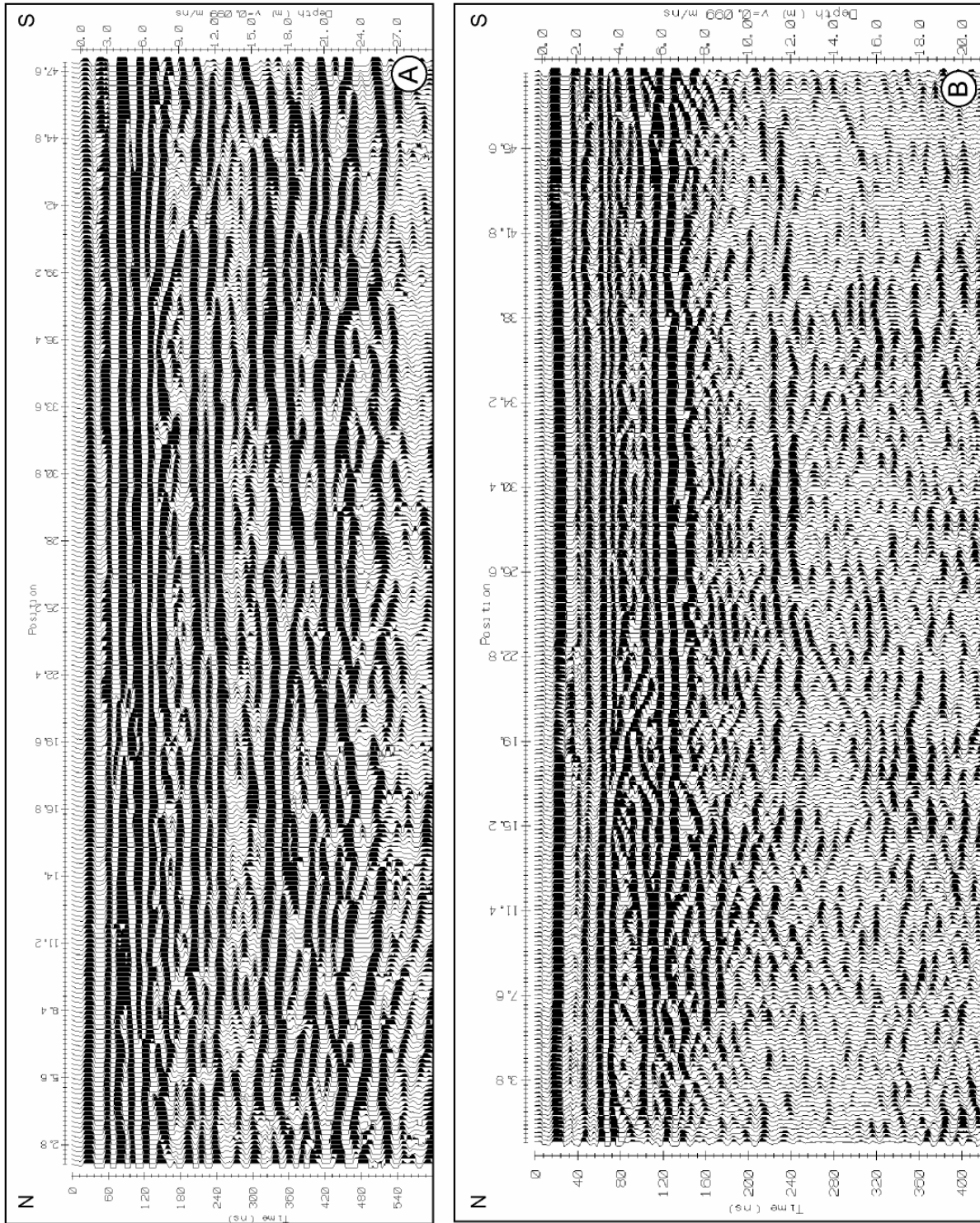


Figure 6.13: 50 MHz (left) and 100 MHz (right) GPR profiles from Line 5 in the southwest quadrant of the OSLW Quarry reveal a strong similarity in reflectors seen in Lines 1 and 2 from the northwest quadrant of the quarry. Strong reflectors separate the Lions Head, Colpoy Bay, and Eramosa members.

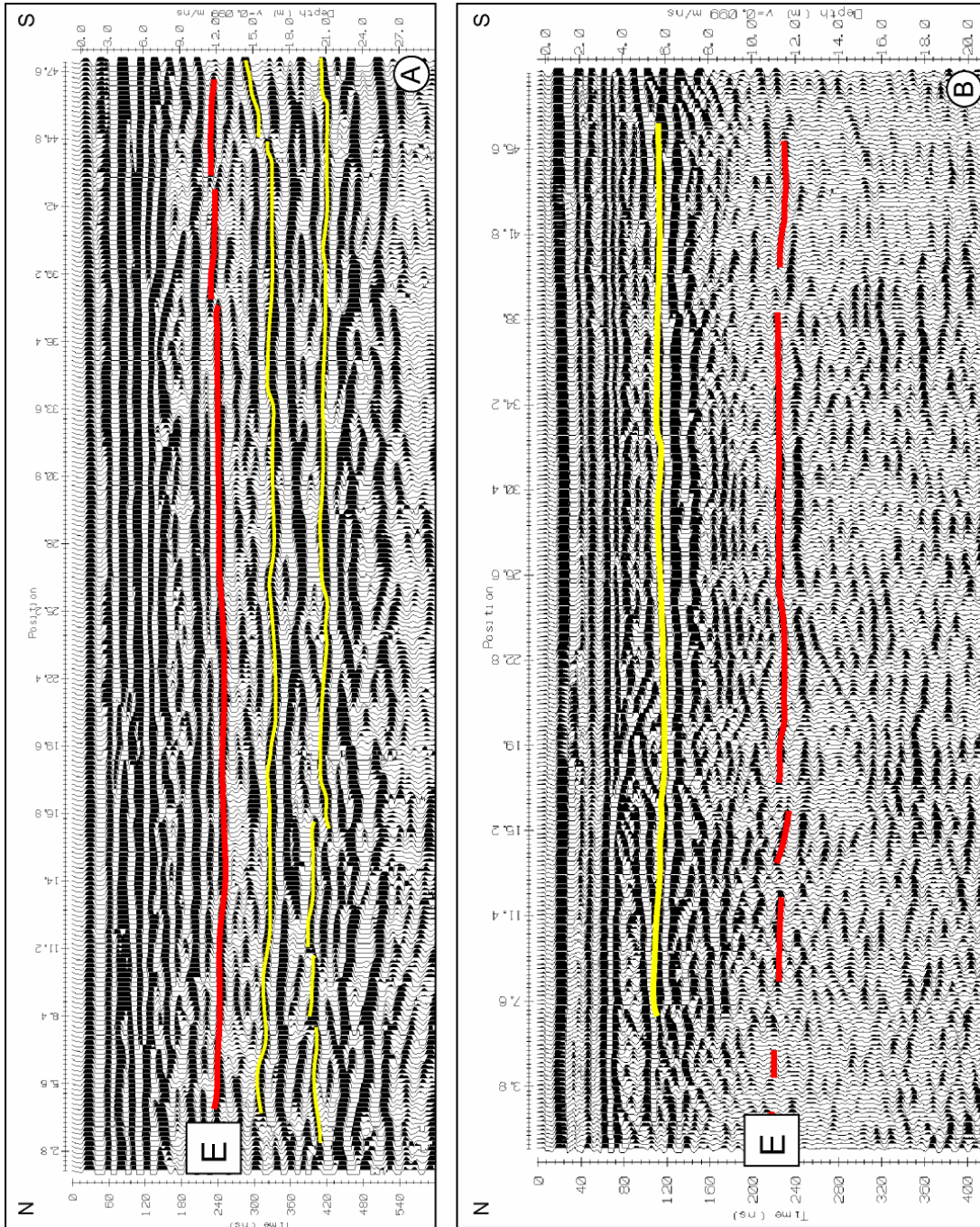


Figure 6.14: 50 MHz (A) and 100 MHz (B) GPR profiles from Line 5 in the southwest quadrant of the OSLW Quarry reveals a strong similarity in reflectors seen in Lines 1 and 2 from the northwest quadrant of the quarry. **A)** A strong reflector separates the Colpo Bay Member and the Eramosa (E) Member (red). This profile resolves the strong planar internal reflections within the Colpo Bay Member (yellow). **B)** Although the 100 MHz profile does not show reflectors within the deeper Colpo Bay Member, the strong planar internal reflectors are shown in the Eramosa Member (yellow).

6.4.3 Correlating GPR with geology at Borehole 90-3

One radar line was performed along a wide dirt and gravel road surrounded by heavy tree and vegetation and adjacent to borehole OGS-90-3. This site has less than 1 m of overburden at surface and a bedrock surface composed of relatively porous dolostones. Adjacent to the side road and < 3 m from the radar line borehole 90-3 was drilled (Fig. 6.15B). A monitoring well was installed with metal casing surrounding the upper few metres after the borehole was drilled in 1990. The scattered radar waves from the metal casing are observed in the radar profile (Fig. 6.15A).

For the correlation with the carbonate geology observed in borehole 90-3, we present the 50 MHz profile which optimizes the deeper radar reflections. The 100 MHz and 200 MHz profiles are available in Appendix C. Figure 6.15 illustrates the correlation between the GPR profile and the borehole. The uppermost ~ 21 m at the 90-3 site is composed of brown to tan massive, fossil-rich, medium crystalline dolostone of the Guelph Formation. Numerous diffractions that make up this GPR facies package may have resulted from the chaotic heterogeneous internal structure that is typical of bioherm or reefal facies. Alternatively, diffractions may have resulted from karstic features such as large vuggy pores or dissolution joints. The very hummocky surface observed in the forest along the profile line may be the result of extensive dissolution at the vicinity of the bedrock surface.

The contact between the upper Guelph Formation and underlying Eramosa Member is characterized by a transition from chaotic reflectors to more planar continuous reflectors. The Eramosa Member at the OSLW Quarry was similarly characterized by planar reflectors associated with laminated to bedded argillaceous dolostone interbedded with massive

fossiliferous dolostone. From the photo of the top of borehole 90-3, an abrupt change in colour and apparent bedding (stylolite seams) is evident (Fig. 6.15C). An increase in porosity in the Guelph Formation is shown with zones of broken core, which generally indicates that more water was available at that horizon to dissolve the carbonate rocks. The underlying Eramosa Member is composed of grey-brown, stylolitic, fine crystalline dolostone with minor coral and shelly fragments.

90-3 Site: Line 0 – 50 MHz

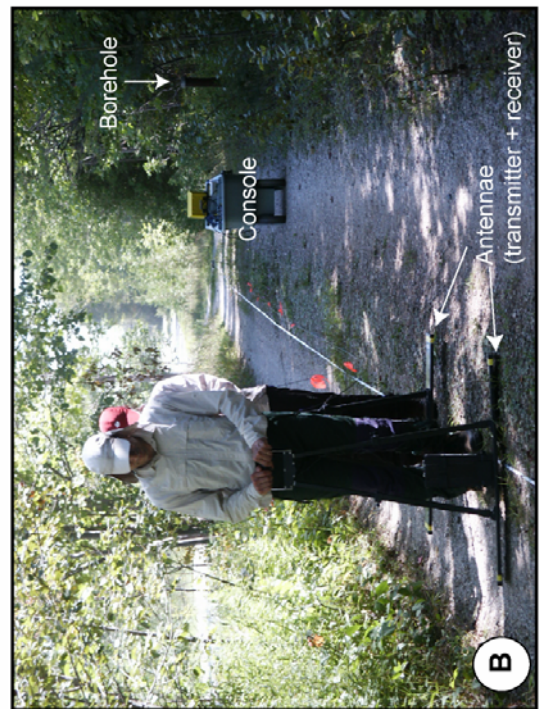
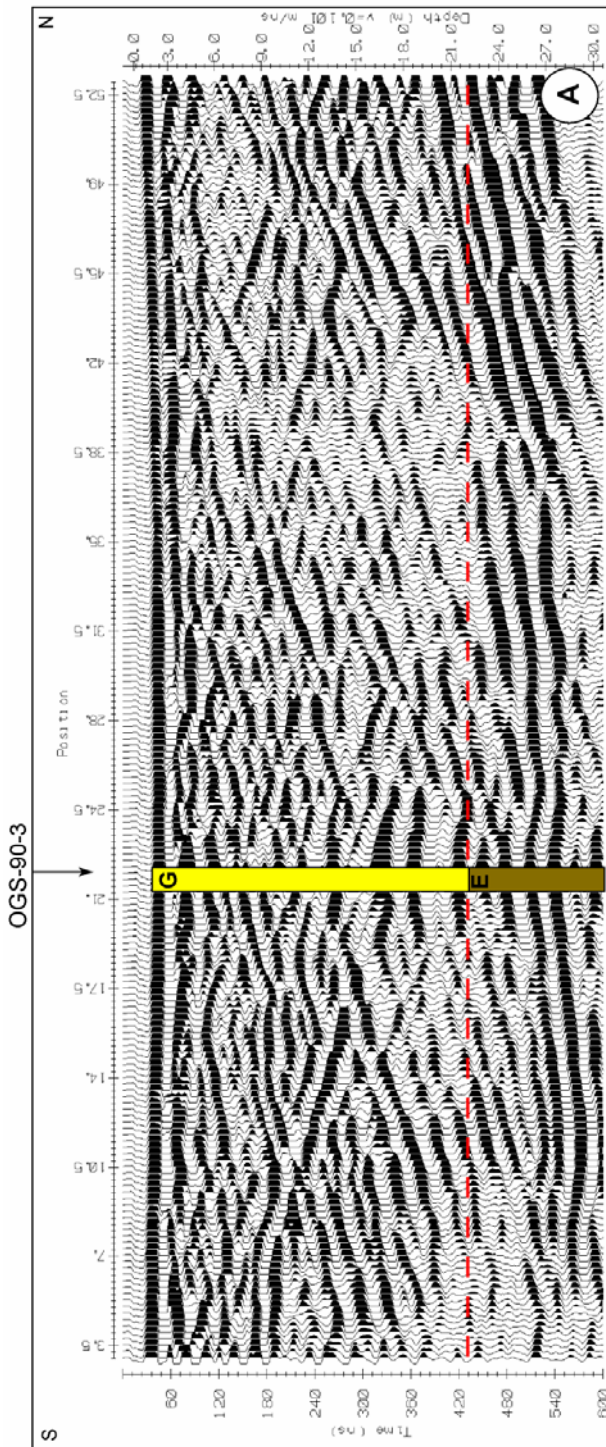


Figure 6.15: A) Radar profile from Line 0 at the 90-3 borehole site reveals a thick succession of the Guelph Formation (G) overlying the Eramosa Member (E), which is divided by an obvious change in reflectors; B) The borehole is situated at position 21.80 m on the survey line; C) Photo of core from the top of the borehole illustrates colour and porosity differences between the Eramosa Member and the Guelph Formation.

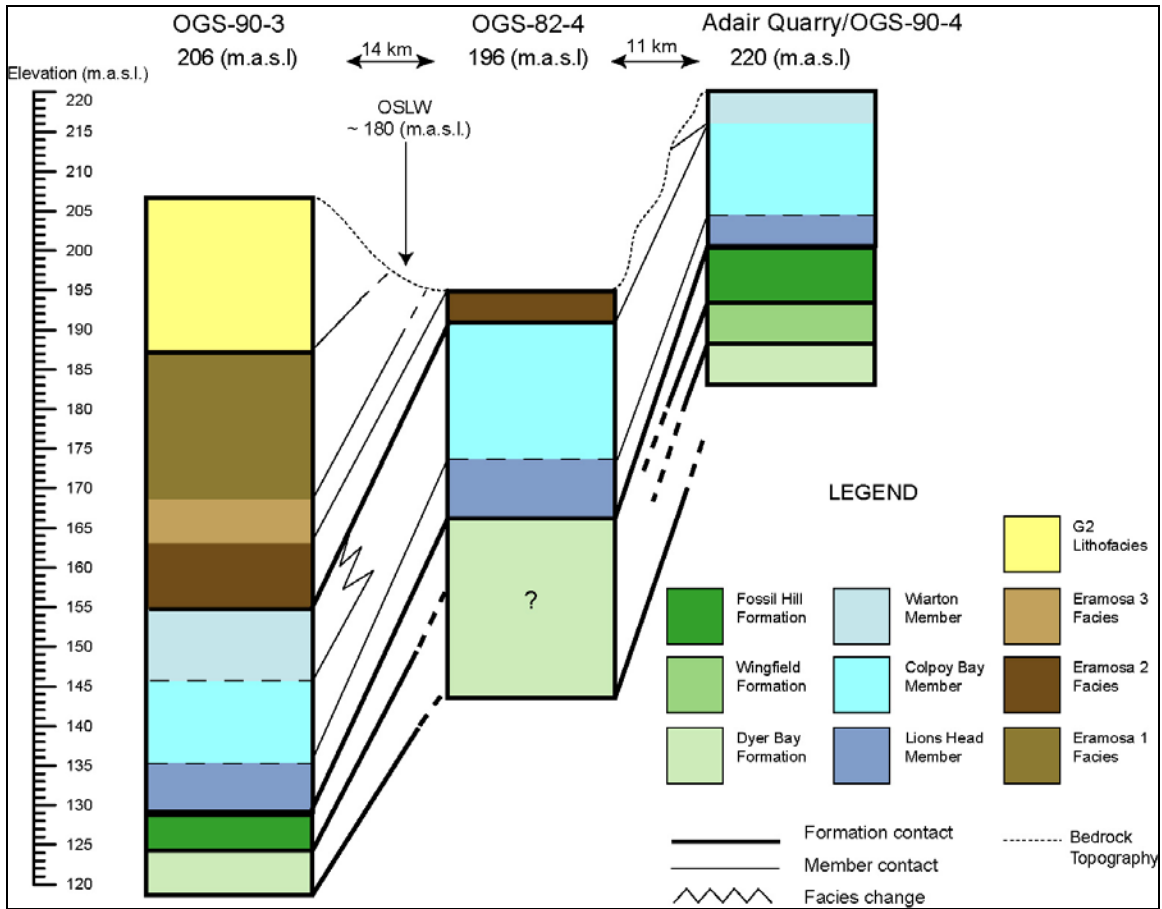


Figure 6.16: Borehole correlation from south to north along the Bruce Peninsula and superimposed location of the OSLW Quarry. The legend in the lower right hand corner illustrates the Clinton Group (green), Amabel Formation (blue), Eramosa Member (brown), and the Guelph Formation (yellow). The question mark within the Dyer Bay Fm. at the base of borehole OGS-82-4 reflects possible pinch-out of the Wingfield and Fossil Hill formations.

A stratigraphic cross-section at each borehole site surrounding the OSLW Quarry is illustrated in Figure 6.16. The Guelph 1 lithofacies is likely only present in borehole 90-3 due to the dip angle of the Silurian strata to the west and the erosional pattern on the Peninsula. Where porosity and density variations occur within the OSLW Quarry, radar responses have similar properties. In low porosity facies (e.g., the Eramosa Member), planar reflectors are more common. In the heterogeneous porous facies (e.g., the Guelph Formation), more

chaotic discontinuous reflectors are imaged. Similar radar responses are shown in the high frequency profiles in Chapter 5.

Within the Adair Quarry and the OSLW Quarry, the transition between the overlying Colpoy Bay Member of the Amabel Formation and the underlying Lions Head Member is consistently imaged throughout the quarry. At the OSLW Quarry and the 90-3 site the transition from the Wiarton and Colpoy Bay members to the overlying Eramosa Member is also readily apparent in the radar sections.

6.5 Conclusions

Low frequency GPR profiling was successfully used to image vertical stratigraphic changes at the OSLW and Adair quarries, as well as the site of borehole 90-3 on the Bruce Peninsula. From correlations with stratigraphic logs of boreholes, we observed that major vertical facies changes within the stratigraphy correlated with strong continuous GPR reflectors. Further, the GPR facies between these boundaries varied in their internal reflection pattern. Our study also found that lateral facies changes were clearly imaged in the radar profiles at Line 2 in the OSLW Quarry, where reflectors from the south appeared to onlap a buildup/mound on the northern side of the profile. Mounds or buildups are a negative feature for quarry operators as they generally contain solution-enhanced porosity or impurities within vugs in the form of lead sulphides (iron, sphalerite).

GPR is an economical tool that provides quarry operators with the locations of such features and lateral continuity/discontinuity of facies that is otherwise costly to acquire. This field-based study clearly demonstrates that low-resolution, deep penetration GPR techniques

in combination with detailed geologic mapping can be employed as a cost effective exploration method for resource estimates in building-stone quarries, especially where the lack of subsurface data limits other means of assessing the resource potential.

Chapter 7: Concluding Remarks and Future Recommendations

7.1 Overall Conclusions

The Silurian Amabel Formation in the subsurface of the Bruce Peninsula is composed of three members - in ascending order these are the: Lions Head, Colpoy Bay and Wiarion members. Within core, the two lowermost members of the Amabel Formation are laterally continuous across the Bruce Peninsula and exhibit distinct core and petrographic characteristics. A hardground surface, mottling resulting from pyrite content, finely crystalline dolomite and chert nodules characterize the Lions Head Member. The Colpoy Bay Member exhibits irregular elongate mottles containing undifferentiated organics that concentrated within higher porosity zones, which reflect bioturbation. The Colpoy Bay Member is more fossiliferous than the underlying Lions Head Member, although recognition of fossils is equally difficult. The distinct mottles in the Lions Head Member and the increased porosity and fossil content in the Colpoy Bay Member allows these two members to be readily discernable in both core and thin section. The uppermost crinoid-rich Wiarion Member is not laterally continuous across the Bruce Peninsula. Although the Wiarion Member may be mistaken as the Colpoy Bay Member where crinoids are more difficult to recognize, the Wiarion Member is easily distinguished from the Guelph Formation. A tan-brown colour and noticeable increase in the abundance and size of brachiopods, bivalves, and/or gastropods characterizes the Guelph Formation.

The replacement dolomite within the Amabel Formation is generally anhedral, cloudy, and finely crystalline whereas replacement dolomite within the Guelph Formation is

commonly subhedral to euhedral, slightly clearer and medium to coarsely crystalline. The amount of replacement nodular silica is noticeably less within the Guelph Formation versus the underlying Amabel Formation. The Lions Head Member of the Amabel Formation represents quieter water conditions, and the increase in fossil content in the Colpoy Bay Member is suggestive of a gradually shallowing environment. Overlying Warton Member crinoidal grainstones with minor corals are indicative of a high energy shoal environment proximal to a bioherm.

The Eramosa Member is found within six of the eight boreholes from this study. The Eramosa Member is subdivided into four lithofacies (E1 through E4) that range from sparsely fossiliferous, light tan, massive and vuggy to fossiliferous and dark brown to argillaceous and laminated. Although these lithofacies are relatively distinct in core, there are few discernible differences petrographically. Similar to the upper undifferentiated Guelph Formation, the Eramosa Member contains little silica and preservation of fossils is generally poor. Replacement dolomite within both the Eramosa Member and the undifferentiated Guelph Formation is distributed such that the precursor fabric is somewhat easier to infer. The tan to light grey E1 and E3 lithofacies may contain abundant closely-spaced wispy stylolites which differentiate them from the E2 lithofacies. The E2 lithofacies is more fossiliferous and darker brown in colour than the E1 and E3 lithofacies. The E4 lithofacies is characterized by thin dark brown to black laminations. The Eramosa Member contains minor secondary minerals in the form of sphalerite and fluorite as well as silica, pyrite and calcite. Silica was observed within the E1 and E2 lithofacies and is much rarer within the E3 and E4 lithofacies. Evaporite mineral molds are filled with late-stage calcite cement. Dolomite

replaced the majority of recognizable fossils within the Eramosa Member and the upper Guelph Formation, with remaining recognizable fossils being replaced with silica or left as biomoldic pores. Silica predominantly replaces recognizable fossils in the Amabel Formation, with a lower abundance of replacement by dolomite. Nodules within the Eramosa Member are composed of a mixture of chert and ~ 30 % dolomite, or more rarely up to 60–80 % dolomite. A prominent decrease in the silica content occurs proceeding stratigraphically upwards from the Amabel Formation into the Eramosa Member and Guelph Formation. Minor sphalerite mineralization observed in thin section indicates that later fluids containing sulfides permeated the Eramosa Member. The four lithofacies of the Eramosa Member represent depositional environments which range from less-oxygenated lagoonal to a possible bioherm-proximal environment subject to periodic storm influxes.

The Guelph Formation is not laterally continuous across the Bruce Peninsula, although the absence of this formation in the cores in the central area of the Peninsula is likely due to erosion. The three lithofacies that make up the Guelph Formation are all fossiliferous. Fossils are generally replaced with dolomite, as silica is rare in this formation. Large (> 4 cm) megalodont-bivalves and gastropods were observed in core within the Guelph Formation. The abundance of coral and stromatoporoid fragments found within the Guelph Formation across the Bruce Peninsula are suggestive of a relatively normal saline environment.

Ground-penetrating radar (GPR) is a useful tool which aids in the shallow subsurface profiling of the members of the Amabel and Guelph formations. The members of the Amabel Formation and the Eramosa Member consistently show similar radar responses in the Adair

Quarry and the Owen Sound Ledgerrock Warton Quarry. The Eramosa Member contains conductive argillaceous units interbedded with more homogeneous dolostones and produces strong planar reflectors at both the OSLW and 90-3 borehole sites. GPR has also been useful in imaging karstic features such as large dissolution joints and fractures, as well as units that contain abundant vugs and nodules. Solution-enhanced joints and fractures, vugs and mounds are negative attributes of these carbonates that, if imaged with high frequency GPR, may be avoided by quarry operators in their search for suitable building stone or aggregate. Vugs, nodules and karstic horizons within the Amabel Formation are problematical due to the impurities sometimes associated with them. Silica and sulfide (pyrite and sphalerite) impurities exist within the Amabel and Guelph formations and are concentrated within vugs, nodules, and along stylolite seams (Brunton and Dekeyser, 2004; Brunton et al., 2005). Bioherms or reef mounds are generally localized heterogeneous features that may contain vugs and nodules, which decrease the quality of the rock for aggregate usage. Lateral facies changes imaged with the GPR unit provide quarry operators with particular measurements of the extent of a particular lithofacies. Quarry operators on the Bruce Peninsula would greatly benefit from GPR images of the shallow subsurface for their exploration of pure carbonates (e.g., Colpoy Bay Member of the Amabel Formation) or lateral extensions of the Eramosa Member, which has been exploited for its use as a building and ornamental stone.

7.2 Recommendations for Future Work

Although this study covers a broad spectrum of the stratigraphy and petrography of the Amabel and Guelph formations on the Bruce Peninsula, additional research could shed

further light on the interpretation of the depositional and diagenetic history. Potential additions to this project are the following:

- 1) Incorporation of geochemical data in the form of (a) Sr concentrations, (b) oxygen, carbon, and radiogenic strontium isotopes, and (c) fluid inclusions would allow comparison of the diagenesis of Bruce Peninsula carbonates with correlative carbonates elsewhere in the Michigan Basin area;
- 2) Additional core and outcrop analysis of the Clinton and Albemarle groups on Manitoulin Island and the northern Bruce Peninsula in order to assess the suggestion made by Briggs et al. (1980) that an inlet existed during the Early Silurian; and
- 3) Increase the length of ground-penetrating radar lines and/or create a three-dimensional model within or adjacent to current quarries where there is interest in continued or new exploration of strata of the Amabel and Guelph (including the Eramosa Member) formations.

7.2.1 Geochemical contributions

Sr concentrations would be useful to compare to those obtained by Land (1980), Zheng (1999), Banner (1995), and Machel and Anderson (1989) to help determine the type of diagenetic environment the dolomites were precipitated from.

Oxygen isotopic values are controlled by temperature and oxygen isotopic composition of the precipitating fluid (Land, 1980). Oxygen isotopic values in dolostones

could be compared to calcite cements within each of the members and lithofacies, which would provide evidence for dolomitization timing relative to calcite precipitation. This would be particularly useful where dedolomitization may have occurred but was not observed using petrography. Oxygen isotopic values would also provide more information on the nature of the burial dolomitizing fluids, and insights into the temperature at which dolomite precipitated (Land, 1980).

Carbon isotope values would also characterize the dolomitizing fluid composition. Enriched values may be related to an increase in organic-derived CO₂ due to methanogenesis (Lohmann, 1988). Depleted values would possibly provide details regarding other organic-related reactions such as sulphate reduction, hydrocarbon degradation, or the oxidation of methane.

Strontium isotopic ratios provide evidence for the nature of the dolomitizing fluids and their original Sr composition. These values would add to the data obtained from carbon and oxygen isotopes to indicate the composition of the dolomitizing fluids.

Lastly, fluid inclusions help infer the chemistry of the precipitating or recrystallizing solutions, which would aid in determining the burial depth at which dolomite or calcite may have precipitated. However, acquisition of reliable fluid inclusion data from correlative carbonates in southwestern Ontario have proven to be challenging, due to their small size (M. Coniglio, personal communication, 2006), and it is likely that dolostones on the Bruce Peninsula will be equally problematical.

7.2.2 Georgian Bay Inlet

Currently there is very little evidence for the hypothesized inlet that existed during the Early Silurian on the northeastern margin of the Michigan Basin. The most northerly borehole within this study (OGS-89-3) did not reveal any significant changes in member thicknesses to support the interpretation by others (Briggs et al., 1980; Gill, 1985; Armstrong, 1993) that a channel or deeper waters existed north of the Bruce Peninsula. Boreholes drilled closer to the northern tip of the Peninsula, as well as core and outcrop analyses on the southeastern edge of Manitoulin Island, may shed light on the existence and nature of the Georgian Bay inlet.

7.2.3 Extensive GPR profiles and a three-dimensional GPR-stratigraphy model

The radar facies packages and correlations with Silurian strata determined from this project could be used in addition to extensive radar profiles or multiple closely-spaced GPR lines to create a three-dimensional model of exploitable rock. Alternatively, GPR survey extensions on the survey lines imaged in this study may provide current quarry operators with the ability to avoid karstic zones or potential reef mounds that generally contain vuggy porosity or nodular bedding which may include unwanted impurities.

References

- Alling, H.R. and Briggs, L. I. 1961. Stratigraphy of the Upper Silurian Cayugan evaporites. *American Association of Petroleum Geologists Bulletin*, v. 45, p. 515-547.
- Anastas, A.S. and Coniglio, M. 1991. Sedimentology and depositional environments of the Manitoulin Formation, Lower Silurian, southern Ontario. In: *Proceedings with Abstracts, Geological Association of Canada-Mineralogical Association of Canada, Joint Annual Meeting with Society of Economic Geologists*, p. A3.
- Annan, A.P. 2005a. Chapter 11 Ground-Penetrating Radar. In: *Near-Surface Geophysics*. D.K. Butler (ed.). Society of Exploration Geophysicists, Tulsa. p. 357-438.
- Annan, A.P. 2005b. Chapter 7 GPR methods for hydrogeological studies. In: *Hydrogeophysics*. Y. Rubin and S.S. Hubbard (eds.). Springer, Dordrecht, 523p.
- Armstrong, D.K. 1988. Paleozoic geology of the central Bruce Peninsula. In: *Summary of Field Work and Other Activities 1988*, Ontario Geological Survey, Miscellaneous Paper 141, p. 446-453.
- Armstrong, D.K. 1993a. Paleozoic geology of the central Bruce Peninsula; Ontario Geological Survey, Open File Report 5856, 19p.
- Armstrong, D.K. 1993b. Paleozoic Geology of Southern Bruce Peninsula, Southern Ontario; Ontario Geological Survey, Open File Report 5875, 19p.
- Armstrong, D. K., and Dubord, M. P., 1992, Paleozoic geology, northern Bruce Peninsula, southern Ontario: Ontario Geological Survey, Open File Map 198, scale 1:50,000.
- Armstrong, D.K. and Goodman, W.R. 1990. Stratigraphy and depositional environments of Niagaran carbonates, Bruce Peninsula, Ontario; American Association of Petroleum Geologists, 1990 Eastern Section Meeting, hosted by Ontario Petroleum Institute, Field Trip Guidebook no.2, 59p.
- Armstrong, D. K., and Meadows, J. R., 1988, Stratigraphy and resource potential of the Eramosa member (Amabel Formation), Bruce Peninsula, Ontario: Ontario Geological Survey, Open File Report 5662, 89p.
- Armstrong, D.K., Goodman, W.R., and Coniglio, M. 2002. Stratigraphy and depositional environments of Niagaran carbonates, Bruce Peninsula, Ontario; Guidebook for 2002 Ontario Petroleum Institute fall fieldtrip, September 20-22, 2002, London, Ontario, 56p.
- Asprion, U. and Aigner, T. 2000. An initial attempt to map carbonate buildups using ground-penetrating radar: an example from the Upper Jurassic of SW-Germany. *Facies*, v. 42, p. 245-252.
- Asprion, U., Aigner, T., and Westphal, H. 2004. Refining sedimentological information of carbonate environments with ground-penetrating radar (GPR). Tenth International Conference on Ground Penetrating Radar, 21-24 June, Delft, The Netherlands.
- Banner, J.L. 1995. Application of the trace element and isotope geochemistry of strontium to studies of carbonate diagenesis. *Sedimentology*, v. 42, p. 805-824.
- Bathurst, R.G.C. 1975. Carbonate sediments and their diagenesis. Elsevier, Amsterdam, 658p.
- Beales, F. W. 1953. Dolomitic mottling in Palliser (Devonian) Limestone, Banff and Jasper National Parks, Alberta. *Bulletin of the American Association of Petroleum Geologists*, v. 37, p. 2281-2293.
- Brett, C.E. and Brookfield, M.E. 1984. Morphology, faunas and genesis of Ordovician hardgrounds from southern Ontario, Canada. *Paleogeography, Paleoclimatology, Palaeoecology*, v. 46, p. 233-290.
- Brett, C.E., Goodman, W.M., and LoDuca, S.T. 1990. Sequences, cycles, and basin dynamics in the Silurian of the Appalachian Foreland Basin. *Sedimentary Geology*, v. 69, p. 191-244.

- Brett, C.E., Tepper, D.H., Goodman, W., LoDuca, S.T., Eckert, B. 1995. Revised stratigraphy and correlations of the Niagaran Provincial Series (Medina, Clinton, and Lockport Groups) in the type area of western New York: U. S. Geological Survey Bulletin 2096, 66p.
- Brett, C.E., Goodman, W.M., LoDuca, S.T., and Tetreault, D. 1999. Silurian-Early Devonian sequence stratigraphy, events, and paleoenvironments of western New York and Ontario, Canada: New York Geological Association, 71st Annual Meeting Field Trip Guidebook, p. B1-B36.
- Briggs, L.I. and Briggs, D. 1974. Niagara-Salina relationships in the Michigan Basin. In: Silurian Reef-Evaporite Relationships. R.V. Kesling (ed.). Michigan Basin Geological Society Field Guidebook, p. 1-30.
- Briggs, L.I., Gill, D., Briggs, D.Z., and Elmore, R.D. 1980. Chapter 17: Transition from open marine to evaporite deposition in the Silurian Michigan Basin. In: Developments in Sedimentology 28: Hypersaline Brines and Evaporitic Environments A. Nissenbaum (ed.). Elsevier Scientific Publishing Company, New York, p. 253-270.
- Bolton, T.E. 1953. Silurian formations of the Niagara Escarpment in Ontario. Geological Survey of Canada, Paper 53-23, 19p.
- Bolton, T.E. 1957. Silurian stratigraphy and paleontology of the Niagara Escarpment in Ontario. Geological Survey of Canada, Memoir 289, 145p.
- Brunton, F.R., and Copper, P. 1994. Paleoecologic, temporal and spatial analysis of Early Silurian patch reefs of the Chicotte Formation, Anticosti Island, Canada. *Facies*, v. 31, p. 57-80.
- Brunton, F.R., and Dixon, O.A. 1994. Siliceous sponge-microbe biotic associations and their recurrence through the Phanerozoic as reef mound constructors. *Palaios*, v. 9, p. 370-387.
- Brunton, F.R., Copper, P., and Dixon, O.A. 1997. Silurian reef-building episodes. In: Lessios, H. A., and Macintyre, I. A. (eds.). Proceedings of the 8th International Coral Reef Symposium, Panama City: Smithsonian Tropical Research Institute, v. II, p. 1643-1650.
- Brunton, F.R., Smith, L., Dixon, O.A., Copper, P., Nestor, H., and Kershaw, S. 1998. Silurian reef episodes, changing seascapes and paleobiogeography; *in* Silurian Cycles and Sequences: The James Hall Symposium, Second International Symposium of the Silurian System, New York State Museum Bulletin 491, p.259-276.
- Brunton, F.R. and Dekeyser, L. 2004. Industrial mineral potential of the Guelph Formation and the Eramosa Member of the Amabel Formation, southwestern Ontario. In: Summary of Fieldwork, Ontario Geological Survey, 2004 Ontario Mining Review, p. 19-1–19-5.
- Brunton, F.R., Dekeyser, L., and Coniglio, M. 2005. Diagenetic history of the Guelph Formation, Eramosa Member, and Amabel Formation, southwestern Ontario. In: Summary of Fieldwork, Ontario Geological Survey, 2005 Ontario Mining Review, p. 34-1–34-5.
- Burns, S.J., McKenzie, J.A. and Vasconcelos, C. 2000. Dolomite formation and biogeochemical cycles in the Phanerozoic, *Sedimentology*, v. 47, p. 49-61.
- Carter, T.R. 1990. Subsurface geology of southwestern Ontario: a core workshop. Ontario Petroleum Institute, 146p.
- Cercone, K.R. 1988. Evaporative sea-level drawdown in the Silurian Michigan Basin. *Geology*, v. 16, p. 387-390.
- Cercone, K.R. and Lohmann, K.C. 1987. Late burial diagenesis of Niagaran (Middle Silurian) pinnacle reefs in Michigan Basin. *American Association of Petroleum Geologists Bulletin*, v. 71, p. 156-166.
- Chamberlain, A.T., Sellers, W., Proctor, C., and Coard, R. 2000. Cave detection in limestone using ground-penetrating radar. *Journal of Archaeological Science*, v. 27, p. 957-964.

- Chow, N. and Longstaffe, F.J. 1995. Dolomites of the Middle Devonian Elm Point Formation, southern Manitoba: intrinsic controls on early dolomitization, *Bulletin of Canadian Petroleum Geologists*, v. 43, p. 214-225.
- Charbonneau, S.L. 1990. Subaerial exposure of Middle Silurian Guelph Formation pinnacle reefs of the Michigan Basin, southwestern Ontario: Ontario Petroleum Institute Inc., Twenty-Ninth Annual Conference, Technical Session No. 4, Paper No. 17, London, Ontario, p. 1-22.
- Cheel, R.J. 1991. Sedimentology and Depositional Environments of Silurian Strata of the Niagara Escarpment, Ontario and New York, GAC, MAC, SEG, Joint Annual Meeting Toronto '91, Field Trip B4: Guidebook, 99p.
- Clarke, J.M., and Ruedemann, R. 1903. Guelph fauna in the state of New York: New York State Museum, Memoir 5, 195p.
- Coniglio, M. 1987. Biogenic chert in the Cow Head Group (Cambro-Ordovician), western Newfoundland: *Sedimentology*, v. 34, p. 813-823.
- Coniglio, M., James, N.P., and Aissaoui, D.M. 1988. Dolomitization of Miocene Carbonates, Gulf of Suez, Egypt, *Journal of Sedimentary Petrology*, v. 58, p. 100-119.
- Coniglio, M., Zheng, Q. and Carter, T.R. 2003. Dolomitization and recrystallization of middle Silurian reefs and platformal carbonates of the Guelph Formation, Michigan Basin, southwestern Ontario. *Bulletin of Canadian Petroleum Geology*, v. 51, p. 177-199.
- Coniglio, M., Frizzell, R. and Pratt, B.R. 2004. Reef-capping laminites in the Upper Silurian carbonate-to-evaporite transition, Michigan Basin, southwestern Ontario. *Sedimentology*, v. 51, p. 653-668.
- Cowell, D.W., and Ford, D.C. 1980. Hydrochemistry of a dolomite karst: the Bruce Peninsula of Ontario. *Canadian Journal of Earth Sciences*, v. 17, p. 520-526.
- Crowley, D.J. 1973. Middle Silurian patch reefs in Gasport Member (Lockport Formation), New York. *American Association of Petroleum Geologists Bulletin*, v.57, p.283-300.
- Dagallier, G., Laitinen, A.I., Malatre, F., van Campenhout, I.P.A.M., and Veeken, P.C.H. 2000. Ground-penetrating radar application in a shallow marine Oxfordian limestone sequence located on the eastern flank of the Paris Basin, NE France. *Sedimentary Geology*, v. 130, p. 140-165.
- Daniels, D. J. (ed.), 2004. *Ground Penetrating Radar (2nd Edition)*. The Institution of Electrical Engineers, London., 726 pp.
- de Freitas, T.A., Brunton, F.R. and Bernecker, T. 1993. Silurian megalodont bivalves of the Canadian Arctic and Australia: Paleoecology and evolutionary significance; *Palaios*, v. 8, p. 450-464.
- Dietrich, R.V., Hobbs Jr., C.R.B., and Lowry, W.D. 1963. Dolomitization interrupted by silicification, *Journal of Sedimentary Petrology*, v. 33, p. 646-663.
- Derry Michener Booth and Wahl and Ontario Geological Survey 1989a. *Limestone industries of Ontario, Volume 1-Geology, Properties and Economics*; Ontario Ministry of Natural Resources, Land Management Branch, 158p.
- Droste, J.B., and Shaver, R.H. 1985. Comparative stratigraphic framework for Silurian reefs - Michigan Basin to surrounding platforms. In: *Ordovician and Silurian rocks of the Michigan Basin and its margins*. Cercone, K.R., and Budai, J.M. (eds.). Michigan Basin Geological Society, Special Paper 4, p. 73-93.
- Droste, J.B., and Shaver, R.H. 1987. Paleooceanography of Silurian seaways in the midwestern basins and arches region. *Paleooceanography*, v. 2, p. 213-227.
- Dunham, R.J. 1962. Classification of rock types according to depositional texture. In: *Classification of carbonate rocks*. W.E. Ham (ed.). American Association of Petroleum Geologists, Memoir 1, p. 108-121.

- Eley, B.E., and Jull, R.K. 1982. Chert in the Middle Silurian Fossil Hill Formation of Manitoulin Island, Ontario. *Bulletin of Canadian Petroleum Geology*, v. 30, p. 208-215.
- Eley, B.E., and von Bitter, P.H. 1989. Chert of Southern Ontario: Royal Ontario Museum Miscellaneous Publication, 51 p.
- El-Tabakh, M., Mory, A., Schreiber, C., and Yasin, R. 2004. Anhydrite cements after dolomitization of shallow marine Silurian carbonates of the Gascoyne Platform, Southern Carnarvon Basin, Western Australia. *Sedimentary Geology*, v. 164, p. 75-87.
- Fisher, D.W. 1962. Silurian Rocks of the Southern Lake Michigan Area, Michigan Basin Geological Society, Annual Field Conference 1962.
- Flügel, E. 1982. *Microfacies analysis of limestones*. Springer-Verlag, New York, 633p.
- Folk, R.L. 1959. Practical petrographic classification of limestones. *Bulletin of the American Association of Petroleum Geologists*, v. 43, p. 1-38.
- Folk, R.L. and Weaver, C.E. 1952. A study of the texture and composition of chert. *American Journal of Science*, v. 250, p. 498-510.
- Gill, D. 1977. The Bell River Mills gas field, productive Niagaran reefs encased by sabkha deposits, Michigan Basin. Michigan Basin Geological Society, Special Papers, no.2, 187p.
- Gill, D. 1985. Depositional facies of Middle Silurian (Niagaran) pinnacle reefs, Belle River Mills gas field, Michigan Basin, southeastern Michigan. In: *Carbonate Petroleum Reservoirs*. Roehl, P.O. and Choquette, P.W. (eds.). Springer-Verlag, 622p.
- Grimwood, J.L., Coniglio, M. and Armstrong, D.K. 1999. Blackriveran carbonates from the subsurface of the Lake Simcoe area, southern Ontario: Stratigraphy and sedimentology of a low-energy carbonate ramp. *Canadian Journal of Earth Sciences*, v. 36, p. 871-889.
- Hagan, T.H., Coniglio, M., and Edwards, T.W.D. 1998. Subfossil bioerosion of mollusc shells from a freshwater lake, Ontario, Canada. *Ichnos*, v. 6, p. 117-127.
- Harland, W.B., Armstrong, R.L., Cox, A.V., Craig, L.E., Smith, A.G., and Smith, D.G. 1990. *A geologic time scale*. Cambridge University Press, Cambridge, 263p.
- Huh, J.M., Briggs, L.I., and Gill, D. 1977. Depositional environments of pinnacle reefs, Niagara and Salina Groups, northern shelf, Michigan Basin. In: *Reefs and evaporites, Concepts and depositional models*. J. H. Fisher, (ed.). American Association of Petroleum Geologists, Studies in Geology no. 5, p. 1-21.
- James, N.P., and Ginburg, R.N. 1979. The seaward margin of Belize barrier and atoll reefs, morphology, sedimentology organism distribution and Late Quaternary History. *International Association of Sedimentologists, Special Publication 3*, 191 p.
- Jeppsson, L., Aldridge, R.J., and Dorning, K. 1995. Wenlock (Silurian) oceanic episodes and events. *Journal of the Geological Society*, v. 152, p. 487-498.
- Jodry, R. L. 1969. Growth and dolomitization of Silurian Reefs, St. Clair County, Michigan. *American Association of Petroleum Geologists Bulletin*, v. 52, p. 957-981.
- Johnson, M.D., Armstrong, D.K., Sanford, B.V., Telford, P.G., and Rutka, M.A. 1991. Paleozoic and Mesozoic Geology of Ontario. In: *Geology of Ontario: Ontario Geological Survey, Special Volume 4*, pt. 2, p. 907-1008.
- Johnson, M.E. and McKerrow, W.S. 1991. Sea level and faunal changes during the latest Llandovery and earliest Ludlow (Silurian). *Historical Biology*, v. 5, p. 153-169.
- Kendall, A.C. 1977. Origin of Dolomite Mottling in Ordovician Limestones from Saskatchewan and Manitoba. *Bulletin of Canadian Petroleum Geology*, v. 25, p. 480-504.

- Kershaw, S., and Brunton, F.R. 1999. Paleozoic stromatoporoid taphonomy: ecologic and environmental significance. *Palaeogeography, Palaeoclimatology, Palaeoecology*, v. 149, p. 313-328.
- Kobluk, D.R. and Brookfield, M.E. 1982. Excursion 12A: Lower Paleozoic carbonate rocks and paleoenvironments in southern Ontario. International Association of Sedimentologists, Field Excursion Guidebook – 11th International Congress on Sedimentology, McMaster University, Hamilton, Ontario. 62p.
- Kruger, J.M., Martinez, A., and Franseen, E.K. 1997. A high-frequency ground-penetrating radar study of the Drum limestone, Montgomery County, Kansas. Kansas Geological Survey Open File Report 96-49.
- Kunert, M., Coniglio, M., and Jowett, E.C. 1998. Controls and age of cavernous porosity in Middle Silurian dolomite, southern Ontario. *Canadian Journal of Earth Sciences*, v. 35, p. 1044-1053.
- Kunert, M. and Coniglio, M. 2002. Origin of vertical shafts in bedrock along the Eramosa River valley near Guelph, southern Ontario. *Canadian Journal of Earth Sciences*, v. 39, p. 43-52.
- Land, L. S. 1980. The isotopic and trace element geochemistry of dolomite: the state of the art. In: *Concepts and models of dolomitization*. Zenger, D. H., Dunham, J. B., and Ethington, R. L. (eds.). Society of Economic Paleontologists and Mineralogists, Special Publication no. 28, p. 87-110.
- Liberty, B.A., and Bolton, T.E. 1971. Paleozoic geology of the Bruce Peninsula area, Ontario: Geological Survey of Canada, Memoir 360, 163p.
- Logan, W.E. 1863. Geology of Canada; Geological Survey of Canada, Progress Report to 1863, 336p.
- Lowenstam, H.A. 1957. Niagaran reefs in the Great Lakes area. Geological Society of America, Memoir 67, p. 215-248.
- Lowenstein, T.K. 1983. Deposition and alteration of an ancient potash evaporite: the Permian Salado Formation of New Mexico and West Texas. Ph.D. thesis, The Johns Hopkins University, Baltimore, MD, 411p.
- Machel, H.G. 2004. Concepts and models of dolomitization: a critical reappraisal. In: *The geometry and petrogenesis of dolomite hydrocarbon reservoirs*. Braithwaite, C. J. R., Rizzi, G. and Darke, G. (eds.). Geological Society, London, Special Publications, 235, p. 7-63.
- Machel, H.G. and Anderson, J.H. 1989. Pervasive subsurface dolomitization of the Nisku Formation in central Alberta. *Journal of Sedimentary Petrology*, v. 59, p. 891-911.
- Machel, H.G. and Lonnee, J. 2002. Hydrothermal dolomite – a product of poor definition and imagination. *Sedimentary Geology*, v. 152, p. 163-171.
- McIlreath, I.A., and Morrow, D.W. (eds.). 1990. Diagenesis, Geoscience Canada Reprint Series 4, 338p.
- Mesolella, K.J., Robinson, J.D., McCormick, L.M. and Ormiston, A.R. 1974. Cyclic deposition of Silurian carbonates and evaporites in Michigan Basin. *American Association of Petroleum Geologists Bulletin*, v. 58, p. 34-62.
- Middleton, K., Coniglio, M., Sherlock, R. and Frape, S.K. 1993. Dolomitization of Middle Ordovician carbonate reservoirs, southwestern Ontario. *Bulletin of Canadian Petroleum Geology*, v. 41, p. 150-163.
- Mosher, R.E., Lilienthal, R.T., and Sanford, J.T. 1978. The lithostratigraphy of the Warton Silurian section, Bruce Peninsula, Ontario, Canada. In: *Geology of the Manitoulin area*. Sanford, J.T., and Mosher, R.E. (eds.). Michigan Basin Geological Society, Special Papers, No. 3, p. 101-106.
- Noble, J.P.A. and Van Stempvoort, D.R. 1989. Early burial quartz authigenesis in Silurian platform carbonates, New Brunswick, Canada. *Journal of Sedimentary Petrology*, v. 59, p. 65-76.
- Nowlan, J.P. 1935. The Silurian Stratigraphy of the Niagaran Escarpment in Ontario. Unpublished Ph. D. Thesis, University of Toronto, Canada.
- Pounder, J.A. 1962. Guelph-Lockport Formation of southwestern Ontario: Ontario Petroleum Institute, Inc., 1st Annual Conference, Paper 5, p. 1-29.

- Pratt, B.R. and Miall, A.D. 1993. Anatomy of a bioclastic grainstone megashoal (Middle Silurian, southern Ontario) revealed by ground-penetrating radar. *Geology*, v. 21, p. 223-226.
- Reid, A. 1989. Principles of Applied Carbonate Petrography, Permian Basin Graduate Center Pub. No. 3-89, 51p.
- Reineck, H., Gerdes, G., Claes, M., Dunajtschik, K., Riege, H. and Krumbein, W.E. 1990. Microbial modification of sedimentary surface structures. In: *Sediments and environmental geochemistry: selected aspects and case histories*. D. Heling, P. Rothe, U. Forstner and P. Stoffers (eds.). Springer-Verlag, p. 254-276.
- Roberts, M.C., Niller, H. and Helmstetter, N. 2003. Sedimentary architecture and radar facies of a fan delta, Cypress Creek, West Vancouver, British Columbia. In: Bristow, C.S. and Jol, H.M. (eds.). *Ground Penetrating Radar in Sediments*. Geological Society, London, Special Publications, 211, p. 111-126.
- Sanford, B.V. 1969. Silurian of southwestern Ontario; Ontario Petroleum Institute, 8th Annual Conference Proceedings, Technical Paper No. 5, p.1-44.
- Sanford, B.V., Thomson, F.J., and McFall, G.H. 1985. Plate tectonics- a possible controlling mechanism in the development of hydrocarbon traps in southwestern Ontario. *Bulletin of Canadian Petroleum Geology*, v. 33, p. 52-71.
- Sanford, J.T., and Mosher, R.E. (eds.). 1978. *Geology of the Manitoulin area, including the Road Log to the Michigan Basin Geological Society Field Trip, Sept. 29-Oct. 1, 1978*: Michigan Basin Geological Society, Special Papers, No. 3, 111p.
- Schneiderman, N. and Harris, P.M. 1985. Carbonate cements. *Society of Economic Paleontologists, Special Publication 36*, 379p.
- Scholle, P.A. 1978. A colour illustrated guide to carbonate rock constituents, textures, cements and porosities. *American Association of Petroleum Geologists, Memoir 27*, 241p.
- Sears, S.O., and Lucia, F.J. 1980. Dolomitization of northern Michigan Niagara reefs by brine refluxion and freshwater/seawater mixing. In: *Concepts and models of dolomitization*. Zenger, D.H., Dunham, J.B., and Ethington, R.L. (eds.). *SEPM Special Publication 28*, p. 215-235.
- Shaver, R.H. 1991. A history of study of Silurian reefs in the Michigan Basin environs. *Geological Society of America, Special Paper 256*, p. 101-138.
- Shaver, R.H., Ault, C.H., Ausich, W.I., Droste, J.B., Horowitz, A.S., James, W.C., Okla, S.M., Rexroad, C.B., Suchomel, D.M. and Welch, J.R. 1978. The search for a Silurian reef model, Great Lakes area; Department of Natural Resources, Geological Survey Special Report 15, 36p.
- Shaw, E.W. 1937. The Guelph and Eramosa formations of the Ontario Peninsula. *Transactions of the Royal Canadian Institute*, v. 21 p. 317-362.
- Sibley, D.F. and Gregg, J.M. 1987. Classification of Dolomite Rock Textures. *Journal of Sedimentary Petrology*, v. 57, p. 967-975.
- Siever, R. 1962. Silica solubility, 0-200degrees C, and the diagenesis of siliceous sediments. *Journal of Geology*, v. 70, p. 127-150.
- Smith, L. 1990. Geologic controls on porosity and permeability variation in Silurian pinnacle reef bioherms, southwestern Ontario: Ontario Petroleum Institute Inc. Twenty-Ninth Annual Conference, Technical Session No. 2, Paper No. 4, London, Ontario, p. 1-19.
- Stott, C.A. and von Bitter, P.H. 1999. Lithofacies and age variation in the Fossil Hill Formation (Lower Silurian), southern Georgian Bay region, Ontario. *Canadian Journal of Earth Sciences*, v. 36, p. 1743-1762.
- Telford, P.G. 1978. Silurian stratigraphy of the Niagara Escarpment, Niagara Falls to the Bruce Peninsula. In: *Toronto '78 Field Trip Guidebook: GSA-GAC-MAC, Meeting*. Currie, A.L., and Mackasey, W.O. (eds.). p. 28-42.

- Tetreault, D.K. 2001. A new Silurian Konservat-Lagerstätte from the Eramosa Dolostone of the southern Bruce Peninsula, Ontario. University of Western Ontario, unpublished Ph.D. thesis, 194p.
- Textoris, D.A. and Carozzi, A.V. 1964. Petrography and Evolution of Niagaran (Silurian) Reefs, Indiana. *Bulletin of the American Association of Petroleum Geologists*, v. 48, p. 397-426.
- Torok, A. 2000. Formation of dolomite mottling in Middle Triassic ramp carbonates (Southern Hungary). *Sedimentary Geology*, v. 131, p. 131-145.
- Tucker, M.E. 2001. *Sedimentary Petrology: an introduction to the origin of sedimentary rocks*. 3rd Edition, Oxford: Blackwell Science Ltd., 262p.
- Tucker, M.E. and Bathurst, R.G.C. 1990. *Carbonate diagenesis*. International Association of Sedimentologists, Reprint Series 1, Blackwell Scientific Publications, Oxford, U.K., 312p.
- Tucker, M.E., Wilson, J.E., Crevello, P.D. Sarg, J.R. and Read, J.F. 1990. Carbonate platforms, facies, sequence and evolution. International Association of Sedimentologists, Special Publication 9, Blackwell Scientific Publications, Oxford, U.K., 328p.
- Tucker, M.E., and V.P.Wright. 1990. *Carbonate sedimentology*. Blackwell Scientific Publications, Oxford, U.K., 482p.
- Twoo, A.G. 1985. The nature and origin of lead-zinc mineralization, Middle Silurian dolomites, southern Ontario. University of Waterloo unpublished M. Sc. thesis, 276p.
- Walker, R.G. and James, N.P. 1992. Facies Models, response to sea level change. Geological Association of Canada, 409p.
- Wilkinson, B.H., Owen, R.M. and Carroll, A.R. 1985. Submarine hydrothermal weathering, global eustasy and carbonate polymorphism in Phanerozoic marine oolites. *Journal of Sedimentary Petrology*, v. 55, p.171-183.
- Williams, M.Y. 1915a. The Middle and Upper Silurian of southwestern Ontario: Geological Survey of Canada, Summary Report 1914, p. 82-86.
- Williams, M.Y. 1915b. An eurypterid horizon in the Niagara Formation of Ontario: Geological Survey of Canada, Museum Bulletin No. 20, 21p.
- Williams, M.Y. 1919. The Silurian geology and faunas of Ontario Peninsula, and Manitoulin and adjacent islands: Geological Survey of Canada, Memoir 111, 195p.
- Wright, V.P. 1992. A revised classification of limestones. *Sedimentary Geology*, v. 76, p. 177-185.
- Wright, D.T. and Wacey, D. 2004. Sedimentary dolomite: a reality check. In: *The Geometry and Petrogenesis of Dolomite Hydrocarbon Reservoirs*. Braithwaite, C.J.R., Rizzi, G. and Darke, G. (eds.). Geological Society, London, Special Publications, 235, p. 65-74.
- Zenger, D.H. 1965. Stratigraphy of the Lockport Formation (Middle Silurian) in New York State: New York State Museum and Science Service, Bulletin No. 404, 210p.
- Zheng, Q. 1999. Carbonate diagenesis and porosity evolution in the Guelph Formation, southwestern Ontario. M. Sc. thesis, University of Waterloo, Canada. 265p.

Appendix A
Geologic Data

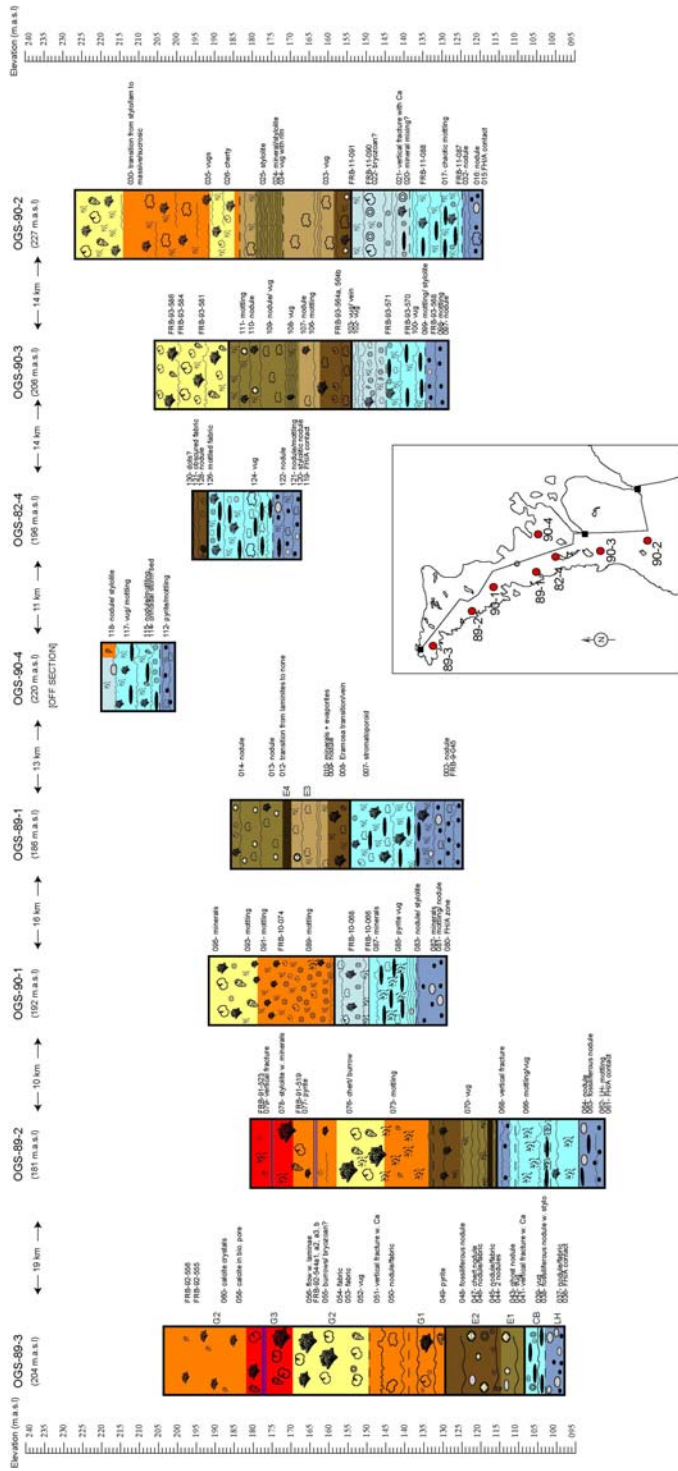


Figure A-1: Cross-section of boreholes with distribution of thin sections.

Table A1: Samples from the Owen-Sound Ledgerrock Wiarnton Quarry

Sample #	Location	Depth	Purpose	Thin Section
LD-191	L6'04	top of quarry/top of 1st bench	chert nodule	yes
LD-192	L6'04	top of quarry/top of 1st bench	chert nodule	yes
LD-193	L4'05	112 cm from top of section (2nd bench)	vug in light gray/tan nodular	yes
LD-194	L4'05	112 cm from top of section (2nd bench)	"matrix" material	yes
LD-195	L4'05	190 cm from t.o.s. (2nd bench)	I-beam bed: "I"	yes
LD-196	L4'05	190 cm from t.o.s. (2nd bench)	I-beam bed: "matrix"	yes
LD-197	L4'05	202 cm from top of section (2nd bench)	nodule in brown bed under I-beam	yes
LD-198	L4'05	176 cm from t.o.s. (2nd bench)	nodule within brown mottled	yes
LD-199	L4'05	55 cm from t.o.s. (1st bench)	dark brown/black/gray laminated	yes
LD-200	L4'05	25cm from top of section (1st bench)	massive tan	yes
LD-201	L4'05	202 cm from top of section (2nd bench)	stylolitic with mini-vug	yes

Table A2: Samples from borehole OGS-89-3

Sample #	Depth (feet)	Box #	Purpose	Thin Section
893-036	348'6"	38	FH/Amabel contact	yes
37	345'6"	38	nodule/fabric	yes
38	332'	37	fossiliferous nodule with stylo.	yes
39	330'	36	vug	yes
40	326'	36	flow around vug	
41	313'	35	vertical fracture with Ca	yes
42	309'2"	34	vug	yes
43	307'2"	34	ghost nodule	yes
44	293'	32	2 nodules	yes
45	290'8"	32	nodule/fabric	yes
46	276'	31	nodule/fabric	yes
47	273'4"	30	chert nodule	yes
48	260'4"	29	fossiliferous nodule	yes
49	243'10"	27	pyrite	yes
50	199'2"	22	nodule/fabric	yes
51	186'	21	vertical fracture with Ca	yes
52	173'	19	vug	yes
53	162'	18	fabric	yes
54	155'	17	fabric	yes
55	142'	16	burrows?/bryozoan	yes
56	128'	14	flow with laminae	yes
58	66'10"	8	calcite in biomoldic pore	yes
59	57'10"	7	vug and mottling	
60	54'	6	calcite crystals	yes

Table A2: Samples from borehole OGS-89-2

Sample #	Depth (feet)	Box #	Purpose	Thin Section
892-061	304'5"	34	FH/Amabel contact	yes
62	302'	34	LH-mottling	yes
63	288'8"	33	fossiliferous nodule	yes
64	288'	32	nodule	yes
65	266'7"	30	mottling with stylolite	
66	232'	27	mottling/vug	yes
67	215'	25	pyrite and mottle	
68	211'	25	vertical fracture	yes
69	186'6"	22	nodule and pyrite	
70	181'8"	21	vug	yes
71	151'3"	18	stylolite and mineral	
72	142'8"	17	chert nodule	
73	118'	15	mottling	yes
74	107'	14	small biomold. Vug with minerals	
75	104'	13	strom? With minerals	
76	79'8"	10	chert + burrows	yes
77	41'6"	6	pyrite	yes
78	21'	3	stylo. With minerals	yes
79	8'8"	2	vertical fracture	yes

Table A3: Samples from borehole OGS-90-1

Sample #	Depth (feet)	Box #	Purpose	Thin Section
901-080	204'	15	FH/Amabel zone	yes
81	196'8"	14	mottling/nodule	yes
82	192'	14	minerals	yes
83	178'	13	nodule/stylo.	yes
84	177'	13	vug and stylolite	
85	162'6"	12	pyrite vug	yes
86	152'8"	11	bio/chert/mottle	
87	143'8"	10	minerals	yes
88	123'	9	odd flow?	
89	87'4"	7	mottling	yes
90	86'	6	mottling/stylolite	
91	49'1"	4	mottling	yes
92	47'10"	4	compaction/transition zone?	
93	35'7"	3	mottling	yes
94	10'6"	1	mottling	
95	8'10"	1	minerals	yes

Table A4: Samples from borehole OGS-89-1

Sample #	Depth (feet)	Box #	Purpose	Thin Section
891-001	200'5"	23	Lions Head mottling	
891-002	189'	21	nodule	yes
3	163'2"	19	minerals in mottling	
4	154'1"	18	mottling	
5	148'	17	chaotic to regular mottling	
6	129'11"	15	coral in mottling	
7	117'	14	stromatoporoid	yes
8	96'2"	12	Eramosa transition/vein	yes
9	87'6"	11	nodule	yes
10	83'	10	minerals + evaporites	yes
11	65'8"	8	transition to Eramosa	
12	44'6"	6	transition from laminites/none	yes
13	35'1"	5	nodule	yes
14	7'3"	2	nodule	yes

Table A5: Samples from borehole OGS-90-4

Sample #	Depth (feet)	Box #	Purpose	Thin Section
904-112	53'	6	pyrite/mottling	yes
113	51'	6	nodule surrounded by mottling	
114	39'8"	4	crinoidal storm bed	yes
115	36'4"	4	nodule/mottling	yes
116	32'4"	4	mottling	
117	19'6"	2	vug/mottling	yes
118	5'10"	1	nodule/stylo.	yes

Table A6: Samples from borehole OGS-82-4

Sample #	Depth (m)	Box #	Purpose	Thin Section
824-119	47.3	12	FH/Amabel contact	yes
824-120	46.95	12	stylolitic nodule	yes
121	45.43	11	nodule/mottling	yes
122	42.63	10	nodule	yes
123	38.9	8	mottling/nodule/stylolite	
124	35.22	7	vug	yes
125	27.94	4	mottled fabric	
126	23.9	3	mottled fabric	yes
127	23.19	2	mottled/Guelph contact?	
128	21.6	1	nodule	yes
129	19.98	1	minerals (calcite/pyrite) in vug	
130	19.42	1	dots?	yes
131	19.47	1	obscured fabric	yes

Table A7: Samples from borehole OGS-90-3

Sample #	Depth (feet)	Box #	Purpose	Thin Section
90-3-096	260'3"	19	pyrite nodule	
903-097	249'10"	18	nodule	yes
98	248'	18	mottling	yes
99	231'8"	17	mottling/stylo	yes
100	223'	16	vug	yes
101	194'	14	crinoid mottled	
102	168'8"	13	vug	yes
103	165'4"	12	vug/vein	yes
104	151'	11	vug with outline/nodule	
105	138'10"	11	vug and minerals	
106	130'3"	10	mottling	yes
107	122'6"	9	nodule	yes
108	111'4"	8	vug	yes
109	93'	7	nodule/vug	yes
110	76'6"	6	nodule	yes
111	68'8"	5	mottling	yes

Table A8: Samples from borehole OGS-90-2

Sample #	Depth (feet)	Box #	Purpose	Thin Section
902-015	334'9"	22	FH/Amabel contact	yes
16	329'6"	21	nodule	yes
17	309'	20	chaotic mottling	yes
18	301'	19	chaotic biostrat	
19	280'6"	18	chaotic mottling with pyrite	
20	277'	17	mineral mixing?	yes
21	270'7"	17	vertical fracture with Ca	yes
22	250'3"	16	bryozoan?	yes
23	215'5"	13	minerals in lower Guelph	
24	170'	10	mineral/stylo	yes
25	155'10"	9	stylo.	yes
26	126'	7	cherty	yes
27	99'	5	mottling and stylolite	
28	77'2"	3	texture/stylo/min?	
29	50'8"	2	sucrosic porosity	
30	47'6"	1	transition stylo lam to mas. Suc.	yes
31	329'	21	vug and nodule	
32	326'3"	21	nodule	yes
33	208'4"	13	vug	yes
34	171'	10	vug with rim	yes
35	109'11"	6	vugs	yes

Stratigraphic descriptions of the Amabel and Guelph formations from the boreholes on the Bruce Peninsula are illustrated in the following figures:

Figure A2: OGS-89-3

Figure A3: OGS-89-2

Figure A4: OGS-90-1

Figure A5: OGS-89-1

Figure A6: OGS-82-4

Figure A7: OGS-90-4

Figure A8: OGS-90-3

Figure A9: OGS-90-2

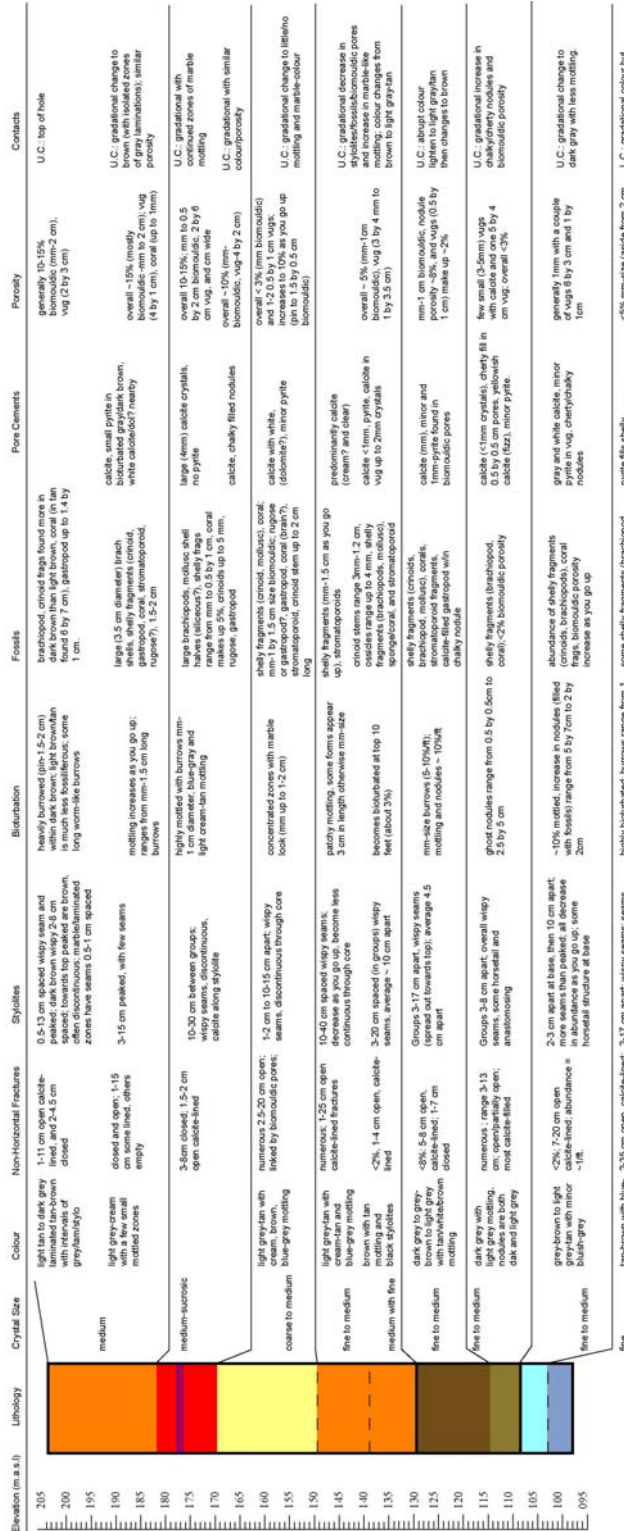


Figure A2: OGS-89-3

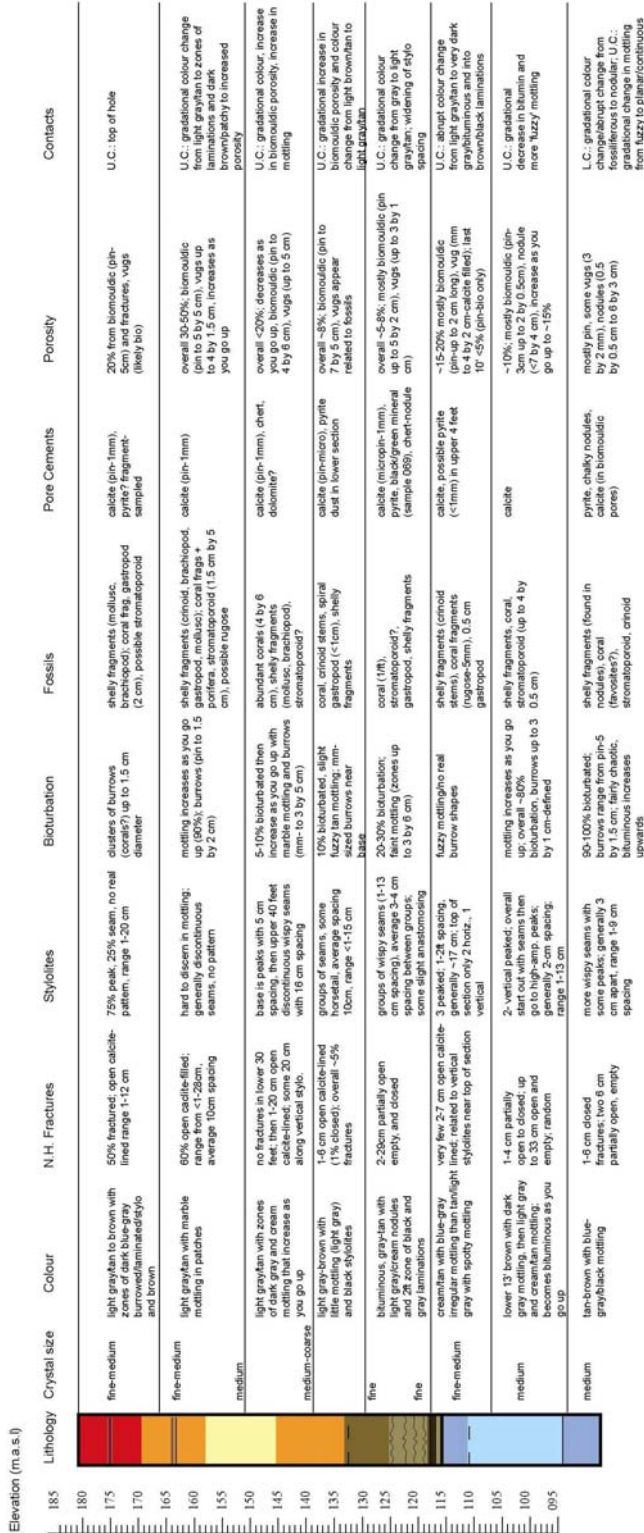


Figure A3: OGS-89-2

OGS-90-1

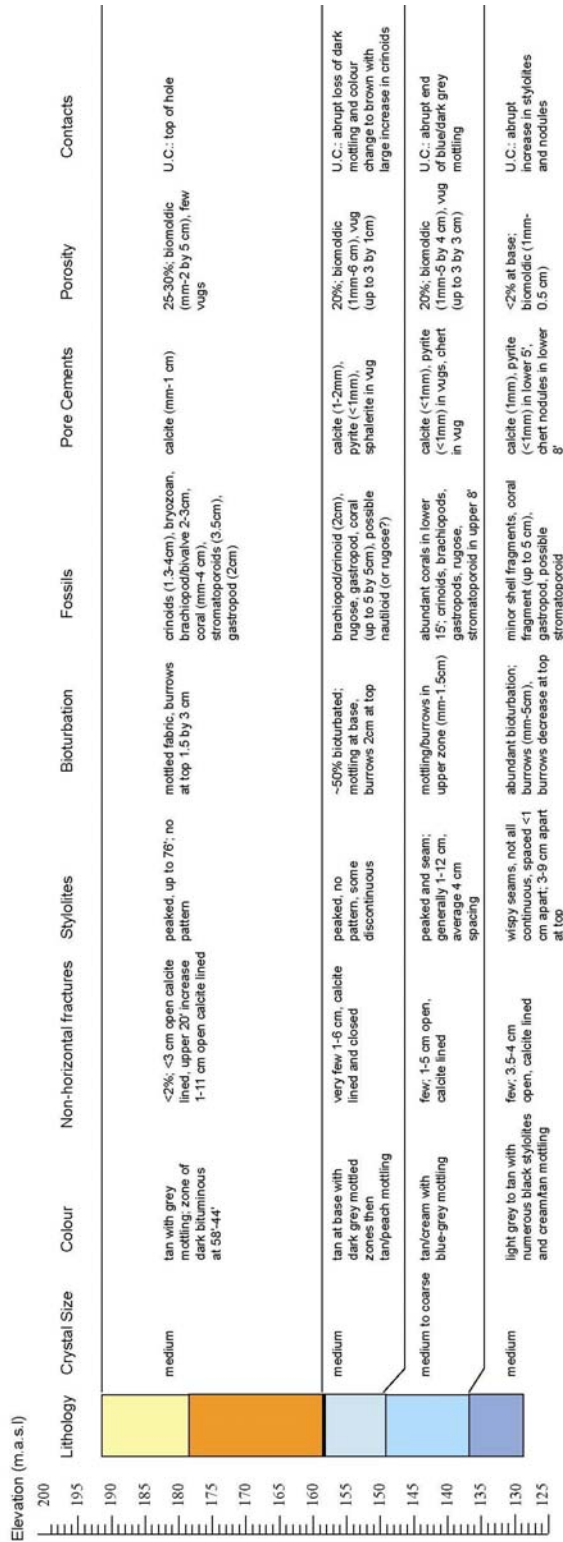


Figure A4: OGS-90-1

Crystal size	Colour	N.H. Fractures	Stylolites	Bioturbation	Fossils	Pore Cements	Porosity	Contacts
fine	chocolate brown, darkens towards top, mottling/nodule s light tan-grey	from 23 cm, 1-3 cm open (95%) Ca-lined and closed (5%)	wispy seams spaced 1-15 cm, no peaks	burrows not abundant up to 22; zoned bioturbation and nodules every 2-6 cm (abundance increases upwards)	crinoid ossicles, stems; favosites coral, brachiopods	calcite with pyrite in vug, green mineral in biomouldic pore	Overall < 5% then increases upwards to 10-20% with zones up to 60%; pores are biomouldic (pin-2mm)	U.C.: T.O.H. (Eramosa contact hard to discern)
fine	tan-grey to light grey with black and brown laminae	only one 2cm closed	random spacing of wispy seams	abundant burrows in lower 4', and again at 44'	shelly fragments (crinoid, brachiopod), coral (branching), stromatoporoids	Calcite (vugs), pyrite (pin-mm)	Overall 5%, biomouldic, 3 vugs (4 by 3 cm)	U.C.: abrupt end of laminations and start of nodules
fine	light grey-tan, minor mottling	only found above BS; 2, 10 cm closed and 7 cm partially open	Abundant seams (anastomosing) for lower 3'; then gradually spaced at 4-20 cm intervals	pin-size to mottled (20%)	Shelly fragments (crinoids, gastropod, peltepod), coral fragments, black branch-like fauna	pyrite (pin-mm), calcite, (veins, pin, mm), green surrounded by possible evaporite/cementation,	10-20% then decreases to 5-10%, pin with odd vug (1 by 1 up to 3.5 by 4cm)	U.C.: gradational colour and structure
fine	chocolate brown with tan mixing	2-9 cm open Ca-lined; one 2 cm open empty; one 6 cm closed.	Mainly wispy seams, few singular; spacing ranges from 1.5 - 8 cm, average <5 cm.	1mm-sized burrows; approximate 50% mottled	shelly fragments (crinoids, brachiopod), coral bits, strom.	pyrite, calcite crystals, calcite veins	Overall 50-60% (pin-size), vugs up to 3.5 by 4 cm; fractures up to 4mm wide, biomouldic up to 0.5 by 2 cm.	U.C.: abrupt reduction in biomouldic porosity and colour changes from brown to light gray.
medium	dark-light grey with cream-tan and bluish mottling	2-17 cm open Ca-lined	Mainly seam, some peak; range from 4-30 cm spacing, average 12 cm spacing	Irregular burrows, more bituminous at base of section	abundance increases upwards; coral fragments increase upwards (rugose); shelly fragments (crinoids- ossides and stems in tact as you go up), gastropods, brachiopods, stromatoporoids	Calcite, minor pyrite, yellow mineral (calcite- fazz)	Vugs increase as you go upwards, generally 2 by 4 cm, pin-sized biomouldic porosity increases upwards near 104'	U.C.: abrupt colour change to brown, less chaotic mottling
fine-medium	light grey with tan zones and blue-grey to black mottling	3-14 cm open and closed; open are Ca-lined	peak and seam; wispy with some horsetail; range 2-15 cm; average 7 cm spacing.	Bioturbation decreases as you go up; mottling is planar	80% bioturbation; shelly fragments increase as you go up (including gastropods). Coral fragments increase as you go up.	Calcite, minor pyrite, Vugs contain calcite; nodules don't fazz (chalky), up to 3 by 6 cm.	pin-sized biomouldic porosity and vugs up to 3 by 6 cm	L.C.: FRB sample; U.C.: gradational- mottling becomes more chaotic

Elevation (m. a.s.l)

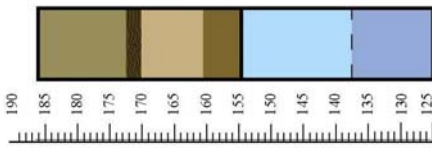


Figure A5: OGS-89-1

OGS-90-4
 Description: L. DeKeyser
 University of Waterloo
 June, 2005

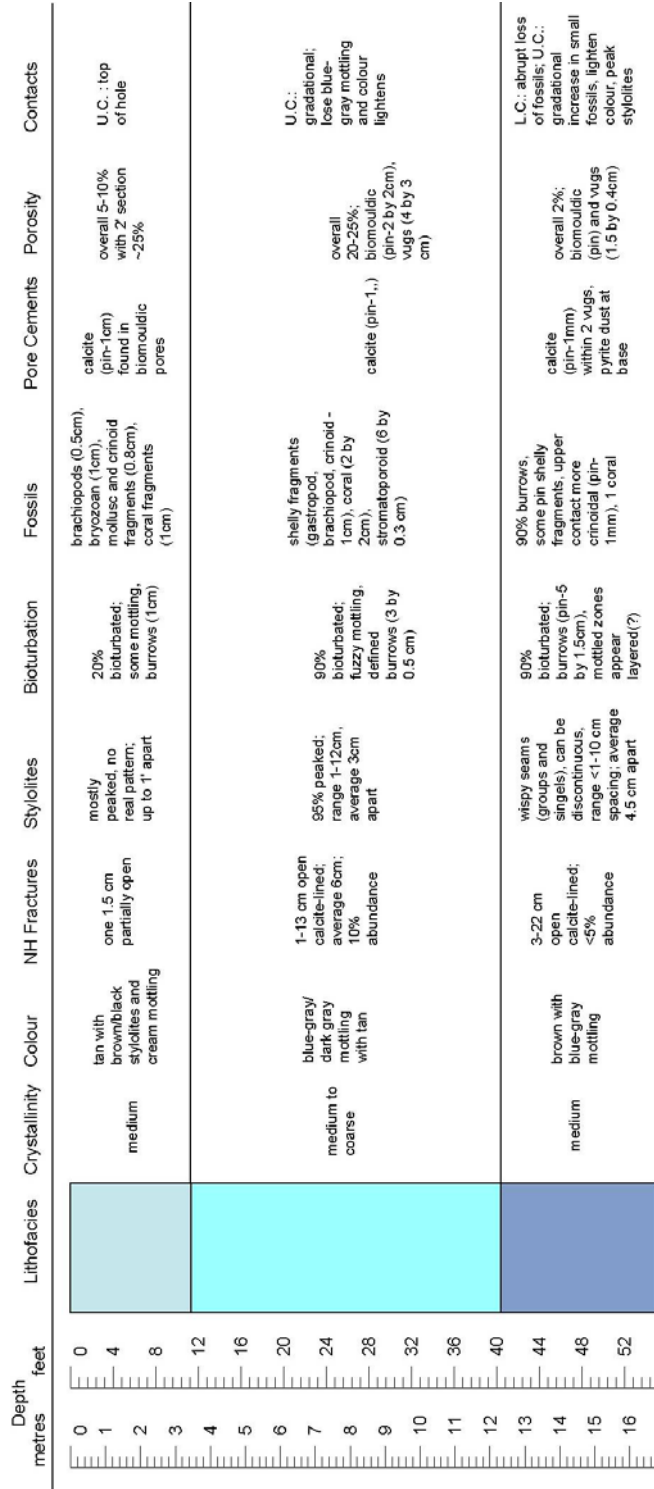


Figure A6: OGS-90-4

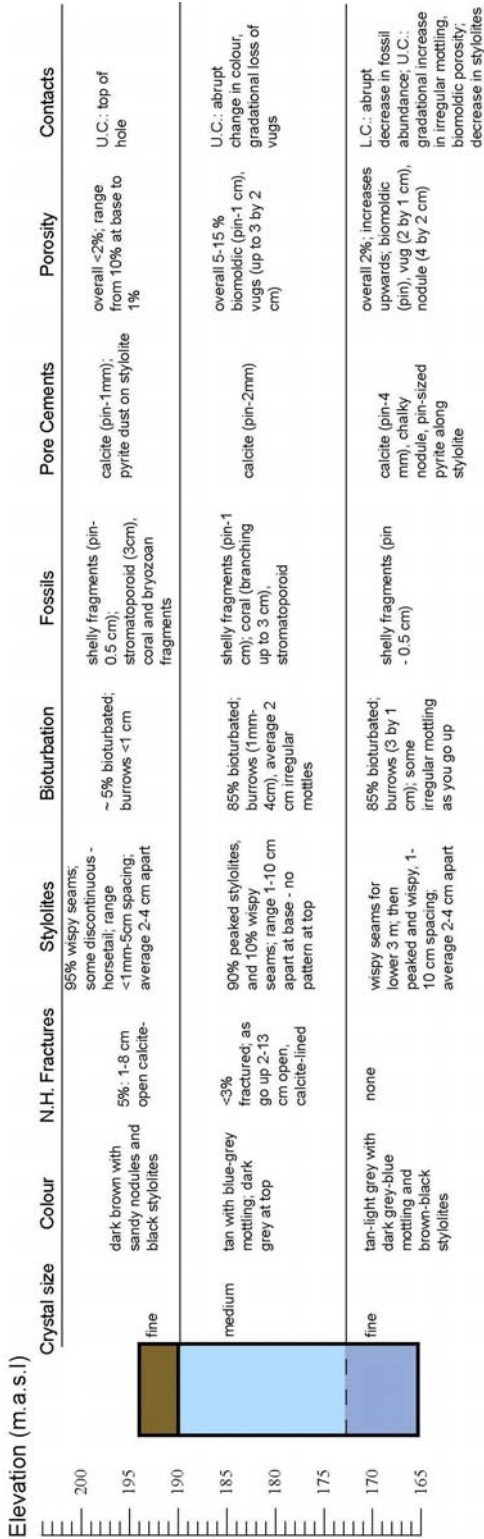


Figure A7: OGS-82-4

OGS-90-3
 Description: L. Deleyser
 University of Waterloo
 June, 2005

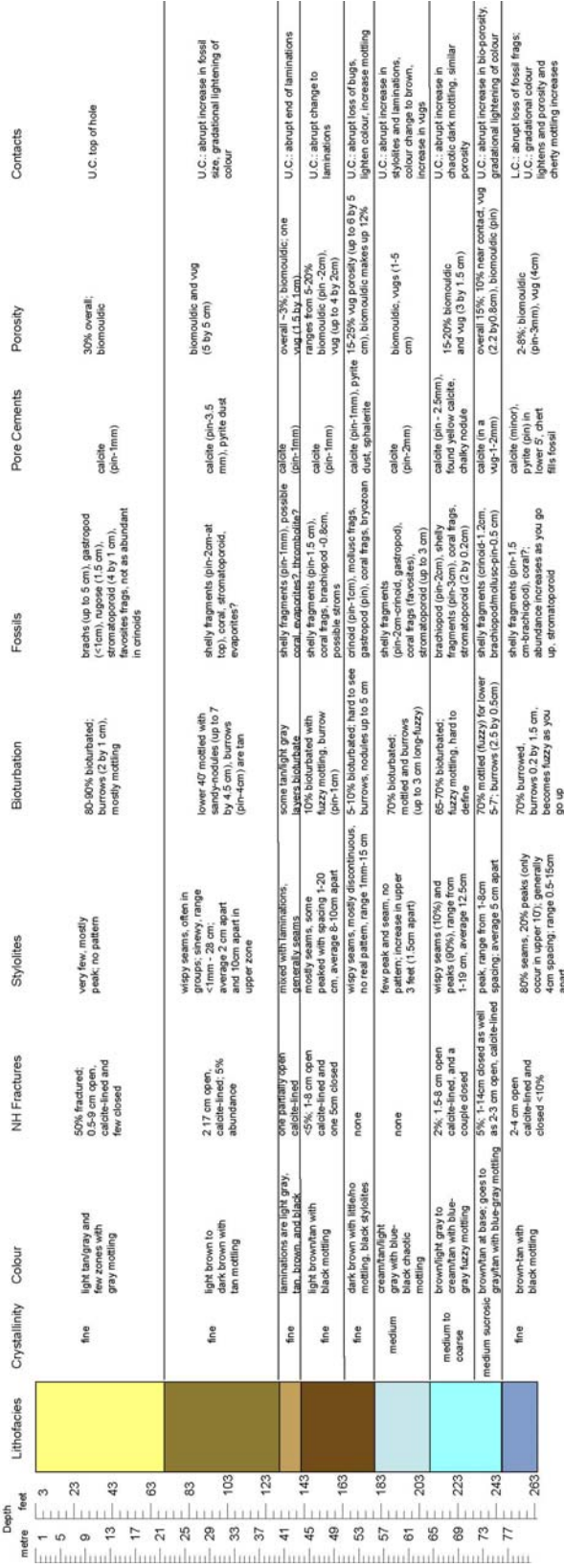


Figure A8: OGS-90-3

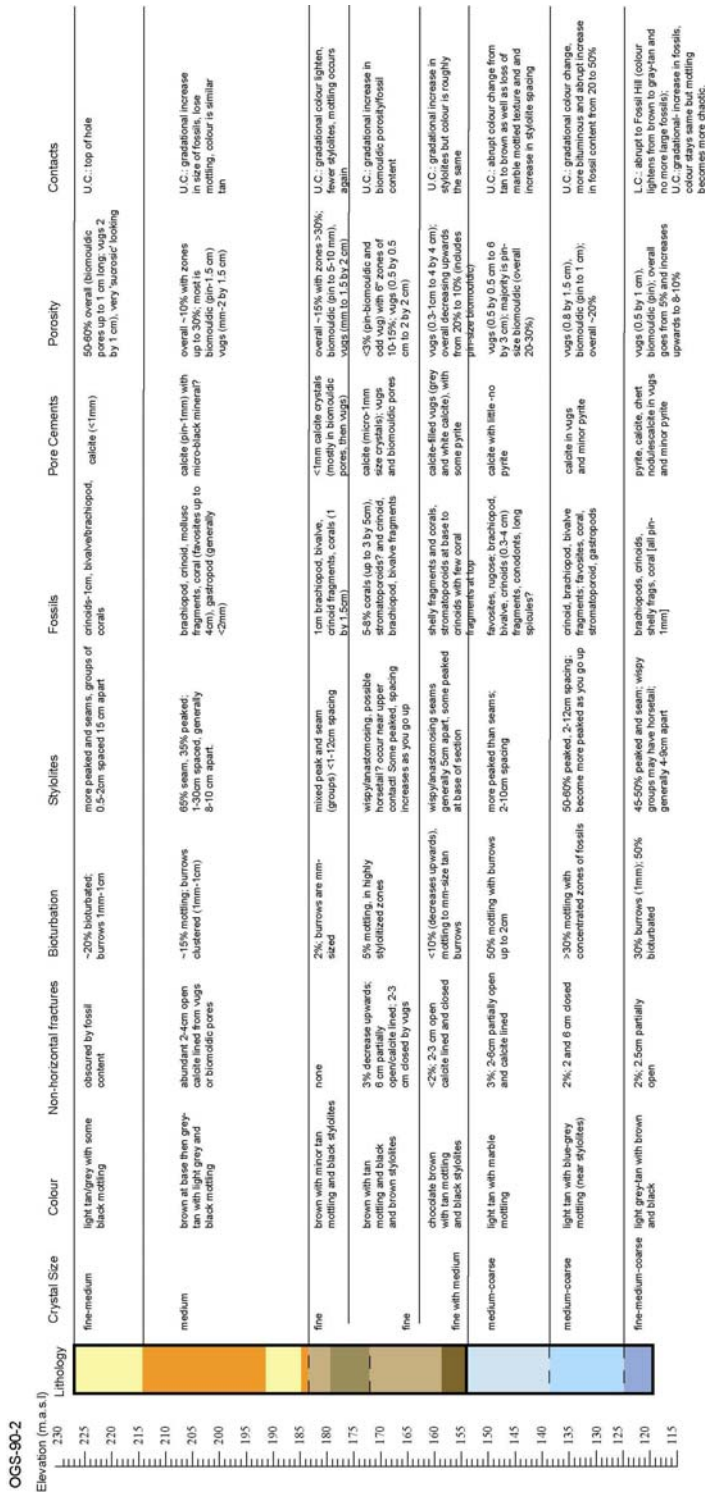


Figure A9: OGS-90-2

Appendix B– High Frequency Shallow Subsurface GPR

Table B1: CMP velocity analysis at Line 2 at the Adair Quarry

Line 2 Adair - 900 MHz
 CMP analysis
 CMP file: Line0006
 AGC = 1000
 Window width = 1
 Traces per inch = 15
 Down the trace = 3
 Trace to trace = 1

Velocity file: Line06V2
 CON gain = 6-60
 Traces per inch = 10
 Down the trace = 1

			Lower Limit	Upper Limit
CON gain max	Time (ns)	Vave (m/ns)	velocity (m/ns)	velocity (m/ns)
6	36	0.1	0.098	0.102
12				
20	52	0.098	0.096	0.1
30				
60	57	0.104	0.102	0.106
		0.10066667		

Table B2: CMP velocity analyses at Line 7 in the OSLW Quarry

Line 7 (OSLW) - 225 MHz

CMP analysis
 CMP file: Line13
 SEC = 1000
 Attenuation = 1.2
 Traces per inch = 15
 Down the trace = 3
 Trace to trace = 1

Velocity file: Line13V2
 CON gain = 4-50
 Traces per inch = 10
 Down the trace = 1

			Lower Limit	Upper Limit
CON gain max	Time (ns)	Vave (m/ns)	velocity (m/ns)	velocity (m/ns)
4	24	0.102	0.1	0.104
6	40	0.099	0.098	0.1
8	54	0.098	0.096	0.1
25	132	0.098	0.096	0.1
		0.09925		

Line 7 (OSLW) - 450 MHz

CMP analysis

CMP file: Line12

SEC = 1000

Attenuation =1.2

Traces per inch = 20

Down the trace = 3

Trace to trace = 1

Velocity file: Line12V2

CON gain = 3-20

Traces per inch = 10

Down the trace = 1

			Lower Limit	Upper Limit
CON gain max	Time (ns)	Vave (m/ns)	velocity (m/ns)	velocity (m/ns)
3	24	0.102	0.1	0.104
8	54	0.098	0.096	0.1
		0.1		

Line 7 (OSLW) - 900 MHz

CMP analysis

CMP file: Line11

SEC = 1000

Attenuation =0.8

Traces per inch = 30

Down the trace = 3

Trace to trace = 1

Velocity file: Line11V2

CON gain = 3-15

Traces per inch = 10

Down the trace = 1

			Lower Limit	Upper Limit
CON gain max	Time (ns)	Vave (m/ns)	velocity (m/ns)	velocity (m/ns)
3	8	0.107	0.102	0.112
3	24	0.102	0.098	0.106
10	38	0.1	0.098	0.102
15	54	0.098	0.096	0.1
		0.10175		

Table B3: WARR velocity analyses at Line 6 in the OSLW Quarry

Line 6 - 225 MHz

WARR analysis

WARR file: REEF6

velocity file: REEF6V

CON gain max: range from 1.5 - 80

AGC gain max = 1000

down the trace = 1

window width =3

traces per inch = 10

Down the trace = 6

traces per inch = 10

			Lower Limit	Upper Limit
CON gain max	Time (ns)	Vave (m/ns)	velocity (m/ns)	velocity (m/ns)
1.5	33	0.1	0.1	0.1
3	64	0.1	0.1	0.1
8	138	0.0995	0.099	0.1
15	162	0.1	0.1	0.1
40	191	0.1	0.1	0.1
60	208	0.105	0.1	0.11
80	208	0.105	0.1	0.11
		0.101357143		

Line 6 - 900 MHz

WARR analysis

WARR file: REEF10

velocity file: REEF10V

CON gain max: range from 1.5 - 30

AGC gain max = 1000

down the trace = 1

window width =3

traces per inch = 10

Down the trace = 3

traces per inch = 10

			Lower Limit	Upper Limit
CON gain max	Time (ns)	Vave (m/ns)	velocity (m/ns)	velocity (m/ns)
1.5	10.5	0.1	0.1	0.1
3	12.5	0.1	0.1	0.1
4	19	0.11	0.11	0.11
5	26	0.105	0.1	0.11
8	36	0.105	0.1	0.11
15	56	0.105	0.1	0.11
20	60	0.105	0.1	0.11
30	60	0.105	0.1	0.11
		0.104375		

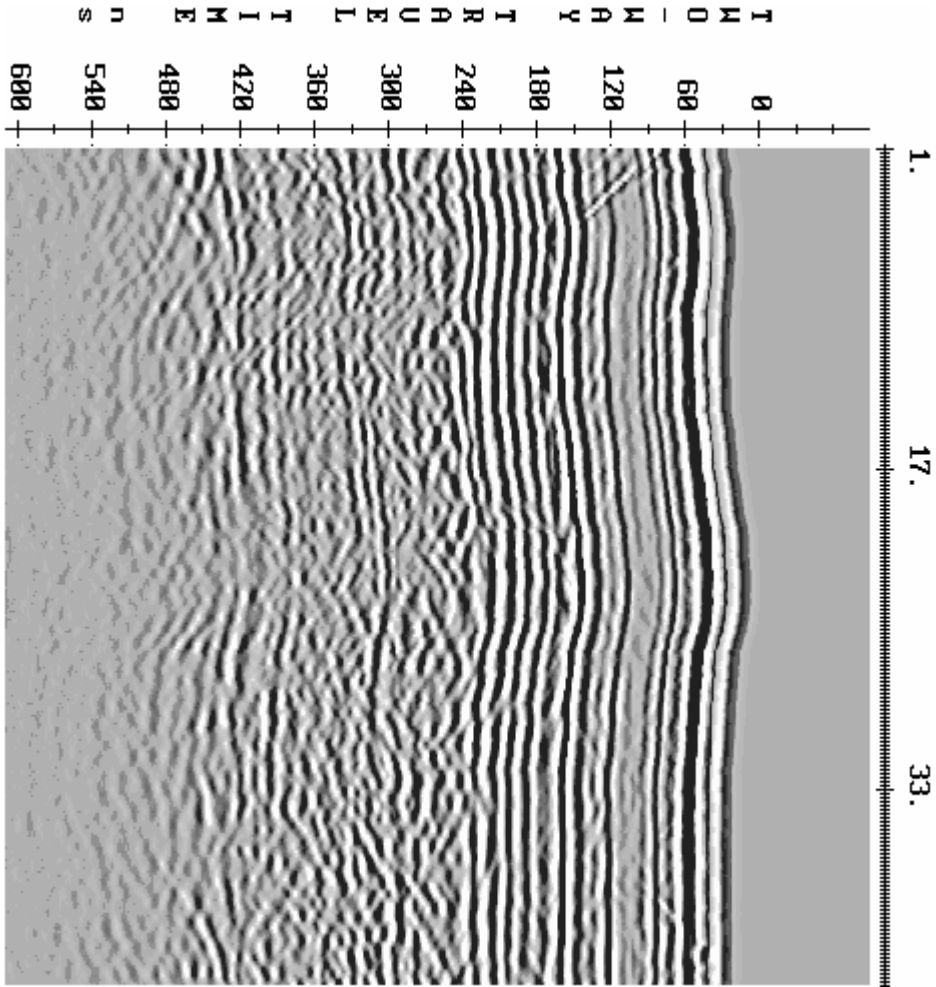


Figure B1: 450 MHz profile at Line 4 in the OSLW Quarry.
 File: OSLW'04/Elev/Line4el
 Processing included: SEC = 1000, Attenuation = 0.7, Down the trace = 3, Traces per inch = 30, V= 0.095 m/ns

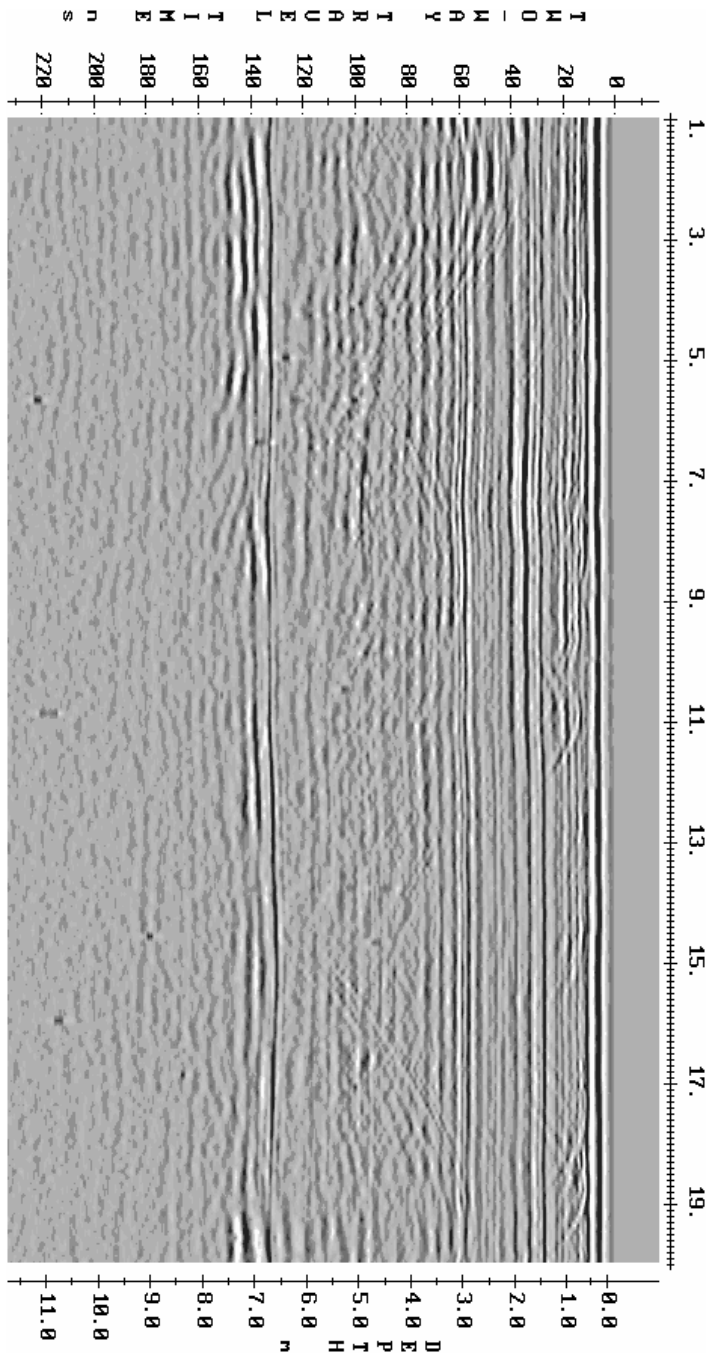


Figure B2: 225 MHz profile at Line 6 in the OSLW Quarry.

File: OSLW'04/REEF 4

Processing included: SEC = 500, Attenuation = 1, Down the trace = 5, Traces per inch = 20

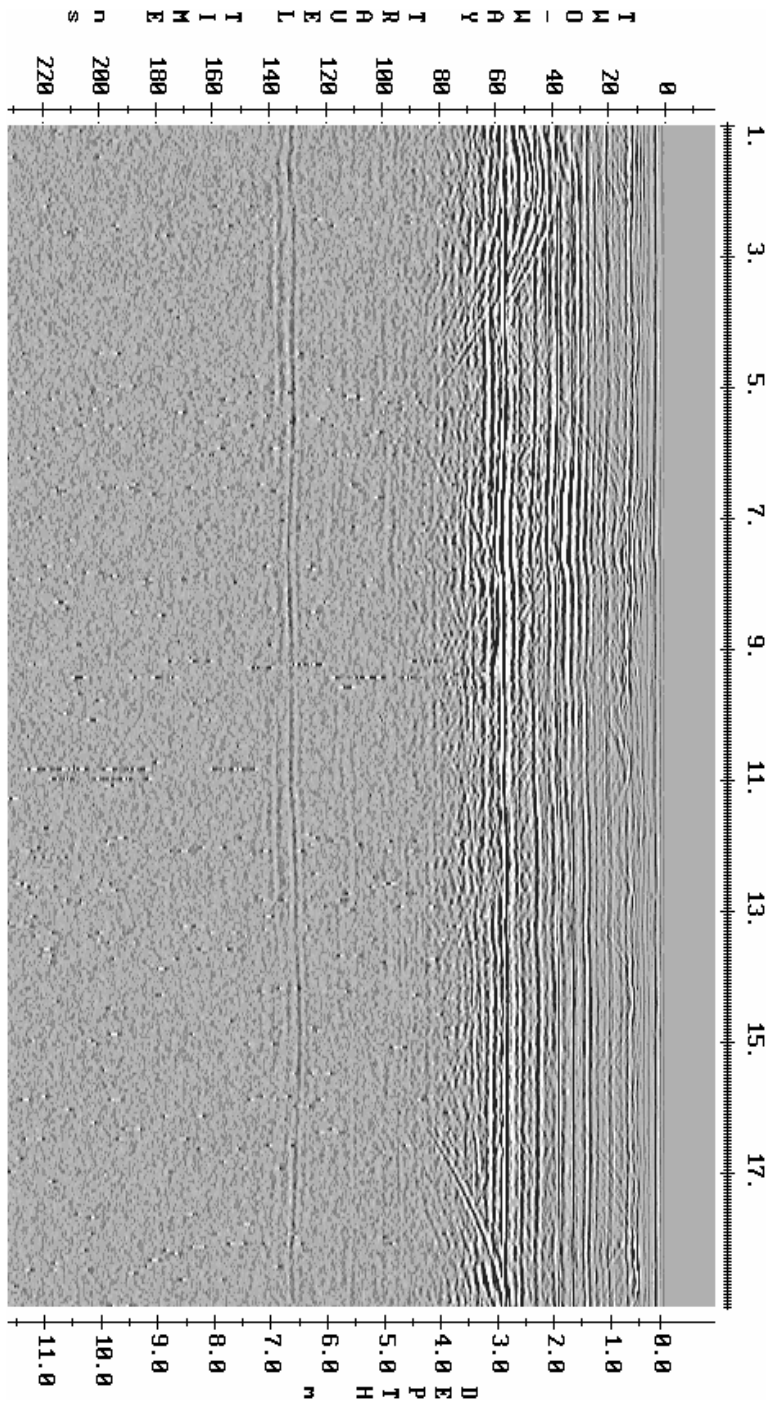


Figure B3: 450 MHz profile at Line 6 in the OSLW Quarry.
 File: OSLW'04/REEF 7
 Processing included: SEC = 1000, Attenuation = 0.7, Down the trace = 3, Traces per inch = 40

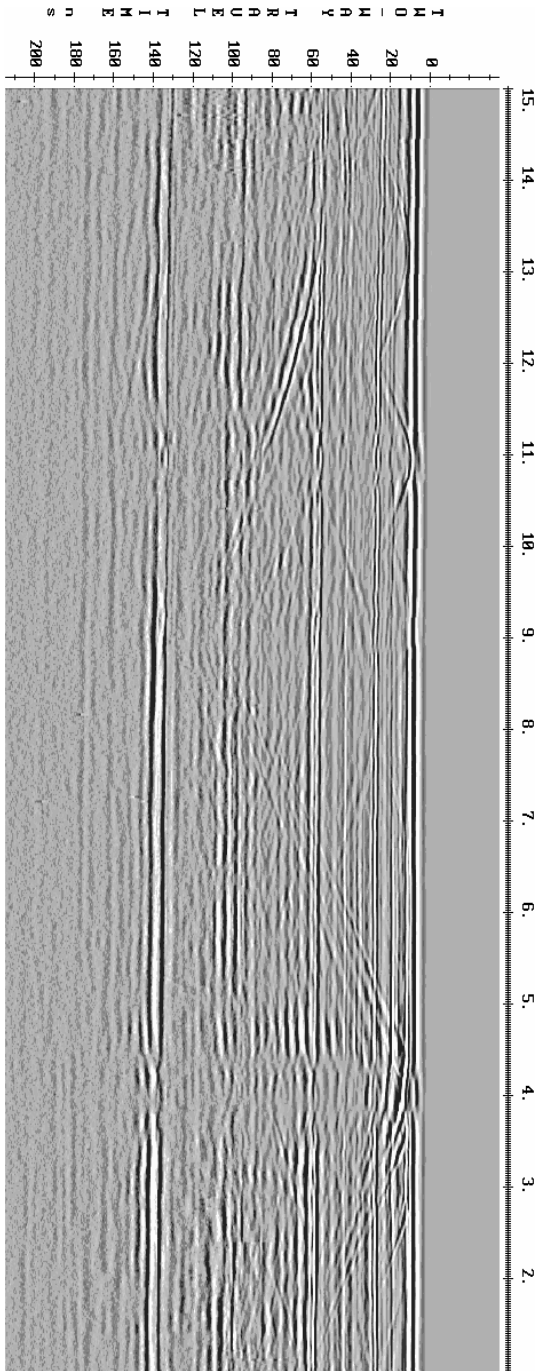


Figure B4: 225 MHz profile at Line 7 in the OSLW Quarry.
 File: Wiarnton2/ Field 2/Line7el
 Processing included: SEC = 1000, Attenuation = 1.2, Down the trace = 3, Traces per inch = 40, V=0.099 m/ns

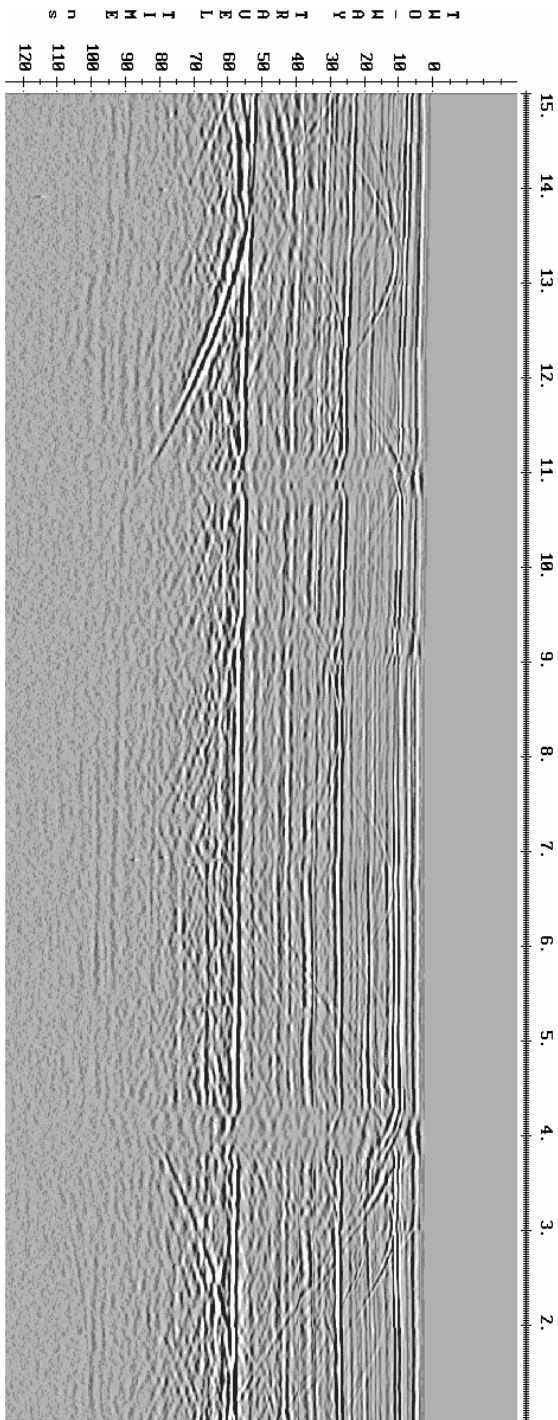


Figure B5: 450 MHz profile at Line 7 in the OSLW Quarry.
 File: Wiarton2/ Field 2/Line8el
 Processing included: SEC = 1000, Attenuation = 1.2, Down the trace = 3, Traces per inch = 40, V=0.1 m/ns

Line 6 - Stratigraphic Log

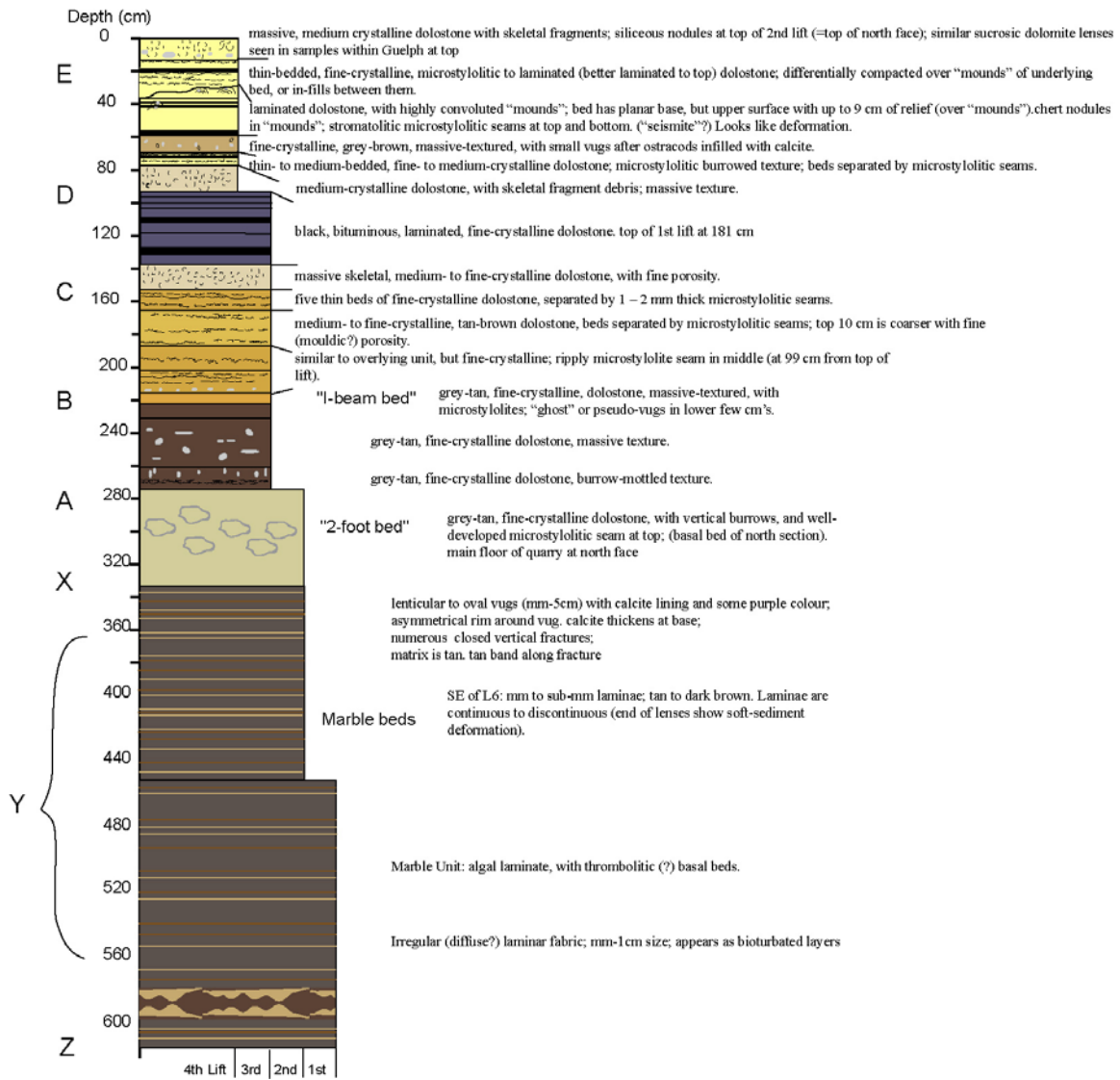


Figure B6: Stratigraphic log with descriptions of each unit at the OSLW Quarry.

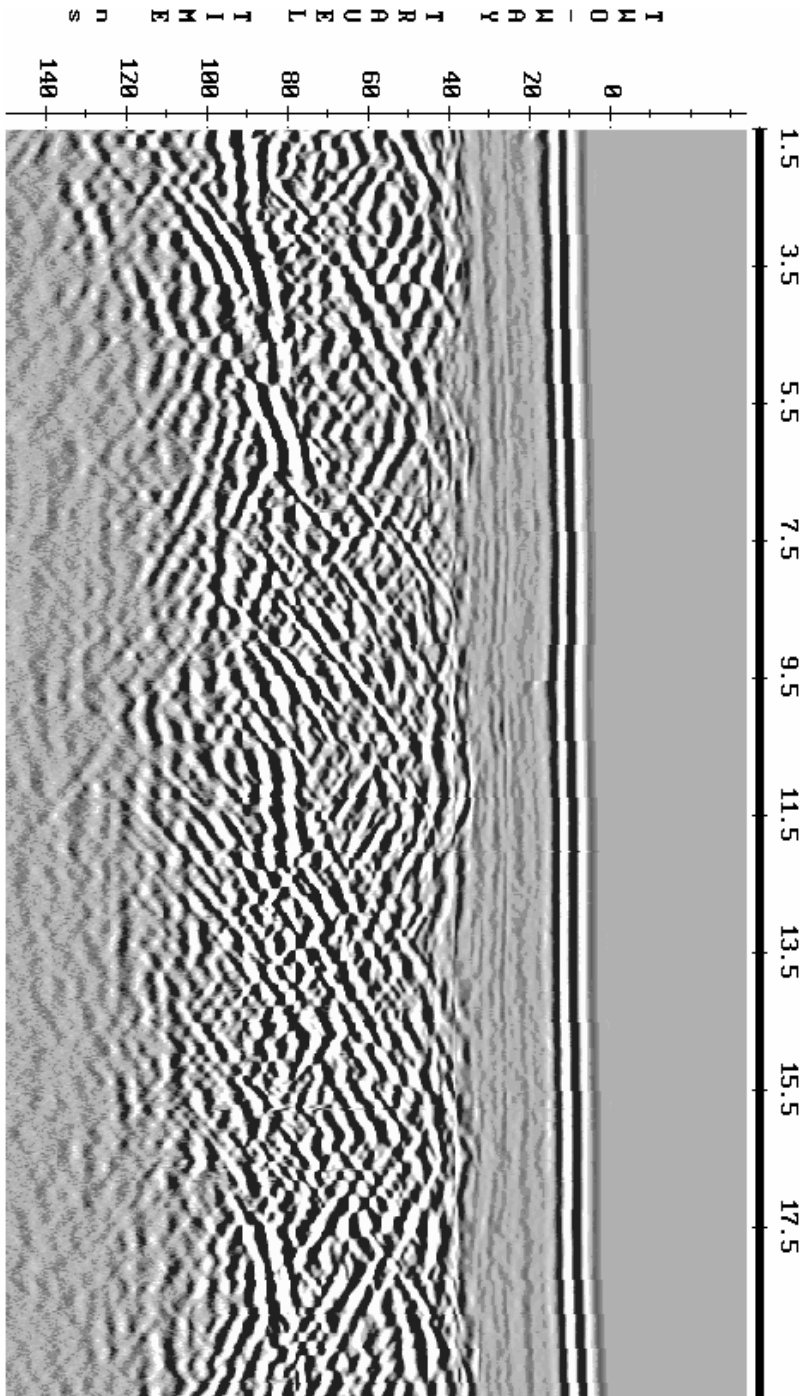


Figure B7: 225 MHz profile at Line 2 in the Adair Quarry.
 File: Wiarton2/Field: Line002el
 Processing included: SEC = 1000, Attenuation = 1.8, Traces per inch = 60, Down the trace = 3

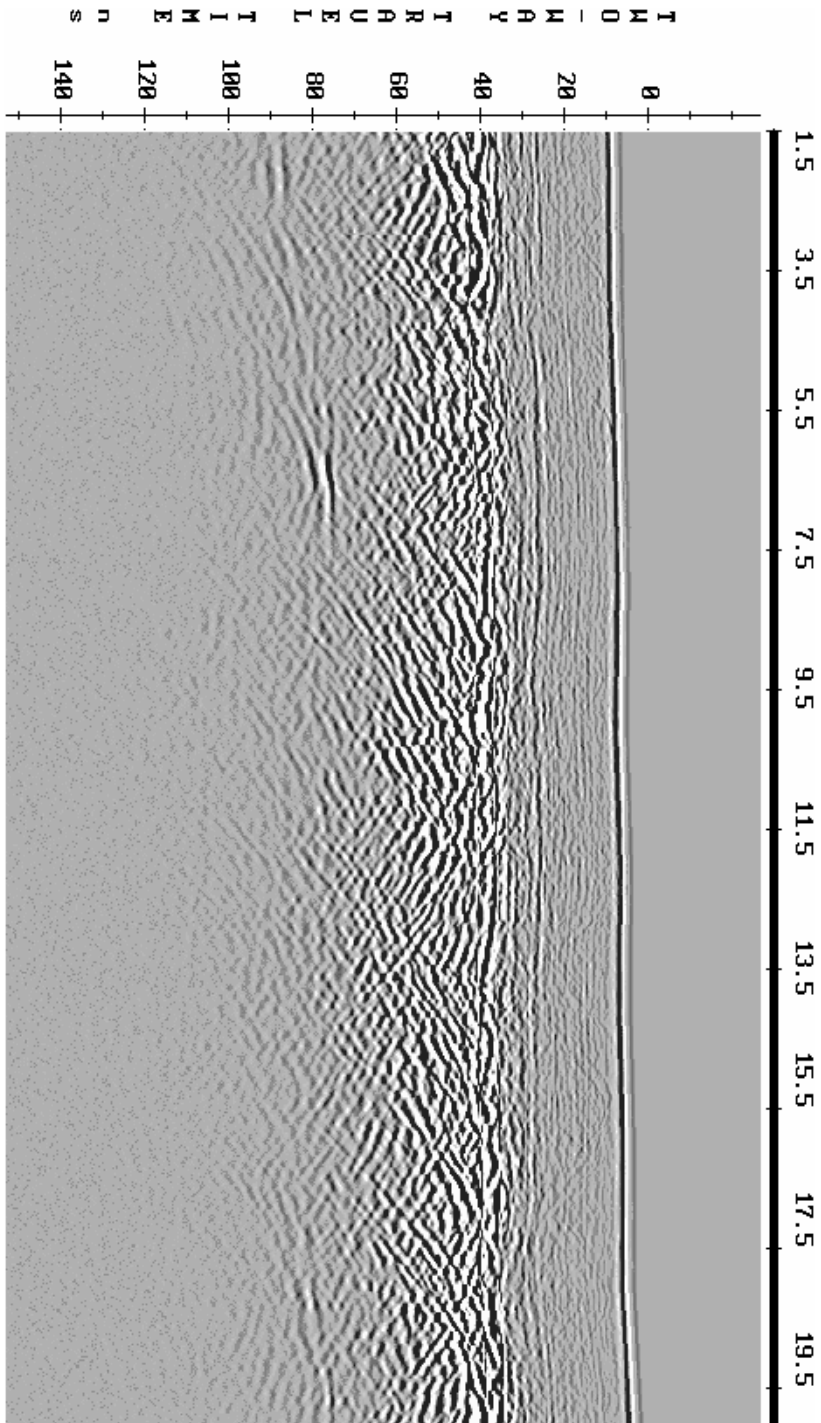


Figure B8: 450 MHz profile at Line 2 in the Adair Quarry.

File: Warton2/Field: Line003el

Processing included: SEC = 500, Attenuation = 2, Traces per inch = 60, Down the trace = 3

Appendix C– Low Frequency Shallow Subsurface GPR

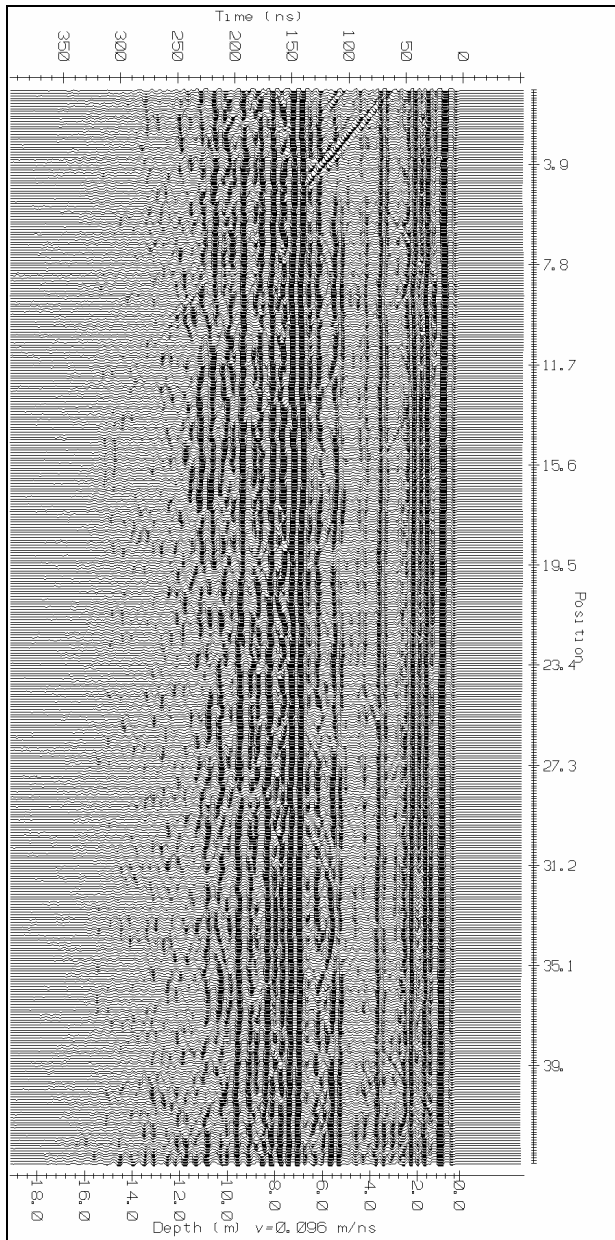


Figure C1: 200 MHz profile at Line 1 in the OSLW Quarry.

File: OSLW'04; Elev; L1-200e1

Processing included: SEC = 1000, Attenuation = 1.8, Down the trace = 3, Traces per inch = 40

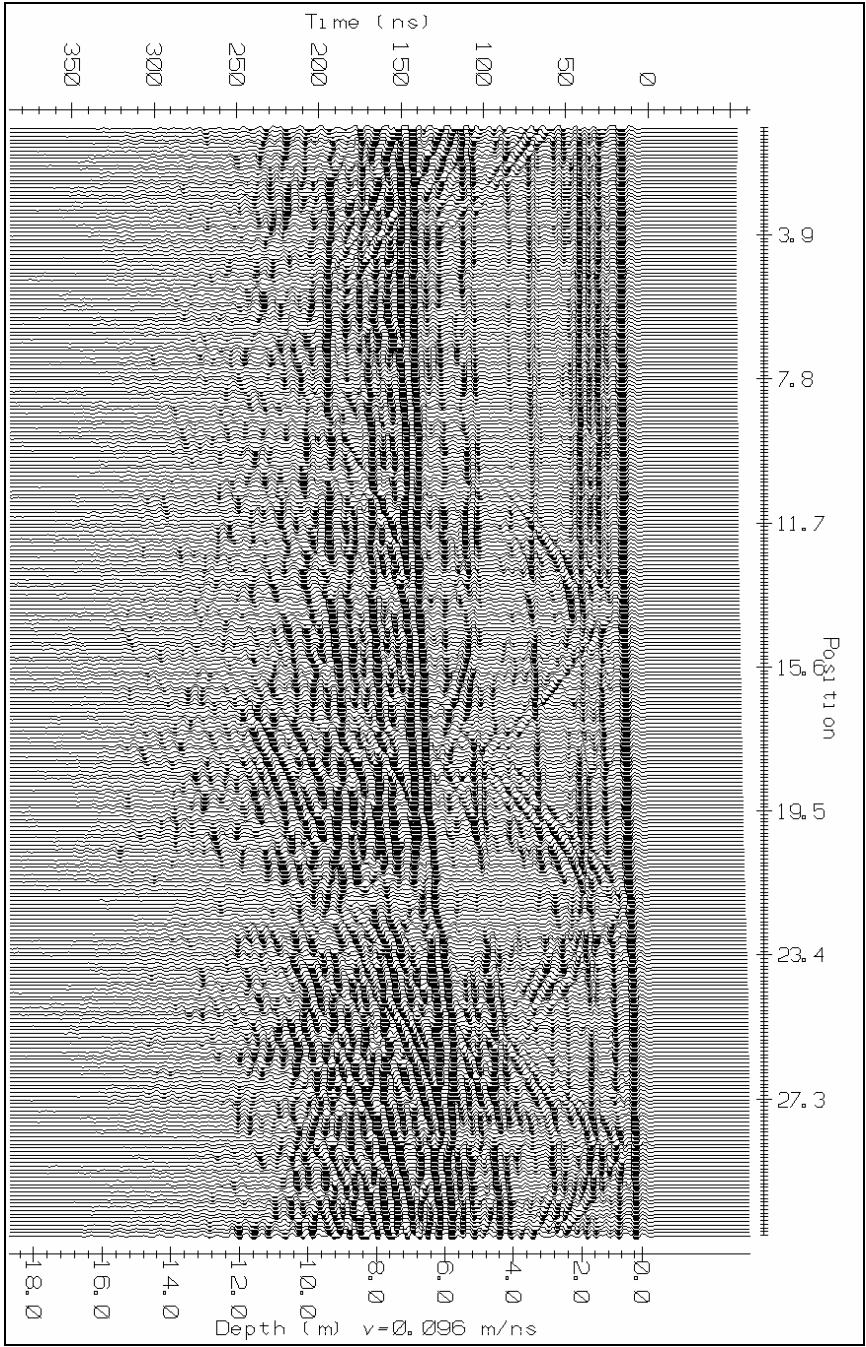


Figure C2: 200 MHz profile at Line 2 in the OSLW Quarry.
 File: OSLW'04; Elev; L2-200el
 Processing included: SEC = 1000; Attenuation = 1.8; Down the trace = 3; Traces per inch = 40

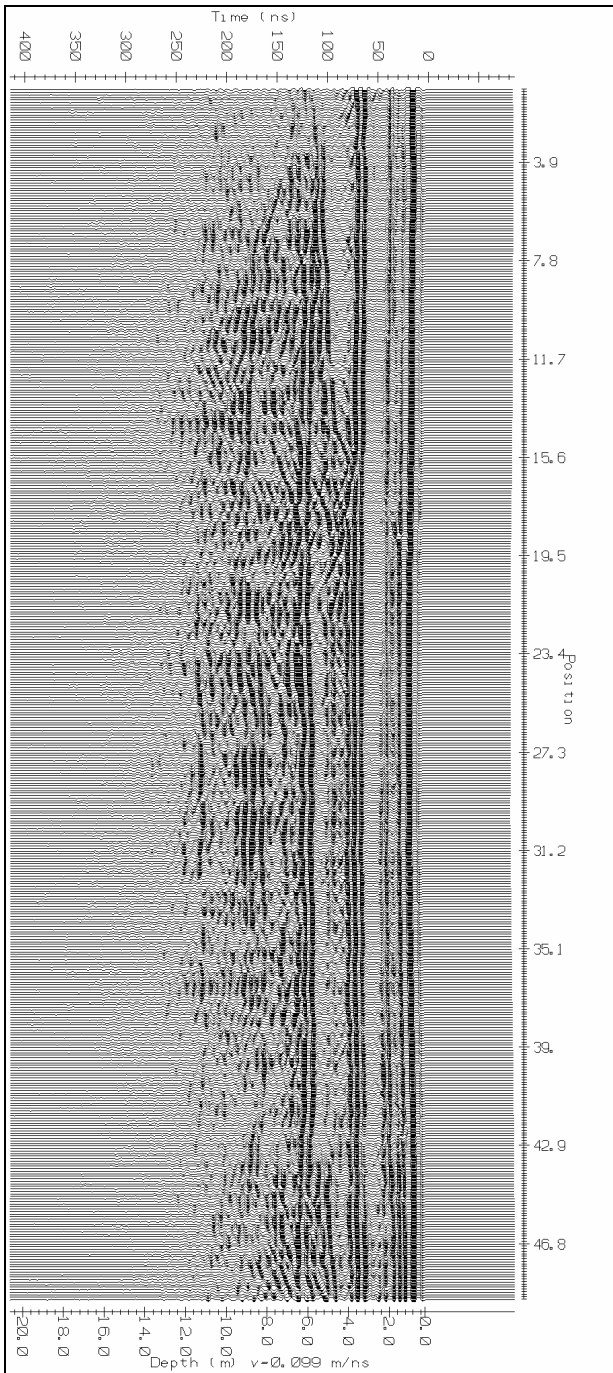


Figure C3: 200 MHz profile at Line 5 at the OSLW Quarry.

File: OSLW'04, Elev

Processing included: SEC = 1000, Attenuation = 1.2, Down the trace = 3, Traces per inch = 40

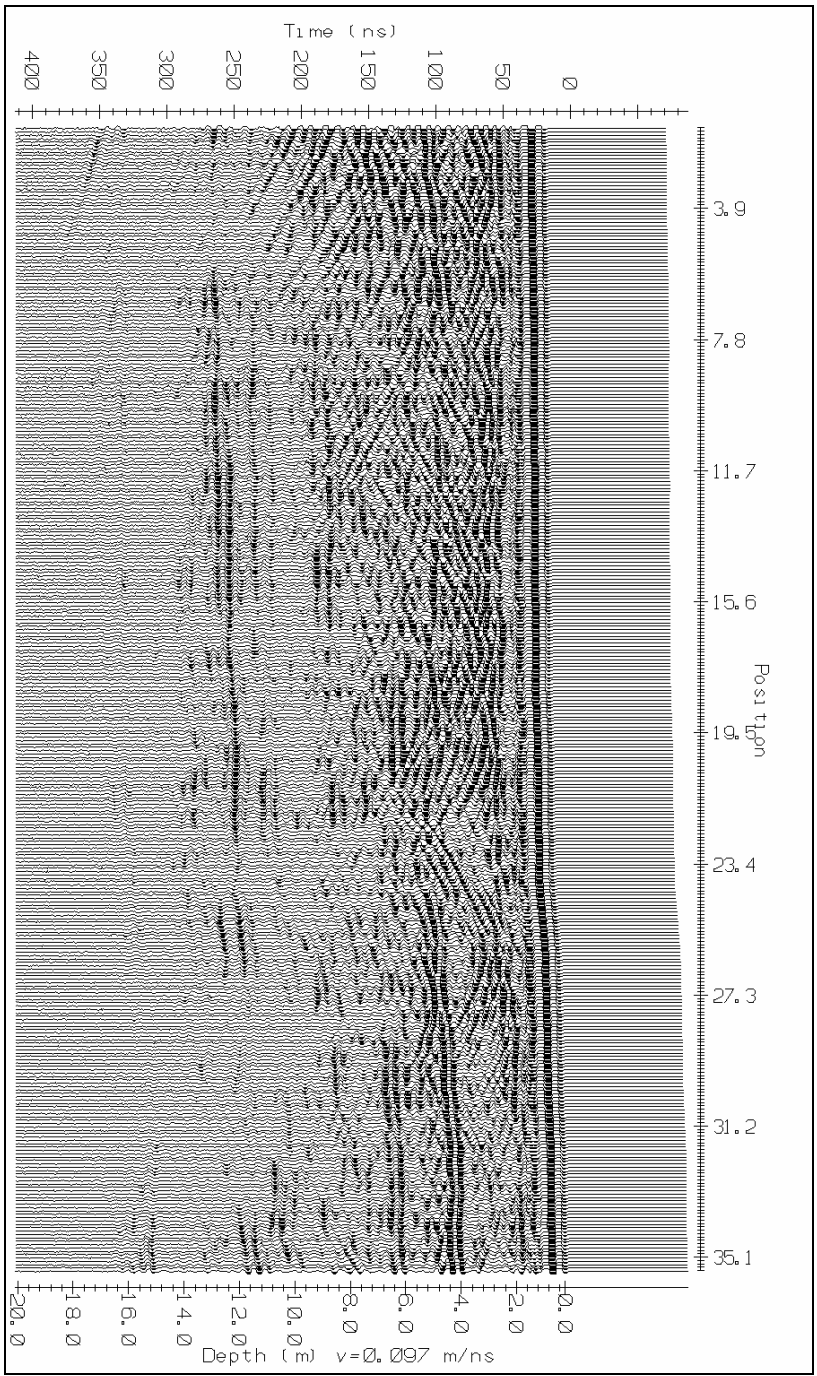


Figure C4: 200 MHz profile at Line 2 at the Adair Quarry.
 File: Wiarnton2/Field 1: Line15ele
 Processing included: SEC = 1000, Attenuation = 1.7, Down the trace = 1, Traces per inch = 40

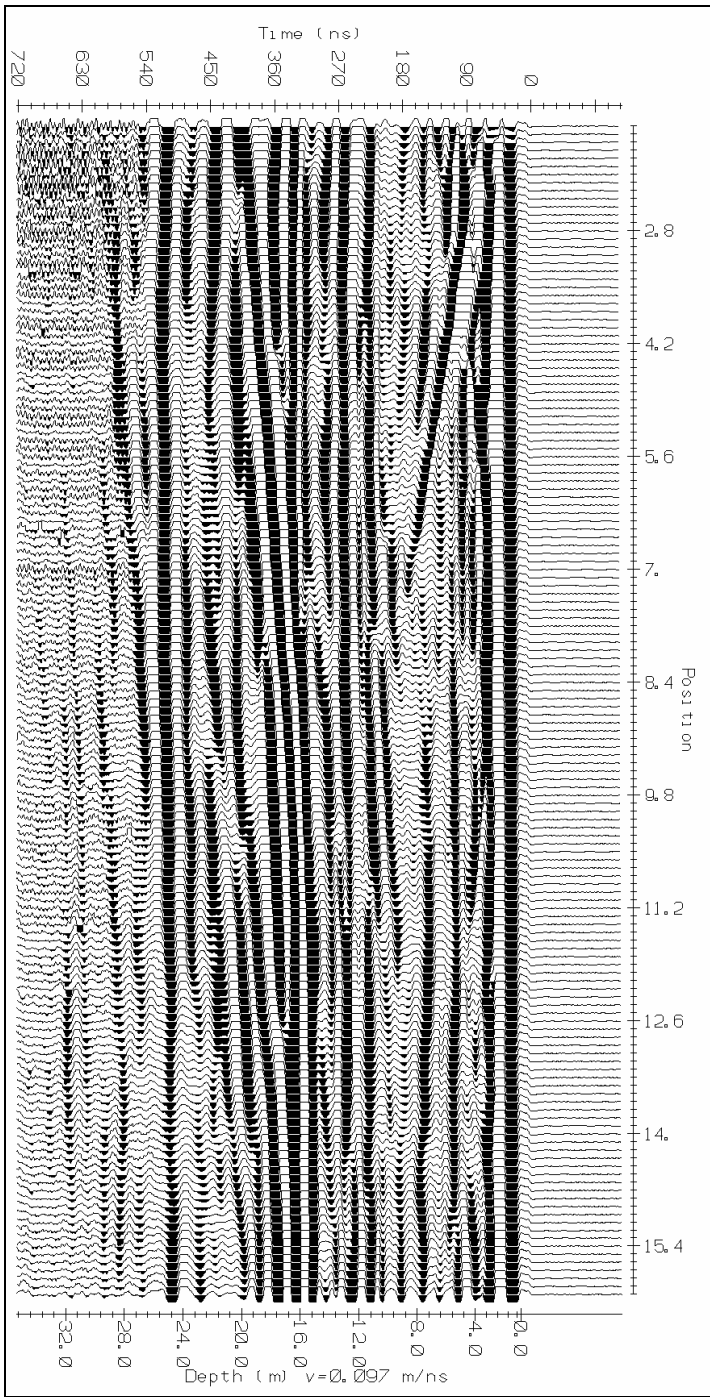


Figure C5: 50 MHz profile at Line 3 in the Adair Quarry.

File: Warton2/Field 1: Line8ele

Processing included: SEC = 1000, Attenuation = 0.5, Down the trace = 7, Traces per inch = 15

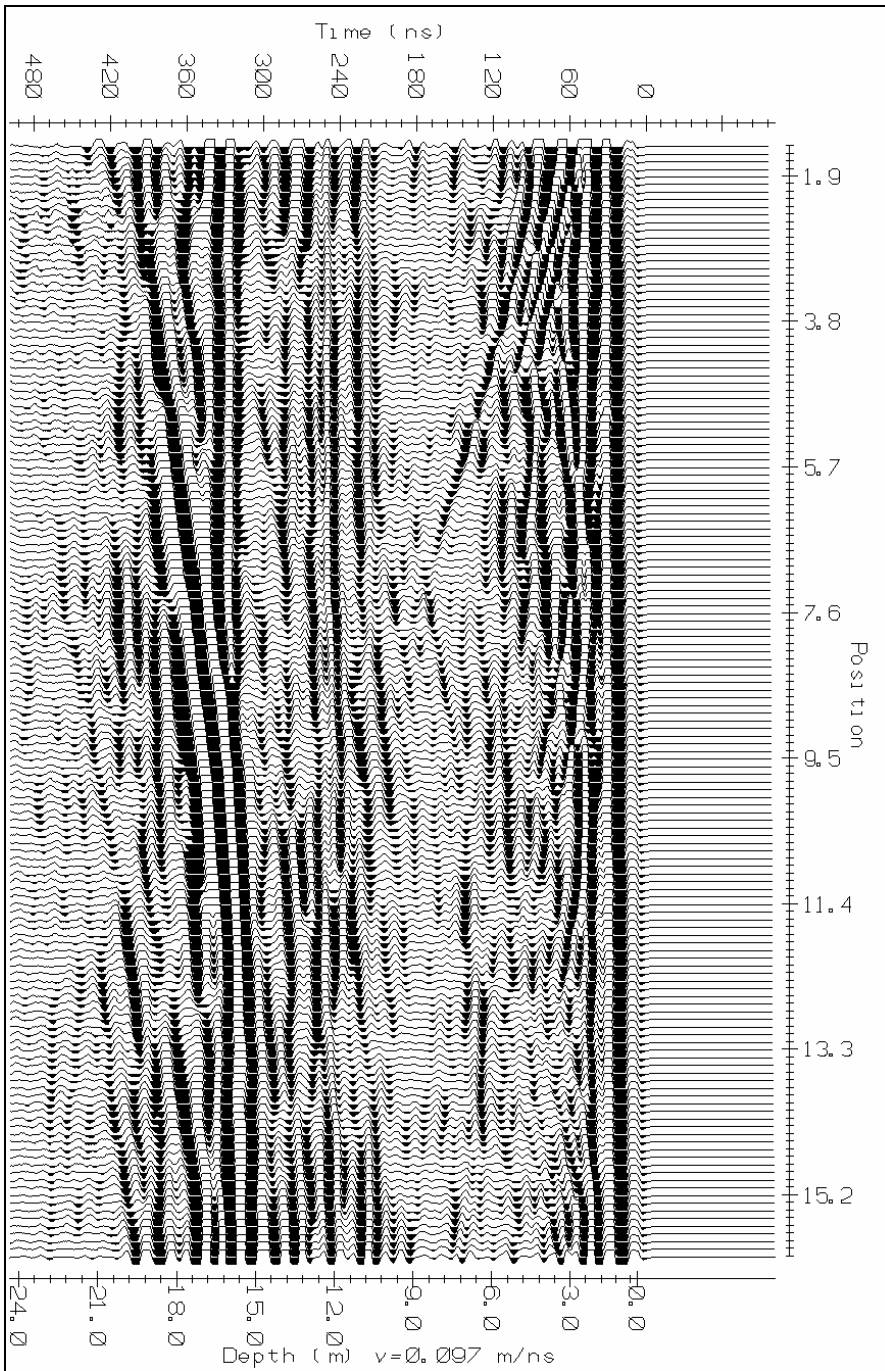


Figure C6: 100 MHz profile at Line 3 at the Adair Quarry.
 File: Warton2/Field 1: Line12ele
 Processing included: SEC = 1000, Attenuation = 0.8, Down the trace = 5, Traces per inch = 20

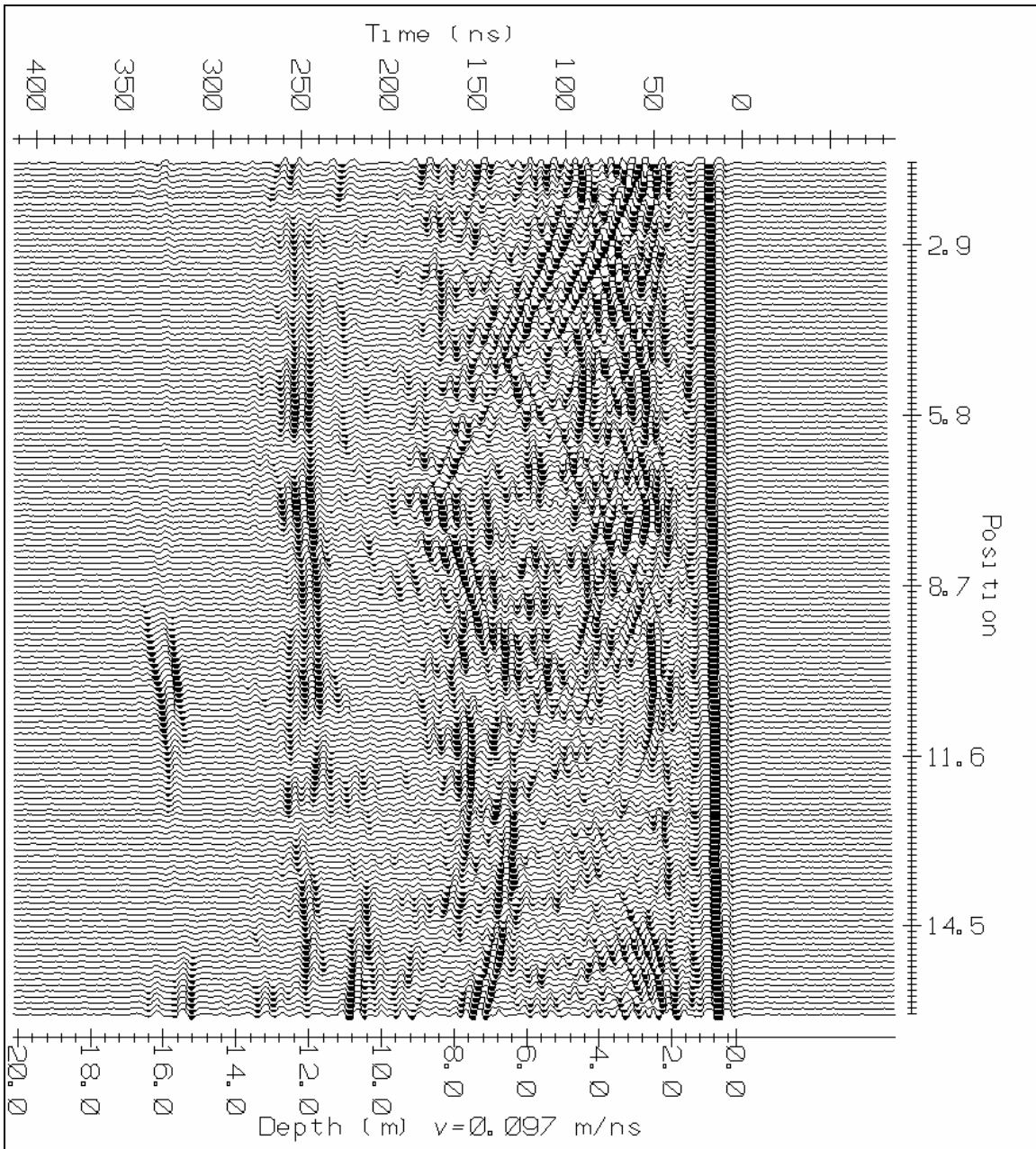


Figure C7: 200 MHz profile at Line 3 at the Adair Quarry.

File: Wiarnton2/Field 1: Line16ele

Processing included: SEC = 1000, Attenuation = 1.2, Down the trace = 3, Traces per inch = 30

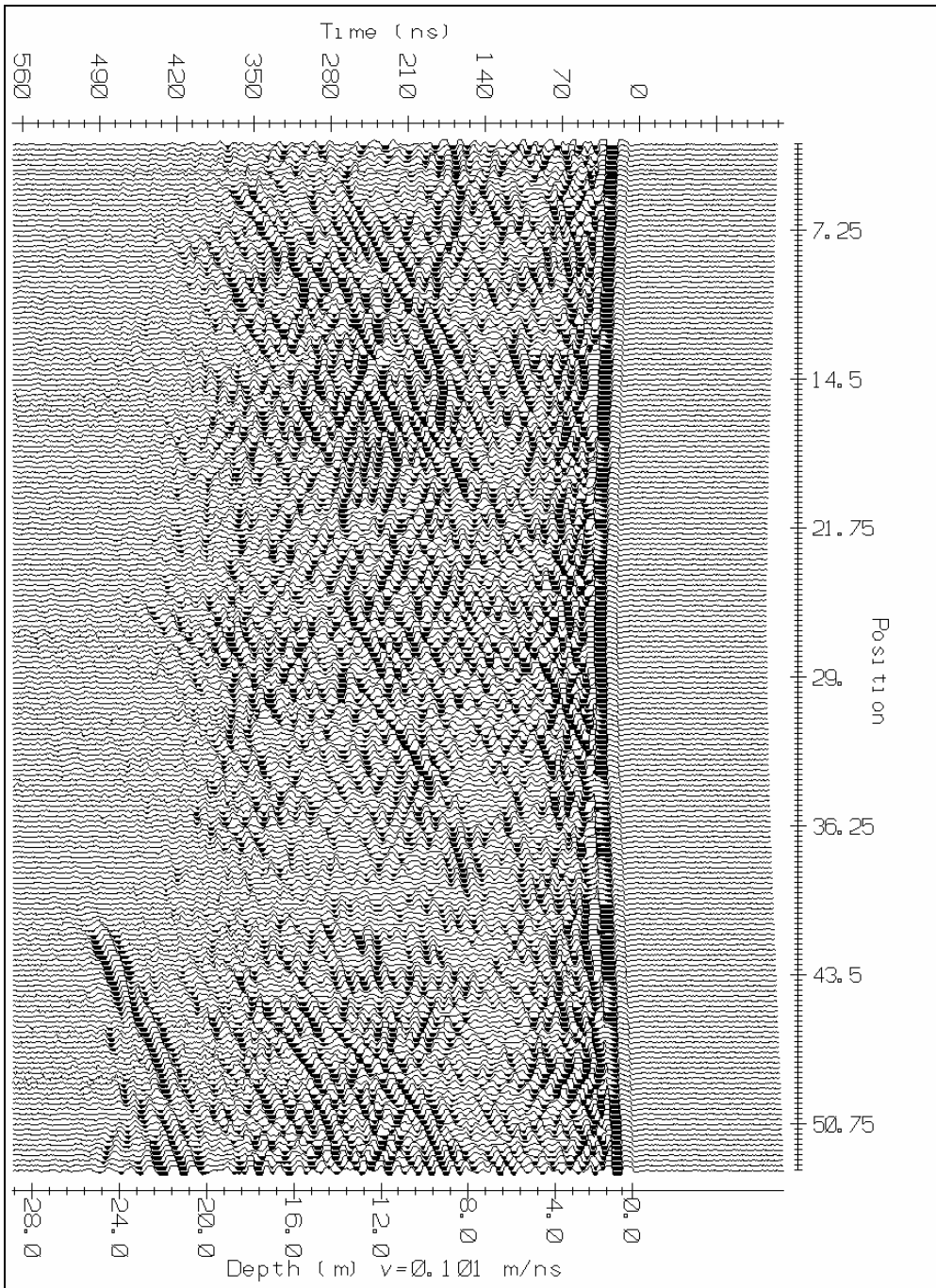


Figure C8: 100 MHz profile at the 90-3 borehole site.

File: Warton2/Field 1: Line3ele

Processing included: SEC = 1000, Attenuation = 0.8, Down the trace = 3, Traces per inch = 30

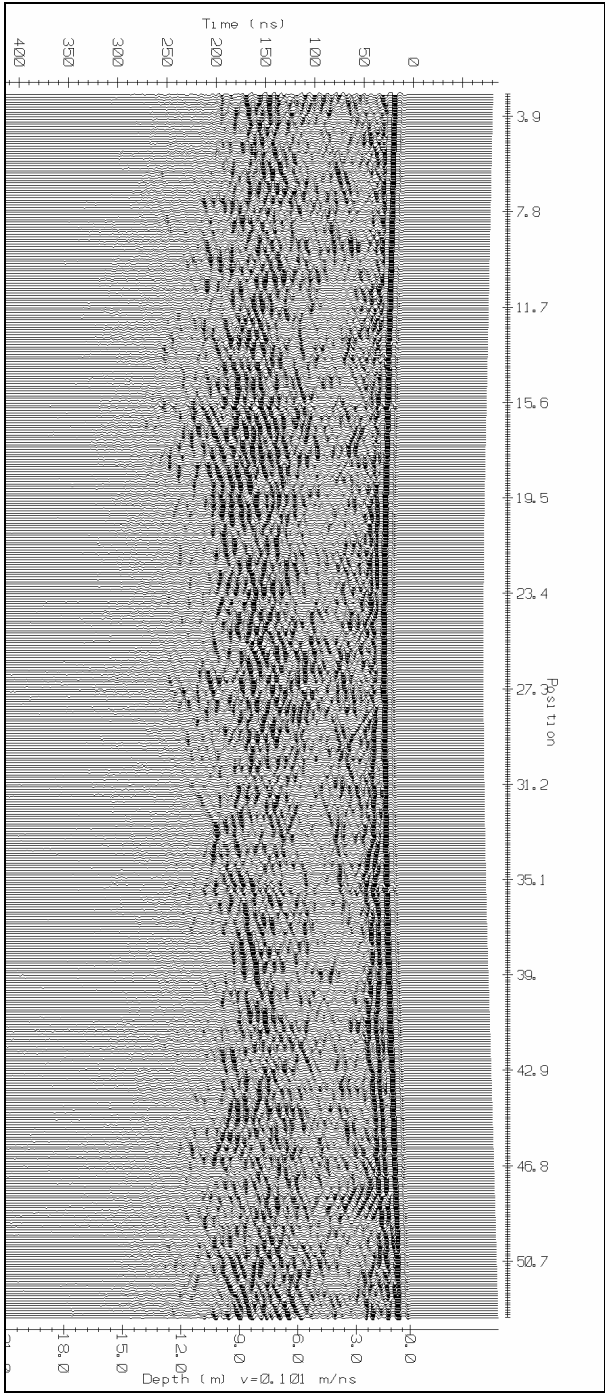


Figure C9: 200 MHz profile at the 90-3 borehole site.

File: Wiarion2/Field 1: Line5ele

Processing included: SEC = 1000, Attenuation = 1.2, Down the trace = 3, Traces per inch = 30

Appendix D – Data on CD-ROM

1. Thesis in .pdf format
2. Elevation data for each site
3. TOP files for topographic correction
4. Raw DT1 and HD files:

Folder: OSLW'04

2004

File

Name	Location	Line	Frequency	
WIART1	OSLW	1	50 MHz	
WIART2	OSLW	1	50 MHz	CMP
WIART4	OSLW	2	50 MHz	
WIART5	OSLW	1	100 MHz	
WIART6	OSLW	1	100 MHz	CMP
WIART7	OSLW	2	100 MHz	
WIART8	OSLW	1	200 MHz	
WIART9	OSLW	1	200 MHz	CMP
WIART11	OSLW	2	200 MHz	
REEF2	OSLW	3	450 MHz	
REEF3	OSLW	4	450 MHz	
WIART15	OSLW	5	50 MHz	
WIART16	OSLW	5	50 MHz	CMP
WIART17	OSLW	5	100 MHz	
WIART19	OSLW	5	100 MHz	CMP
WIART20	OSLW	5	200 MHz	
WIART21	OSLW	5	200 MHz	CMP
REEF4	OSLW	6	225 MHz	
REEF6	OSLW	6	225 MHz	WARR
REEF7	OSLW	6	450 MHz	
REEF8	OSLW	6	900 MHz	
REEF10	OSLW	6	900 MHz	WARR

Folder: Field 1

2005

File

Name	Location	Line	Frequency	
Line0000	90-3	1	50 MHz	
Line0002	90-3	1	50 MHz	CMP
Line0003	90-3	1	100 MHz	
Line0004	90-3	1	100 MHz	CMP
Line0005	90-3	1	200 MHz	
Line0006	90-3	1	200 MHz	CMP
Line0007	Adair	2	50 MHz	
Line0008	Adair	3	50 MHz	
Line0009	Adair	2	50 MHz	CMP
Line0010	Adair	2	100 MHz	
Line0012	Adair	3	100 MHz	
Line0013	Adair	2	100 MHz	CMP
Line0015	Adair	2	200 MHz	
Line0016	Adair	3	200 MHz	
Line0017	Adair	2	200 MHz	CMP

Folder: Field 2

2005

File

Name	Location	Line	Frequency	
Line0002	Adair	2	225 MHz	
Line0003	Adair	2	450 MHz	
Line0004	Adair	2	900 MHz	
Line0006	Adair	2	900 MHz	CMP
Line0007	OSLW	7	225 MHz	
Line0008	OSLW	7	450 MHz	
Line0010	OSLW	7	900 MHz	
Line0011	OSLW	7	900 MHz	CMP
Line0012	OSLW	7	450 MHz	CMP
Line0013	OSLW	7	225 MHz	CMP